

**Evaluating a bioprosthetic anterior mitral valve leaflet made from autologous jugular vein and expanded polytetrafluoroethylene (Gore-Tex) chordae in a sheep model.**

**Jacques Janson**

MB ChB M Med (Thor) FCS (Cardio)

*Dissertation presented for the Degree of Doctor of Philosophy in the Faculty of Medicine and Health Sciences, at Stellenbosch University*



**Supervisor: Prof Andre Coetzee**

MB ChB M Med (Anes) FFA (SA) FFARCS PhD MD PhD DSc

Professor and Executive Head

Anesthesiology and Critical Care, Stellenbosch University

March 2016

**Declaration**

By submitting this dissertation electronically, I declare that the entirety of the work contained therein is my own, original work, that I am the sole author thereof (save to the extent explicitly otherwise stated), that reproduction and publication thereof by Stellenbosch University will not infringe any third party rights and that I have not previously in its entirety or in part submitted it for obtaining any qualification.

**Signature .....**      **Date .....**

## Abstract

The purpose of this study was to evaluate whether an autologous vein graft supported by expanded polytetrafluoroethylene (Gore-Tex) chordae can be used to replace an anterior mitral valve leaflet and whether the vein will be able to withstand the stress and strain of deformation, remain viable in the intracardiac environment and be able to adapt morphologically and grow as a valve leaflet.

An autologous jugular vein graft, used as a double layer, supported by Gore-Tex chordae was used to create a functional anterior mitral valve leaflet in 21 sheep. No ring annuloplasty was used to support the annulus. The average cross-clamp time was 99 minutes (76 to 151 min) and the average bypass time was 137 minutes (109 to 188 min). One sheep died intra-operatively. The post-operative echocardiogram demonstrated laminar diastolic flow across the mitral valve with an average opening area of 2.8cm<sup>2</sup>. Fourteen sheep had trace to mild mitral regurgitation (MR), 5 sheep had mild to moderate MR and 1 sheep had moderate to severe MR. The body of the vein leaflet tends to billow during systole which increases stress on the Gore-Tex chordae.

Three sheep died 2 to 3 days postoperatively from mitral regurgitation due to Gore-Tex chordae that were too long, causing prolapse in 2 cases and 1 case developed a hematoma between the 2 vein layers. Seven sheep died between 1 and 6 months. Four sheep developed infective endocarditis on the mitral valve.

Echocardiography at 6 months showed that the mitral regurgitation (MR) progressed with time in most of the sheep: 3 out of 11 sheep had mild MR, 5 had mild to moderate MR and 3 had moderate to severe MR. The progression of MR was due to lack of secondary chordal support of the vein leaflet and mitral annulus, leading to progressive annular dilatation, decreased leaflet coaptation length and increased tension on the primary Gore-Tex chordae. Durability of the valve should be improved by adding an annuloplasty ring and supporting the leaflet with secondary chordae. The 10 surviving sheep were euthanized between 6 to 10 months. All vein implants were examined histologically.

The vein leaflet developed intimal fibroplasia and fibrous proliferation between the 2 vein layers as a response to the increased stress upon the tissue. This caused leaflet thickening, but the vein remained flexible without shortening or contracture. The 6 to 10 month vein

implants showed viable endothelium and the underlying vein layers clearly showed viability with myofibroblasts, collagen and elastin. A normal healing pattern was seen at the suture lines and no calcification was seen in the vein leaflet apart from the Gore-Tex sutures. No vein growth was demonstrated.

Autologous vein has the potential to be used as a valve leaflet substitute, because it remains viable in the intracardiac position for up to 10 months and is able to withstand the stress and deformation of a valve leaflet. Histologically it showed the ability to heal and to morphologically adapt to the new environment.

## Opsomming

Die doel van hierdie studie was om te sien of outologiese lewendige vene weefsel, ondersteun deur politetrafluoroetileen (Gore-Tex) chordae, gebruik kan word om die anterior mitraalklepsuil te vervang. Daar wou gesien word of die vene die druk, spanning en vervorming in die mitraalklep posisie sal kan hanteer en of die vene lewensvatbaar sal bly en morfologies sal aanpas en groei.

'n Outologiese jugulêre veen transplantaat is gebruik, as 'n dubbel laag, ondersteun deur Gore-Tex chordae om 'n funksionele anterior mitraalklepsuil te skep in 21 skape. Geen ring annuloplastiek is gedoen om die mitraalklep annulus te ondersteun nie. Die gemiddelde klem tyd was 99 minute en die gemiddelde kardiopulmonale omleiding tyd was 137 minute. Een skaap is intra-operatief dood. Post-operatiewe eggokardiografie het laminêre diastoliese vloei oor die mitraalklep demonstreer met 'n gemiddelde kleparea van 2.8 cm<sup>2</sup>. Veertien skape het baie geringe tot geringe mitraal inkompetensie (MI) gehad, 5 skape het gering tot matige MI getoon en 1 skaap het matig tot strawwe MI gehad. Die veenklep was geneig om uit te bult na die linker atrium tydens ventrikulêre sistolie wat spanning op die primêre Gore-Tex chordae verhoog het.

Drie skape is 2 tot 3 dae post-operatief dood as gevolg van mitraal inkompetensie omdat die Gore-Tex chordae te lank was in 2 skape met veenklep prolaps en 'n hematoom het gevorm in een klepsuil tussen die 2 veen lae. Sewe skape is dood tussen 1 tot 6 maande. Vier skape het infektiewe endokarditis op die mitraalklep ontwikkel.

Eggokardiografie op 6 maande het getoon dat die mitraalinkompetensie (MI) progressief vererger het in die meeste skape met 3 uit 11 skape wat geringe MI getoon het tussen 6 en 10 maande. Die progressie van die MI was as gevolg van die verlies van sekondêre Gore-Tex chordae wat die veenklep en die mitraalklep annulus ondersteun het. Dit het gelei tot progressiewe annulus dilatasie, verminderde koaptasie lengte en verhoogde spanning op die primêre Gore-Tex chordae. Die klepfunksie behoort beter behou te word deur die veenklep te ondersteun met 'n klepring annuloplastiek en sekondêre Gore-Tex chordae. Die 10 oorlewende skape het eutanase ondergaan tussen 6 tot 10 maande. Alle veen klepsuile is histologies evalueer.

Die veen klep het intimale fibroplasie ontwikkel met fibreuse proliferasie tussen die 2 veen lae as aanpassing tot die verhoogde drukspanning op die weefsel. Dit het verdikking van die klepsuil veroorsaak, maar die klepsuil was steeds vervormbaar sonder verkorting of kontrakture. Die 6 tot 10 maande veen oorplantings het lewensvatbare endoteel getoon en die onderliggende veen lae was lewensvatbaar met miofibroblaste, kollageen en elastien. 'n Normale genesingsproses is gesien by die steke lyne en geen kalsifikasie is in die vene gesien nie, behalwe by van die Gore-Tex steke. Veen groei is nie gedemonstreer nie.

Outologiese veen het die potensiaal om gebruik te word vir die vervanging van 'n klepsuil, want dit bly lewensvatbaar in die hart vir tot 10 maande. Die veenklep kan die druk, spanning en vervorming van 'n klepsuil hanteer en histologies toon die veen die potensiaal om te genees en morfologies aan te pas by die intra-kardiale milieu.

## Acknowledgements

Many people have helped and contributed to this dissertation and for that I am extremely grateful. Without their help this project would not have been possible. Specifically I would like to thank the following people:

**Prof Andre Coetzee**, my supervisor and head of Anaesthesia and Critical Care at the University of Stellenbosch. He was very efficient in reviewing my writing, from the protocol to the final discussion. His years of research experience and critical thinking guided me to focus my ideas. Prof Coetzee taught me how to question thoughts and express ideas. His words of encouragement were also valuable and a comfort when faced with the challenges of the study.

**Prof Gawie Rossouw**, head of Cardiothoracic Surgery at the University of Stellenbosch, for his insightful comments and practical support given during different stages of the research. He also helped logistically to make this study a reality by departmental research funding.

**Dr Izak Loftus**, Pathologist at Pathcare, Somerset West, for all his hard work in preparing the histological samples of all the specimens. He reviewed all the histology with me, mostly after hours. His enthusiasm for histopathology is contagious and reviewing the histology with him opened my eyes again as a surgeon of how fascinating living tissue is. His knowledge of histopathology was a tremendous contribution to this study.

**Dr Pieter Rossouw and Dr Philip Herbst**, Cardiologists at the University of Stellenbosch, for their help with echocardiography to evaluate the mitral valve function. Dr Rossouw made a few trips with me to do post-operative echocardiography on the sheep at the experimental farm in Stellenbosch. Their experience in echocardiography helped us to obtain good images in difficult circumstances.

**Dr Riaan Murray**, Anaesthetist at the University of Stellenbosch, for managing the sheep anaesthetic and helping with the post-operative care. He was guided by **Prof Andre Coetzee** and helped a few times by **Dr Francois Retief**. Dr Murray was a pleasure to work with and he

helped with the success of the experiments. It was a steep learning curve for us all, but his dedication and perseverance helped to get the sheep through complex heart surgery.

**Mr Noel Markgraaf**, head of the animal laboratory with his staff, **Mr David Jackson, Mr William Waldeck, Mr Deon Douglas, Mr Romano Markgraaf and Ms Sharon Meyer**. They were always friendly, ready to help and took great care of the animals.

**Mr Hannes Engelbrecht and Ms Annerie Muller**, both perfusionists, managed the perfusion of the sheep during cardiopulmonary bypass. They are both a pleasure to work with and their experience and dedication helped us to successfully do cardiac surgery on the sheep with cardiopulmonary bypass and cardiac arrest.

**Ms Sue Henderson** is an exceptional scrub nurse. She has years of experience in cardiac surgery and she came out of retirement to help us with this project. She had the ability to make the animal laboratory feel like an operating room. Her assistance helped me to focus on the procedure while she took care of the rest. **Ms Marie Dawidse** often assisted us as the floor nurse and made sure the instruments and sutures are always ready.

My wife, **Janet** and our 3 daughters, **Dayna, Lana and Christie** for their love, patience and support during this study. They are a constant source of joy in my life. My wife, Janet was also my reliable assistant during the surgeries and truly stood by my side during this study!

Above all, I would like to thank our heavenly Father, for by Him all things were created, in heaven and on earth, visible and invisible. As the Psalmist David wrote: "I praise you for I am fearfully and wonderfully made. Wonderful are your works; my soul knows it very well." (Psalm 139:14). The mitral valve is an example of beautiful design with precision. I am humbled when I look at the mitral valve because it shows the work of a Master!



I dedicate this thesis to my parents, Peter and Elana Janson.

## Table of Contents

<b>Abstract</b> .....	1
<b>Opsomming</b> .....	3
<b>Acknowledgements</b>	
<b>1. Literature Review</b> .....	10
1.1 Mitral valve anatomy.....	10
1.1.1 The fibrous skeleton of the heart.....	10
1.1.2 The mitral annulus.....	13
1.1.3 The mitral leaflets.....	18
1.1.4 The subvalvular apparatus.....	29
1.2 Blood flow through the normal mitral valve.....	31
1.3 The burden of mitral valve disease.....	33
1.4 Current valve prostheses.....	46
1.5 Tissue engineering of heart valves.....	58
1.6 The pulmonary autograft.....	60
1.7 The ideal prosthetic valve.....	61
1.8 Creating a prosthetic valve from autologous tissue.....	62
1.9 The autologous vein graft.....	63
1.10 The proposed study.....	69
<b>2 Methods</b> .....	70
2.1 Anaesthesia.....	70
2.2 Surgical procedure.....	71
2.2.1 Harvesting the internal jugular vein.....	71
2.2.2 Creating the anterior mitral leaflet from the internal jugular vein.....	72
2.2.3 Insertion of the vein leaflet.....	77
2.2.4 Post-operative care.....	86
2.3 Echocardiography.....	88
2.4 Pathology and histology.....	90

<b>3</b>	<b>Results</b> .....	92
	3.1 General remarks.....	92
	3.2 Echocardiographic result.....	95
	3.3 Early postoperative mortality (0-3 days).....	105
	3.4 Intermediate mortality (1-6 months).....	110
	3.5 Euthanized sheep.....	118
	3.6 Histology results.....	124
<b>4</b>	<b>Discussion</b> .....	182
	4.1 Technical aspects of vein implantation and the reproducibility of the procedure .....	182
	4.2 The nature of the linkage between the vein leaflet and the host.....	204
	4.3 Opening resistance and forward flow across the valve.....	206
	4.4 Valve closure and competence.....	207
	4.5 Activation of the coagulation system.....	212
	4.6 Tissue response to the vein leaflet and Gore-Tex chordae and effect on blood elements.....	214
	4.7 Durability of the vein leaflet.....	220
<b>5</b>	<b>Conclusion</b> .....	225
<b>6</b>	<b>References</b> .....	229

## **1.Literature review.**

### **1.1 Mitral valve anatomy**

The mitral valve is a remarkable structure which regulates unidirectional blood flow from the left atrium to the left ventricle. The valve is a functional complex which consists of the left atrium, mitral annulus, valve leaflets, chordae tendineae, papillary muscles and left ventricle. Each part of this complex plays an important role for the mitral valve to function properly.

Since the development of mitral valve surgery in the late 1950's and early 1960's there has been renewed interest in the detailed anatomy and function of the mitral valve (Du Plessis and Marchand 1964). Understanding the normal valve structure and ultrastructure gives us better insight into mitral valve function, valve dynamics, mitral valve disease and the surgical treatment of valve pathology.

#### **1.1.1 The fibrous skeleton of the heart:**

The fibrous skeleton of the heart provides the key to understanding the anatomical relationships of the mitral valve (Du Plessis and Marchand 1964). It is found at the base of the heart and consists of densely collagenous fibres with the aortic annulus forming the central part of the skeleton. Fibrous extensions from the aortic annulus form the scaffold for the pulmonary, tricuspid and mitral rings (Fig 1.1 and Fig 1.2). The fibrous skeleton is anchored to the myocardium in a similar way as tendons are attached to muscles (Misfeld and Sievers 2007).

**Fig 1.1:** Diagram of the fibrous skeleton of the heart (Du Plessis and Marchand 1964).

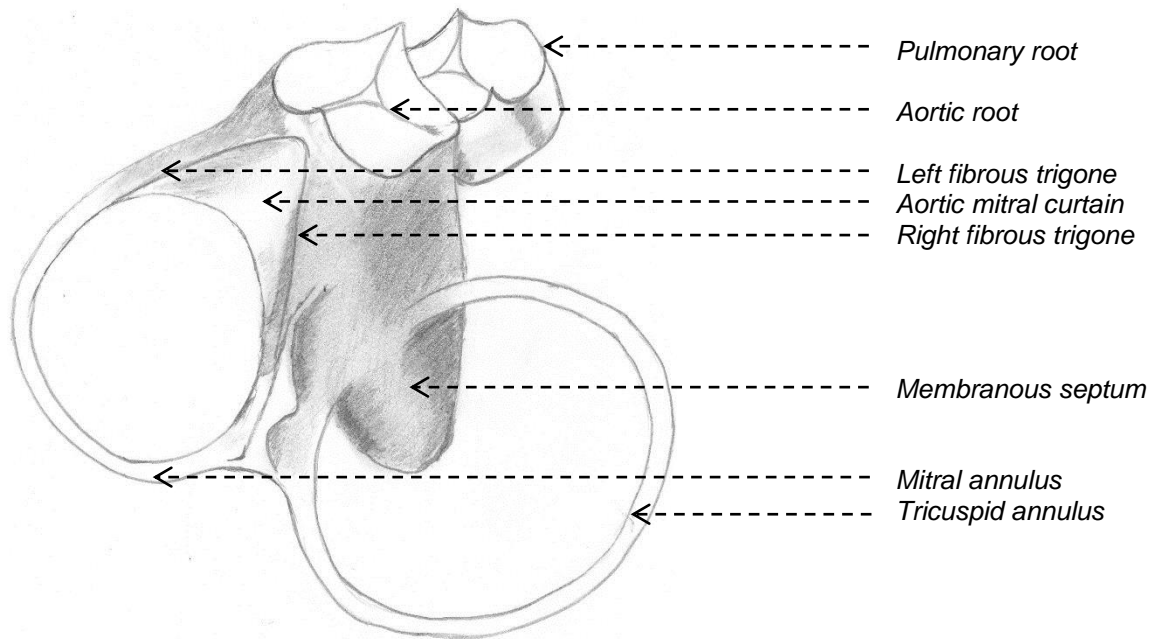
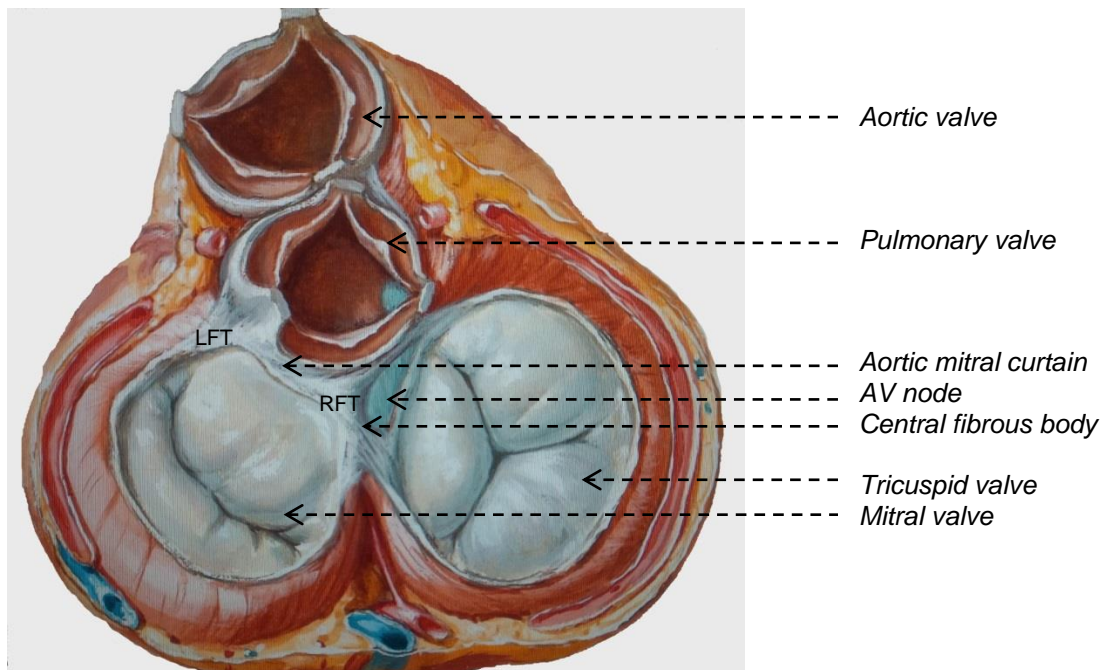
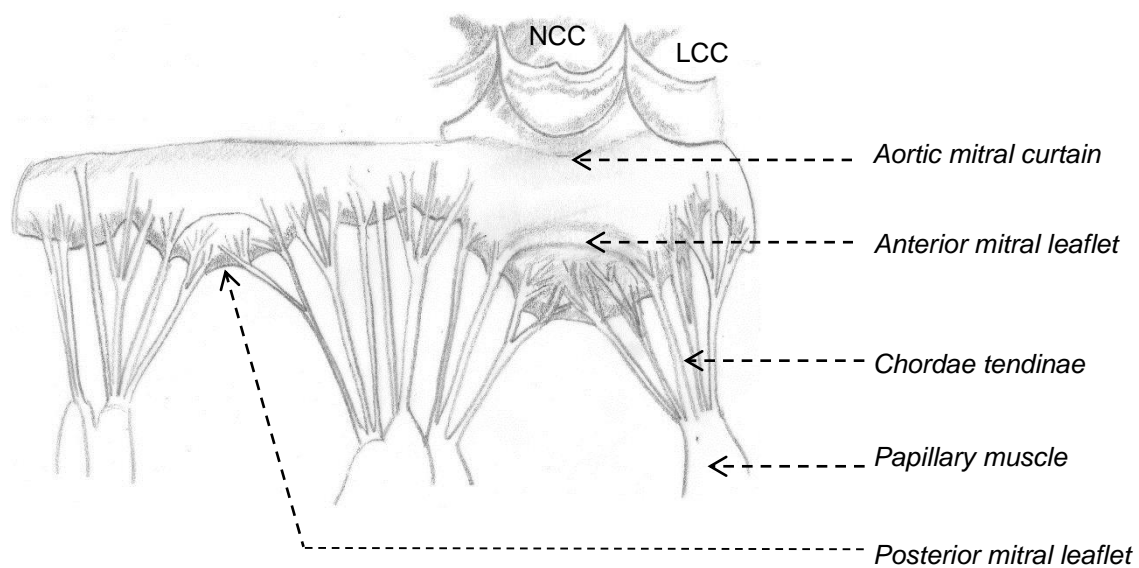


**Fig 1.2:** Fibrous skeleton of the heart showing the close relationship of the aortic, mitral and tricuspid valve. The AV node lies in the central fibrous body. The intervalvular fibrosa (aortic mitral curtain) is bordered on the left and right by the left fibrous trigone (LFT) and right fibrous trigone (RFT) (Netter 2010).



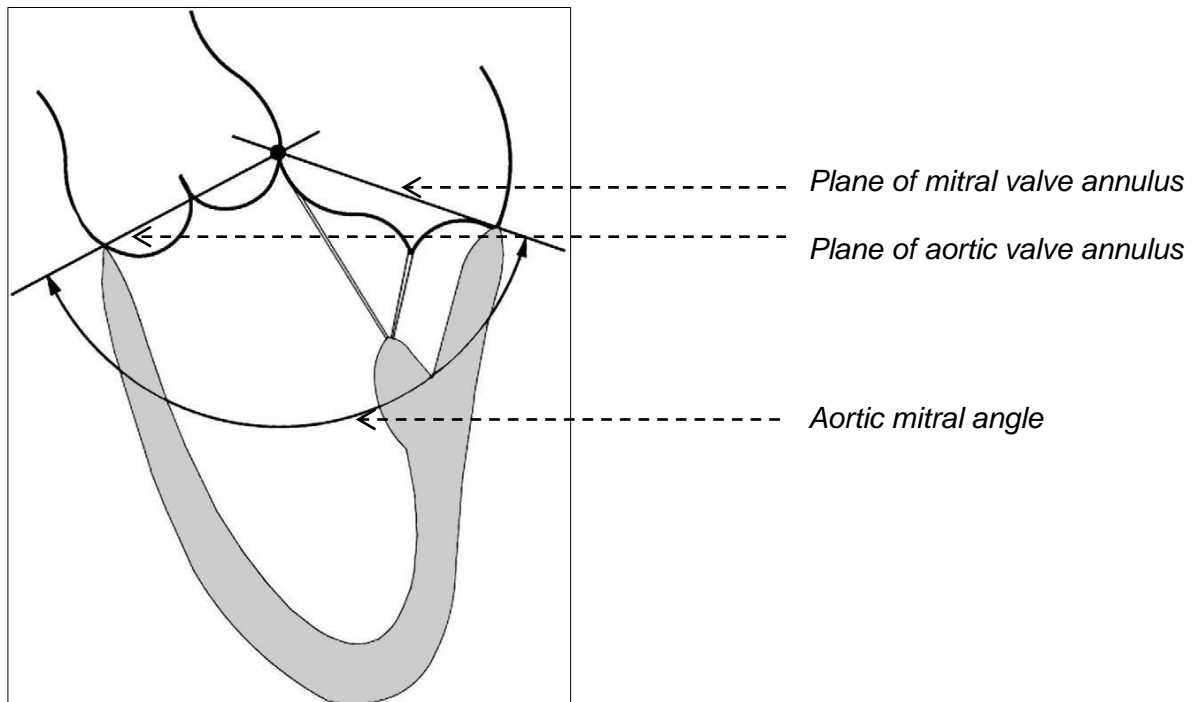
The position of the valves in the fibrous skeleton shows the close relationship of the four heart valves to each other. The tricuspid and pulmonary valves occupy two openings within the right ventricle and are separated by ventricular muscle called the conus arteriosus or infundibulum. The aortic and mitral valve occupy the same opening in the left ventricular myocardium (Du Plessis and Marchand 1964). The aortic and mitral valves are connected by the intervalvular fibrosa or aortic mitral curtain which stretches from the base of the left and non-coronary aortic cusps to the anterior mitral annulus (Silbiger and Bazaz 2009) (Fig 1.1, 1.2, 1.3).

**Fig 1.3:** Left ventricular view of the aortic and mitral valve which are opened up to show the aortic mitral curtain (Du Plessis and Marchand 1964, Carpentier et al 2010). The aortic mitral curtain stretches from the base of the left coronary aortic cusp (LCC) and non-coronary aortic cusps (NCC) to the anterior mitral annulus.



The anterior mitral leaflet forms a divide between the left ventricular inflow and outflow streams. The angle between the aortic and mitral valve, also called the aortic-mitral angle is about 120 degrees in diastole and 110 degrees during systole (Fig 1.4) (Komoda et al. 1997).

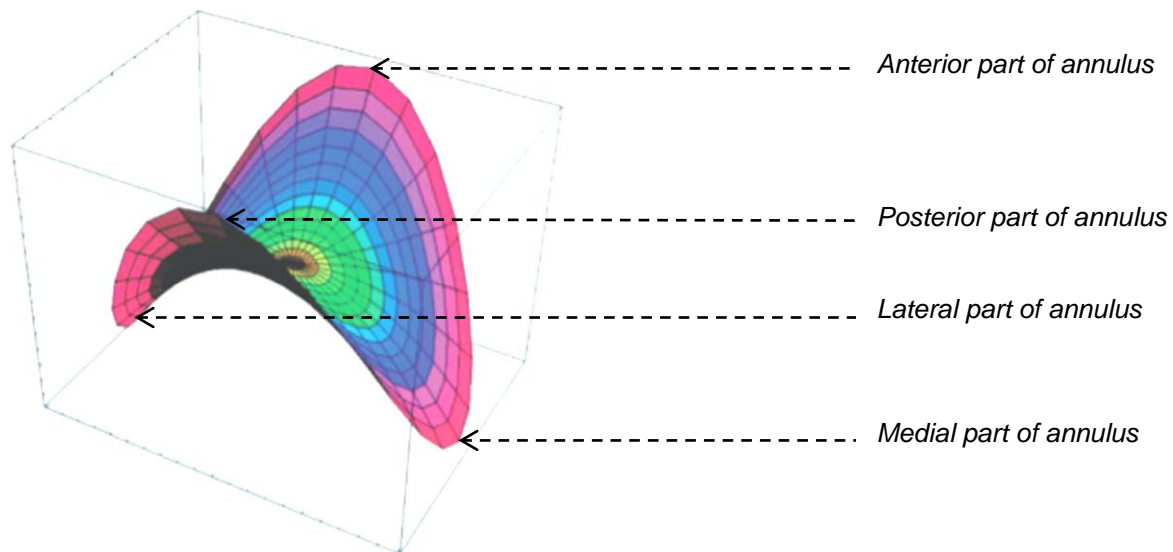
**Fig 1.4:** Left ventricular inflow and outflow with aortic-mitral angle (Komoda et al 1997).



### 1.1.2 The mitral annulus

The mitral annulus forms the hinge point from where the valve leaflets arise. It is at the annulus where the valve leaflets are anchored to the myocardium by the elastic and collagenous fibres that radiate into the myocardium (Misfeld and Sievers 2007). The shape of the mitral annulus resembles a hyperbolic paraboloid, a geometric shape which looks like a riding saddle, with its peaks located anteriorly and posteriorly and its valleys located medially and laterally at the commissures (Silbiger and Bazaz 2009). This three-dimensional shape of the annulus reduces the mechanical stress on the valve leaflets (Fig 1.5) (Salgo et al. 2002; Jimenez et al. 2007).

**Fig 1.5:** Saddle shape of the mitral annulus (Salgo et al. 2002).



The mitral annulus can be divided into an anterior third to which the base of the anterior leaflet is attached and the posterior two thirds from where the posterior leaflet arises. The anterior annulus is connected to the aorta by the intervalvular fibrosa which is bordered on the left and right side by the left and right fibrous trigones (Fig 1.1 and Fig 1.2). The right fibrous trigone is continuous with the membranous part of the interventricular septum and these two components together form the central fibrous body which is the strongest part of the fibrous skeleton of the heart (Fig 1.2) (Wilcox et al. 2005). The atrioventricular conduction bundle passes through the right fibrous trigone. The posterior two thirds of the annulus is a fibrous thickening at the base of the left ventricle extending from the left to the right fibrous trigone, but this part of the fibrous annulus is often incomplete where the leaflets are attached directly to the endocardium of the left ventricle (Angelini et al 1988).

The annulus is not a rigid structure but changes shape during the cardiac cycle. The posterior mitral annulus contracts during atrial and ventricular systole with maximal shortening at the midportion of the posterior annulus (Glasson et al. 1996). The anterior annulus lengthens slightly during systole, with movement of the anterior annulus towards the posterior annulus and towards the left atrium. This movement happens because the anterior part of the annulus is closely connected to the aorta and it stretches passively with systole and gets pushed towards the posterior annulus (Fig 1.6) (Lansac et al. 2001; Timek et al. 2003). The total effect is an increase in aortic diameter with reduction of the mitral annular circumference and the

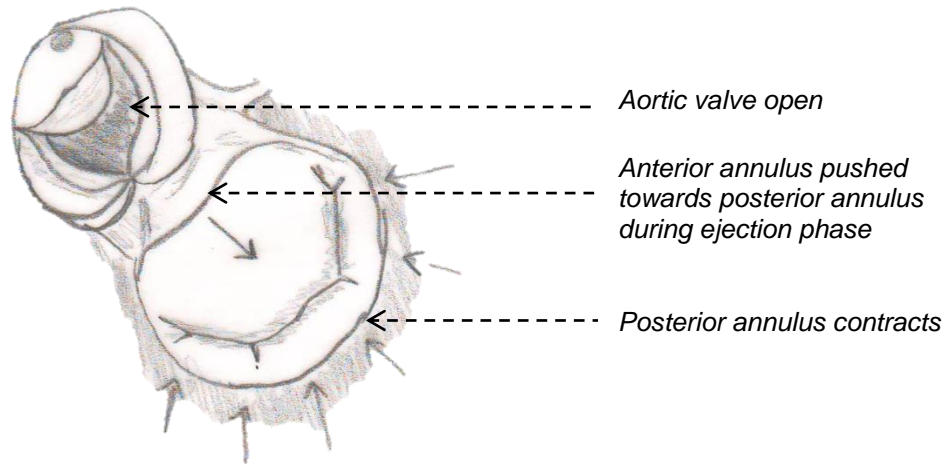


mitral orifice area during systole (Fig 1.6). This results in a larger aortic diameter which facilitates ventricular ejection and a smaller mitral orifice area which gives better mitral leaflet coaptation during systole.

During early diastole the posterior mitral annulus dilates as the ventricle relaxes and the anterior annulus shifts towards the aorta and left ventricle (Fig 1.6) (Lansac et al. 2001; Timek et al. 2003). This causes a larger mitral annular area during diastole to allow for more efficient filling of the left ventricle. The normal mitral annular area index changes from 2.8 cm<sup>2</sup>/ m<sup>2</sup> in systole to 3.85 cm<sup>2</sup>/ m<sup>2</sup> in diastole, an increase of about 25% (Fig 1.7) (Orniston et al 1981). Prosthetic devices and rigid mitral rings fixate the mitral annulus and do not allow for systolic and diastolic changes in the mitral annular diameter (Timek and Miller 2001).

**Fig 1.6:** The mitral annulus changes shape during the cardiac cycle so that the mitral orifice area is smaller in systole than diastole (Lansac et al. 2001; Timek et al. 2003).

a) Systole:



b) Diastole:

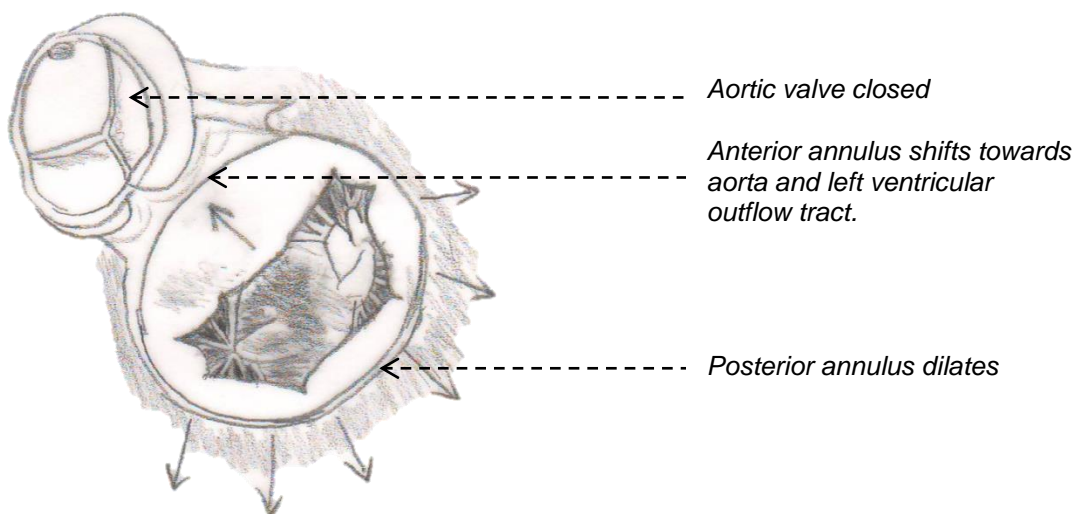
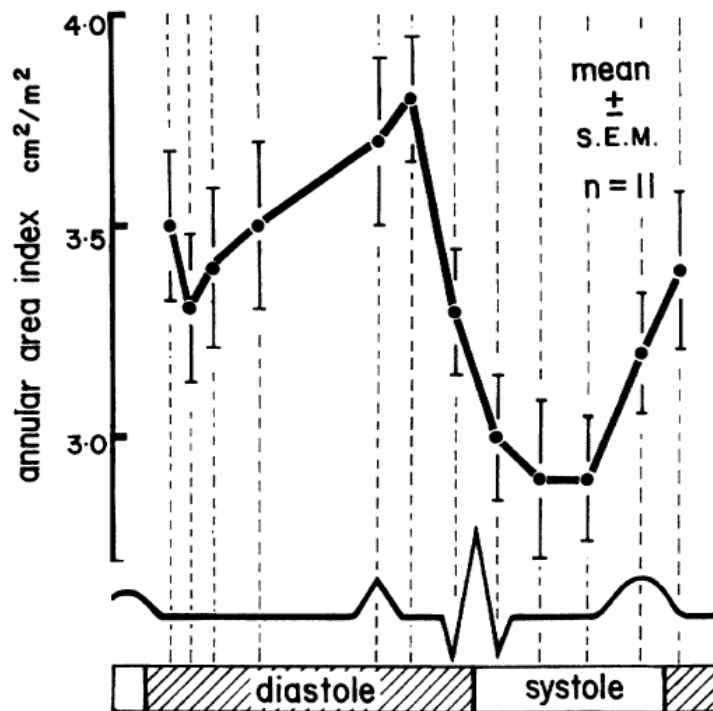


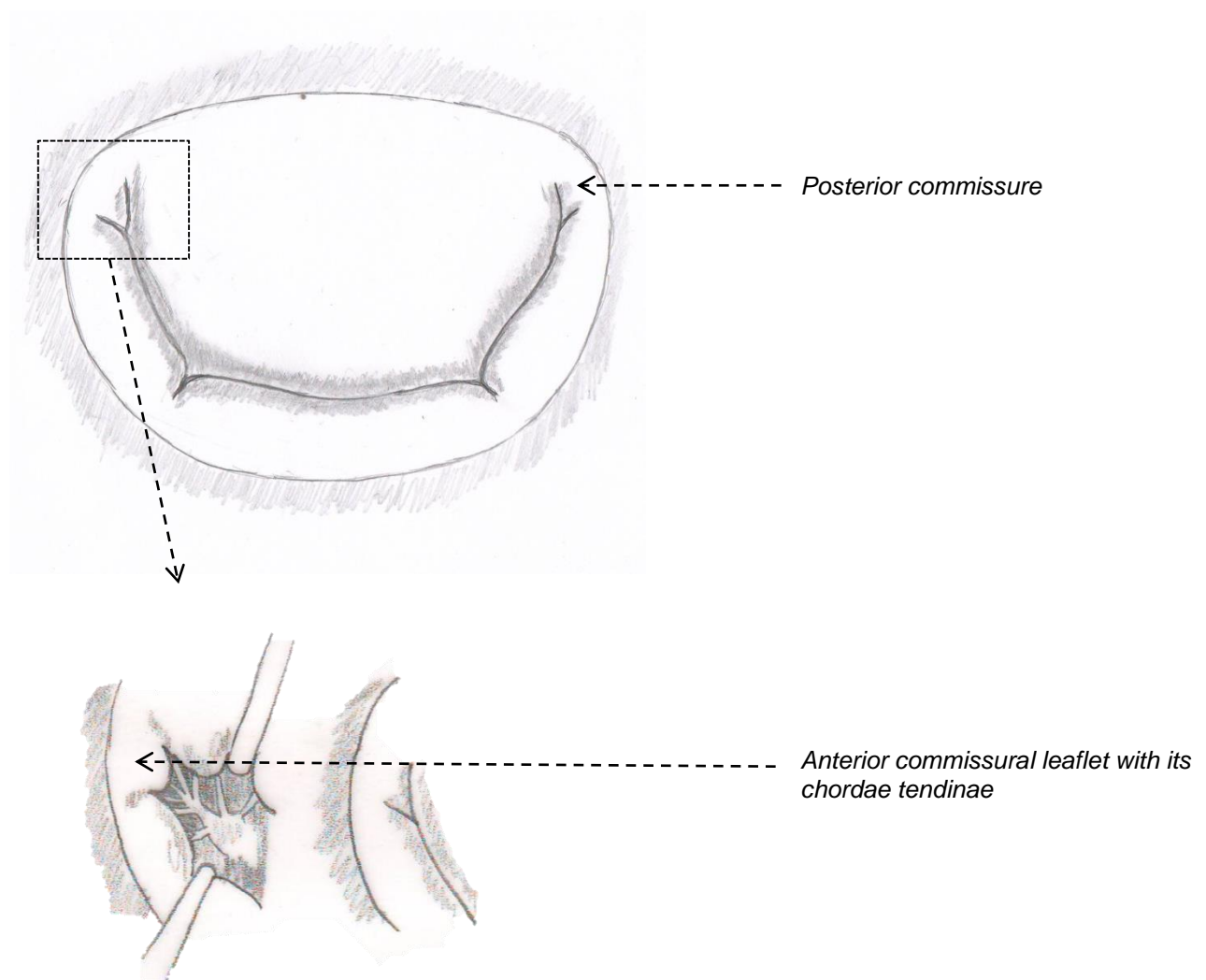
**Fig 1.7:** Changes in mitral annular area index during the cardiac cycle in 11 normal subjects (Ormiston et al 1981).



### 1.1.3 The mitral leaflets:

The mitral valve has 2 leaflets, an anterior leaflet which arises from the anterior third of the mitral annulus and a posterior leaflet which arises from the posterior two thirds of the annulus. The 2 leaflets are actually a single continuous structure which hangs into the left ventricle like a veil with indentations at the commissures. These indentations are partial and do not extend all the way to the annulus, which leaves bridging commissural tissue between the anterior and posterior leaflets (Fig 1.8) (Silverman and Hurst 1968; Silbiger and Bazaz 2009).

**Fig 1.8:** Anatomy of the mitral commissures. The commissural leaflet has its own chordae (Carpentier et al 2011).



The anterior leaflet is roughly triangular in shape with a rounded free edge and the leaflet depth is about twice as long as the posterior leaflet. This gives the anterior and posterior leaflet about the same surface area, because the posterior leaflet is attached to two thirds of the annular circumference (Fig 1.9 and Fig 1.10).

The posterior valve leaflet can be divided into 3 parts namely, P1, P2 and P3 (Carpentier et al 2010). There are indentations between P1, P2 and P3 and these indentations are important for the valve to open properly during diastole (Fig 1.6). The anterior leaflet is also divided into 3 parts A1, A2 and A3 which corresponds to the area which coapts with the posterior leaflet (Fig 1.9). This is very useful when describing valve pathology for example a valve may be leaking at the level of P2 and A2 with prolapse of P2. The atrial surface of both leaflets has a smooth zone and a rough zone. The rough zone is the area where both leaflets coapt (Fig 1.10).

**Fig 1.9:** Different parts of the anterior and posterior leaflets (Carpentier et al 2010).

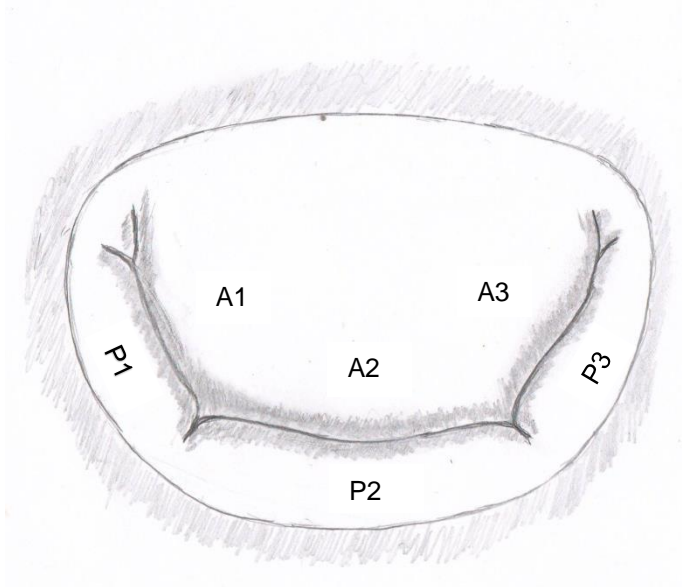
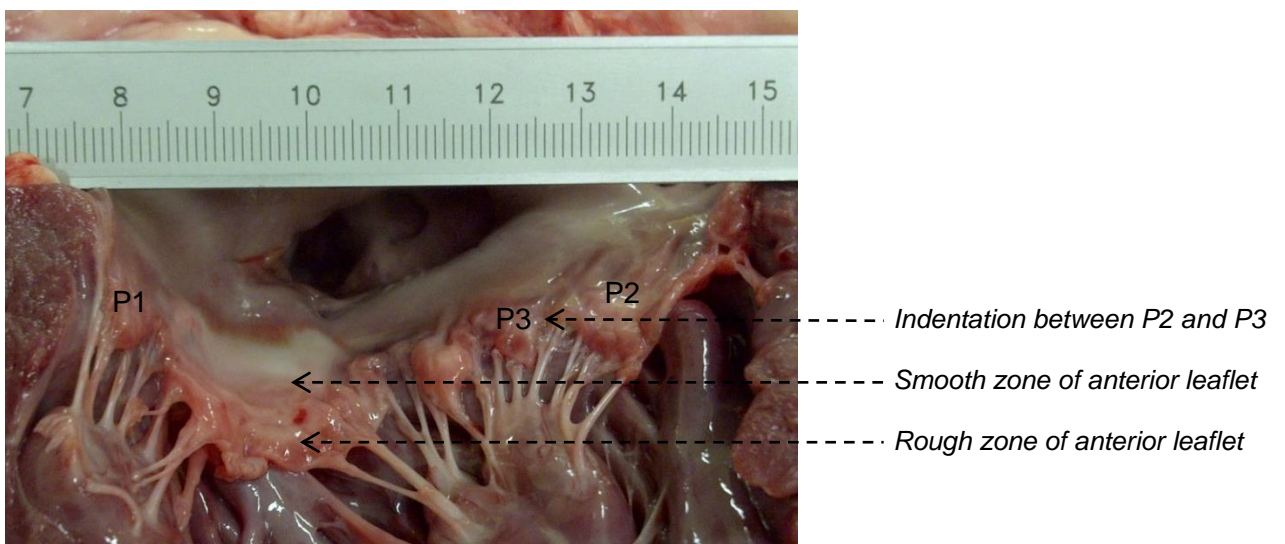


**Fig 1.10:** Mitral annulus opened between P1 and P2 showing the smooth zone and the rough zone where the leaflets coapt. Also note the indentations between P1, P2, and P3:



Ultrastructurally the mitral valve leaflets are metabolically active and consist of an extracellular fibro-elastic matrix filled with valvular interstitial cells which is covered with a continuous monolayer of valvular endocardial cells (Fig 1.11) (Fenoglio et al 1972). These cells also cover the chordae tendinae (Fig 1.12). The proximal third of the valve leaflets also have smooth muscle, cardiac muscle and nerve cells present (Filip et al. 1986). Capillaries may be present at the bases of the leaflets but the body of the leaflets do not have any capillaries which means the valvular interstitial cells receive their gas exchange and nutrition directly from the intracardiac blood that bathes the leaflets (Gross and Kugel, 1931).

**Fig 1.11:** Electron micrograph of a mitral valve leaflet. Note the endocardial cells on the atrial side (AE) and the ventricular side (VE). The valvular interstitial cells are also seen in the extracellular matrix which contains collagen, elastin, proteoglycans and glycoproteins (Fenoffio et al 1972).

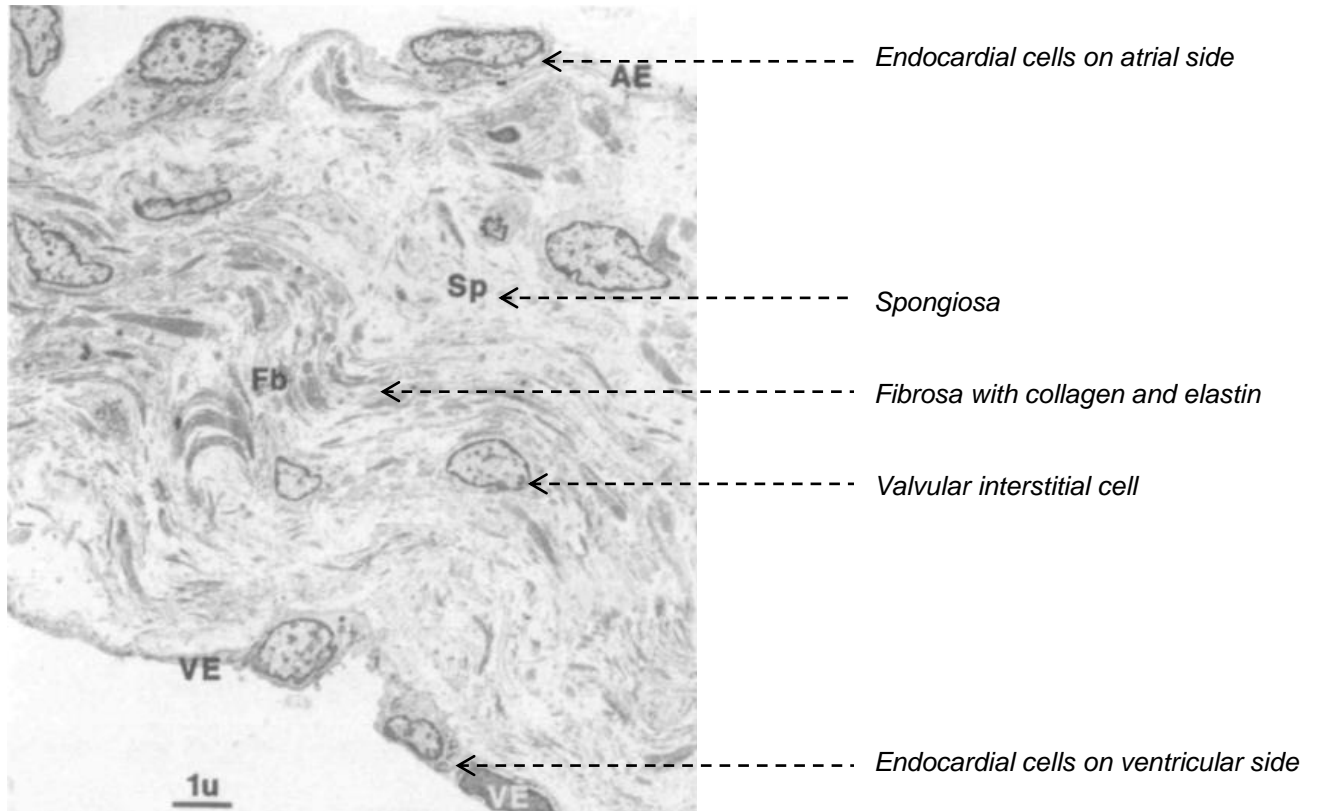
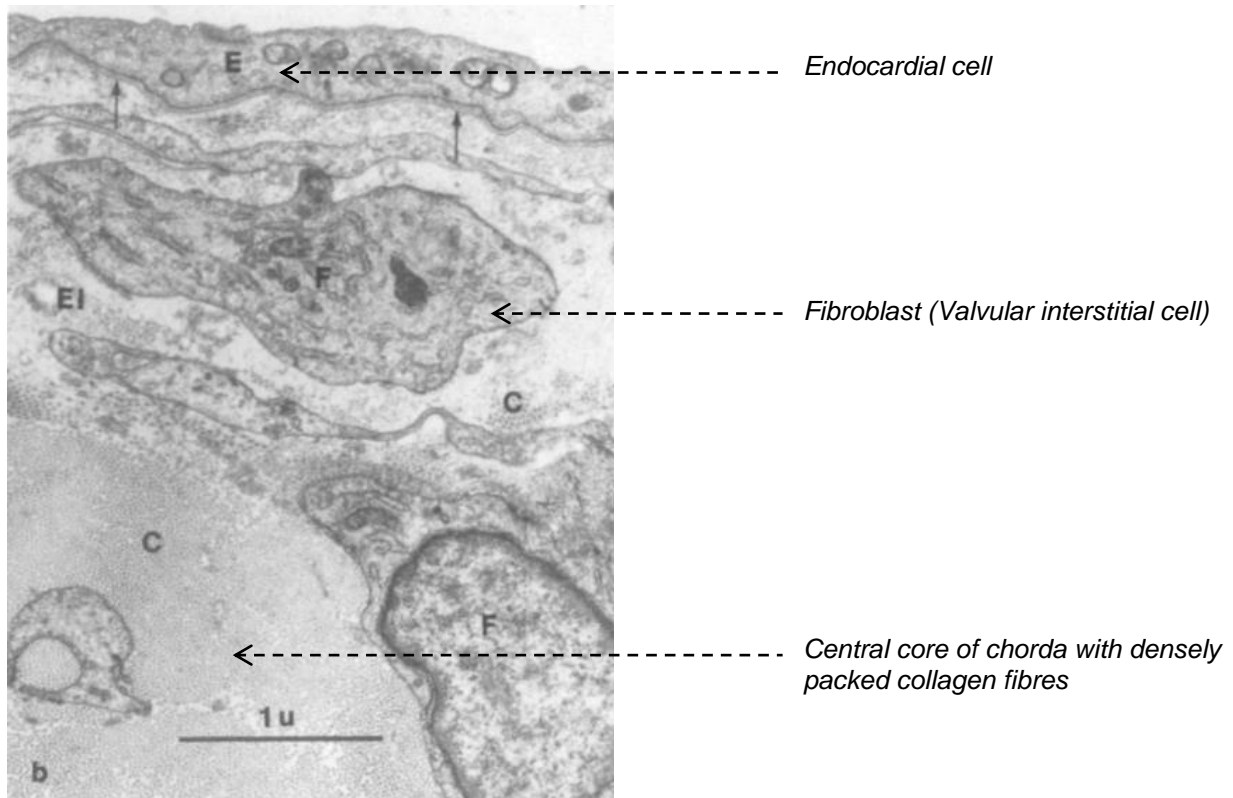




**Fig 1.12:** Electron micrograph cross section of a chorda tendinae. Note the endocardial cell lining (E) with a distinct basal lamina (arrows). The spongiosa contains scattered collagen fibres (C) and elastic fibres (EI). The central core of the chorda consists of densely packed parallel collagen fibres and fibroblasts (Fenoglio et al 1972).



The extracellular matrix consists of the fibrous macromolecules collagen and elastin, proteoglycans and glycoproteins. The collagen provides most of the mechanical strength of the valve and is mostly type I and III collagen. The collagen fibres are surrounded by an elastin matrix which provides interconnections with collagen fibres (Fig 1.11) (Flanagan and Pandit 2003).

Valvular interstitial cells (fibroblasts, myofibroblasts, and undifferentiated mesenchymal cells) are numerous elongated cells with many long, slender processes. They connect to each other to form a three dimensional network throughout the entire valve matrix. They have the following characteristics:

- Are coupled by communicating junctions which connect them functionally,
- Are innervated and closely related to motor nerve terminals (Marron et al. 1996)
- Show secretory properties, forming collagen, elastin, laminin, fibronectin, chondroitin sulphate to help with extracellular matrix formation (Flanagan & Pandit, 2003)
- Show mitogenic activity to platelet derived growth factor (PDGF) (Johnson et al. 1987)
- Possess characteristics similar to smooth muscle cells in the media of arteries and veins cells, namely, abundance of actomyosin filaments, cGMP dependent proteinkinase and contractile response to epinephrine and angiotensin II. (Filip et al. 1986, Della Rocca et al 2000).

The valvular interstitial cells are believed to be responsible for the maintenance and repair of valvular structure. The constant motion of the valve leaflets during the cardiac cycle produces deformation and damage in the cell matrix. The interstitial cells respond to these changes and maintain valvular integrity. They are connected to each other and with the extracellular matrix through focal adhesion molecules and these cell-matrix attachment sites link the cytoskeleton to matrix proteins via integrins. This also acts as signal transduction sites which transmit mechanical information from the extracellular matrix to the valvular interstitial cells. This information then elicits a response such as matrix secretion, migration, cell adhesion, growth and differentiation. The latter being very important for valvular integrity, valve repair and regeneration (Flanagan and Pandit 2003). A major drawback of current bioprosthetic valves is that the valve leaflets are not living tissue and do not possess the regenerative potential of a living native valve (Hopkins 2007).

The cell biology of valvular interstitial cells is not fully understood, but it is key to understand how these cells interact with each other and their environment. Knowledge of this cellular biology is especially important for tissue engineering of heart valves (Hopkins 2007). The precise balance between stiffness and flexibility of the leaflets depends heavily on the correct distribution of the extracellular matrix components (collagen, elastin, glycoproteins and proteoglycans) and this is regulated by the valvular interstitial cells. This is critical for proper valve function and there is growing evidence that valvular heart disease is the consequence of abnormal remodelling and regeneration of heart valve extracellular matrix (Hinton and Yutsi

2011). Biochemical studies of normal and diseased valves showed that collagen content is increased in rheumatic mitral valves and myxomatous valves (Lis et al. 1987). The abnormalities in myxomatous valves include disorganization of the bundles of collagen fibrils, alterations in the aggregation and organization of the amorphous components and microfibrils of the elastic fibers and accumulation of proteoglycans (Tamura et al. 1995). These changes are seen in the leaflets and the chordae tendinae.

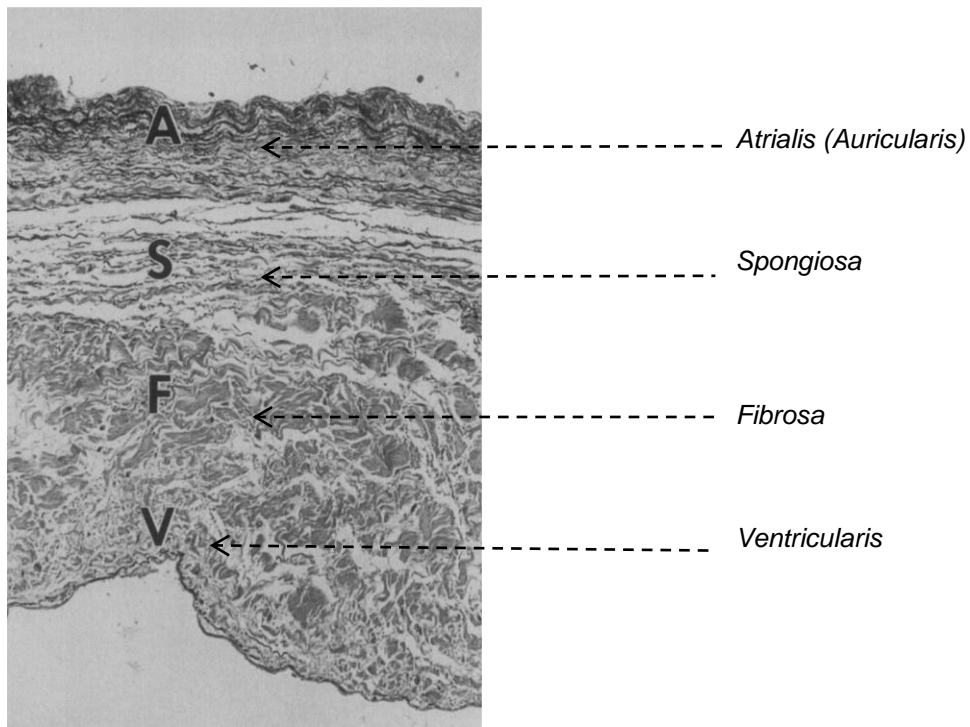
The valvular endocardial cells form a functional envelope around the mitral leaflets. These cells function to maintain a non-thrombogenic valve surface, similar to vascular endothelium (Frater et al. 1992). They are linked together by tight junctions and gap junctions and have overlapping marginal edges (Flanagan and Pandit 2003). The cells secrete nitric oxide (NO), endothelium-derived relaxing factor (EDRF) and vasodilatory prostanoids. NO and EDRF have both been shown to be potent inhibitors of platelet aggregation (Furlong et al. 1987), (Radomski et al. 1987). The valvular endocardial cells also regulate the underlying interstitial cells by secreting soluble factors. This is similar to vascular endothelium regulating the underlying smooth muscle (Mullholland and Gotlieb 1997). They may also play a sensory role as they present a large surface area which is exposed to metabolites in the circulating blood (Flanagan and Pandit 2003).

The metabolically active valve leaflets are in stark contrast to current biological prostheses which is either a glutaraldehyde treated xenograft or cryopreserved homograft. These treatments remove cells and debris from the graft to lower the immune response between the host and the graft. The graft then gets colonized with a neointima and pseudo intima of fibroblasts and smooth muscle cells from the host. This acellular graft is not capable of regeneration and repair and degenerates with time with fibrosis and calcification (Hopkins 2007)

Histologically, the mitral valve leaflets can be divided into 4 layers (Fig 1.13) (Gross and Kugel 1931):

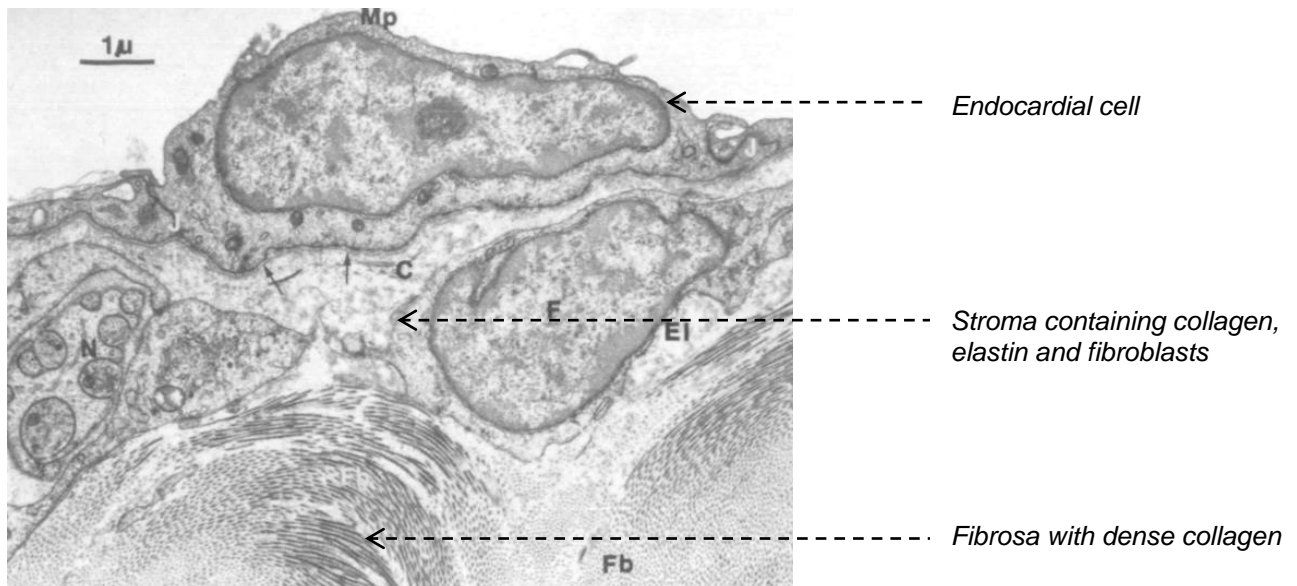
1. Auricularis or atrialis
2. Spongiosa
3. Fibrosa
4. Ventricularis

**Fig 1.13:** Histological section of a normal mitral valve (Tamura et al 1995)



The fibrosa forms the structural core of the mitral valve leaflets and is covered by the spongiosa and atrialis on the atrial side and the ventricularis on the ventricular side. The fibrosa consists of dense collagen fibres which are arranged in an orderly and parallel pattern. These collagen fibres are continuous with the annulus and fibrous skeleton of the heart and also continuous with the core of the chordae tendinae which connect the leaflet to the papillary muscles (Fig 1.14). Small numbers of elastic fibres are found in the fibrosa between the dense collagen fibres. (Tamura et al. 1995)

**Fig 1.14:** Electron micrograph of the ventricular surface of the mitral leaflet near the insertion of a chorda tendinae. Note the endocardial cell and the underlying stroma with collagen (C), elastic fibres (E) and fibroblasts (F). The fibrosa contains a band of dense, wavy collagen which is an extension of the core of the chorda tendinae (Fenoglio et al 1972).



The atrialis layer consists of an endothelial layer of valvular endocardial cells. Between the endothelial layer and the most superficial elastic fibres lies a layer of extracellular matrix with very few collagenous fibres and a gelatinous consistency. (Gross and Kugel, 1931). This layer is more prominent at the leaflet tips or coaptation zone and facilitates a good seal during valve closure. The elastic fibres in the atrialis run in a radial direction between the valve ring and free edge of the leaflet. The atrialis also contains some smooth muscle cells. (Tamura et al. 1995)

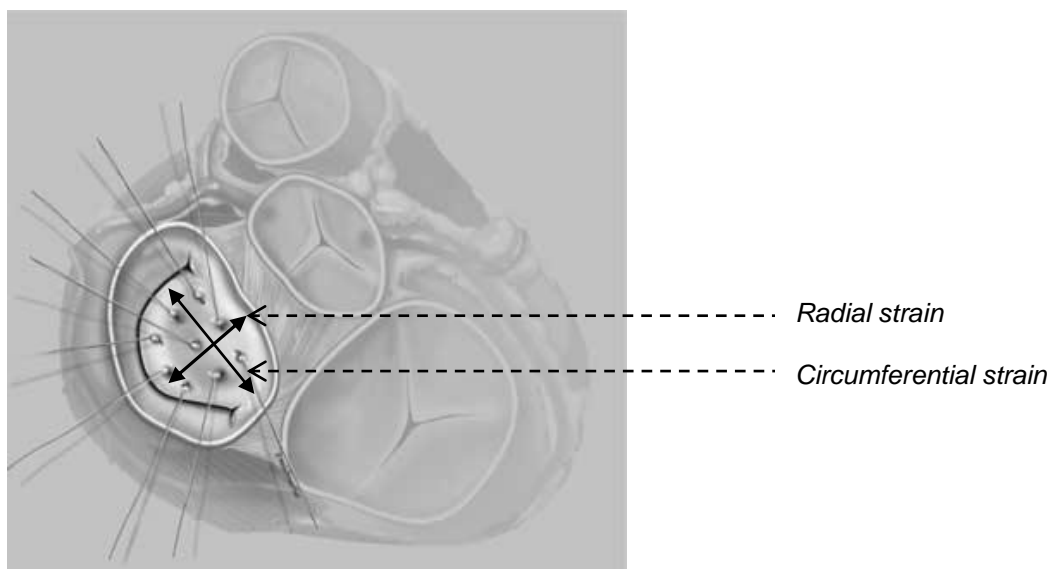
The valvular interstitial cells are mainly found in the spongiosa. The spongiosa is also rich in proteoglycan and contains small amounts of elastic fibres and collagen. Near the valvular annulus the spongiosa contains some cardiac muscle cells which are a continuation of the left atrial myocardium (Tamura et al. 1995).

The ventricularis layer is covered with endocardium on the ventricular side and contains a thin layer of linearly arranged elastic fibres. This layer is continuous with the elastic layer of the chordae tendinae (Tamura et al. 1995).

The interconnected sheets of collagen and layers and tubes of elastin give the valve tissue viscoelasticity, anisotropy and highly non-linear mechanics (Sacks and Yoganathan 2007). The valve leaflets stretch during closure and once the valve is closed, further leaflet deformation ceases. The closing deformation reverses again during valve opening.

Anisotropy is a term used to describe the direction-dependent properties of materials and valve tissue show larger strain in the radial direction than in the circumferential direction (Fig 1.15). The maximum anterior mitral valve leaflet extension ratio is 1.18 in the circumferential direction and 1.34 in the radial direction (May-Newman and Yin 1995). In vivo studies on sheep have been done to measure the strain of the anterior mitral valve leaflet (Sacks et al 2006). Nine 1mm hemispherical piezo-electric transducers were implanted on the anterior mitral valve leaflet in a 15 mm square array (Fig 1.15). Three-dimensional crystal spatial positions were recorded at 250 Hz over several cardiac cycles. Mean peak strain rates were approximately 300–400% per second in the radial direction and 100–130% per second in the circumferential direction.

**Fig 1.15:** Mitral valve strain measured with piezo-electric transducers on the anterior mitral valve leaflet during the cardiac cycle. Peak radial strain is 16-22% and peak circumferential strain is 2.5-3.3% (Sacks et al 2006).



#### 1.1.4 The subvalvular apparatus:

Both leaflets are attached to the ventricular cavity by the subvalvular apparatus which consist of chordae tendinae and the papillary muscles. The papillary muscles provide a contractile element and the chordae tendinae have elastic properties.

Chordae tendinae attach to the free edge and ventricular surface of the leaflets and then insert into 2 well defined anterior and posterior papillary muscles which form part of the left ventricular myocardium. Functionally the anterior and posterior mitral valve leaflets can be divided into lateral and medial halves by an imaginary mid-mitral line. The lateral halves are anchored by chordae from the anterior papillary muscle and the medial halves are anchored by chordae from the posterior papillary muscle (Kumar et al 1995).

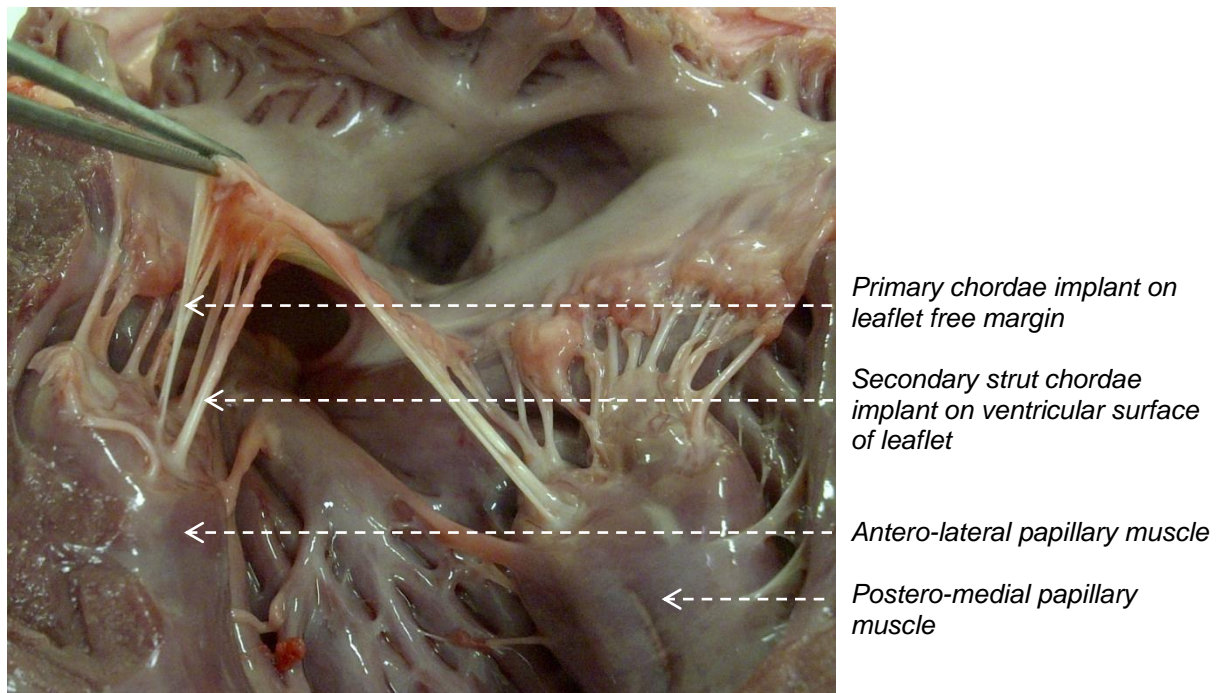
The chordae tendinae are composed of collagenous and elastic fibres and are covered with a smooth layer of endothelial cells (Fig 1.12, Fig 1.14). They support the free edge of the mitral valve during closure and also help to maintain left ventricular geometry during systole. The chordae branch out in a fan like configuration from the papillary muscles and form a sophisticated network which transmits the contractions of the papillary muscles to the valve leaflets (Fig 1.16) (Misfeld and Sievers, 2007).

Three types of chords have been described: primary, secondary and tertiary (Lam et al 1970). Primary chordae attach to the free margin of the leaflet and secondary chordae to the ventricular surface of the mitral leaflet. Tertiary chords arise directly from the left ventricular wall and insert only to the posterior mitral leaflet. Primary and secondary chordae have very distinct functions. The thinner primary chordae maintain leaflet apposition and facilitate valve closure. When primary chords are sectioned or rupture, it results in acute mitral regurgitation. Sectioning of secondary chordae does not produce mitral regurgitation, but they do serve an important function in maintaining left ventricular size, geometry and function (Silbiger and Bazaz 2009). The anterior leaflet has some thick secondary chordae, also called strut chordae which insert into the 4 o'clock and 8 o'clock positions on the under surface of the leaflet to the dense collagen network that ultimately terminates at the fibrous trigones (Fig 1.16). No strut chordae attach to the posterior mitral leaflet. The strut chordae connect the musculature of the left ventricle (at the papillary muscles) to the mitral annulus (at the fibrous trigones) and maintains papillary-annular continuity (David 1994). The strut chords are under continuous

tension, like a stretched rubber band, and this tension is transmitted to the papillary muscles and the fibrous trigones (Nielsen et al 2003). When these strut chordae are severed it results in papillary muscle retraction and change in left ventricular geometry with decreased systolic function.



**Fig 1.16:** Photo of a porcine mitral valve to show the anterior mitral leaflet with its primary and secondary chordae

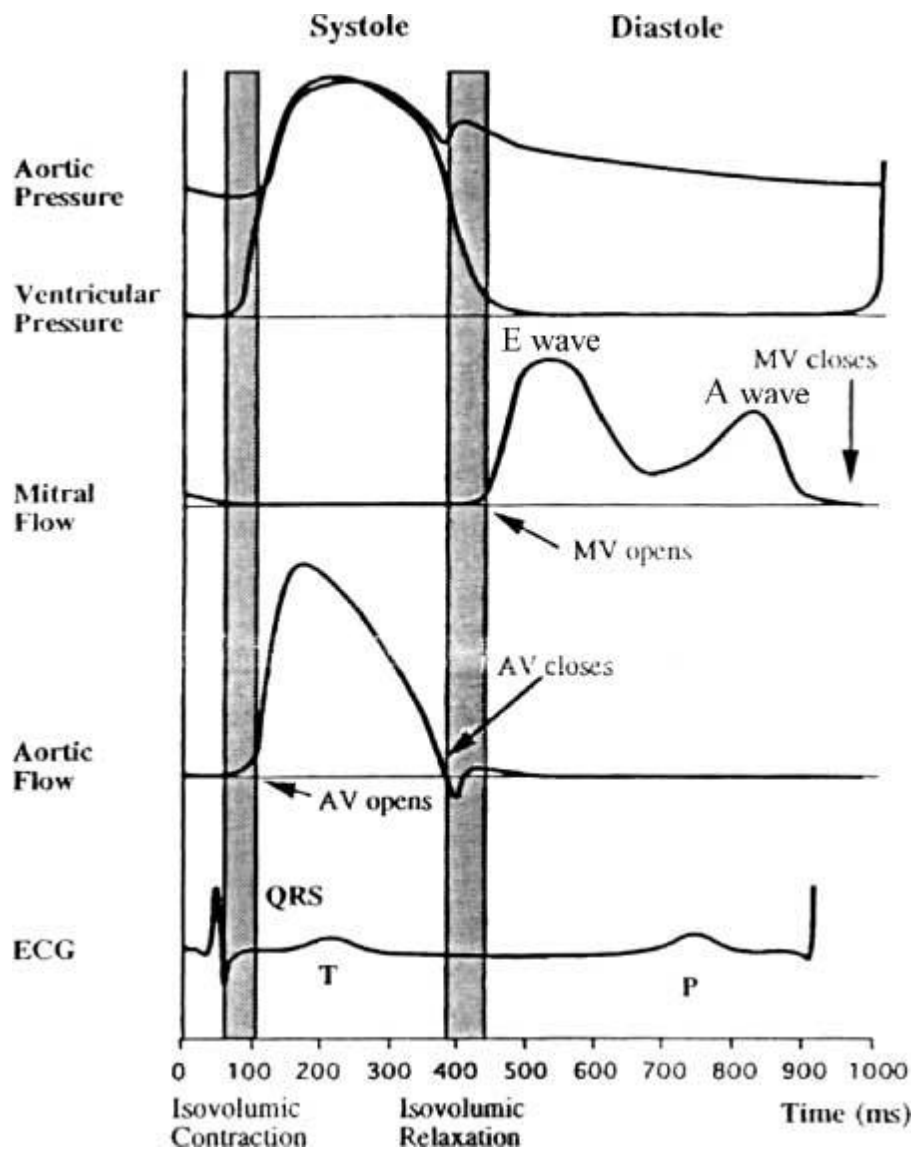


## 1.2 Blood flow through the normal mitral valve:

The left atrium, left ventricle, mitral valve leaflets, chordae tendinae and papillary muscles all play an important role to ensure normal functioning of the mitral valve. Blood flow through the mitral valve is biphasic during diastole. The first peak, called the E-wave (early ventricular filling), is due to ventricular relaxation. The second peak, the A-wave (atrial contraction) is caused by contraction of the left atrium (Fig 1.17) (Yoganathan et al. 2004). During isovolumic relaxation the pressure in the left ventricle drops to below that of the left atrium which causes the mitral valve leaflets to open. The initial filling is enhanced by the active relaxation of the ventricle and results in the E-wave of the mitral flow curve. The peak velocity in the normal E-wave range from 0.5-0.8 m/s (Oh et al. 1997). After active ventricular relaxation, the fluid begins to decelerate and the mitral valve closes partially. The atrium then contracts and blood flow through the mitral valve increases and gives rise to the A-wave in the mitral flow curve. This increased flow opens the mitral valve again. The peak velocity in the normal A-wave is typically lower than the E-wave.

Magnetic resonance phase-velocity mapping of normal human hearts has expanded our knowledge of blood flow through the heart (Kilner et al 2000, Markl 2011). The left atrium functions as a conduit during ventricular diastole and a reservoir during ventricular systole. Flow patterns of left atrial filling revealed vortical flow during systole and diastole. The principal vortex originated mainly from the left pulmonary veins and inflow from the right pulmonary veins joined the vortex periphery between the vortex and the atrial wall. These consistent patterns and their progression through the cardiac cycle may help to minimize stasis and energy dissipation and allows the momentum of the inflowing streams to be redirected towards the mitral valve (Kilner et al 2000, Markl et al 2011).

**Fig 1.17:** Pressure flow curves of the aortic and mitral valve (Yoganathan et al 2004).



The mitral valve starts closing at the end of atrial contraction because of the changing pressure gradient from the left ventricle to left atrium as the left ventricular pressure increases (Reul et al 1981). With ventricular contraction, the mitral annulus diameter decreases, mainly the posterior annulus and this helps to give better leaflet coaptation (Glasson et al. 1996). The anterior part of the annulus is closely connected to the aorta and it stretches passively with systole and gets pushed towards the posterior annulus as discussed before (Fig 1.6).

The anterior and posterior leaflets coapt and the chordae tendinae and papillary muscles prevent the leaflets from prolapsing into the atrium. The papillary muscles shorten during systole and this maintains a constant distance between the papillary muscle tips and the mitral annulus as the ventricle contracts. The papillary muscles can be seen as the shock absorber of the mitral valve complex, keeping the chordae tendinae tension constant. (Joudinaud et al 2007). In patients with mitral valve prolapse the papillary muscles do not shorten as efficiently and this shortens the distance between the papillary muscle tips and the mitral annulus, causing leaflet prolapse and eventually regurgitation (Sanfilippo et al 1992).

The mitral valve is exposed to high ventricular pressures during systole which can be as high as 150 mm Hg in normal individuals. Three basic loading states affect the valve tissue during the cardiac cycle: flexure, shear and tension (Hinton and Yutsey 2011). Flexure occurs when the valve leaflets are opening or closing, shear occurs when blood flows through the open valve and tension occurs when the valve is closed and exposed to ventricular pressure. Mitral valve tissue has exceptionally high strain because the tissue cycles from a completely unloaded state in diastole to the high tension during left ventricular systole (Sacks and Yoganathan 2007).

### **1.3 The burden of mitral valve disease:**

Mitral valve disease may manifest as stenosis or obstruction of outflow, or as regurgitation from defective closure. Since 1950, the predominance of mitral valvular disease in industrialised countries has shifted from a rheumatic origin to a degenerative etiology (Lung and Vahanian 2011). The incidence of rheumatic heart disease in industrialised countries declined since the widespread use of penicillin and the incidence of degenerative mitral valve disease became better known with the introduction of cardiac imaging such as echocardiography. In developing countries valvular disease is still mainly caused by rheumatic heart disease (Soler-Soler and Galve 2000, Lung and Vahanian 2011).

Mitral stenosis occurs mainly as a result of rheumatic heart disease and is the least common valvular disease in industrialised countries. It is, however, the most common form of valvular disease in developing countries. Degenerative calcification of the mitral annulus can cause mitral stenosis in older patients, but seldom causes clinically important mitral stenosis.

Mitral regurgitation can be caused by primary abnormalities of the valvular apparatus (organic mitral regurgitation) or by left ventricular remodelling, which causes incomplete valvular coaptation (functional mitral regurgitation). Functional mitral regurgitation is caused by the incomplete closure of a structurally normal valve because of valve tethering by the subvalvular apparatus due to left ventricular remodelling or dysfunction (Lung and Vahanian 2011). Functional mitral regurgitation is a good example of how the whole mitral valve complex needs to work together to create a competent mitral valve. Even with normal leaflets, a valve can still leak if the subvalvular apparatus or left ventricle is tethering the valve. Techniques to repair functional mitral regurgitation have all been suboptimal, because none can address the primary problem which is left ventricular dysfunction, remodelling or dilatation. Instead, repair techniques have focused on decreasing the septolateral distance of the mitral annulus or resuspending the papillary muscles to create better leaflet coaptation (Langer et al. 2009).

Carpentier's classification for mitral regurgitation is useful for understanding the different causes of mitral regurgitation (Table 1.1). It is very important to understand the mechanism of regurgitation and have a systematic approach when repairing a valve (Carpentier 1983).

**Table 1.1** Carpentier's classification of mitral regurgitation (Carpentier 1983).

Functional type	Pathology	Leaflet motion	Regurgitation jet
I	Annular dilatation	Normal	Central
	Leaflet perforation		
	Dilated left ventricle		
II	Chordal rupture/elongation	Excessive (anterior, posterior or bileaflet leaflet prolapse)	Eccentric
	Papillary muscle rupture		
IIIa	Commissural fusion, Leaflet thickening	Restricted leaflet motion in systole and diastole (Rheumatic heart disease)	Eccentric
IIIb	Papillary muscle displacement	Restricted leaflet motion in systole (Ischaemic mitral regurgitation)	Eccentric

The main etiology for organic mitral regurgitation in industrialised countries is mitral valve prolapse caused by myxomatous degeneration of the mitral valve (lung and Vahanian 2011). This is a degenerative disease of the mitral valve with leaflet billowing and shift of leaflet coaptation above the level of the annulus. The leaflet billowing and shortening of the coaptation distance between the leaflets places more stress on the chordae tendinae. This causes the chordae to elongate and rupture, leading to mitral regurgitation. The prevalence of myxomatous mitral valve disease was 2.4% in a USA population based study of 3491 people with only 3.5 % of these cases having severe mitral regurgitation (Freed et al. 1999). The

prevalence of degenerative mitral valve disease increases significantly with age, with a prevalence of over 6% above the age of 65 (Nkomo et al 2006).

The prognosis of myxomatous mitral valve disease depends on the severity of the mitral regurgitation and the left ventricular function. An ejection fraction less than 50% and severe mitral regurgitation is associated with a higher mortality and higher cardiovascular events such as heart failure, endocarditis, atrial fibrillation and mitral valve surgery (Avierinos et al. 2002). Asymptomatic patients with myxomatous mitral valve disease and severe mitral regurgitation at initial diagnosis (effective regurgitant orifice  $>0.4\text{cm}^2$ ) have a 80-100% chance of having a cardiovascular event over 10 years, that is a risk of 8-10% per year (Topilsky et al. 2010). Valve repair is possible in most patients with myxomatous mitral valve prolapse, with experienced centres achieving successful repair rates of 85-95% in patients referred for mitral valve surgery. The following repair techniques can be used during mitral valve repair (Carpentier 1983, Filsoufi & Carpentier 2007, Carpentier et al 2011):

1. Annuloplasty with a mitral valve ring. This reduces the mitral annulus and restores the normal antero-posterior dimension during systole. The mitral valve annuloplasty ring is very important to strengthen and stabilize any repair (Fig 1.18).
2. Quadrangular resection of the prolapsing segment of the posterior leaflet (Fig 1.18).
3. Quadrangular resection and sliding plasty for excision of a larger prolapsing segment of the posterior leaflet (Fig 1.19).
4. Chordal transfer from posterior leaflet to anterior leaflet (Fig 1.20) (Gillinov & Cosgrove 2004).
5. Chordal shortening was used in the past, but fell out of favour because of the risk of chordal rupture (Fig 1.21) (Smedira et al 1996).
6. Papillary muscle shortening or papillary muscle sliding plasty (Fig 1.22) (Dreyfus et al 2001).
7. Replacement of ruptured or elongated chordae with artificial PTFE (Gore-Tex) sutures (David 2004) (Fig 1.23).
8. A commissural leaflet prolapse can often be repaired with a commisuroplasty. This means suturing the anterior leaflet to the posterior leaflet at the commissure. For this technique to work, one of the leaflets must be normal without prolapse to support the prolapsing leaflet (Fig 1.24).

**Fig 1.18:** *Quadrangular resection of the posterior leaflet and annuloplasty with mitral ring (Carpentier and Filsoufi 2007).*

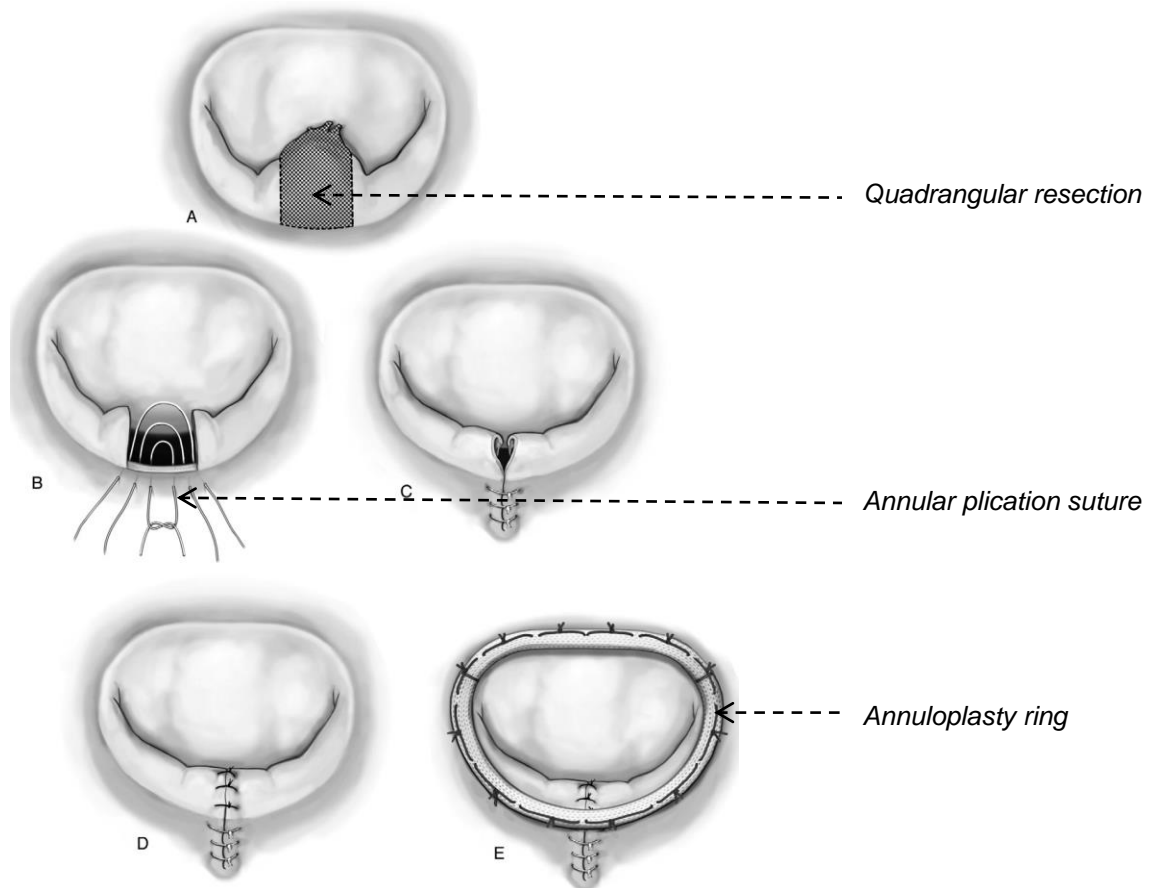


**Fig 1.19:** *Quadrangular resection and sliding plasty (Carpentier and Filsoufi 2007)*

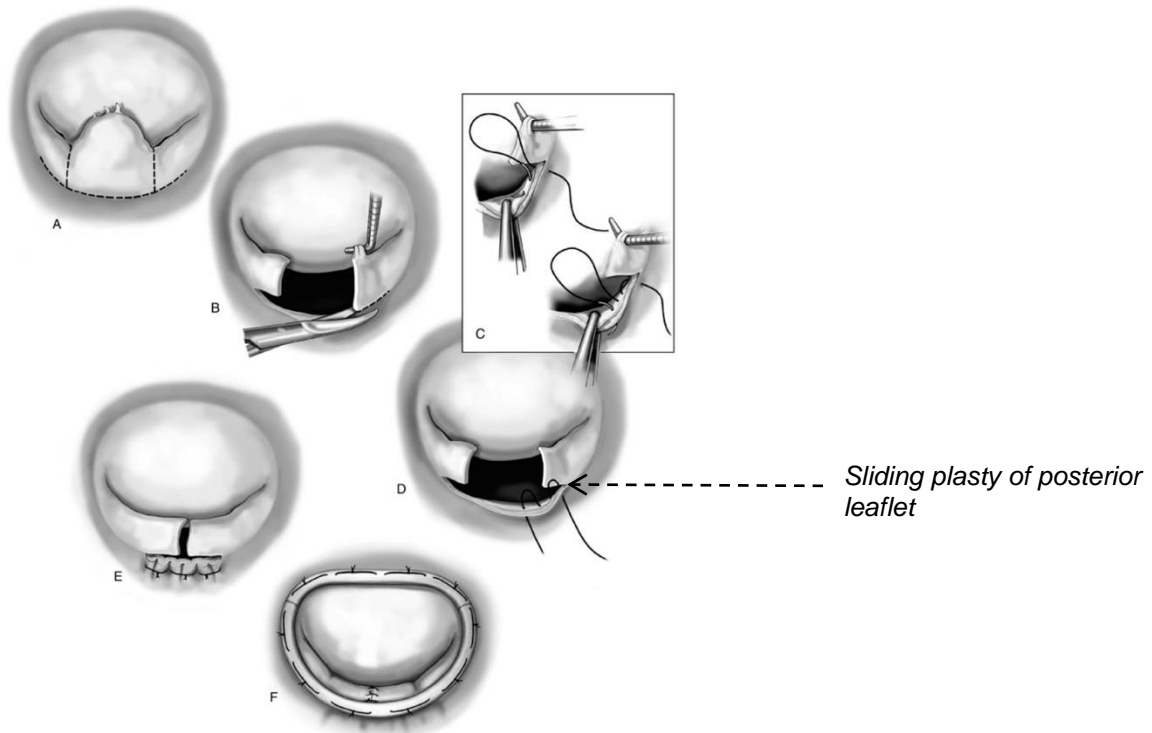


**Fig 1.20:** *Chordal transfer (Gillinov & Cosgrove 2004).*

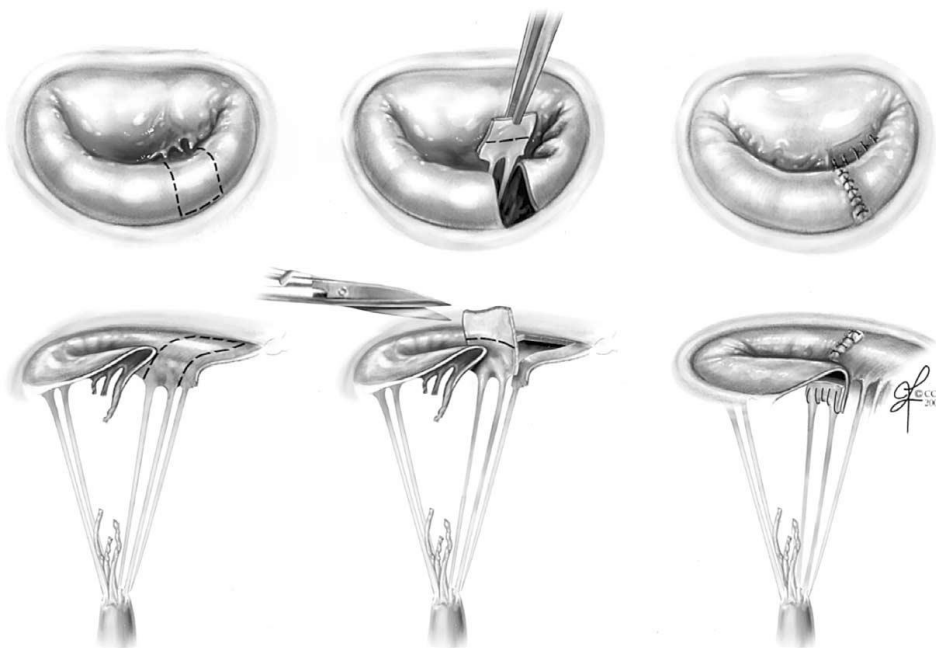




**Fig 1.21:** Chordal shortening (Smedira et al 1996).

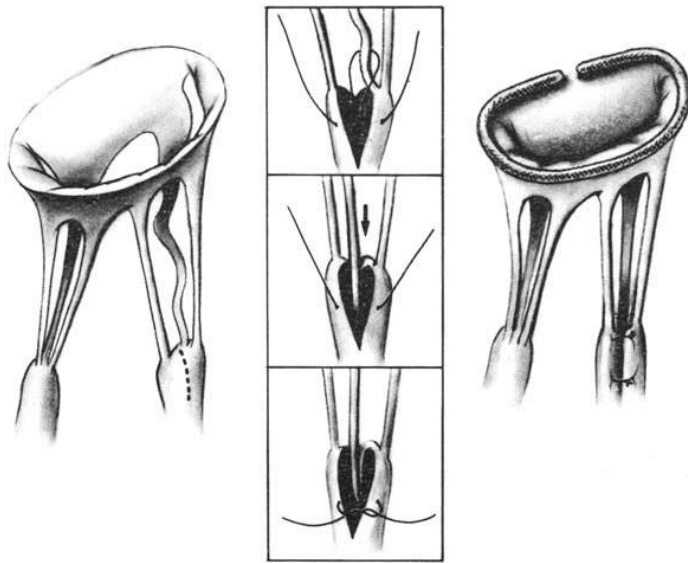


**Fig 1.22:** Papillary muscle shortening (Dreyfus et al 2001).

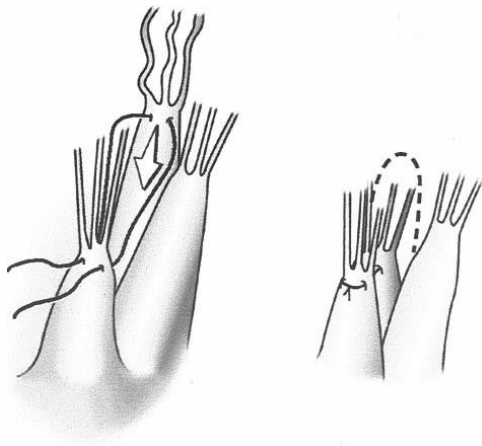


**Fig 1.23:** Artificial chordae with Gore-Tex sutures (David 2004).

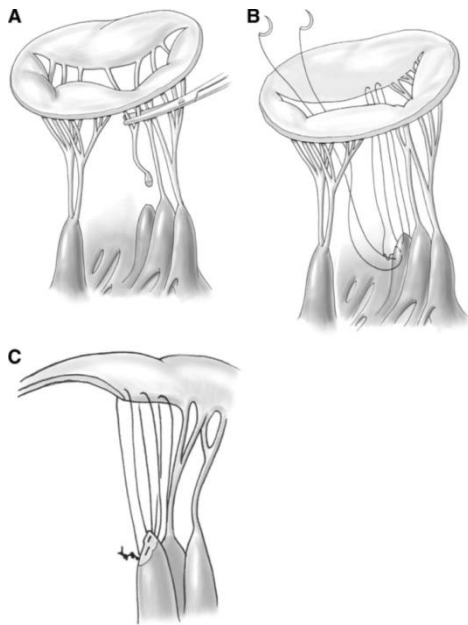
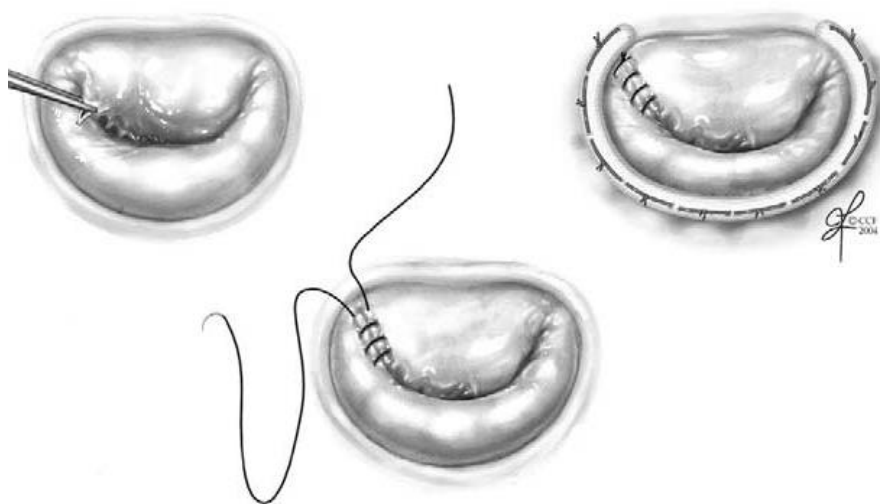


**Fig 1.24:** Commisuroplasty (Gillinov et al 2005).



There is a growing body of evidence supporting the American College of Cardiology (ACC)/ American Heart Association (AHA) guidelines' recommendation of early surgery for severe mitral regurgitation, in asymptomatic patients (Guyton et al 2014). Early surgery can restore normal life expectancy when it is done in an advanced repair centre that can provide an operative risk of less than 1%, high repair rates (85%-90%) and high durability of repair (5-10% reoperation rate after 10 years) (David et al 2003, Adams & Anyanwu 2009, Gillinov et al 2010, Topilsky 2010). Repair of posterior leaflet prolapse have a better durability than anterior and bileaflet prolapse. In a long term follow-up from Toronto the freedom from moderate to severe MR was 80% at 12 years for posterior leaflet prolapse and 65% and 67% for anterior and bileaflet prolapse. The introduction of Gore-Tex chordae to repair a prolapsing leaflet has improved the durability of anterior leaflet repair (David et al 2005). Gore-Tex chordae have made it possible to do complex repairs where the mitral valve have multiple segments of prolapse. Extensive leaflet resections, chordal shortening and papillary muscle shortening have largely been abandoned in favour of supporting prolapsing segments with Gore-Tex chords (Perier et al 2008, Lawrie et al 2011, David et al 2013).

Long term survival for mitral valve repair is reduced with increasing NYHA functional class, impaired left ventricular function, pulmonary hypertension, atrial fibrillation and tricuspid regurgitation (Gillinov et al 2010). It is still beneficial to offer these symptomatic patients with mitral valve prolapse and regurgitation valve repair surgery since they have less morbidity and mortality compared to the natural history of the disease (Topilsky 2010).

Studies have shown that all the connective tissue components of the mitral valve are abnormal in patients with myxomatous mitral valve disease (Tamura et al. 1995, Lis et al 1987). These abnormalities are:

1. Spiralling collagen fibrils and alteration in the pattern of arrangement of collagen bundles.
2. Structural changes in the arrangement of the amorphous components and microfibrils of elastic fibres.
3. Increase in the number of elastic fibres and decrease in the size of elastic fibres.
4. Extensive accumulations of proteoglycans.

Myxomatous mitral valve disease is more common in patients with gene mutations that affect connective tissue homeostasis such as Marfan syndrome, Williams syndrome, Loeys-Dietz syndrome, Osteogenesis imperfecta, Ehlers-Danlos syndrome type IV (lung and Vahanian 2011, Hinton and Yutsi 2011).

Family based linkage studies have identified disease loci on chromosomes 16p, 11p and 13q for mitral valve prolapse. Current evidence suggest that valve malformation may be the result of multiple predisposing genotypes in combination with maladaptive valve tissue maintenance which leads to valve disease (Hinton and Yutsi 2011).

Other causes of organic mitral regurgitation are rheumatic heart disease, infective endocarditis, and congenital heart disease such as atrioventricular septal defects.

Rheumatic heart disease (RHD) is the leading cause of valvular heart disease in children and young adults in Africa. It is estimated that globally between 15.6 million and 19.6 million people suffer from RHD (Nkomo 2007). The highest prevalence of RHD is in sub-Saharan Africa with a prevalence of 5.7 per 1000, compared with 1.8 per 1000 in North Africa, and 0.3 per 1000 in economically developed countries (Carapetis and Steer 2005). In South Africa, rheumatic valvular disease complicates 0.6% of pregnancies of black women from low socioeconomic background, with a maternal mortality rate of 9.5%. (Schoon et al. 1997)

Rheumatic heart disease is a late consequence of acute rheumatic fever with carditis which is initiated by a pharyngeal infection by group A beta-hemolytic Streptococci. An exaggerated immune response to specific bacterial epitopes in a susceptible host leads to acute rheumatic fever with multi-organ involvement and valvular inflammation. (Carapetis et al 2005) (lung and Vahanian 2011). There are more than 60 rheumatogenic serologic types of group A Streptococci (Denny 1987).

Streptococcal pharyngitis typically occurs in school-age children with the peak between 6 and 14 years (Denny 1986). In susceptible individuals, acute rheumatic fever will then follow after 10 to 35 days (average 3 weeks) after untreated infections. The risk of a first attack of acute rheumatic fever is 2-3% but the risk increases to 25-75% for subsequent streptococcal infections (Denny 1987).

Rheumatic heart disease can result from a single attack of acute rheumatic fever with carditis, but more commonly it is caused from cumulative damage from repeated attacks of rheumatic fever. Repeated attacks of rheumatic fever can be prevented by secondary prophylaxis programmes. These programmes have been successful in New Zealand and India, where they have resulted in lower rates of acute rheumatic fever recurrences and also ensuring good clinical follow up of patients with acute rheumatic fever and rheumatic heart disease. (Carapetis et al 2005).

There has been an initiative by the Pan African Society of Cardiology (PASCAR) in 2005 at the first All Africa Workshop on Rheumatic Fever and Rheumatic Heart disease to launch an effective prevention strategy for rheumatic fever and rheumatic heart disease in Africa. The programme in Africa is similar to the World Heart Federation Pacific Islands Rheumatic Heart Disease Control Programme (World Heart Federation 2014). Children are screened for heart valve damage and those found to have RHD are provided the monthly penicillin injections that prevent the progression of the disease. The strategy focuses on Awareness, Surveillance, Advocacy and Prevention (A.S.A.P) (Robertson et al 2006).

- A. Awareness: raising the awareness of the public and health care workers on the impact of rheumatic heart disease.
- S. Surveillance: improving the quality of information available on the incidence, prevalence and burden of rheumatic heart disease through epidemiological surveillance.
- A. Advocate: working together as advocates to change public policy for the improvement of health care facilities to treat and prevent the disease
- P. Prevention: working towards the establishment of national primary and secondary prevention programmes.

The programme is setting up demonstration sites in Egypt, Eritrea, Ethiopia, Ghana, Kenya, Mozambique, Nigeria, Rwanda, South Africa and Zambia (World Heart Federation 2014).

The prevalence of RHD increases with age, peaking in adults aged 25-34 years. In young patients mitral regurgitation is the predominant lesion with annular dilatation, chordal elongation or rupture and anterior leaflet prolapse. With increasing age and progression of the valvular inflammation and fibrosis the leaflets thicken, shorten and valve commissures fuse. This results in mitral stenosis with or without incompetence (Carapetis et al 2005).

Rheumatic heart disease with mitral incompetence or stenosis affects a patient's quality of life and also life expectancy. The prognosis of a patient depends on the severity of the valvular lesion. The natural history of mitral valve disease has been described in the era before cardiac surgery was available.

In a series of 271 patients from Denmark with mitral stenosis the 10 year survival after first diagnosis was a dismal 34% and 20 year survival was 14% for the whole group. Patients with NYHA class II symptoms in sinus rhythm had an 82% 10 year survival. Those patients with NYHA class II symptoms with atrial fibrillation and NYHA class III symptoms had a 10 year survival of 34% and 35% respectively. There were no survivors after 10 years in patients with NYHA class IV symptoms (Olesen 1962).

In a study from California, patients with mitral incompetence and stenosis were followed for 10 years on medical treatment. Seventy patients with mitral incompetence had a 10 year survival of 60%. Another group of 102 patients with combined mitral stenosis and incompetence had a 10 year survival of only 33% (Rapaport 1975). A study from France showed an 8 year survival in patients with severe mitral regurgitation of 33% (Delahaye 1991).

Mitral valve repair and replacement have improved the quality of life and the prognosis of patients with RHD. Percutaneous balloon valvuloplasty is the procedure of choice for patients with mitral stenosis and favourable valvular morphology (Reyes et al. 1994). The mitral valve morphology is scored echocardiographically using the Wilkins score (Table 1.2). This scoring system looks at leaflet mobility, leaflet thickening, subvalvular thickening and calcification (Wilkins et al. 1988). If the valve scores favourable on all these criteria, that is a Wilkins score of 8 or less out of 16, it is a good predictor that a balloon valvuloplasty will be successful.

**Table 1.2** Wilkins score: Grading of mitral valve characteristics from the echocardiographic examination (Wilkins et al. 1988).

Grade	Mobility	Subvalvular thickening	Thickening	Calcification
1	Highly mobile valve with only leaflet tips restricted	Minimal thickening just below the mitral leaflets	Leaflets near normal in thickness (4-5mm)	A single area of increased echo brightness
2	Leaflet mid and base portions have normal mobility	Thickening of chordal structures extending up to one third of the chordal length	Mid-leaflets normal, considerable thickening of margins (5-8mm)	Scattered areas of brightness confined to leaflet margins
3	Valve continues to move forward in diastole, mainly from the base	Thickening extending to the distal third of the chords	Thickening extending through the entire leaflet (5-8 mm)	Brightness extending into the mid-portion of the leaflets
4	No or minimal forward movement of the leaflets in diastole	Extensive thickening and shortening of all chordal structures extending down to the papillary muscles	Considerable thickening of all leaflet tissue	Extensive brightness throughout much of the leaflet tissue

Long term results of mitral valve balloon valvuloplasty in patients with rheumatic mitral stenosis show an event free survival of 88% at 10 years and 60% at 15 years. (Fawzy 2009). Open surgical mitral commissurotomy is indicated in patients with favourable valvular anatomy, but have a contra-indication to balloon valvuloplasty such as a left atrial thrombus, significant subvalvular disease, mitral valve calcification or concomitant cardiac pathology that requires corrective surgery (Choudhary 2003). Operative mortality for open mitral commissurotomy is less than 0.5% and the 10 year survival is 87% (Gross 1981). Freedom from reoperation at 10 years ranges from 78%-87% and by 20 years about half of the patients need a reoperation (Choudhary 2003, Hickey 1991). This means that a significant number of these patients require

a second procedure which is most often a valve replacement, because the valvular fibrosis and calcification progress and the valve becomes unsuitable for a valvuloplasty.

Patients with rheumatic mitral regurgitation can be treated with mitral valve repair if the valve is suitable for repair. That means there must be sufficient leaflet tissue and mobility to ensure a proper coaptation surface (Kumar et al 1995). Operative mortality for rheumatic mitral valve repair is superior to that of mitral valve replacement, ranging from 0.7-4% (Duran et al 1991). Five and 10 year survival for rheumatic mitral repair is 97% and 88% respectively and is better than the survival of mitral valve replacement which is between 60 and 70% at 10 years. (Yau et al 2000, Baudet 1995). At Tygerberg Hospital (Cape Town, South Africa) a 5 year survival of 81% was found after mitral valve replacement (Barnard et al 2010).

Unfortunately not all rheumatic mitral valves are suitable for repair and even if they can be repaired, there is often a progression of RHD, which is the main indication for re-operation (Chauvaud et al 2001). The freedom from re-operation ranges from 66%-82% at 10 years and 55% at 20 years (Chauvaud et al 2001, Yau et al 2000, Di Bardino et al 2010). Repaired degenerative mitral valves (myxomatous valves) have a higher freedom of reoperation which ranges from 90-95% at 10 years (David et al 2013, Di Bardino et al 2010).

A large portion of patients with rheumatic mitral valve disease will not be suitable for a repair and will need a mitral valve replacement. At Tygerberg Hospital 497 mitral valve procedures were done from 2006-2013 of which only 91 (18%) of the mitral valves could be repaired and 82% needed replacement (Janson 2013). This is because of the high prevalence of rheumatic heart disease.

#### **1.4 Current valve prostheses:**

Diseased cardiac valves are replaced with either mechanical or biological tissue prostheses. Mechanical valves are more durable, but require long-term anticoagulation therapy with warfarin to prevent surface clotting. Bioprosthetic valves do not require anticoagulation therapy, but have limited durability secondary to structural degeneration and calcification (Edmunds et al 1996). The long term outcome of a mitral valve replacement is inferior to that of a valvuloplasty or repair. (Baudet et al 1995, Duran et al 1991, Yau et al 2000, Kim et al 2010). This is because current mechanical and bioprosthetic valves are not ideal substitutes for a functioning native valve and have prosthetic related complications.



Heart valve prostheses have been used successfully since the first complete replacement of the mitral valve in 1960 (Braunwald et al 1960). In the sixties mechanical valves were popular and saw the development of many mechanical designs. The 3 main mechanical designs were the ball and cage, tilting disc and bileaflet designs. All these valves create turbulent blood flow with increased fluid stresses. It is very complex to model the flow across these valves, because of the complex geometric shapes and the pulsatile nature of blood flow (Yoganathan 2005). This can cause platelet destruction and activation and hemolysis of red blood cells. Direct mechanical trauma of blood cells and platelets by impact with the prosthetic valve structure and leaflets and the shearing forces of the turbulent flow across these valves are the possible mechanisms for this destruction. The same fluid stresses which can lead to the damage of red cells and platelets can also affect the endothelial cells. When the endothelial cells are stripped from their biological substrates by high fluid shear stress, it exposes the extracellular matrix proteins lining the surface. This can lead to the adherence, activation and aggregation of platelets causing thrombo-emboli (Yoganathan et al 2005). The presence and severity of hemolysis in patients can be correlated with elevated concentrations of serum LDH, serum haptoglobin and blood haemoglobin (Skoularigis 1993).

The introduction of pyrolytic carbon in the late 1960's as a valve material and the design of bileaflet valves in the 1970's were developmental milestones that contributed to improvements in the durability and performance of mechanical prosthetic heart valves (Giddens et al 1993, Bokros 1989). Today, almost 50 years after the introduction of pyrolytic carbon as a valve material, there is not another rigid biomaterial available that has more thromboresistant properties. Unfortunately, even pyrolytic carbon is not perfect as a valve substitute and patients with mechanical valves need to take lifelong anticoagulation to prevent prosthetic valvular thrombo-emboli.

Prosthetic heart valves not only have the risk of hemolysis, thrombo-embolism and valve thrombosis. There is also the risk of anticoagulant related bleeding, tissue overgrowth over the valve sewing ring (pannus formation) with valve dysfunction, prosthetic valve endocarditis and paravalvular leaks (Baudet 1995, Giddens et al 1993).

There are 6 categories of prosthetic valve related morbidities which are specified in the Southern Thoracic Society (STS)/ American Association for Thoracic Surgery (AATS) guidelines for reporting morbidity and mortality after cardiac valvular operations (Edmunds et al. 1996):

1. Structural valvular deterioration,
2. Non-structural dysfunction,
3. Valve thrombosis,
4. Embolism,
5. Bleeding and
6. Endocarditis.

All these events, except structural valve deterioration, have a relatively constant rate (hazard function) after the first postoperative month and are reported as a linearized rate in the surgical literature. Linearized rates are calculated as follows (Grunkemeier et al 2000):

Number of events

----- X 100 = Events per 100 patient-years or percent per year (%/y)

Follow up years

A comprehensive literature review covering 165 reported series, 61 455 valve implants and 319 749 patient-years of follow-up showed the following rates of these complications: (Grunkemeier et al 2000)

The risk of thromboembolism is 0.5-3% per year for mechanical mitral valves and 0.5-2% per year for biological valves. The risk for mechanical valves is for patients on anticoagulation therapy and this rate would be even higher if the patient is not using anticoagulants or if the anticoagulant therapy is not well controlled.

Valve thrombosis is a serious complication which can cause valve obstruction and death, or it will require an intervention, such as redo valve replacement or thrombolytic therapy. The risk of valve thrombosis is less than 0.5% per year for mechanical mitral valves and less than 0.2% per year for tissue mitral valves.

The bleeding rate for mechanical mitral valves is between 0.5-3% per year and less than 1.5% per year for biological valves.

Endocarditis risk for mechanical and biological mitral valves is below 1% per year.

Paravalvular leak rates are below 1% per year for both mechanical and biological valves.

These valve related complications add morbidity and mortality to a patient, because each of these complication risks are additive. Over 10 years a patient has a 5-30% chance of thromboembolism and a 5-30% chance of bleeding with a mechanical valve, according to the above complication rates.

Structural valve failure with current mechanical valves is very low and almost all studies report a 0% incidence. The most notorious example of mechanical valve failure was the Bjork-Shiley Convexo-Concave tilting disc valve. Modest design changes from the previous model led to increased stress on the welded outflow strut. This resulted in strut fracture and disc escape which was first described in 1978 with a peak incidence in 1984 (Harrison et al 2013). These valves were withdrawn from the market in 1986. Today most mechanical valves implanted are bileaflet valves with excellent durability (Grunkemeier et al 2000).

In the 1970's there was an increased interest in bioprosthetic valves. Three types of bioprosthetic valves are available commercially:

1. Porcine xenografts (porcine aortic valves mounted on a stent or stentless),
2. Bovine pericardial valves (bovine pericardial tissue is used to shape 3 valve leaflets which are mounted on a stent).
3. Homograft or allograft valves (aortic valves from human cadavers).

It was realised that bioprosthetic valves have less risk of thrombo-embolism and patients did not need anticoagulation with these valves. This lowered the incidence of anticoagulant related bleeding. Unfortunately tissue valves degenerate and calcify with time and this degeneration leads to structural valve failure with stenosis or incompetence of the valve. This degeneration is accelerated in young patients and often requires a reoperation and a new prosthetic valve implant (Grunkemeier et al 2006).

Early experience with xenografts (porcine aortic valves and bovine pericardial valves) showed that the host mounted a strong humoral and cellular immune response to the graft that led to collagen denaturation and early graft failure (Carpentier 1969). To reduce the immune response porcine and bovine pericardial tissue is treated in low concentrations (0.625%) of glutaraldehyde (Carpentier 1969). Collagen is cross-linked by glutaraldehyde in an inter- and intramolecular fashion by the formation of covalent bonds. This can occur in 2 ways: formation of Schiff bases by reaction of an aldehyde group with an amino group of lysine or hydroxylysine or an aldol condensation between 2 adjacent aldehydes. The Schiff base linkage is not a very stable bond, but the aldol condensation is stable (Jayakrishnan 1996). Compared to other aldehydes that can be used to cross-link, glutaraldehyde has the advantage that it reacts relatively quickly, can span various distances between the protein molecule and is able to react with a larger number of amino groups in the protein molecule. This creates a more tightly cross-linked network which stabilizes the collagen proteins and decreases the antigenicity of the graft (Carpentier 1969, Jayakrishnan 1996, Vesely 2005).

Glutaraldehyde also creates a cytotoxic film on the graft which reduces cellular adhesion and causes apoptosis which is programmed cell death without an immune response (Gough et al 2002). The leaflets show some loss of pliability and flexibility, but retain excellent tensile strength. Cross-linking of collagen fibres stiffens the collagen bundles and reduces the possibility of gliding movements of fibres upon itself. After glutaraldehyde treatment, the xenograft is an acellular, nonviable structure with cross-linked collagen leaflets. This can be appreciated when comparing the ultrastructure of fresh porcine valves with glutaraldehyde treated porcine valves (Ferrans et al 1978). The most important alteration is disruption of the endothelial cell layer in the treated valves (Fig 1.25, Fig 1.26). There is also loss of the ground substance of connective tissue including the dense spicules of acid mucopolisaccharides and the network of finely filamentous components. As a consequence the collagen and elastic fibres, which remain structurally normal, appear to be surrounded with less support of the ground substance and with some "loosening" in their arrangement (Fig 1.25, Fig 1.26 and Fig 1.27). The fibroblasts show loss of integrity of cytoplasmic membranes and disruption of organelles (Fig 1.26). Histological examination of valves that have been implanted in humans show disruption of collagen fibres and the formation of a homogenous pale-staining matrix without fibrillary elements. The surface of these valves gets covered with a layer of fibrin with variable numbers of erythrocytes, macrophages and giant cells (Fig 1.28). These structural changes eventually lead to progressive breakdown of the collagen framework with structural failure (Ferrans et al 1978).

**Fig 1.25:** Light microscopy of a normal untreated aortic porcine valve stained with alkaline toluidine blue (Ferrans et al 1978). Note the endothelial cell layer on both surfaces and the distinct layers of the fibrosa, spongiosa and ventricularis.

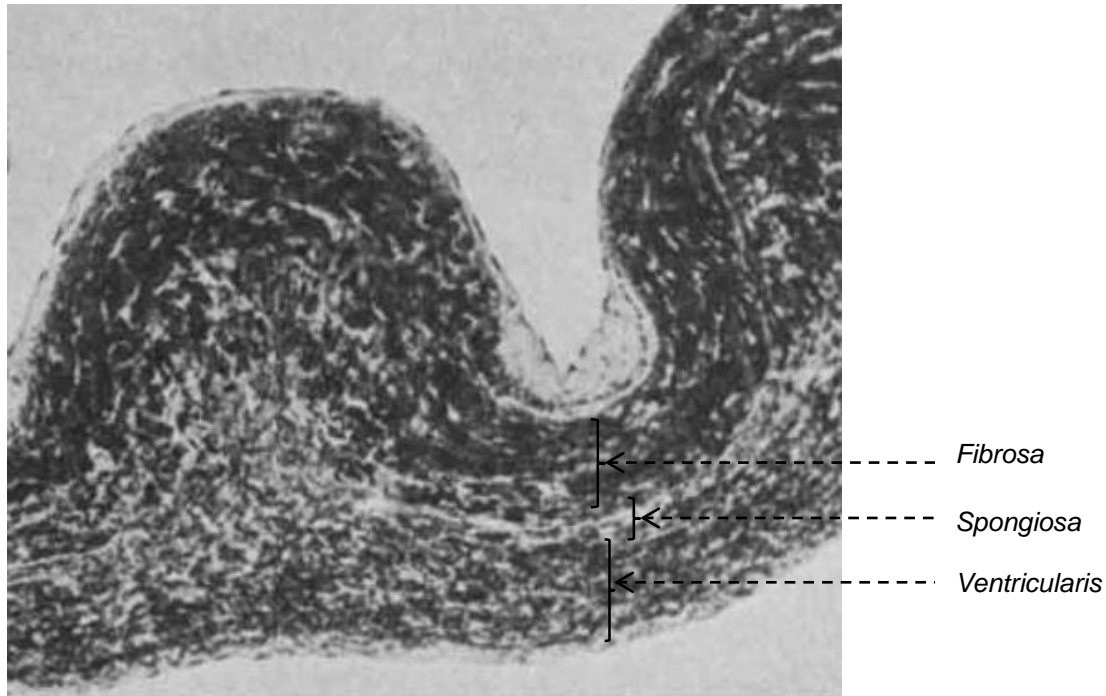


**Fig 1.26:** Light microscopy of a glutaraldehyde treated valve stained with alkaline toluidine blue (Ferrans et al 1978). The fibrosa appears dense and the spongiosa is more loosely arranged than normal. The ventricularis is not well defined. Both surfaces are denuded of endothelium.

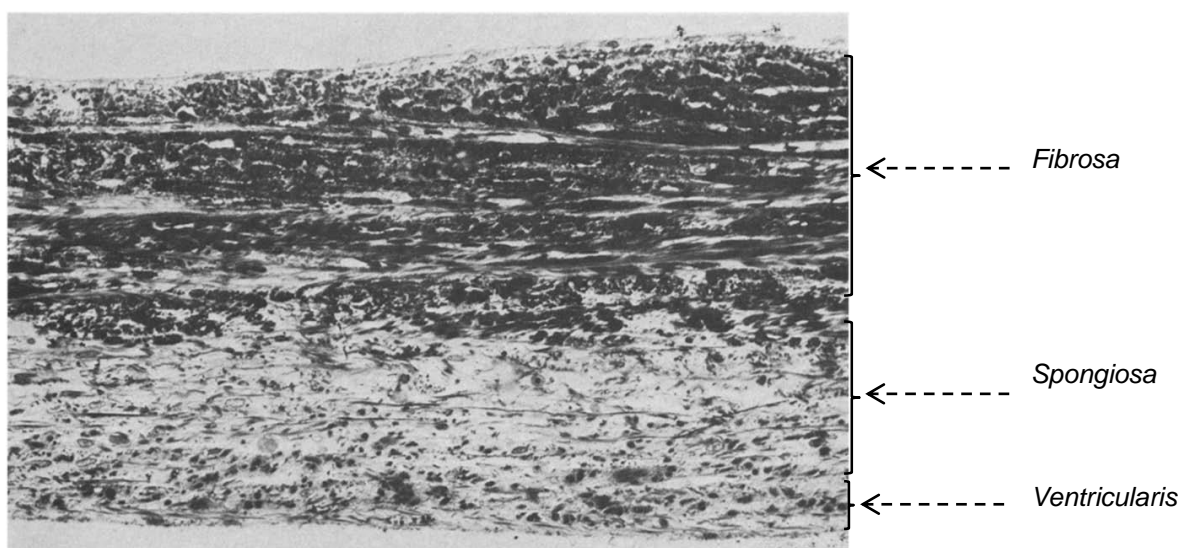


**Fig 1.27:** Electron micrograph of a glutaraldehyde treated porcine valve. The surface lacks an endothelial covering and is composed of loose bundles of collagen and deeper elastic fibres. The morphological features of the valve fibroblast is poorly preserved (arrows) with disrupted organelles (Ferrans 1978).

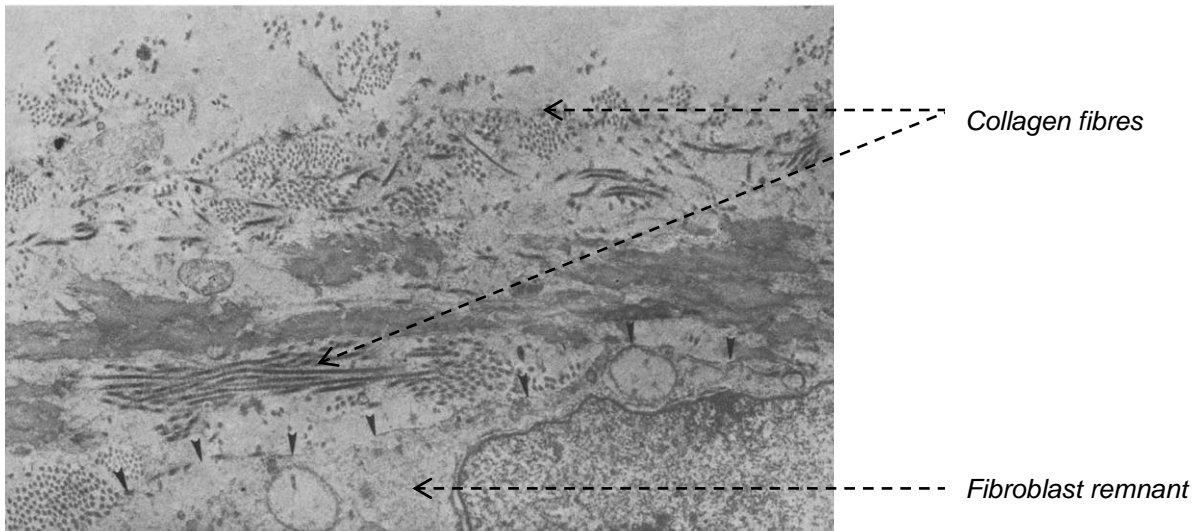
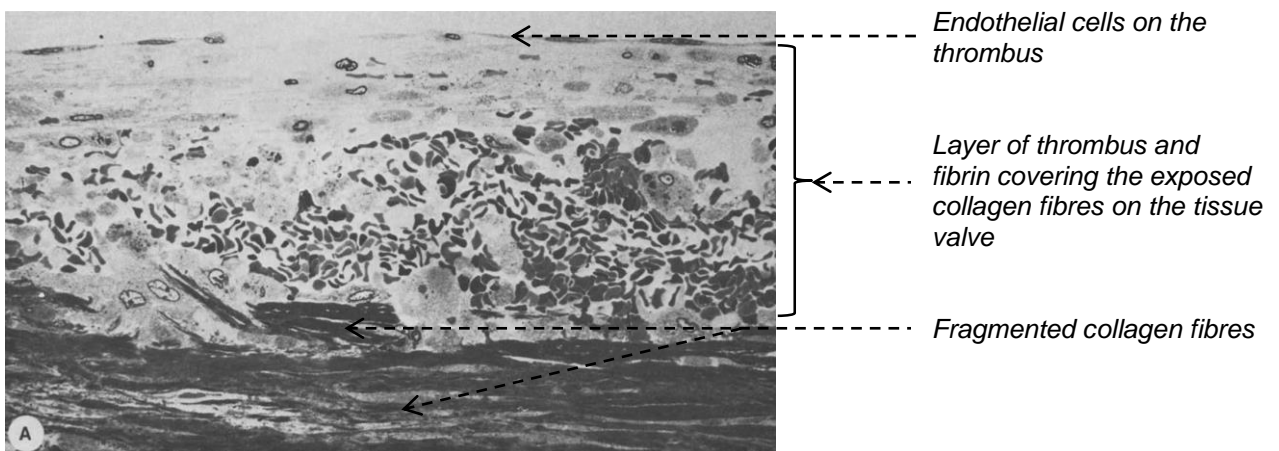


**Fig1.28:** Light microscopy of the surface of a glutaraldehyde treated porcine valve that has been implanted for 21 months. Note the layer of incompletely organised thrombus and fibrin on the collagen fibres. Collagen bundles next to the thrombus are fragmented. This specimen shows a thin layer of neointima (endothelial cells) on the surface of the thrombus (Ferrans et al 1978).



There is growing evidence that, despite glutaraldehyde treatment of xenografts, there may still be a host cellular and humoral immune response against the xenograft. (Dahm et al 1995, Human and Zilla 2001, Manji et al 2006). Not all the antigens on the xenograft are necessarily masked by cross-linking and some antigens may remain unaffected. Devitalized cells and cellular debris remain on the graft. This may explain why tissue valves degenerate and calcify earlier in younger patients, because they have a more reactive immune system and mount a stronger immune response (Manji et al 2006). It could also be that younger patients have a more active calcium metabolism and have more mechanical stress on the leaflets (Schoen and Levy 2005).

Dystrophic calcification of bioprosthetic implants is a clinically important pathologic process that limits the durability and clinical use of these valves in especially younger patients. Dystrophic calcification is seen in soft tissues as a result of injury, disease and aging and these sites often show evidence of tissue alteration or necrosis (Giachelli 1999). Most tissues can undergo calcification but skin, kidney, tendons and cardiovascular tissues are particularly prone to calcification (Giachelli 1999).

The pathophysiology of dystrophic calcification is not fully understood and the sheep model has been used extensively to study the calcification of bioprosthetic valves (Schoen et al 1994, Ozaki et al 2004, Flameng et al 2005). Accelerated calcification is seen in the juvenile sheep model which makes it an ideal model to identify early calcification in bioprostheses. The amount of calcification seen in a bioprosthesis implanted in a sheep for 3 months correlates well with the amount of calcification seen in a bioprosthesis implanted in an elderly person for 10 years (Ozaki et al 2004).

Calcification of bioprosthetic valves is more common in younger age and more pronounced in areas of increased mechanical stress and strain with the highest calcium concentrations shown in the cusps of mitral valve implants where the mechanical stress is higher than in the aortic or pulmonary position (Flameng et al 2005). Glutaraldehyde treatment of tissue also makes it more prone to calcification, because of devitalized connective tissue cells and debris that remain on the valves. (Valente et al 1985, Tamura et al 1995, Flameng et al 2005, Schoen and Levy 2005). Devitalized cells and cell remnants are important foci for early mineralization and calcification. Dystrophic calcification involves the reaction of calcium-containing extracellular fluid with membrane-associated phosphorus, causing calcium phosphate (hydroxyapatite) crystal nucleation. This occurs because the normal extrusion of calcium ions is disrupted in the cells that have been devitalized by glutaraldehyde fixation and calcium

accumulates in the cells (Kim et al 1999). The affinity of cytoplasmic membranes for calcium is related to the high phospholipid component in the membranes. Early detectable crystals of apatite are seen ultrastructurally within matrix vesicles or organelles in close apposition to the inner membrane layer (Fig 1.29) (Valente et al 1985, Schoen and Levy 2005).

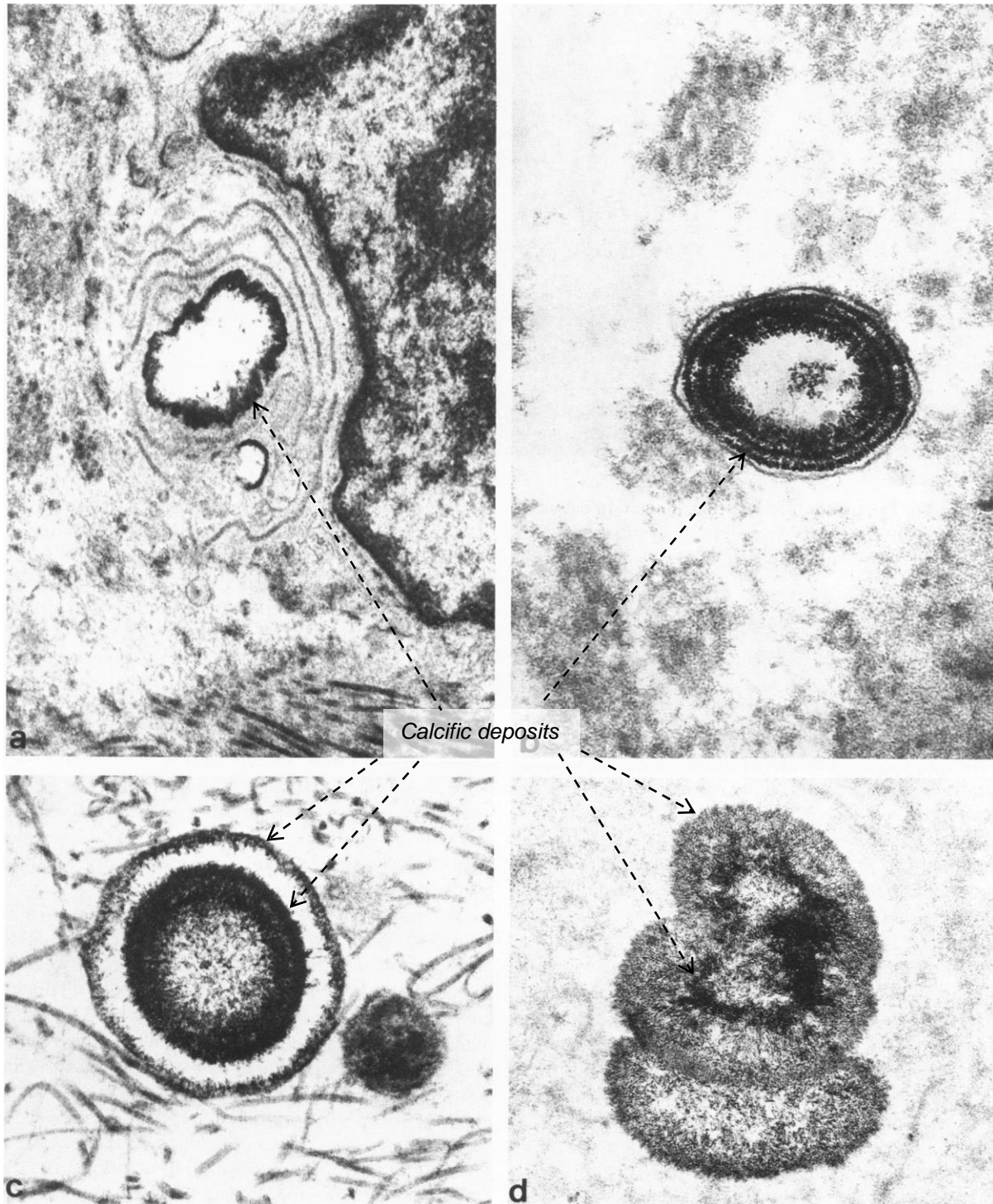
Living tissue have the capacity to curb the spread of calcification, by secreting inhibitors of apatite growth and that is why osteocytes can survive in densely calcified bone (Kim et al 1999). A variety of calcification inhibitors have been identified in tissue fluid and it has been shown that fibroblasts can inhibit calcification of bone cells that are cultured in the same dish through soluble factors including prostaglandins (Kim et al 1999, Ogiso et al 1991). Cells appear to play an active role in regulating mineral deposition and balance between the pro- and anti- calcification mechanisms will dictate the formation of ectopic calcification at a given site (Giachelli 1999).

Elastin and elastolysis with subsequent calcification of the elastic fibres is also an important trigger for calcification as is seen in the aortic wall of stentless valves (Flameng et al 2005). Ultrastructural examination of calcified bioprosthetic valves shows that alteration in collagen plays a role in the progression of calcium deposits. Proteoglycans in the valve matrix act as inhibitors of calcification and removal of proteoglycans during tissue processing may enhance the calcification process (Valente et al 1984).

In an attempt to reduce calcification of the glutaraldehyde treated xenografts, tissue is also treated with calcification inhibitors and other chemical agents to modify or remove calcifiable components and cell debris (Schoen and Levy 2005).



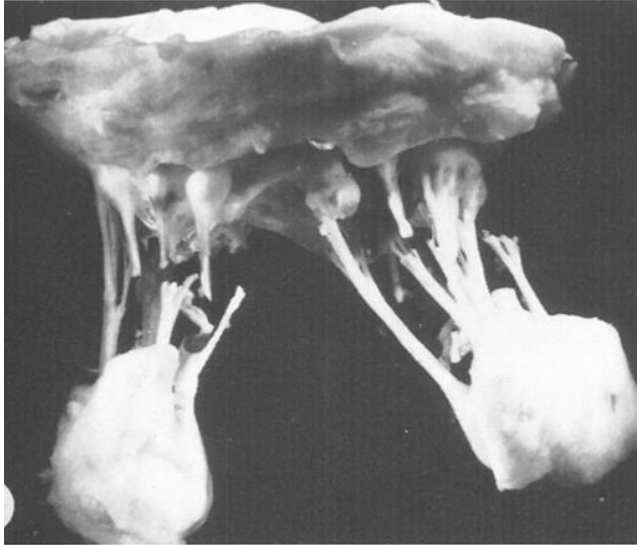
**Fig 1.29:** Electron micrographs of calcific bodies in porcine xenografts. The earliest sign of calcification, before radiological or macroscopic evidence of calcification is seen, is calcific deposits in the form of needle like crystals that occur upon membrane fragments and organelles (x 45000) (Valente et al 1985).



Homografts or allografts obtained from cadaver aortic valves are prepared differently. Viability is reduced and necrotic cells removed by saline washing, leaving behind only the deeply buried myofibroblasts that are viable. This is done to reduce the antigens on the graft and the immune response between the host and the graft. No glutaraldehyde cross-linking is done. It is then stored cryopreserved and when it needs to be used, it is thawed. The allograft then functions as a nonviable, non cellularized scaffold that gets covered by the patient's own neointima and pseudointima which is a fibroblast and smooth muscle sheathing (Hopkins 2007). The homograft can last up to 20 years, as a nonviable piece of tissue, free from mechanical reinforcement by cross-linking agents (Matsuki et al 1988). This shows how remarkable the microstructure and composition of the native aortic valve is. The interconnected sheets of collagen and layers and tubes of elastin give the valve tissue viscoelasticity, anisotropy and highly non-linear mechanics which makes homografts last better than xenografts. The host immune response is also less with homografts than with xenografts. Unfortunately homografts are also unable to regenerate and repair itself from the repeated deformation during systole and diastole and eventually fail, usually by calcification and stenosis (Davila 1989, Vesely 2005).

Bioprosthetic valves show structural degeneration and calcification with a 10% to 20% chance of homograft failure and a 30% chance of xenograft failure within 10 to 15 years (Vongpatanasin et al 1996). A recent study looked at the durability of a porcine aortic bioprosthesis in young patients and showed that patients under 40 years have a 20-year freedom from reoperation due to structural valve failure of only 14 % and patients between 40-49 years have a freedom from reoperation of 21% (Une et al 2014). Young patients with xenograft prostheses and prostheses in the mitral position have a particular high valve failure rate (Vongpatanasin et al 1996). Mitral valve allografts have been tried and tested in animal studies and in humans where a cadaver mitral valve with its papillary muscles are transplanted into the host. The results for mitral homografts in humans were very poor with a 14% early mortality and 85% failure in 5 years (Kumar et al 2000). Early failure occurred because of disruption of one of the donor papillary muscles and late failure occurred because of leaflet and chordal degeneration with calcification. This was also found in other human and animal studies. (Fig 1.30) (Tamura et al 1995).

**Fig 1.30:** *Allograft implanted in the mitral position in sheep for 12 weeks show extensive calcium deposits on the thickened leaflets and some of the chordae are ruptured. (Tamura et al 1995).*



Over the last 30 years, research focused on ways to improve the durability of bioprosthetic valves. The new generation bovine pericardial valves showed some improved durability due to infrastent tissue-mounting, flexible and distendable struts, and better tissue orientation of the leaflets combined with improved tissue preservation techniques, but there is still structural degeneration with time (Aupart et al 2006, Guangqiang et al 2004). The bioprosthetic xenografts and allografts are unable to regenerate and repair the degradation and aging of the collagen fibres which comes from repeated stress and strain and the immune response from the host (Davila 1989, Liao 2008).

Tissue engineered heart valves have been proposed by physicians and scientists to be the ultimate solution for treating heart valve disease. Ideally a tissue engineered valve would be a living tissue valve that would be able to grow, adapt to physiological forces and be able to regenerate and repair itself. (Vesely 2005).

### 1.5 Tissue engineering of heart valves:

The principle of cardiac valve tissue engineering is seeding a scaffold matrix with cells that can differentiate into various cells that are normally found on the native valve. These cells then need to migrate, proliferate and express proteins to regenerate and maintain the extracellular matrix. (Hopkins 2007, Bouten et al 2011).

The scaffold for tissue engineering is a 3-dimensional acellular structure onto which cells are implanted or seeded. The purpose of the scaffold is to give the valve functional structural design, enhance structural properties, deliver biochemical factors for the cells and ensure access to vital nutrients for the cells (Hopkins 2007). Scaffolds that are being used for this purpose are acellular xenograft tissue and bioresorbable synthetic scaffolds. Synthetic scaffolds eventually need to degrade as the endogenous extracellular matrix increases to maintain tissue strength (Bouten et al 2011).

Decellularization of xenografts are made by first breaking apart the cell membranes through lysis in hypertonic and hypotonic solutions. This is followed by extraction with various solutions. Enzymes such as trypsin and nucleases that accompany these detergent treatments have focused mainly on cleaving and removing the DNA that is part of the cellular debris. The entire extraction procedure can last up to a week. The agents that are used for the cell extraction can be detrimental to the matrix by denaturing the matrix proteins or leaving toxic residues. This can affect the mechanical function of the matrix and the cellular seeding. Many studies and patents describe the creation of these acellular matrixes and they vary in the specific detergents used, the sequence of steps and soaking periods in the different solutions (Vesely 2005). Mechanical testing is used to determine the mechanical integrity of the processed tissue. This is then compared to unprocessed controls (Spina et al 2003). The histological morphology of the matrix varies greatly between the different decellularization processes but most of these processes induce mechanical and microstructural defects in the valve matrix and this may impact the durability of the valves (Vesely 2005, Liao et al 2008).

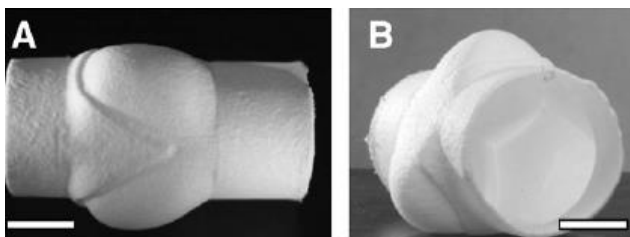
Small intestine submucosa (CorMatrix®) is another popular bio-derived substrate and consists almost entirely of acellular collagen. It does not need to undergo extensive decellularization procedures and have been used in single valve leaflet replacements and even complete valve replacements in animals. (White et al 2005). In a recent study where CorMatrix was used for valvuloplasty in patients with congenital heart defects, the CorMatrix induced an intense

inflammatory reaction, but little or no remodelling of the tissue. It was hoped that the CorMatrix® would remodel into valve tissue, but the tissue did not show resemblance to the 3 layered nature of native valve tissue (Zaidi et al 2014).

The acellular substrates are implanted in vivo or are pre-seeded with various types of cells in vitro and then implanted. Many animal studies have reported repopulation of decellularized matrixes, demonstrating the potential for growth and remodelling, but actual growth has not been reported (Bouten et al 2011). Intra-peritoneal implantation of the grafts have also been done to seed the grafts but it is questionable whether this approach gives the correct cell types for proper in vivo tissue development and remodelling (De Visscher et al 2008).

Synthetic polymers are also being used as substrates for valvular tissue engineering. The most commonly used biodegradable substrates are polylactide (PLA), polyglycolide (PGA), polycaprolacton (PCL) or their co-polymers which can be tailored to meet the mechanical performance and the resorption rates that are required. These scaffolds are biodegradable and give the artificial valve its structure until cells are seeded onto the scaffold in vivo (Fig 1.31) (Bouten et al 2011). With the goal of achieving a fully autologous engineered valve, substrates will have to provide bioactive microenvironments with bioactive molecules that control the adhesion and recruitment of endogenous circulating progenitor cells, cellular differentiation and tissue organisation (Bouten et al 2011).

**Fig 1.31:** An Electrospun polycaprolacton (PCL) valve which is a biodegradable substrate (Bouten et al 2011).



Considerable work still needs to be done to optimize matrix materials and biomolecular approaches to imitate the complex signalling pathways of tissue development and regeneration. This will require collaborative scientific efforts from material scientists, chemists, developmental and cell biologists, tissue engineers and clinicians. Current tissue engineered

heart valves do not possess the strength, durability, growth and remodelling potential of the natural heart valve (Bouten et al 2011, Duan et al 2013, Hinderer et al 2014).

### **1.6 The pulmonary autograft:**

In many ways the pulmonary autograft (replacing the aortic valve with the native pulmonary valve) can be seen as the ideal valve replacement. It has the same architecture as the aortic valve with 3 leaflets, has the same cellular and extra-cellular composition and is a living valve with the potential to grow and remodel. In 1960 the feasibility of replacing the aortic valve with the pulmonary valve was tested and described in dogs (Lower et al 1960). This procedure was first done in humans by Donald Ross in 1967, from there the Ross procedure (Ross 1967). There are 2 ways to implant the pulmonary valve into the aortic position, one is an aortic inclusion technique where the pulmonary valve is implanted in a subcoronary position in the aortic root. The other technique is an aortic root replacement with reimplantation of the coronary arteries into the neo-aortic root.

Long term survival rates for the Ross procedure in the aortic position are very good with 10 year survival similar to the general population when matched for age and gender because of the low rate of valve related complications with the pulmonary autograft (David et al 2000, Elkins et al 2008, Yacoub et al 2006). The valve performs like a normal aortic valve with excellent hemodynamics and no degeneration.

There are drawbacks of the Ross procedure. It is a complex procedure that requires 2 valve replacements because the pulmonary valve that is being harvested for the aortic valve needs to be replaced with a pulmonary homograft. This complexity makes the Ross procedure more difficult and the operative mortality for the Ross procedure is higher than for an aortic valve replacement (3% vs 1%) (David 2009). The pulmonary autograft in the aortic position can dilate and develop late regurgitation in 10-14% of patients over 10-16 years follow-up (Elkins et al. 2008, David 2009).

The pulmonary autograft has also been used to replace the mitral valve on a much smaller scale by placing the autograft in a rigid Dacron tubing and suturing the proximal and distal ends to the tubing (Ross 1967, Ross and Kabbani 1997). The distal end of the autograft and Dacron tubing is sutured to the mitral valve annulus and the proximal end is sutured to the left

atrium with a pericardial skirt. There is a risk of conduit kinking and valve obstruction with this technique which is improved by using stiffer Dacron tubing. Freedom from degeneration of the autograft was 93% at 5 years in 92 patients (Kabbani et al 2007).

The pulmonary homograft (from a human cadaver) is a tissue valve that can degenerate and cause pulmonary stenosis. Between 10-15% of the pulmonary homografts need to be replaced by 10 years (Kouchoukos et al 2004, David 2009).

Mechanical valves, biological valves, tissue engineered valves and the pulmonary autograft are all valve substitutes that palliate the original valve disease, but none of them are perfect substitutes to a normal functioning valve. What are we looking for in the ideal prosthetic valve?

### **1.7 The ideal prosthetic valve:**

The ideal prosthetic heart valve should have the following characteristics (Davila 1989, Harken 1989):

1. It must be safely and easily implantable and the procedure must be reproducible.
2. Implantation should be secure with a permanent linkage between the prosthesis and the host.
3. It must be a unidirectional valve that, within a physiological flow range, offers minimal opening resistance and minimal resistance to forward flow without turbulence.
4. It must close without regurgitation.
5. It must not activate the coagulation system.
6. It must be chemically inert and not damage blood elements.
7. It must be durable and function normally for the rest of the patient's life.

This ideal valve has been eluding scientists and the medical profession for the last 60 years. A living tissue valve that can grow and remodel would fit many of the above criteria. Tissue engineering has not yet been able to produce such a valve. The pulmonary autograft is the most ideal valve replacement with all the characteristics of the original valve, but unfortunately it comes at the cost of sacrificing the native pulmonary valve and having to replace it with a homograft.

## 1.8 Creating a prosthetic valve from autologous tissue

Several investigators have made intra-operative valve prostheses from autologous tissue in an attempt to avoid the immune response (Bjork and Hultquist 1964, Senning 1967, Ionescu and Ross 1969, Fabiani et al 1995, Love 1998). Untreated autologous fascia lata and pericardium have been used to create a biological valve. There are several constraints when making an intra-operative autologous valve (Fabiani 1995). The valve cannot be constructed ahead of time and there is a time constraint when making the valve. There must be a mechanism of quality control after the valve is created and it must be possible to reproduce a comparable valve each time. The method must be simple enough to be taught and learned. There must also be enough autologous tissue available. That is why pericardium has been very popular, because it is easily accessible and it gives enough tissue to build a valve.

Long term results of autologous valves were largely unsuccessful due to tissue shrinkage and thickening. Pericardium and fascia lata do not have an endothelial covering or the viscoelasticity, anisotropy and non-linear mechanics of valvular tissue and cannot sustain the stress and strain of repeated deformations during the cardiac cycle (Fabiani et al 1995, Sacks and Yoganathan 2007). In an attempt to improve these results, autologous pericardium was treated with glutaraldehyde (Fabiani 1995, Love 1998). This helped to improve the tissue shrinkage and thickening but it also fixated the tissue and made it non-viable with an inability to regenerate and repair itself.

Can autologous vein tissue be a suitable substitute for replacing a valve leaflet or a complete valve? When comparing the histology of a vein and a valve leaflet, it can be appreciated that there are many similarities between the two (Fig 1.32, Fig 1.33, Fig 1.34 and Table 1.3). The vein has an endothelial layer, smooth muscle cells (which share many characteristics of the valvular interstitial cells), layers of collagen and elastin. (Jones et al 1973).

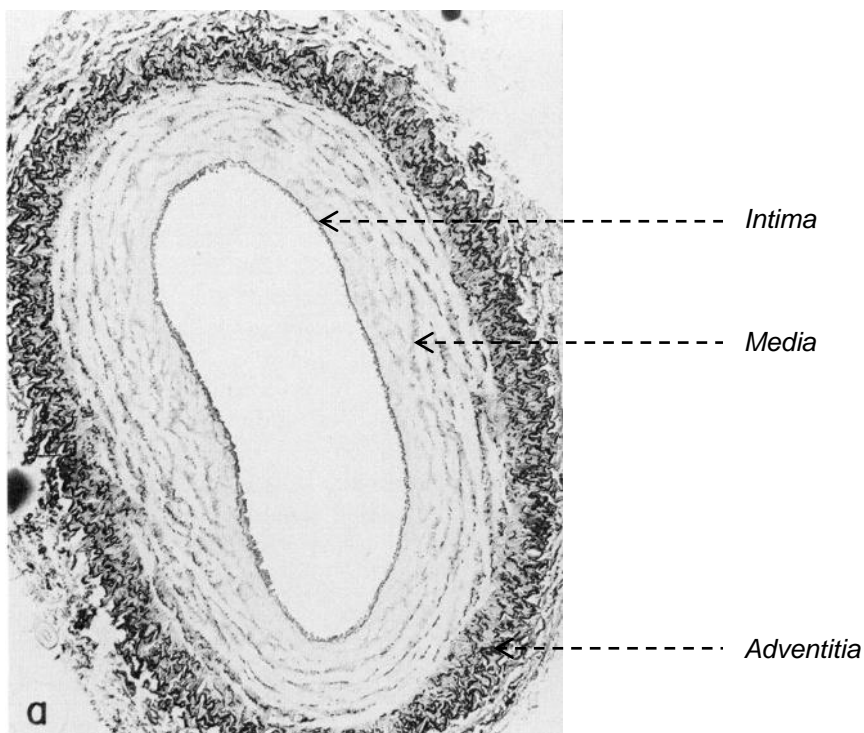


### 1.9 The autologous vein graft.

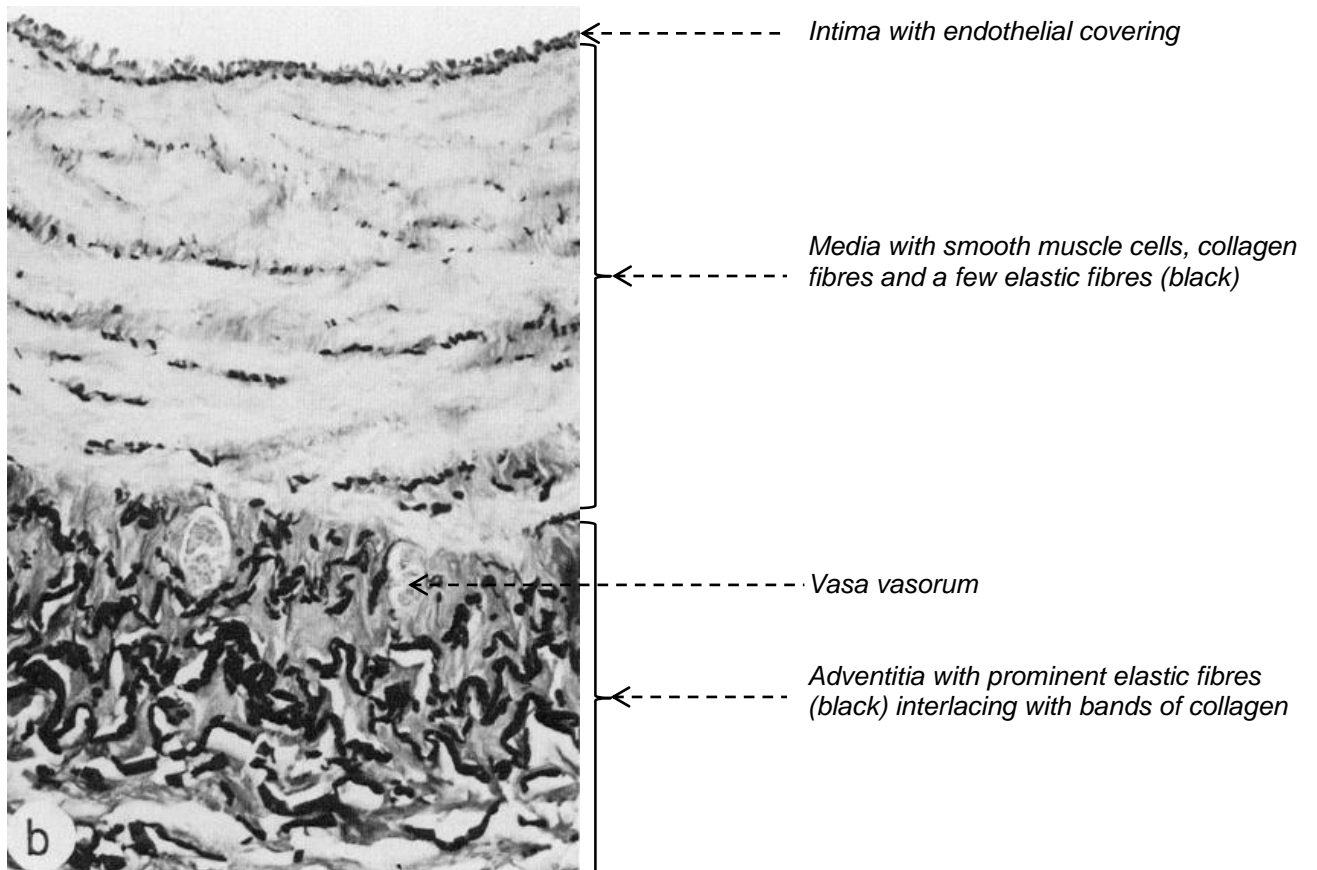
A medium sized vein such as the saphenous vein contains 3 layers (Fig 1.32, Fig 1.33) (Jones et al 1973):

1. The tunica intima which consists of endothelial cells resting on a fenestrated basal membrane and a subendothelial matrix of glycoproteins and connective tissue elements.
2. The tunica media which is well developed and contains concentric layers of smooth muscle cells, collagen fibres and ground substance. The smooth muscle cells contain contractile fibres with dense bodies and the usual organelles. The media contains only scant elastic fibres which are predominantly orientated in a longitudinal direction
3. The adventitia forms the bulk of the vein wall and consists of collagen and elastic fibres. It also contains longitudinal smooth muscle cells and vasa vasorum is also present in this layer.

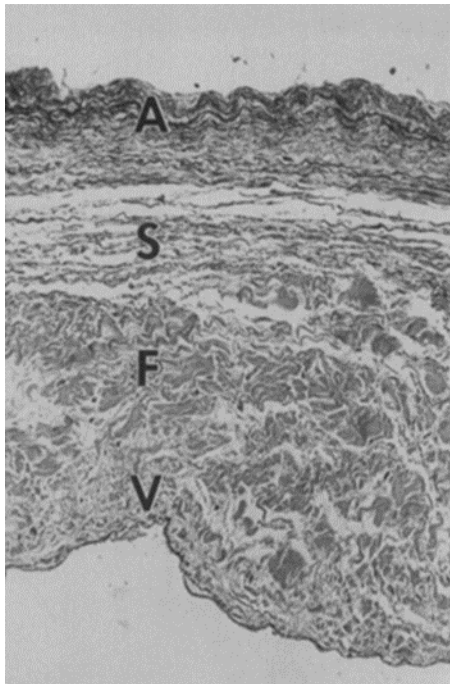
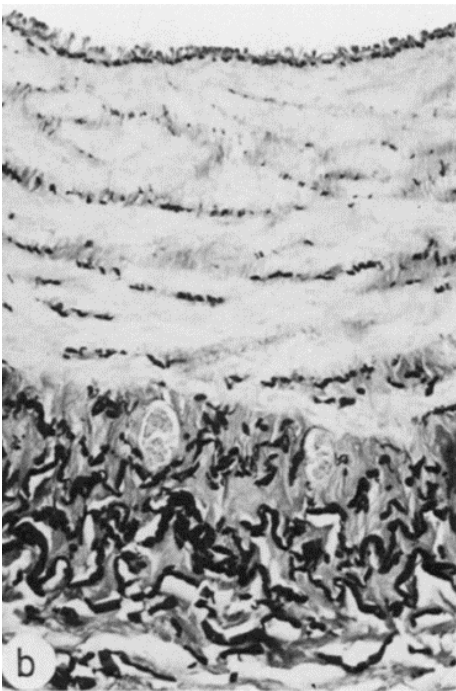
**Fig 1.32:** Histological cross section (low magnification x52) of a normal canine saphenous vein with Van Gieson stain (elastic fibres stain black). (Jones et al 1973).



**Fig 1.33:** Histological section (high magnification x 200) of a normal canine saphenous vein with Van Gieson stain. (Jones et al 1973).



**Table 1.3:** Comparison of the histology of a medium sized vein and a mitral valve leaflet. The histological layers of the mitral valve leaflet are Atrialis/Auricularis (A), Spongiosa (S), Fibrosa (F) and Ventricularis (V)

Mitral valve leaflet (Tamura et al 1995)	Vein (Jones et al 1973)
	
<p><i>Valvular endocardial cell layer on atrial side and ventricular side</i></p>	<p><i>Endothelial cell layer only on intimal side.</i></p>
<p><i>Auricularis (A) and spongiosa (S) contains elastic fibres and some collagen fibres which are more loosely arranged. The spongiosa also contains the most valvular interstitial cells (fibroblasts, myofibroblasts, and undifferentiated mesenchymal cells).</i></p>	<p><i>Media contains smooth muscle cells (which shows similarities with the valvular interstitial cells) collagen fibres, ground substance and few elastic fibres. The collagen fibres are more loosely arranged in the media</i></p>
<p><i>Fibrosa (F) contains, valvular interstitial cells, dense collagen fibres which are arranged in an orderly and parallel pattern and few elastic fibres</i></p>	<p><i>Adventitia contains prominent elastic fibres and bands of collagen which gives strength to the vein wall</i></p>

Veins have been used extensively for coronary artery bypass grafts since the 1960's and also for vascular arterial grafts. The morphological changes observed in saphenous veins when used as an arterial graft have been well described in the literature (Brody et al 1972, Jones et al 1973, Spray and Roberts 1977, Davies and Hagan 1995, O'Brien et al 1997, Kouzi-Koliakos et al 2006). Veins can undergo the following changes:

1. Endothelial damage and disruption
2. Intimal thickening
3. Medial hypertrophy
4. Medial necrosis
5. Graft wall fibrosis
6. Lipid deposition
7. Aneurysmal dilatation

Vein harvesting and preservation may cause mechanical, chemical and ischemic injuries that can cause significant tissue damage. This may result in endothelial cell denudation, endothelial cell injury and smooth muscle cell injury which are important factors for the initiation of intimal hyperplasia. (Davies and Hagan 1995, Cavallari et al 1997, Kalra and Miller 2000). It is very important to handle the vein graft with extreme care during harvesting with minimal instrument contact to the vein wall (Davies and Hagan 1995, Owens 2010). The basic principles of optimal saphenous vein procurement have been established by many studies and includes the use of an appropriate physiological storage solution with a smooth muscle relaxant (Glyceryl trinitrate-verapamil combination or Papaverine) and control of distention pressures to less than 100mm Hg (Gundry et al 1980, Davies and Hagan 1995, Rosenfeldt et al 1999). When the ischemic time of the vein is longer than 90 minutes before transplant, there is significant endothelial cell loss with exposed subendothelial collagen fibres that may aggregate and activate platelets and trigger vascular inflammation (Zou et al 2012).

Veins are highly compliant over the range of venous pressures, but vein tissue loses most of its elasticity at arterial pressure (40 mm Hg for jugular veins and 120mm Hg for saphenous veins) when used as an arterial graft, because its elastic fibres are stretched to the maximum and the inextensible collagen fibres come into play (Wesly et al. 1975). This increase in wall tension and laminar shear stress causes remodeling of the vein wall through endothelium-dependent mechanisms resulting in changes in lumen caliber, wall thickness, composition of

matrix proteins and endothelial cell reactivity (Epstein et al 1994, Owens 2010). This remodeling of the vein is dependent on locally and remotely generated growth factors, vasoactive substances and hemodynamic stimuli.

Intimal thickening of veins implanted in the arterial circulation of dogs was first described in 1906 by Alexis Carrel (Spray and Roberts 1977). This is a universal response of a vein graft implanted in an arterial system and is the result of the migration and proliferation of smooth muscle cells from the media. These smooth muscle cells also deposit an extracellular matrix (Fig 1.33). These hyperplastic lesions appear smooth, firm and homogenous and are located between the endothelium and the medial smooth muscle layer of the vein graft (Davies and Hagan 1995). This intimal hyperplasia is usually a self-limiting process that stabilizes within 2 years after graft insertion, but in focal areas the intimal hyperplastic process can cause significant stenoses in vein grafts (Davies and Hagan 1995).

Early after bypass grafting, the vein graft undergoes significant changes (Brody et al 1972). During the first week there is endothelial cell damage, fibrin deposition, subendothelial edema and necrosis of medial smooth muscle cells with inflammatory cell infiltration. The medial changes are probably initiated by changes in mechanical and chemical stimuli when the vein is transplanted in the arterial system. There is also disruption of vasa vasorum with vascular wall ischemia and denervation of the vascular wall. (Kalra and Miller 2000). With time, the medial smooth muscle cells either undergoes necrosis or fibroblastic transformation which results in medial and intimal fibrous proliferation (Brody et al 1972, Spray and Roberts 1977).

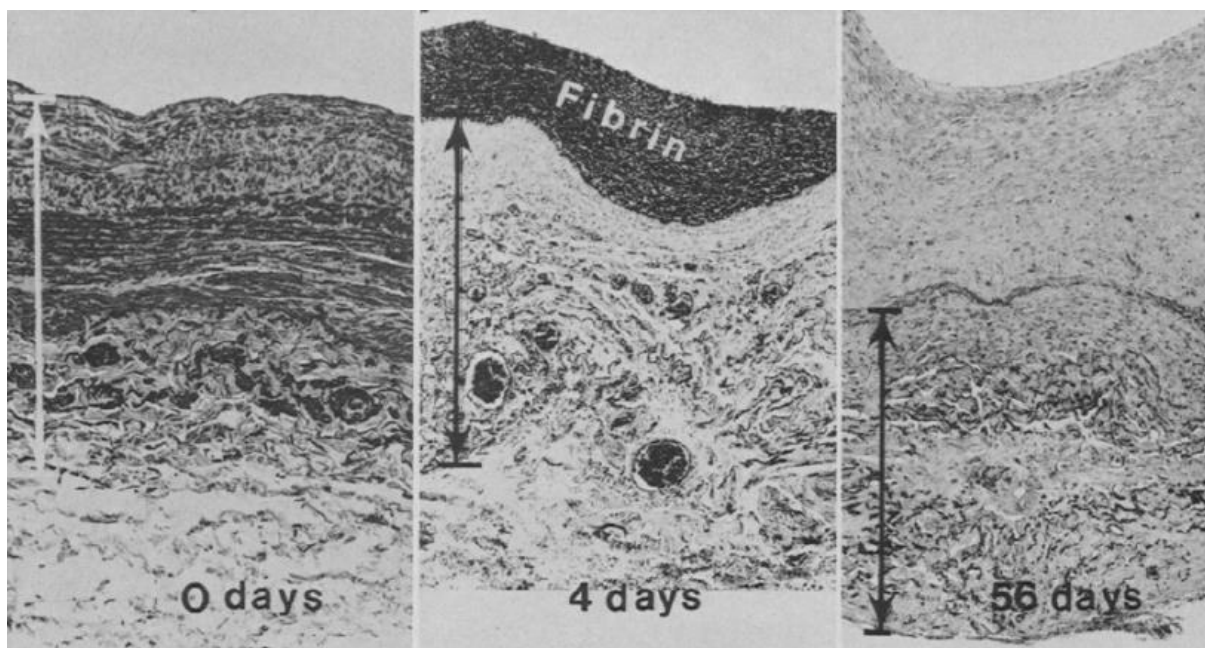
Immunohistochemistry has shed new light on the cellular processes during vein remodeling after arterial grafting (Kalra and Miller 2000). Cell proliferation markers such as MIB-1 immunohistochemistry show increased proliferation of medial and adventitial cells from day 2 in the transplanted vein. This cell proliferation reaches a maximum at 5 days after transplantation and then decreases to minimal levels by 14 days. Phenotypic characterization of proliferating cells by double immunohistochemistry for cytoskeletal markers identifies them as fibroblasts in the adventitia on day 2 (only vimentin positive) and at 5 to 7 the cells appear as myofibroblasts ( $\alpha$ -SM actin positive). This early proliferation of medial and adventitial cells which have phenotypic characteristics of myofibroblasts contribute to the neointimal fibrous proliferation because these cells migrate from the media and adventitia to the neointima by 7-14 days after grafting. Apoptosis was also identified in the vein wall by apoptosis markers and occurred simultaneously with the proliferation and migration (day 2 to 14) which suggests a remodeling process of the vascular wall after arterial transplantation (Kalra and Miller 2000).

**Fig 1.33:** Serial histologic changes in saphenous veins used as aorto-coronary bypass grafts. (Spray and Roberts 1977). Arrows indicate the original vein and thickness.

0 days: Thin intima with marked smooth muscle cell layers.

4 days: Large fibrin deposit over slightly thickened intima. Severe loss of smooth muscle cells in media with cellular infiltration.

56 days: Thickened vein wall with severe intimal fibrous proliferation. Media and adventitia show loss of smooth muscle cells and fibrosis



### **1.10 The proposed study.**

The purpose of this study is to evaluate whether an autologous vein graft can be used to replace a mitral valve leaflet. The fibrous proliferation seen in transplanted vein grafts can cause luminal narrowing when used as a bypass graft, but it might be a useful adaptation when the vein is used to replace a heart valve leaflet by giving the vein extra strength. The questions are:

- Is it technically possible to create a functioning mitral valve leaflet from autologous vein supported by Gore-Tex chordae?
- Will a vein be able to withstand the stress and strain of deformation when used as a valve leaflet and maintain its flexibility?
- Will a vein remain viable in the intracardiac environment when used as a valve leaflet and be able to adapt morphologically and grow?

There is no literature available on the replacement of a heart valve with an autologous vein. In this study a sheep model will be used to replace the anterior leaflet of the mitral valve with an autologous jugular vein and supporting it with Gore-Tex chordae in an attempt to answer the above questions.

## **2. Methods:**

The research was done at the Animal Research Facility at the Tygerberg Campus of the University of Stellenbosch. Animals received humane care in compliance with the Principles of Laboratory Animals Care (NIH 1985). Ethical approval was obtained from the Research Ethics Committee: Animal Care and Use (REC:ACU) of the University of Stellenbosch. (Ref: 11GF\_Jan01).

Twenty one sheep (14 Dorper and 7 Merino) of age 4 to 9 months weighing 26-42 kg were used in the protocol. All animals were fasted for 24 hours prior to surgery with only water given. A pre-operative transthoracic echocardiogram was done as a baseline to measure left ventricular size and function as well as mitral valve function.

### **2.1 Anaesthesia.**

The sheep were premedicated with Ketamine 6-8mg/kg via intramuscular injection. Intravenous access was obtained with an 18 gauge cannula in the right internal jugular vein. This cannula was replaced with a central venous catheter after induction of anaesthesia. Thiopentone 10-14mg/kg was used for induction of anaesthesia. The sheep were then placed in the supine position and intubated with an endotracheal tube and ventilated. Pancuronium bromide 1mg/kg was given as muscle relaxant.

An arterial line was placed in the left or right front leg. The sheep was ventilated with 40% oxygen and alveolar ventilation was monitored with the end-tidal CO<sub>2</sub>, saturation monitoring and arterial blood sampling. The electrocardiogram and temperature were monitored. The sheep's normal temperature is 38.5°C. The sheep's temperature was allowed to drift down before cardiopulmonary bypass and after cardiopulmonary bypass it was controlled by a warming blanket. Intra-operative anaesthesia was maintained with Isoflurane 1.5-2.8% and Pethidien 2-3mg/kg were given for analgesia. Potassium chloride (40mmol) and Magnesium sulphate (1g) were added to the Balsol intravenous fluid and the electrolytes were monitored with arterial bloodgas sampling. Intravenous fluid was limited to 1 litre to avoid hemodilution.



## 2.2 Surgical procedure

### 2.2.1 Harvesting of the internal jugular vein.

The sheep was turned onto its right side with the left neck and chest shaved and cleaned with Hibitane and alcohol solution. Sterile drapes are placed (Fig 2.1). A left sided neck incision was made over the internal jugular vein. The internal jugular vein was exposed for 12 cm, branches were tied and the vein harvested (Fig 2.2). Care was taken not to injure the endothelium. The vein was placed in a 200 ml saline solution with 4000 IU Heparin, 5 mg Verapamil, 2ml Sodium bicarbonate 4.2% and 20 ml autologous blood. The neck incision was closed with 3-0 Vicryl.

**Fig 2.1:** The sheep is anaesthetised, cleaned and draped for the left neck incision and left thoracotomy.

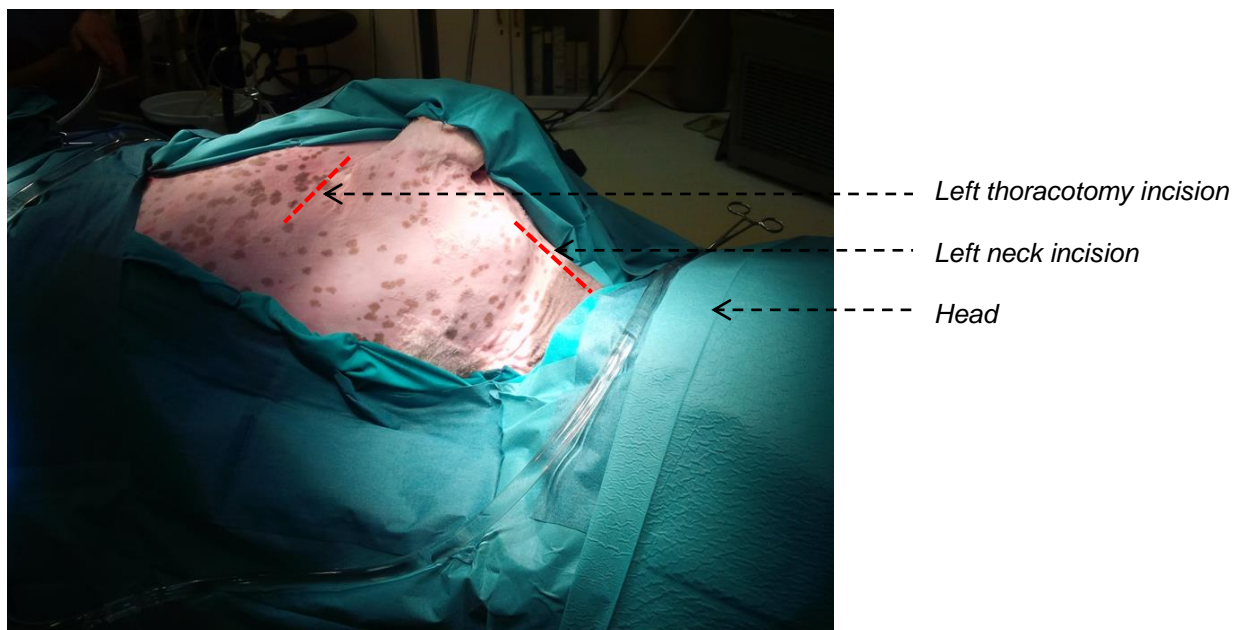


**Fig 2.2:** Left internal jugular vein used for harvesting.



### **2.2.2 Creating the anterior mitral leaflet from the internal jugular vein.**

The vein was then fashioned to form an anterior mitral valve leaflet. The vein was cut open along its length and then folded lengthwise to create a rectangular shaped vein with the endothelial layer on the outside and adventitial layer on the inside (Fig 2.3 to Fig 2.5).

**Fig 2.3:** Left internal jugular vein after harvesting.

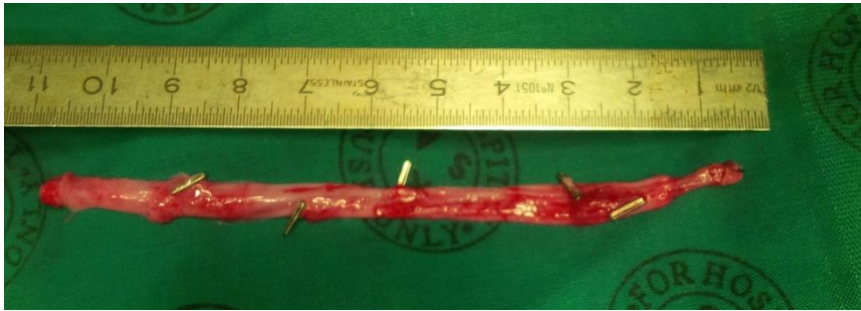


**Fig 2.4:** Liga clips removed and vein cut open along its entire length and opened with intima facing up.

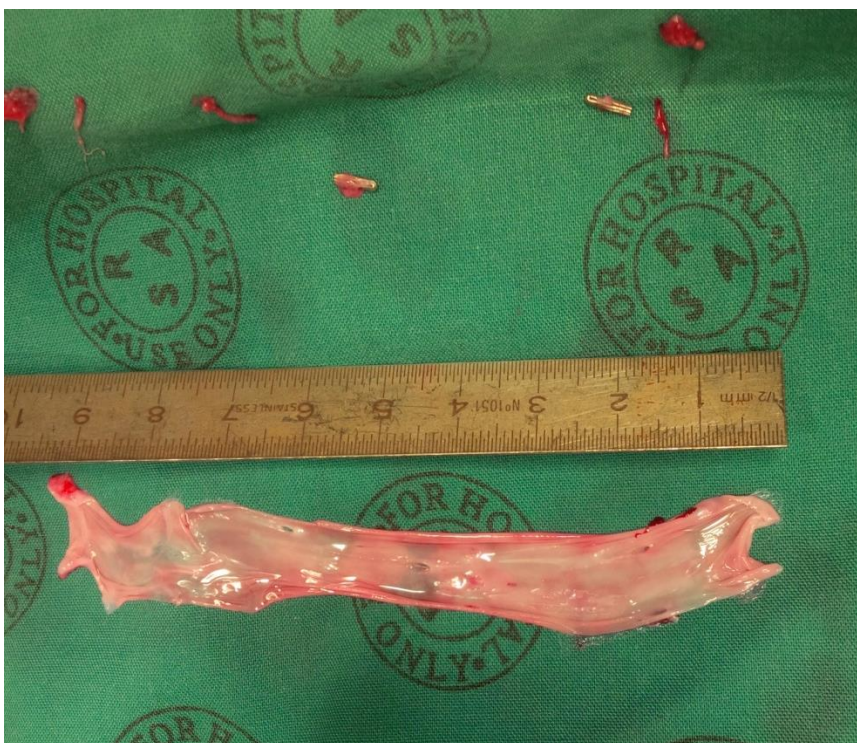


**Fig 2.5:** Vein folded lengthwise with the endothelial layer on the outside and adventitial layer on the inside.



The folded vein was then cut in half (Fig 2.6) and the 2 halves were sewn together side by side with Gore-Tex CV-8 (Fig 2.7) to create an anterior leaflet which measures about 30mm x 20mm or the size of a 28 mitral ring (Fig 2.8).

**Fig 2.6:** The double layered vein is cut in half (along dashed line), creating 2 double layered pieces of vein of about 25mmx14mm

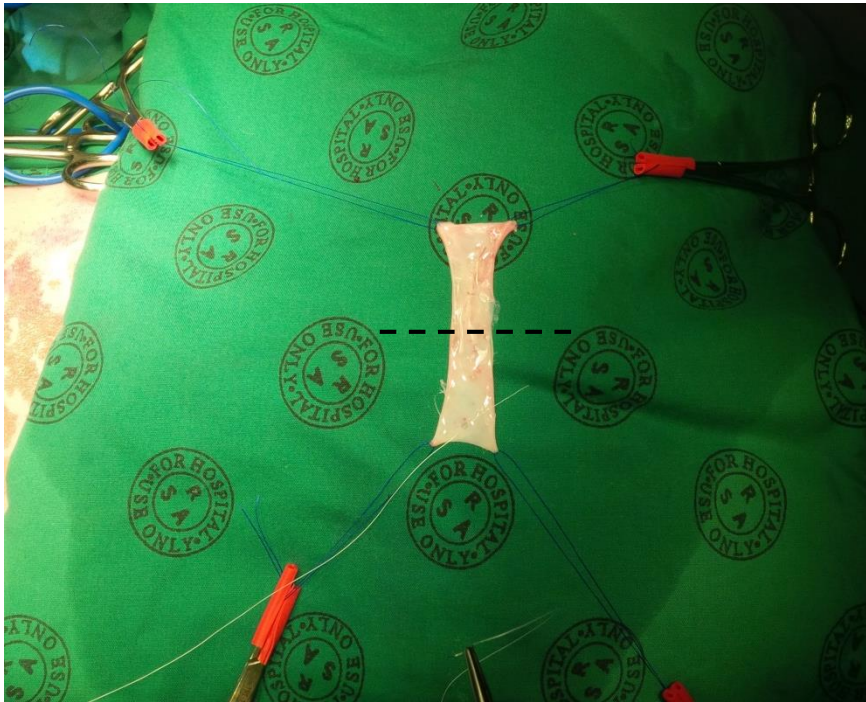


**Fig 2.7:** The 2 double layered halves are sewn together side by side with a Gortex CV-8 suture. Holding sutures on the corners of the vein help with suturing.

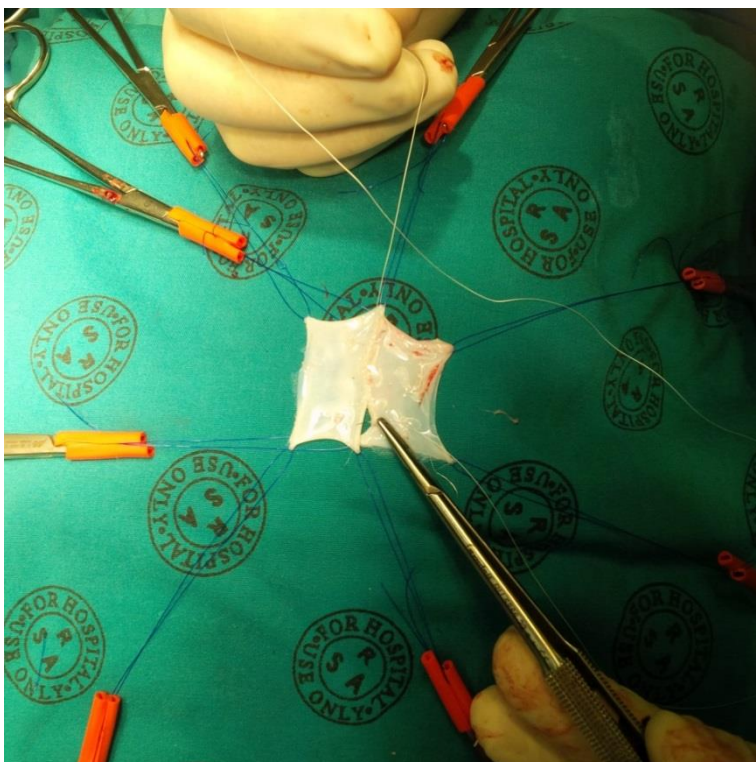
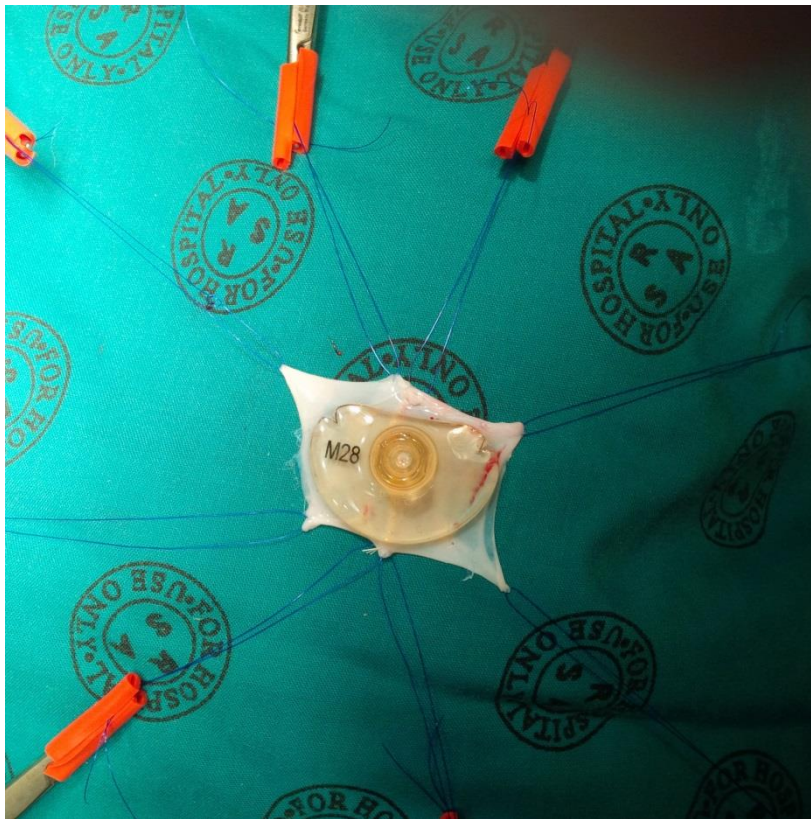
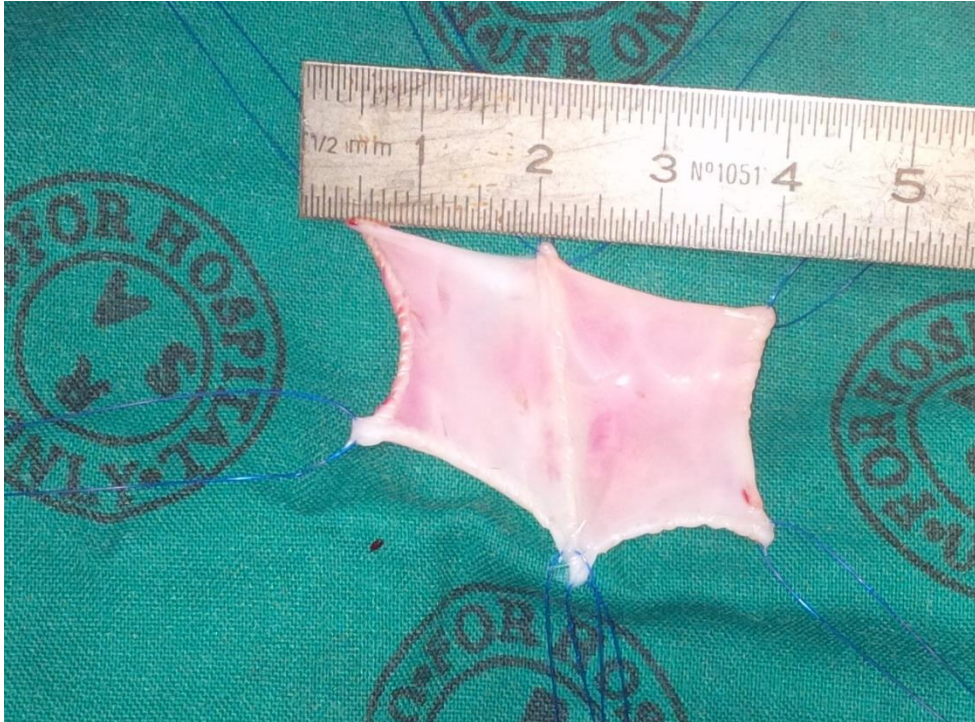


**Fig 2.8:** After suturing the 2 halves together, an anterior leaflet is created that is about the size of a 28mm mitral valve ring.



A simple running suture of Gore-Tex CV-8 was used on the edge of the new vein leaflet around the whole circumference to keep the 2 layers together and strengthen the leaflet edge. All branches were also closed with interrupted Gore-Tex CV-8 sutures. The vein leaflet was then placed in the blood and saline vein mixture.

**Fig 2.9:** A running suture of Gore-Tex CV-8 is used on the edge of the new vein leaflet to keep the 2 layers together and strengthen the leaflet edge.



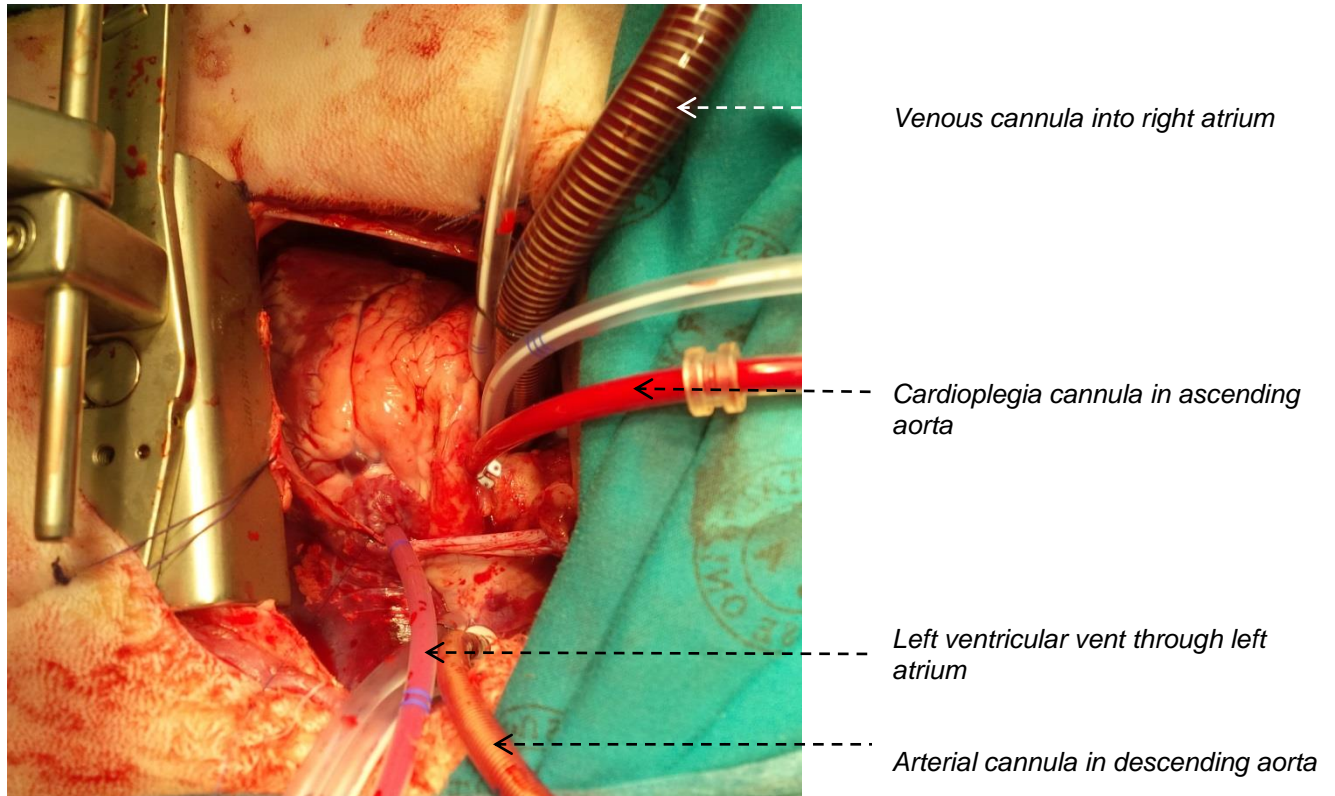
### 2.2.3 Insertion of the vein leaflet.

A left sided thoracotomy was performed in the fourth intercostal space. The pleura was opened and Heparin 1mg/kg was given to raise the activated clotting time (ACT) above 400 seconds. Arterial cannulation of the descending aorta was done with a Medtronic 18 French EOPA cannula (6mm diameter). The ascending aorta in sheep is very short and there was not enough space on the ascending aorta for the aortic cannula, cardioplegia needle and the aortic cross-clamp. The ascending aortic tissue is also delicate and tears easily (as we found during the learning curve).

The pericardium was opened anterior to the phrenic nerve and pericardial stay sutures were placed. A dual stage venous cannula (Medtronic 29/29 French) was placed in the right atrial auricle. This was a challenging exercise because only the tip of the auricle can be seen via the left thoracotomy. Care was taken to guide the cannula down the inferior vena cava,

because the cannula had a tendency to slip through the tricuspid valve into the right ventricle. (Fig 2.10).

**Fig 2.10:** Cardiopulmonary bypass through left thoracotomy.



The cardiopulmonary bypass circuit was primed with one litre of Balsol. Cardiopulmonary bypass was started and the sheep was cooled to 32°C. A cardioplegia needle was placed in the ascending aorta and the aorta was cross-clamped. Cold blood cardioplegia (a mixture of 50% autologous blood and 50% St Thomas cardioplegic solution) was given at 8-10°C. Sixteen mmol of Potassium chloride was added to the first bottle of St Thomas solution to raise the potassium concentration of the first dose to 16 mmol/l. Thereafter, the potassium concentration in the cardioplegia was 8mmol/l. The left atrium was opened and a left ventricular vent cannula was placed through the mitral valve to keep the left ventricle empty during cardioplegia. Cardioplegia was given slowly to prevent the delicate aortic valve from becoming incompetent. Cold saline was poured on the heart after asystole was achieved. The surgical field was flooded with carbon dioxide to limit the possible effects of air-embolism.



The left atrium was opened and the mitral valve was inspected and tested with normal saline in a bulb syringe. Three annular stitches were placed to improve exposure of the mitral valve. The length of the anterior chordae from the anterior and posterior papillary muscle to the leaflet edge was measured with a calliper. The chordal length of the sheep measured between 15mm to 18mm.

The anterior leaflet was then resected 3mm from the mitral annulus to avoid injury to the aortic valve. The anterior leaflet with its chordae was resected up to the level of the commissural leaflets at both commissures. The chordal attachments of the commissural leaflets were left intact (Fig 2.11 and Fig 2.12). The posterior leaflet was left intact and would serve as the control leaflet for this study.

**Fig 2.11:** View of mitral valve from left atrial side.

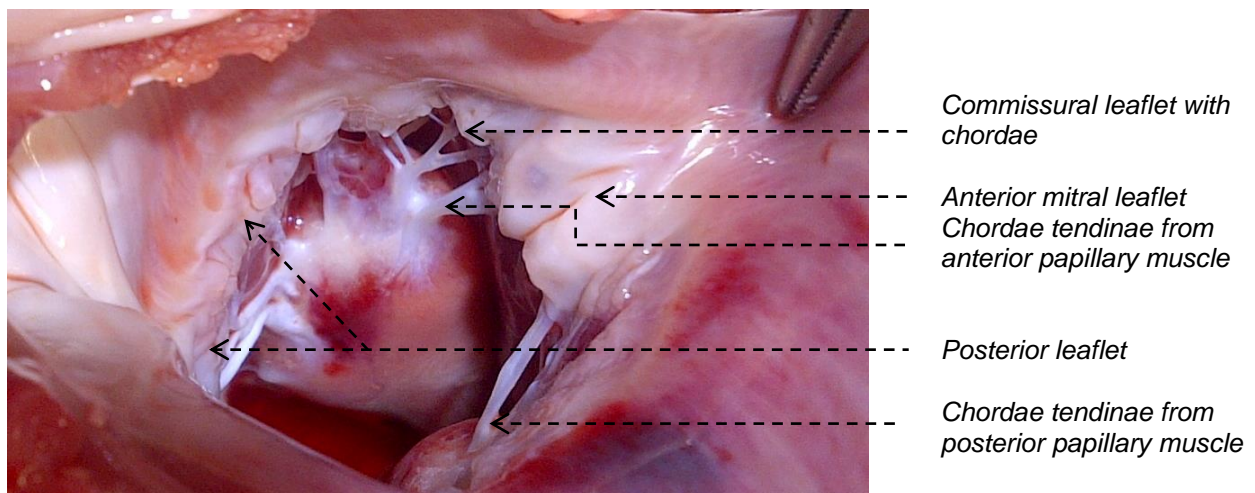
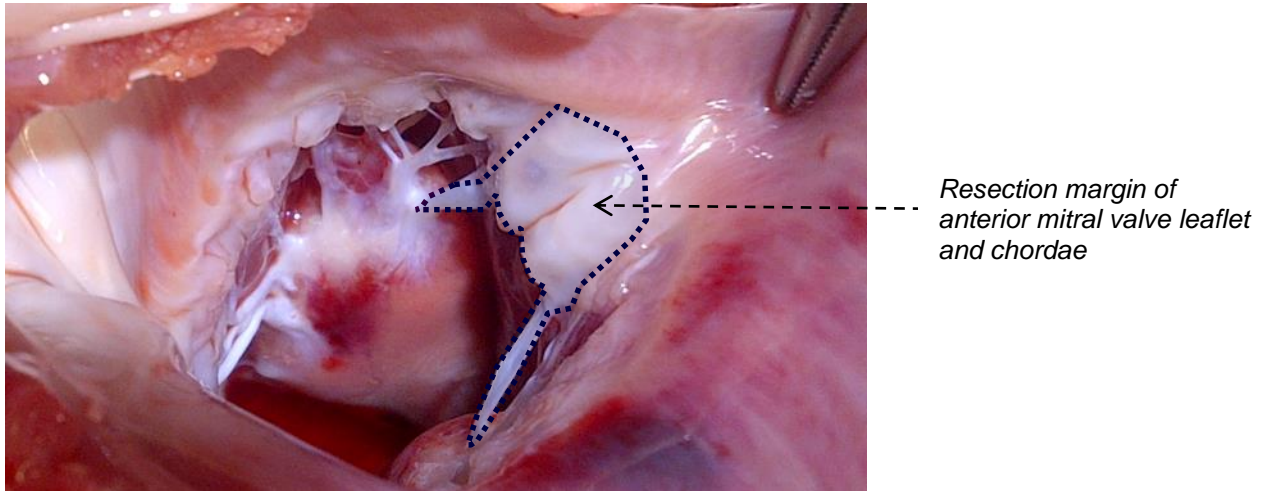
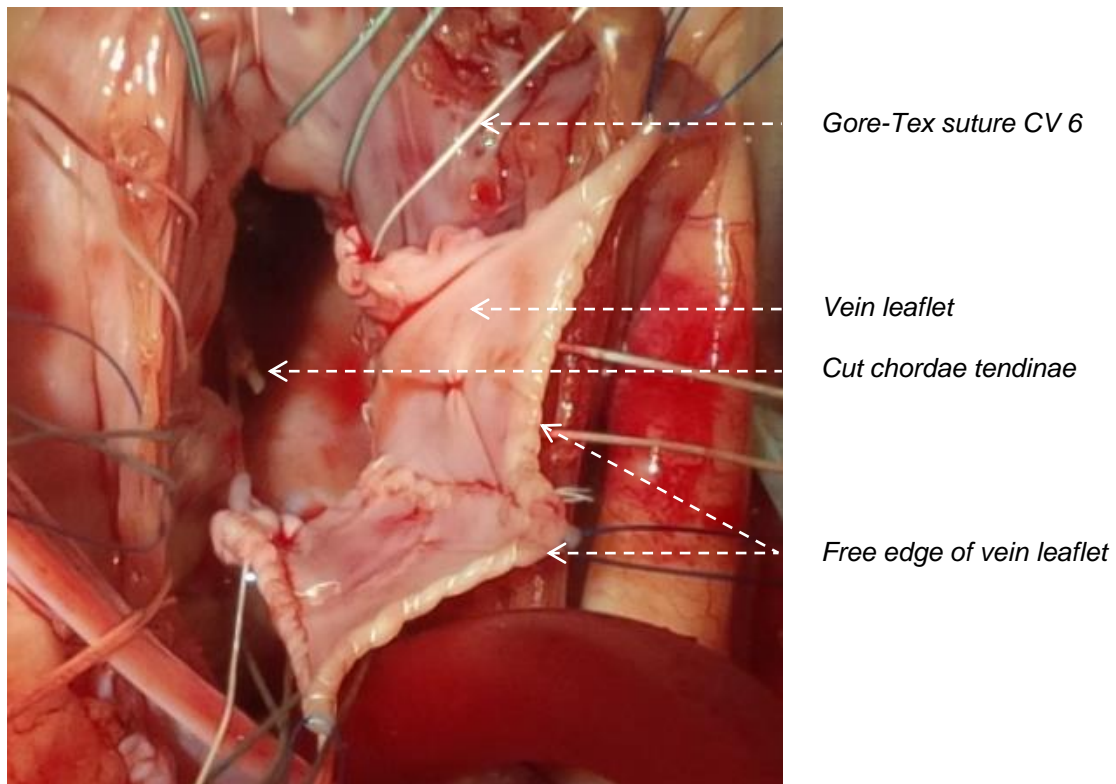


**Fig 2.12:** Anterior mitral leaflet and chordae excised.



The excised anterior mitral valve leaflet dimensions were measured and the newly created vein leaflet was sutured to the anterior mitral annulus with a Gore-Tex CV6 suture (Fig 2.13). The vein was also sutured to the commissural leaflets at both commissures. The free edge of the new vein leaflet was then supported by Gore-Tex chordae.

**Fig 2.13:** Vein leaflet sutured to anterior mitral annulus. The free edge is not supported with Gore-Tex chordae yet and is protruding into the left atrium.



Gore-Tex chordal loops were made intra-operatively from a Gore-Tex CV5 suture according to the length of the native chordae (Fig 2.14 and Fig 2.15). The Gore-Tex loops were tied around a Hegar dilator of the correct size. The principle of obtaining the correct chordal length with a Hegar dilator is as follows: the length of a flattened loop is equal to half the circumference of the Hegar dilator.

The diameter of the correct Hegar dilator needed is calculated from the formula:

$$2L = 2\pi r$$

$$2L = \pi D$$

$$D = \frac{2L}{\pi}$$

$$= \frac{2}{3} L$$

(D=diameter of the Hegar dilator, L=length of the chordae needed and because it is a loop, the length would be 2L,  $\pi = \frac{22}{7}$ ).

To simplify the equation,  $\pi$  is rounded off to 3 and the diameter of the Hegar dilator needed is then 2/3 of the length of the chordae. If the chordae length is 18 mm, the Hegar dilator diameter would be  $\frac{2}{3} \times 18 = 12\text{mm}$ . (Cagli 2009).

**Fig 2.14:** Gore-Tex loops made intra-operatively with a Hegar dilator.

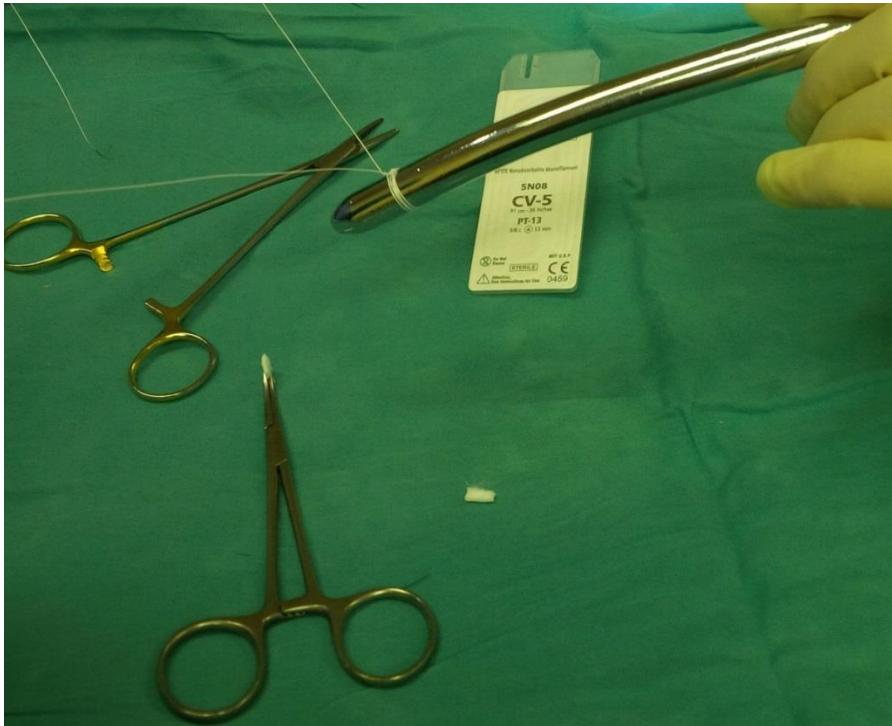
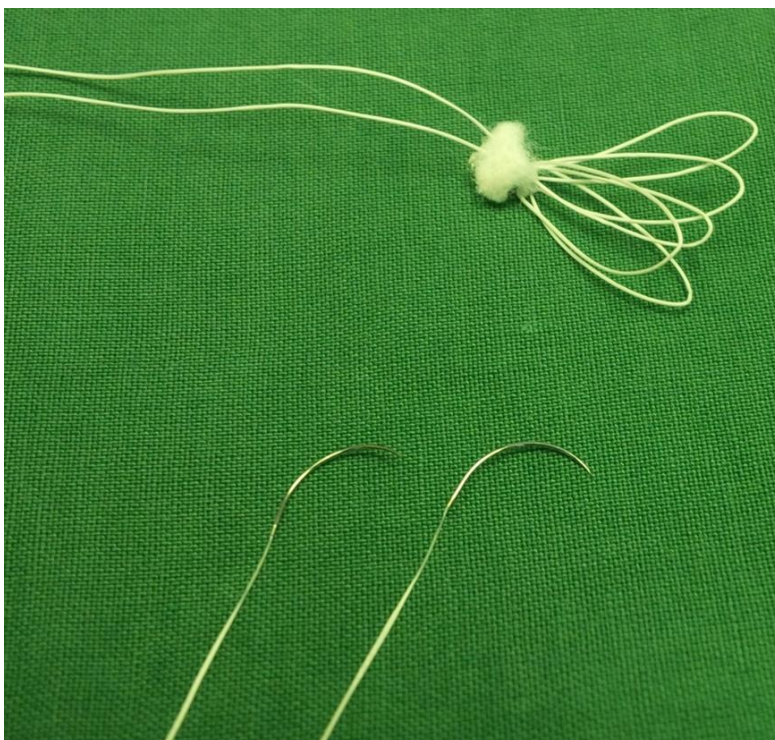


**Fig 2.15:** Completed Gore-Tex loops on a felt pledget ready for implantation.



Six Gore-Tex loops were anchored to the fibrous tip of the anterior papillary muscle with felt pledgets and 6 Gore-Tex-loops were anchored to the posterior papillary muscle. The principles of mitral valve repair were then used to support the edge of the new vein leaflet. The antero-lateral half of the leaflet (A1 and half of A2) was supported with the chordal loops from the anterior papillary muscle and the postero-medial half (half of A2 and A3) was supported with the chordal loops from the posterior papillary muscle (Fig 2.15). Interrupted Gore-Tex CV 5 sutures were used to attach the chordal loops to the free edge of the leaflet.

**Fig 2.16:** Gore-Tex loops support the new mitral valve vein leaflet. Six chordal loops from the anterior papillary muscle support the lateral half of the leaflet and 6 chordal loops from the posterior papillary muscle support the medial half of the leaflet.

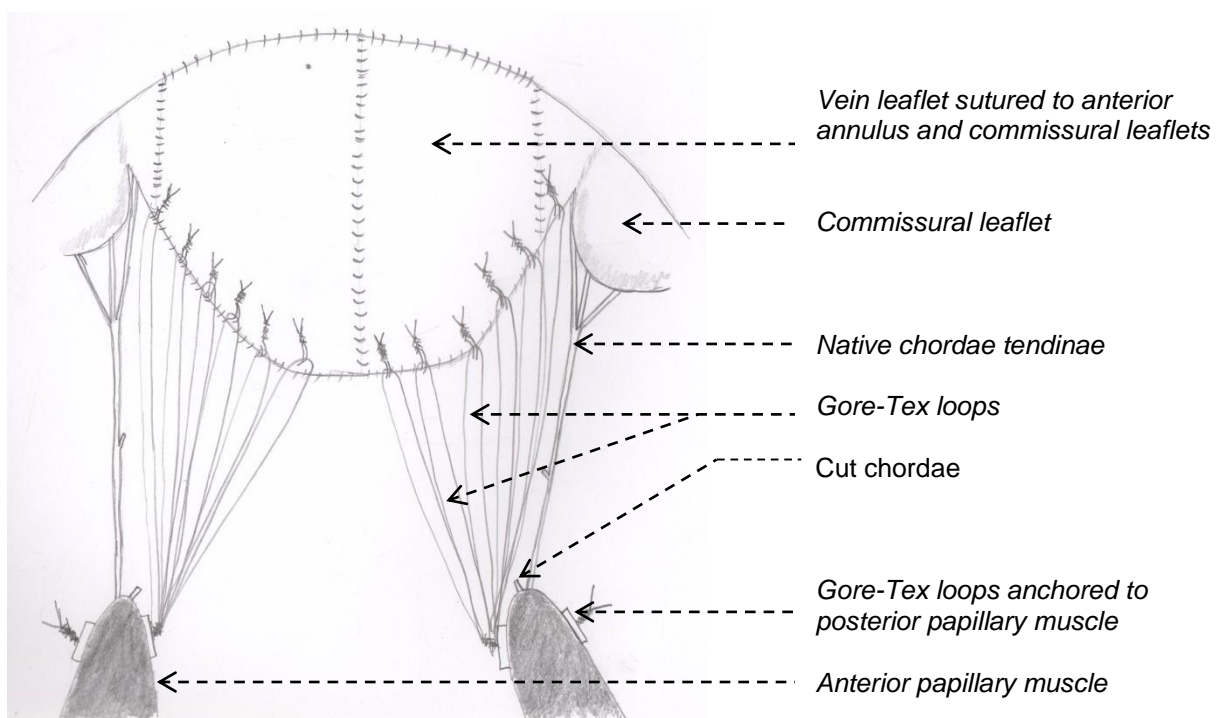
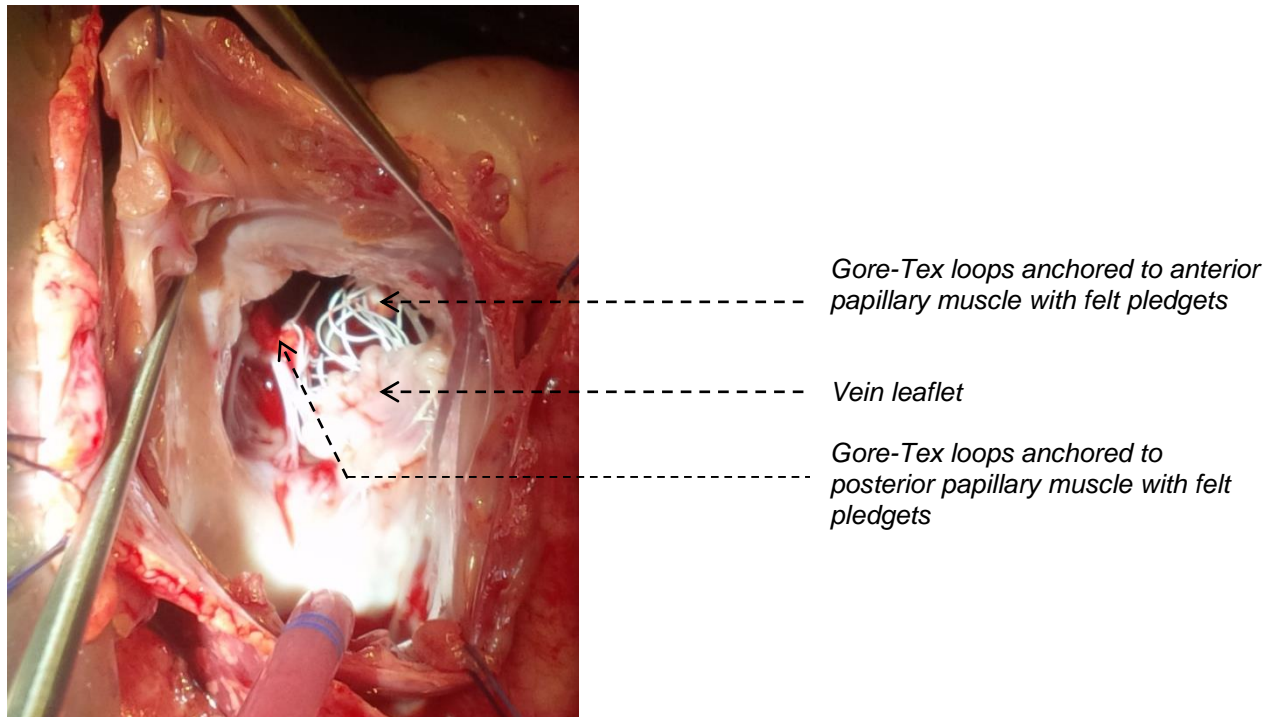


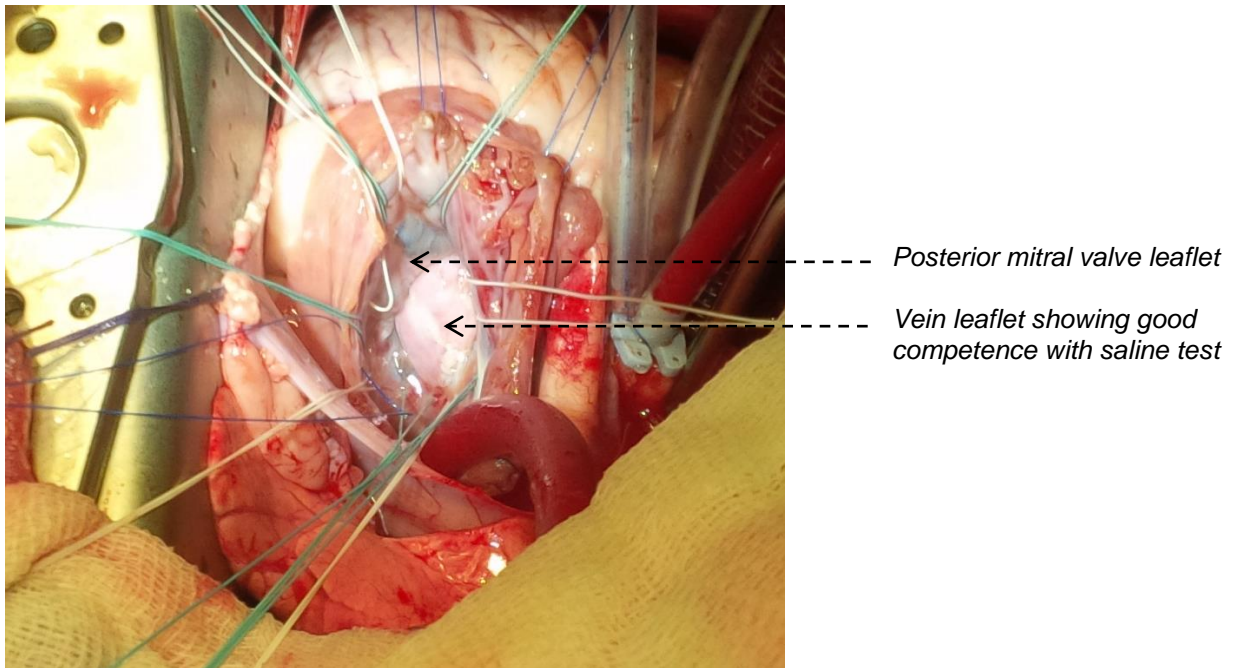
**Fig 2.17:** Vein leaflet supported with Gore-Tex chordae:



The valve was then tested for competence with normal saline. No ring annuloplasty was performed, however 2 sheep had plicating annular sutures in the posterior annulus to improve coaptation. This was done with 2 to 3 Tycron sutures with pledgets.

After the saline test showed the valve to be competent (Fig 2.18), the left ventricular vent was placed through the mitral valve and the left atrium was closed with 5-0 Prolene. The heart was de-aired and the aortic cross-clamp removed. If fibrillation occurred, the heart was defibrillated with internal paddles at 10 Joules and temporary ventricular pacing wires were placed when needed. After 10 minutes of reperfusion, the heart was weaned from cardiopulmonary bypass with a low dose of Adrenalin and Nitroglycerine infusion. The left atrial pressure was measured with a left atrial cannula and then removed. All cannulas were removed and Protamine sulphate (1mg/kg) was given. A pleural drain was placed. An intercostal block was done with 0.5% Bupivacaine (2ml/kg) to help with post-operative analgesia. The pericardium was sutured and the thoracotomy incision was closed. All the blood in the cardiopulmonary bypass circuit was transfused back to the sheep.

**Fig 2.18:** *New anterior mitral valve leaflet tested for competence with saline.*



#### **2.2.4 Postoperative care**

The sheep was monitored and ventilated in theatre until it was awake and breathing spontaneously. The muscle relaxant was reversed with neostigmine (0.04mg/kg) and atropine (0.02mg/kg). Awake extubation was performed, the pleural drain, pacing wires, intra-arterial and intravenous lines were removed (Fig 2.19). The sheep was then transferred to a warm pen with a blanket, food and water (Fig 2.20).

The sheep received Meloxicam 0.5mg/kg per day for analgesia. A long acting opiate was given for the first 2 nights post-operatively (Buprenorphine 0.05mg/kg) and Pethidine 1-2mg/kg every 8 hours during the day. Intramuscular Enrofloxacin was given as an antibiotic for 3 days.



**Fig 2.19:** The sheep was extubated when fully awake and breathing spontaneously. All lines were removed.



**Fig 2.20:** The sheep was transferred to a warm pen after surgery:



## 2.4 Echocardiography

A transthoracic echocardiogram was done post-operatively by Dr Pieter Rossouw a Cardiologist from the Cardiology department at the University of Stellenbosch to evaluate the mitral valve function and cardiac function. The following parameters were recorded:

- Amount of mitral regurgitation
- Position of regurgitation
- Movement of the anterior vein leaflet during the cardiac cycle
- Valve opening area and diastolic flow through the valve
- Left ventricular size
- Left ventricular function

The sheep was kept at the animal laboratory for 1 to 2 weeks and then transferred to the University of Stellenbosch's experimental farm in Stellenbosch (Fig 2.21).

The sheep were monitored on the farm and serial echocardiograms were also done at 1 month, 3months, 6 months and 9 months to evaluate the mitral valve and cardiac function (Fig 2.22)

**Fig 2.21:** *On the farm the sheep grazed in the field during the day and were kept in a shed at night.*



**Fig 2.22:** Serial echocardiograms were done on the sheep to evaluate mitral valve and cardiac function.



## 2.5 Pathology and histology

The sheep were followed up post-operatively for 6 to 10 months. At the time of euthanasia the sheep were first anaesthetised (see before) and a small laparotomy incision was done to do a trans-diaphragmatic echocardiogram. This was done to get better echocardiographic views of the heart and mitral valve. After the echocardiogram was done, the sheep were euthanized with an intravenous bolus of potassium chloride (20 mmol).

The heart and lungs were excised, inspected and photographed. The heart was weighed and the annulus circumference was measured. The vein leaflet was examined for mobility, signs of fibrosis, prolapse and calcification. The Gore-Tex chords and its attachment sites to the free edge of the vein leaflet and papillary muscles were examined and photographed. The lung was examined for signs of pulmonary edema. The hearts and lungs were also retrieved from sheep that died early. The specimens were fixed in a 10% buffered formalin solution for at least 24 hours. Histology was done by Dr Izak Loftus (MBCbB, MMed (Forens Path), FForPath (SA), MMed (Anat Path)) from Pathcare.

Histological samples were taken from the following areas:

1. Left ventricular muscle.
2. Vein leaflet from the leaflet tip to the annulus.
3. Posterior leaflet (control).
4. Gore-Tex chords and its attachments to the papillary muscle and free edge of the vein leaflet.
5. Lungs.

The tissue sections were processed as paraffin blocks and histological sections of 5-6  $\mu$ m thickness were cut from the paraffin blocks.

Haematoxylin and Eosin (H and E) stains were done routinely on all sections. Special stains were also done on the vein and posterior leaflet (control) to stain for specific connective tissue components:

- Alcian blue Periodic Acid Schiff (APAS) stain for acid mucopolisaccharide, proteoglycans and extracellular matrix.
- Verhoeff and Van Gieson stain for collagen and elastic fibres.

- Masson's Trichrome stain for collagen and fibrin.
- Von Kossa stain to identify and quantify calcification.

A gram stain and an APAS stain was used on certain sections where infective endocarditis was suspected. Microbiological culture was also done from valve tissue when infective vegetations were suspected.

Monoclonal Mouse anti-human Ki-67 antigen (clone MIB-1, M7240, Dako Denmark A/S) immunohistochemistry was used in some histological specimens of the vein leaflet as a proliferation marker to identify cell proliferation in the vein leaflet and also to assist indirectly in the distinction between viable and necrotic areas.

Muscle specific Actin (MSA) mouse monoclonal antibody (clone HHF35, NCL-MSA, Novacastra UK) immunohistochemistry was used in some histological specimens of the vein leaflet as an alpha actin marker to identify myofibroblasts and smooth muscle cells in the tunica media and tunica adventitia.

The histological specimens of each vein leaflet were examined for the following:

- Amount of overlying fibrin on the leaflet
- Presence and viability of endothelial cells
- Presence and amount of calcification in the vein leaflet
- Whether the space between the 2 layers of the vein leaflet was obliterated or not and the nature of the obliteration (fibrin, fibrous proliferation, fluid)
- Thickness of the valve
- Presence of infective vegetation
- Presence and amount of calcification and endothelialisation of chordae tendinae
- Presence and amount of calcium in the annulus

The magnification given in the histological sections is the original magnification of the slide with an ocular magnification of 10x multiplied by the objective magnification of 2x, 4x, 10x, 20x or 40x.

### **3. Results**

#### **3.1 General remarks**

**3.1.1** Twenty one sheep (14 Dorper and 7 Merino) of age 4 to 8 months weighing between 26-42kg had replacement of the anterior mitral valve leaflet with an autologous jugular vein leaflet. The average cross-clamp time was 99 minutes (76 to 151 min) and the average bypass time was 137 minutes (109 to 188 min) (Table 3.1).

**3.1.2** Left atrial pressure before cardiopulmonary bypass was between 6-12 mm Hg. After weaning from cardiopulmonary bypass the left atrial pressure was between 14-23 mm Hg. A left atrial pressure above 20 mm Hg was associated with early mortality (Table 3.1).

**Table 3.1: Peri- and post-operative data:**

Sheep	Cross-clamp time (min)	Bypass time (min)	Intra-operative saline test	Left atrial pressure after Bypass (mm Hg)	Post-op echocardiography Amount of Mitral regurgitation (MR) (Trace, mild, moderate, Severe)	Lifespan after surgery	Cause of death
1	115	145	Mild MR at commissures	14	Mild to moderate	4.1 months	2 loose Gore-Tex Chordae with A2 prolapse, severe MR
2	111	144	Mild MR at A3/P3	18	Mild to moderate	1 month	Hematoma in vein at A3. A3 prolapsing segment with Gore-Tex chords loose at A3
3	123	165	Mild MR at commissures	14	Trace	9.7 months	Euthanasia
4	129	154	Mild MR at commissures	18	Moderate to severe	2 days	Leaflet prolapse because Gore-Tex chordae were too long.
5	117	140	Very mild MR at commissures	14	Trace	8.3 months	Euthanasia
6	89	119	mild MR at commissures	15	Mild	7.2 months	Euthanasia
7	100	125	Mild MR	20	Moderate	2 days	Vein leaflet folded in at P3 by chordal knot
8	93	155	Mild MR	18	Mild	6 months	Euthanasia, SBE
9	82	115	Very mild MR at commissures	18	Mild	6.5 months	SBE, with severe MR
10	112	149	Commissural MR Annuloplasty done	14	Mild	6.5 months	Euthanasia
11	151	183	Commissural MR Annuloplasty done	23	Moderate	1 month	Euthanasia for dyspnea. SBE found on histology. Organised hematoma at A2.
12	80	122	Very mild MR at commissures	14	No echo was done	Intra-operative death	Air embolism after bypass when transfusing blood into left atrium.
13	100	188	Very mild MR at commissures	14	Trace	6.4 months	Euthanasia

Sheep	Cross-clamp time (min)	Bypass time (min)	Intra-operative saline test	Left atrial pressure after Bypass (mm Hg)	Post-op echocardiography Amount of Mitral regurgitation (MR) (Trace, mild, moderate, Severe)	Lifespan after surgery	Cause of death
14	76	157	Very mild MR at commissures	14	Trace	6 months	Euthanasia
15	78	110	Mild MR at lateral commissure	19	Trace	4 months	Calcification of the Gore-Tex chords and the Gore-Tex chords from the medial papillary muscle showed a partial disruption from A2
16	76	109	Very mild MR at commissures	17	Mild	6 months	Euthanasia
17	79	111	Very mild MR at commissures	15	Trace	6 months	Euthanasia
18	89	119	Mild MR	18	Mild	4 months	SBE, rupture of chord from A2, A3
19	90	120	Mild MR at commissures	21	Moderate	3 days	Anterior leaflet prolapse from Gore-Tex chordae that were too long
20	82	115	Mild MR at P3/A3 commissure	15	Mild	3 months	Tear in leaflet at Gore-Tex suture line
21	116	154	Mild MR at medial commissures	18	Mild	6 months	Euthanasia

MR = Mitral regurgitation

SBE = Infective endocarditis



### 3.2 Echocardiographic results

The immediate post-operative echocardiogram showed trace mitral regurgitation (MR) in 6 sheep, mild MR in 8 sheep, mild to moderate MR in 2 sheep, moderate MR in 3 sheep and moderate to severe MR in 1 sheep (Table 3.1). The MR was almost always at one or both of the commissures (Fig 3.1) (Table 3.2). The amount of commissural MR was determined by the chordal length of the commissural Gore-Tex chordae. All the Gore-Tex chordae to one half of each leaflet were anchored to one papillary muscle and then fanned out to the leaflet edge (Fig 3.2). When the Gore-Tex chordae length to the commissural areas were not perfect, the vein leaflet would either be tethered slightly or prolapse slightly. The margin for error at the commissures is the smallest because there is a small area of coaptation between the vein leaflet and the commissural leaflet. Native chordae tendinae fan out from the distal part of the chordae and not from the papillary muscle, thus creating a leaflet edge that is aligned in a single plane. This is difficult to recreate with Gore-Tex chords that fan out from the papillary muscle (Fig 3.2).

The vein leaflet opened well during diastole (Fig 3.4 and Fig 3.5) and the diastolic flow through the valves was laminar on colour flow. The opening valve area was measured with planimetry and measured from 2.2 cm<sup>2</sup> to 3.7cm<sup>2</sup> (Average 2.8 cm<sup>2</sup>).

**Fig 3.1:** Echocardiogram of sheep 13 with colour flow Doppler shows 2 incompetence jets at the commissures that was seen in most of the valves.

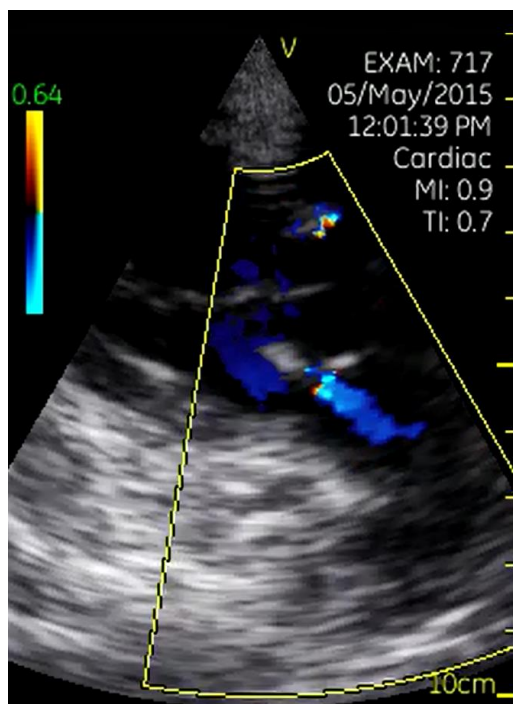
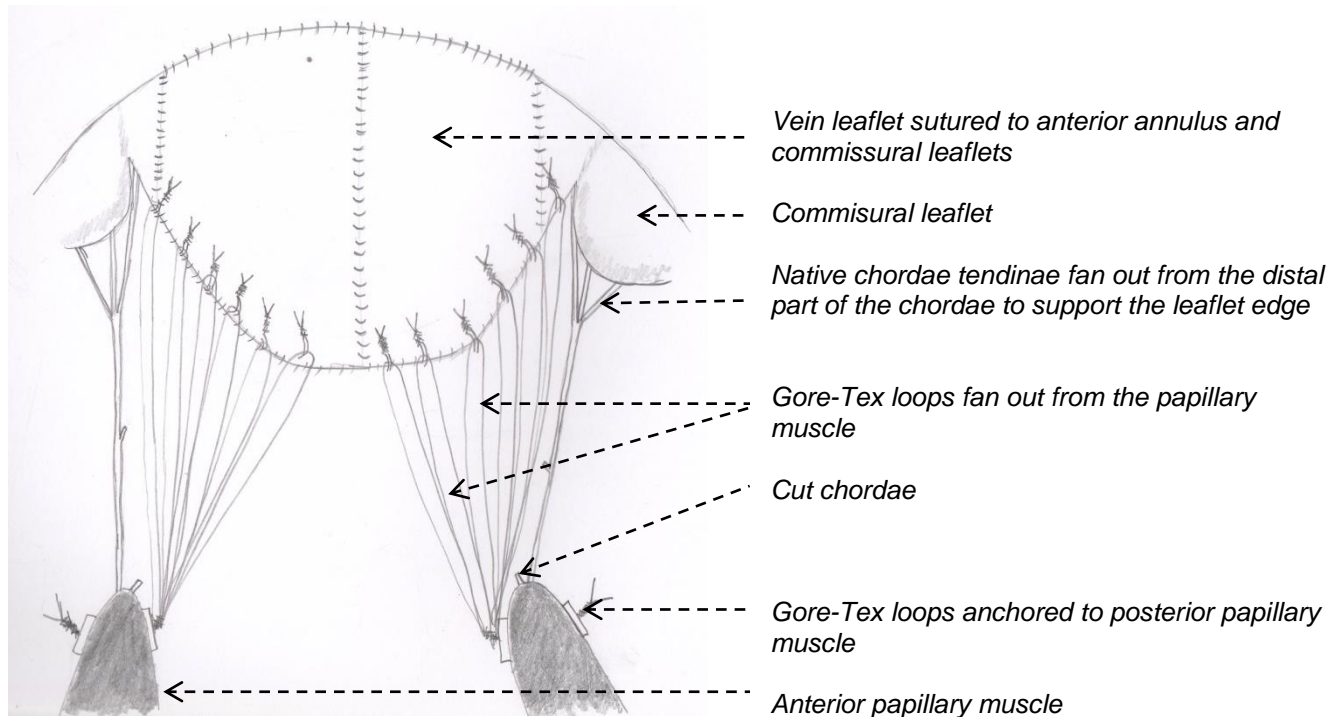


**Fig 3.2:** Suture technique of the Gore-Tex chordae showing the difference in the Gore-Tex chordae and the native chordae tendinae.



The post-operative echocardiogram also showed that the central part of the vein leaflet tends to billow (Fig 3.3 to Fig 3.7). The vein leaflet appears thicker than the posterior leaflet and shows elasticity during the cardiac cycle (Fig 3.4 to Fig 3.6). In diastole it recoils and appears shorter and thicker while in systole it is stretched out, and billows into the left atrium. The billowing of each valve was graded mild, moderate and severe according to the amount of the leaflet body that billows above the mitral annulus (Fig 3.3 to Fig 3.7) (Table 3.2). Although the billowing does not cause prolapse in itself, it does put all the tension on the primary Gore-Tex chordae at the leaflet edge during systole.

**Fig 3.3:** Echocardiogram of sheep 8 to show **severe** billowing of the belly of the vein leaflet (red arrow) during systole. The level of the annulus is shown by the yellow line. The left ventricle (LV) and left atrium (LA) is marked.

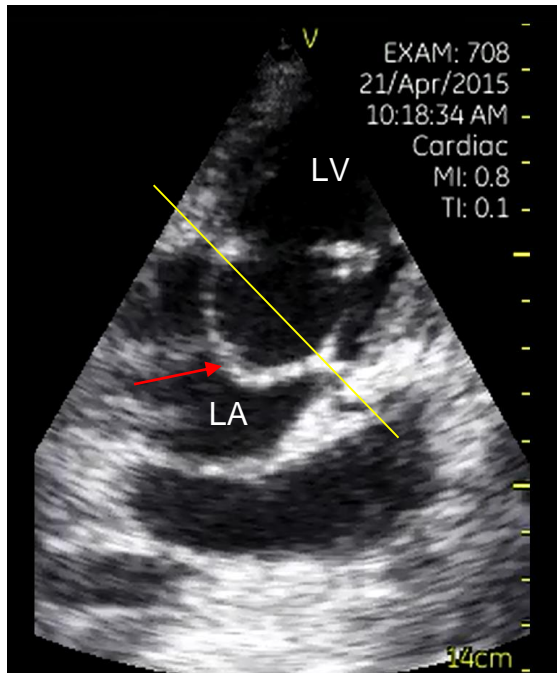
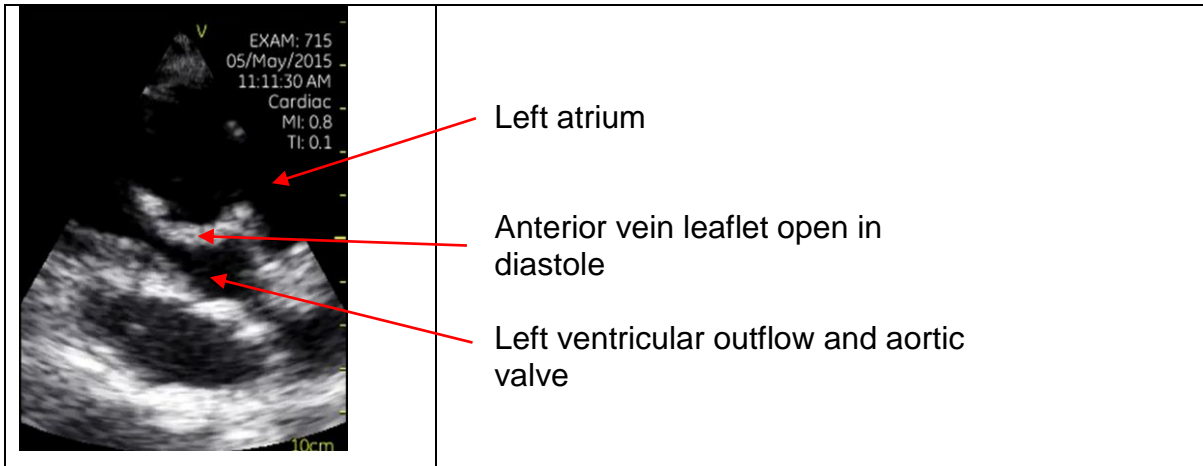


**Fig 3.4:** Echocardiogram of sheep 8 at 6 months post op to show the motion of the anterior vein leaflet during the cardiac cycle. Notice the change in shape of the leaflet and how flexible the leaflet is.

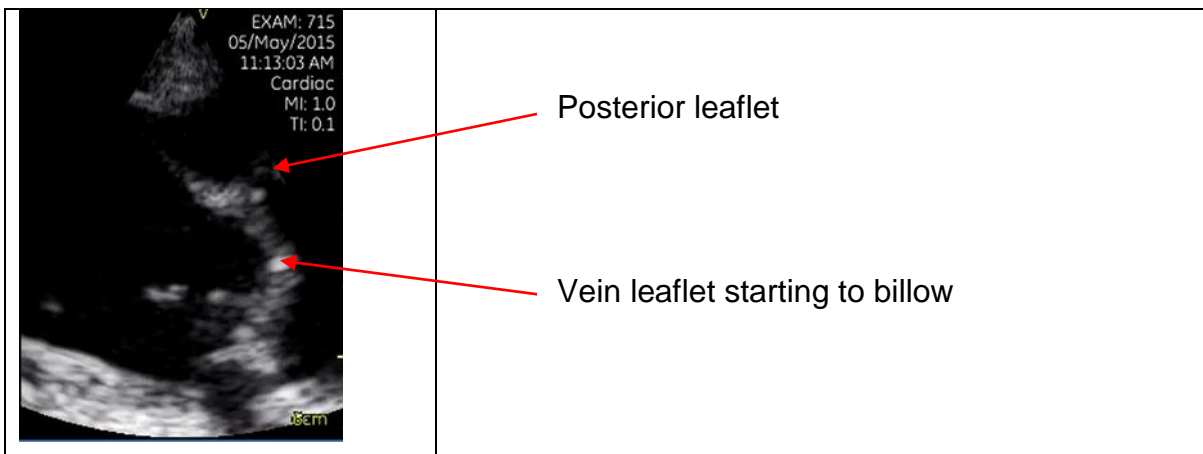
Valve is open in diastole	Valve closing during end of diastole	Valve starting to billow with systole	Final position in systole with even more billowing

**Fig 3.5:** Echocardiogram of sheep 10 shows **moderate** billowing of the anterior mitral valve leaflet

Valve open in diastole



Valve closing during end of diastole



Valve billowing during late systole

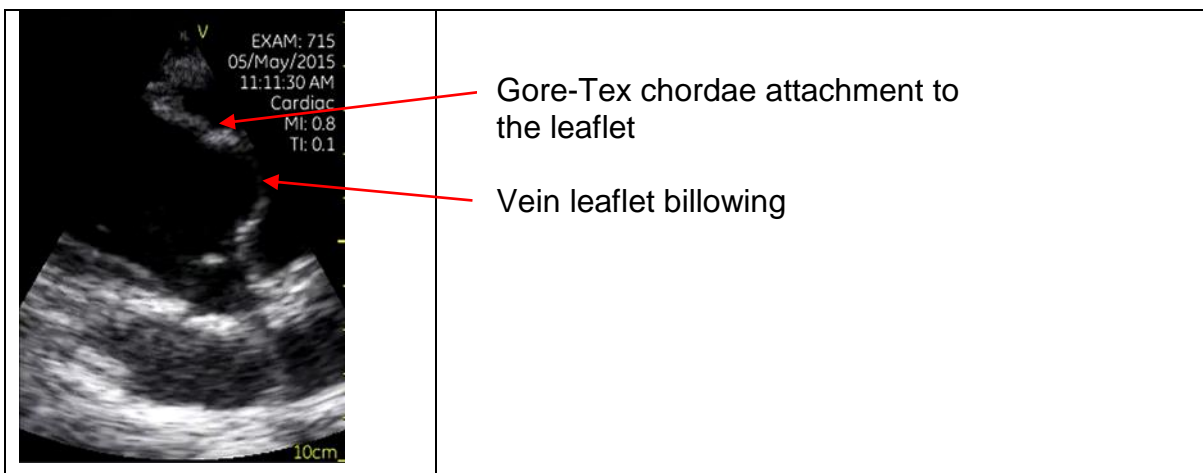
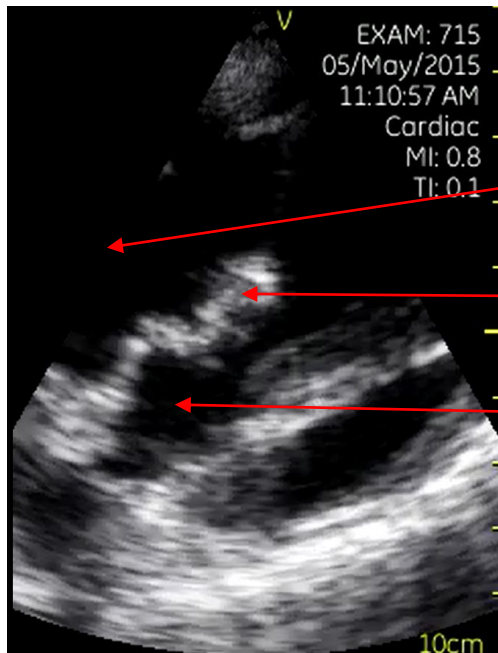


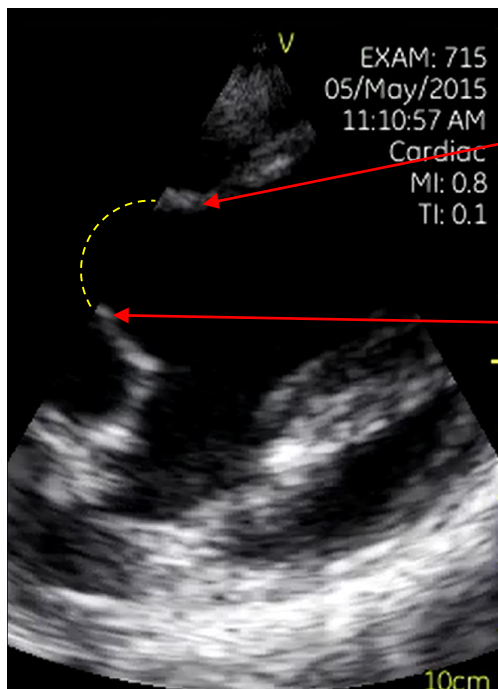
**Fig 3.6:** Echocardiogram of sheep 16 at 6 months to show the elasticity of the leaflet during the cardiac cycle.



Left atrium

Anterior vein leaflet recoils during diastole in the open position

Left ventricular outflow tract

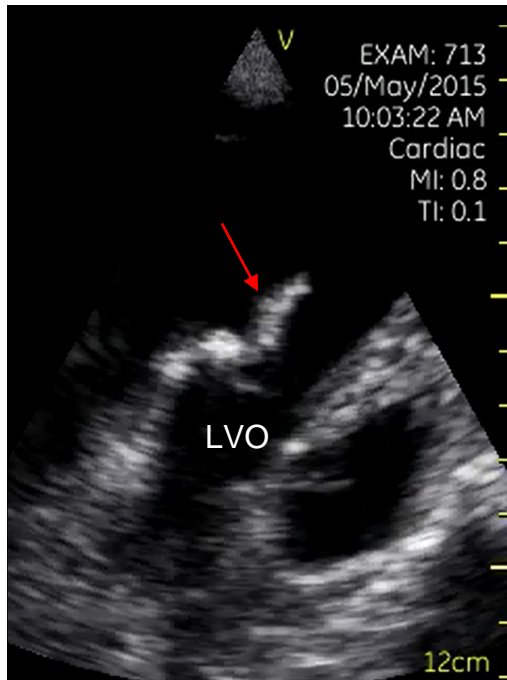


Gore-Tex chordae attachment site

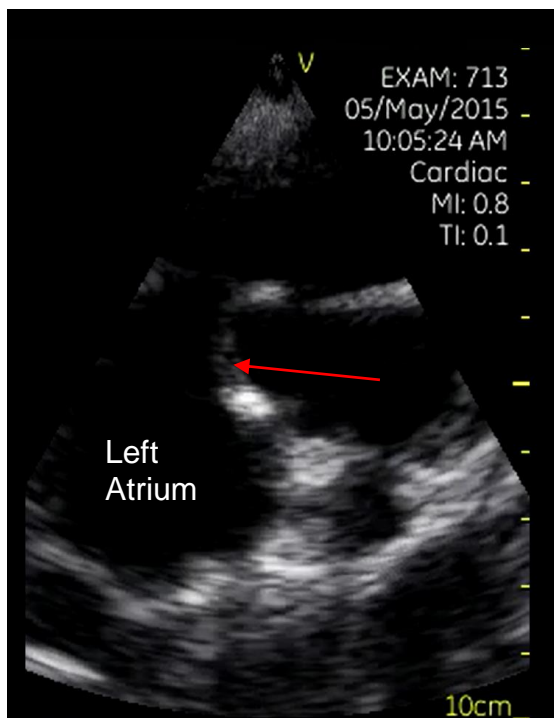
Anterior vein leaflet is stretched during systole and billowing. Part of the leaflet belly is out of the echo window but the course of the leaflet is indicated by the yellow line.

**Fig 3.7:** Echocardiogram of Sheep 3 at 10 months shows **mild billowing** during systole (red arrow). This sheep had mild MR. Left ventricular outflow tract is shown as LVOT

(a) Diastole



(b) Systole



The serial echocardiographic results are summarised in Table 3.2. The 3 month and 6 month echocardiograms showed that the mitral regurgitation (MR) progressed with time in most of the sheep. Fifteen sheep had a 3 month echocardiogram which showed that 7 sheep had mild MR, 4 sheep had mild to moderate MR and 4 sheep had moderate MR.

Eleven sheep had an echocardiogram at 6 months which showed that 3 had mild MR, 1 had mild to moderate MR, 4 had moderate MR and 3 had moderate to severe MR. The increase in MR was most often seen at either one or both of the commissures (Table 3.2).

The left ventricular function remained good in all the sheep except sheep 16 showed poor function from the 3 month echocardiogram with a dilated ventricle. The MR in this sheep was mild and was not the cause of the poor left ventricular function.

The left ventricular end diastolic diameter (LVED) increased in all sheep with time, but was more pronounced in the sheep with moderate and severe MR. The sheep with mild MR at 6 months had an increase in LVED of about 10 mm. This could be attributed to somatic growth of the sheep, because the sheep gained about 7-10 kg in 6 months.



**Table 3.2:** Echocardiographic results directly after surgery and at 3 and 6 months.

Sheep	Amount of mitral regurgitation (MR)			Left ventricular end diastolic diameter (mm)			Area of MR Anterolateral commissure (ALC) Posteromedial commissure (PMC)	Amount of vein leaflet billowing	Ejection fraction on last echo (%)
	Post-operatively	3 months	6 months	Post-operatively	3 months	6 months			
1	Mild to moderate	Mild to moderate		40	45		ALC	Moderate	65
2	Mild to moderate			36			ALC	Moderate	65
3	Trace	Mild	Mild	42	50	52	PMC	Mild	65
4	Moderate to severe			38			ALC	Moderate	60
5	Trace	Mild	Moderate	41	48	52	PMC	Moderate	65
6	Mild	Mild to moderate	Moderate to severe	43	55	60	PMC	Moderate	60
7	Moderate			41	49		PMC	Moderate	60
8	Mild	Mild to moderate	Moderate to severe	32	50	60	ALC and PMC	Severe	65
9	Mild	Mild to moderate	Moderate to severe	40	51	57	ALC	Moderate	65
10	Mild	Mild	Mild	34	42	43	ALC	Moderate	65
11	Moderate			44			ALC and PMC	Mild	55
12	No echo was done								

	Amount of mitral regurgitation (MR)			Left ventricular end diastolic diameter (mm)			Area of MR Anterolateral commissure (ALC)  Posteromedial commissure (PMC)	Amount of vein leaflet billowing	Ejection fraction on last echo (%)
	Post-operatively	3 months	6 months	Post-operatively	3 months	6 months			
13	Trace	Mild	Mild to moderate	40	53	52	ALC	Moderate	60
14	Trace	Mild	Moderate	41	55	58	ALC and PMC	Moderate	55
15	Trace	Moderate		35	54		ALC and PMC	Severe	65
16	Mild	Mild	Moderate	44	58	66	ALC	Moderate	20
17	Trace	Moderate	Moderate	39	44	46	ALC	Moderate	55
18	Mild	Moderate		38	65		ALC	Severe	60
19	Mild			40			PMC	Moderate	65
20	Mild	Moderate		42	52		ALC	Severe	65
21	Mild	Mild	Mild	39	46	48	ALC	Moderate	65

### 3.3 Early post-operative mortality (0-3 days) (Table 3.3)

**Table 3.3:** Results of sheep that died within the first 3 days.

Sheep nr	Time between surgery and death	Lung histology	Vein leaflet morphology	Heart weight (gm)	Annulus length (mm)
4	2 days	Congestion, Edema	Anterior leaflet prolapse from Gore-Tex chordae that were too long	187	63
7	2 days	Congestion	Restriction of the anterior mitral leaflet due to a Gore-Tex suture catching the opposite leaflet edge	215	72
12	Intraoperative death	Congestion	Freshly implanted valve leaflet	179	60
19	3 days	Congestion	Anterior leaflet prolapse at A3 from Gore-Tex chordae that were too long	348	83

Sheep 12 died intra-operatively after being weaned from cardiopulmonary bypass. There was bleeding from the descending aortic cannulation site with the purse string suture tearing out. The bleeding was controlled and blood from the bypass pump was transfused into the left atrium with the arterial cannula. Unfortunately a large air embolism from the bypass circuit went into the left atrium, causing ventricular fibrillation. The heart was massaged and air was aspirated, but the heart could not be resuscitated.

Three sheep died within 3 days after surgery. The cause of death was severe mitral regurgitation. Sheep 4 had anterior leaflet prolapse at A1 from Gore-Tex chordae that were too long and there was also a hematoma between the 2 layers of vein tissue in A3 which caused restriction of the leaflet in A3 (Fig 3.8). Blood entered the space between the veins at the leaflet edge where the 2 veins were sutured together. After seeing this hematoma develop in the leaflet, we were meticulous when suturing the 2 vein layers together to prevent this complication.

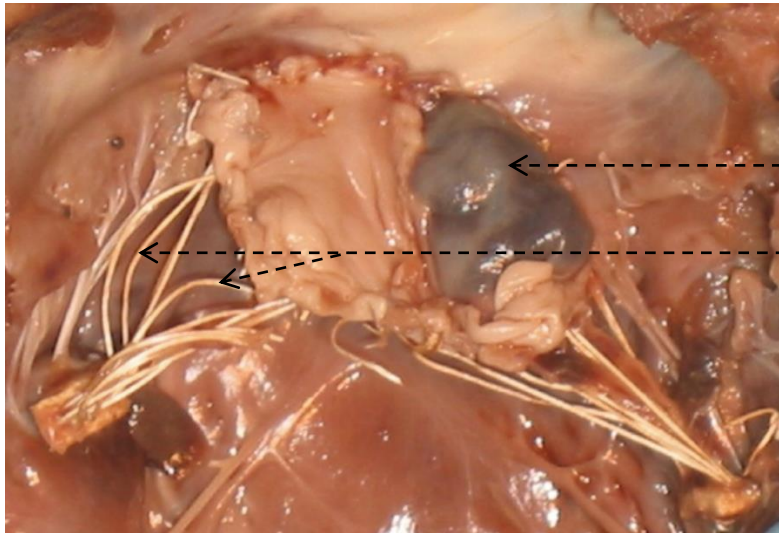
Sheep 7 had restriction of the anterior mitral leaflet due to a Gore-Tex suture catching the opposite leaflet edge. This caused an infolding of the leaflet that could not be seen during surgery, because it was on the underside of the leaflet and was obscured from the atrial view (Fig 3.9).

Sheep 19 had a large pericardial and pleural effusion. This sheep's heart weighed 348gm which is 150 gm more than what is expected for the weight of this sheep (37kg). The normal heart weight for a sheep between 37-38kg is 155-165gm (Fourie et al 2009). On examination of the valve it seemed as if the Gore-Tex chordae were too long and the vein leaflet was prolapsing, especially at the A3 area (Fig 3.10).

The mitral annulus measurements are shown in Table 3.2 and give an idea of the baseline annulus length, since the annulus would not have had a chance to dilate.

The lung histology showed lung congestion (congested capillary vessels and increased interstitial fluid in the alveolar septae) in all the specimens and congestion and lung edema (fluid in the alveolar space) in sheep 4 (Table 3.3).

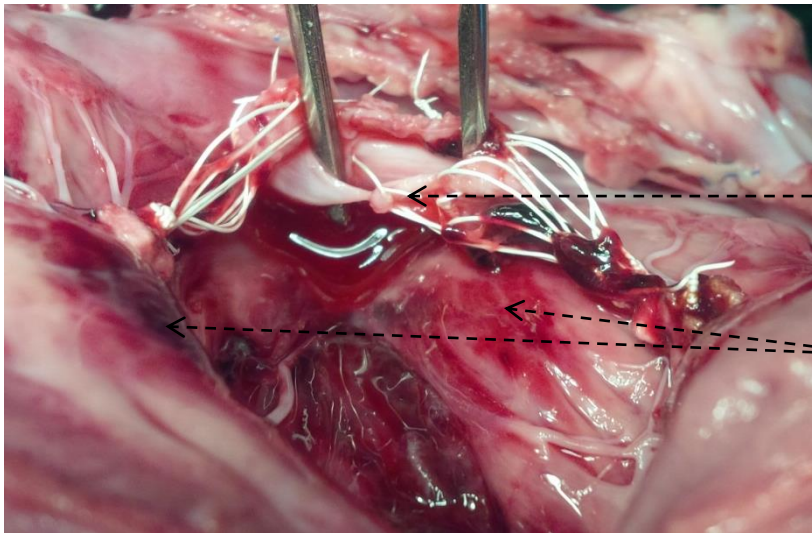
**Fig 3.8:** Mitral valve of sheep 4 shows some Gore-Tex chordae were too long at A1 causing leaflet prolapse. There was also a hematoma that formed between the 2 vein layers at A3.



Hematoma between the 2 vein layers causing leaflet restriction

Gore-Tex chordae too long which caused prolapse of the A1 segment

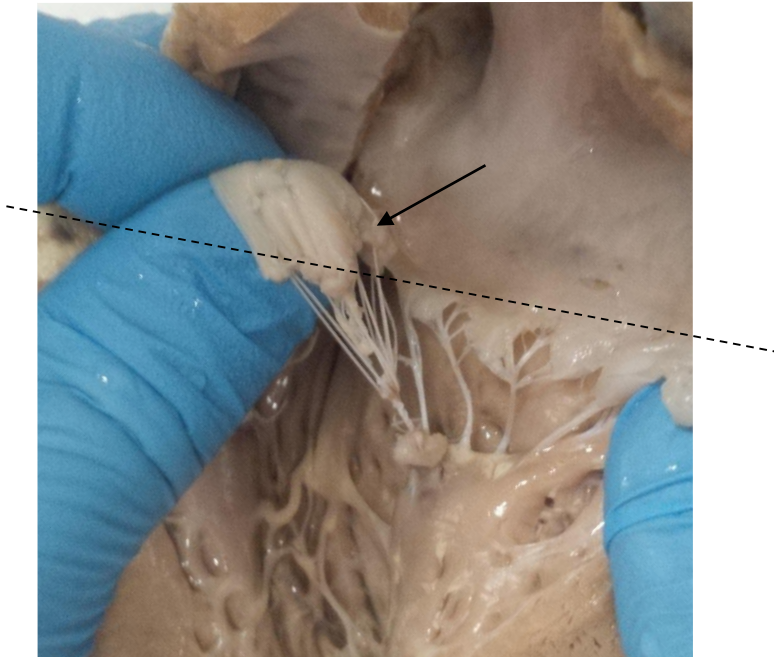
**Fig 3.9:** Sheep 7 died 2 days after surgery from mitral regurgitation due to a restricted anterior mitral valve leaflet. One Gore-Tex suture that was used to tie the Gore-Tex loop to the leaflet edge caught the opposite edge of the underside of the vein leaflet and pulled in the A1 and A3 leaflet edge causing leaflet restriction. Subendocardial hemorrhage is noted in the left ventricle which could be from myocardial ischemia during cardiopulmonary bypass and cardiac arrest.



--- Gore-Tex suture caught the underside of the opposite leaflet edge

--- Subendocardial hemorrhage

**Fig 3.10:** Sheep 19 died 3 days after surgery from mitral regurgitation due to prolapse of the vein leaflet due to Gore-Tex chordae that were too long in the A3 area (arrow). Notice how the leaflet is prolapsing above to the annulus height (dashed line).



### **3.4 Intermediate mortality (1-6 months)**

Seven sheep died between 1 and 6 months (Table 3.4). The lung histology showed pulmonary congestion in all the specimens and sheep 9 had congestion and pulmonary edema (Table 3.4). The hearts of these sheep were enlarged as measured by increased weight and a dilated annulus (Table 3.4). The histology of the left ventricular myocardium in the enlarged hearts showed pleomorphism and enlargement of the cardiomyocytes as a result of volume overload of the left ventricle.

Sheep 1 died 4 months after surgery. The post mortem showed an enlarged heart with increased weight and a dilated mitral annulus (Table 3.4). Two Gore-Tex chordae from the A2 segment pulled loose from the leaflet edge, creating a flail segment (Fig 3.11 and Fig 3.12). Examination of the vein leaflet showed that there was significant tension on the leaflet edge from the primary Gore-Tex chordae (Fig 3.12). As the annulus dilated and the coaptation between the 2 leaflets decreased, the tension on the Gore-Tex chords increased with eventual disruption of the attachment site at the A2 segment.



**Table 3.4:** Results of sheep that died between 1 and 6 months:

Sheep nr	Time between surgery and death	Lung histology	Vein leaflet morphology	Heart weight (gm)	Annulus length
1	4 months	Congestion	Two Gore-Tex chordae from the A2 segment pulled loose from the leaflet edge, creating a flail segment (Fig 3.2 and Fig 3.3).	592	102
2	1 month	Congestion	Hematoma at A3 between the 2 layers of the vein and all the Gore-Tex chords from the medial papillary muscle pulled loose from A2 and A3 creating a large flail segment (Fig 3.4).	625	105
9	6 months	Congestion, Edema	Vegetations on the leaflet tip at A2 and disruption of the Gore-Tex chordae from the medial papillary muscle (Figs 3.11 and 3.12).	240	100
15	4 months	Congestion	Calcification of the Gore-Tex chords and the Gore-Tex chords from the medial papillary muscle showed a partial disruption from A2 (Figs 3.6 and 3.7). The vein leaflet showed good mobility and no calcification.	311	75
18	4 months	Congestion	Severe infection with vegetations over the whole vein leaflet and the native leaflets (Fig 3.13) The medial papillary muscle with its attachments were destroyed	446	85
20	3.2 months	Congestion	Tear in the central suture line between the vein halves at the leaflet edge (Fig 3.8). Thickening of A1 part of leaflet due to organised fibrin between 2 vein layers. The central suture line close to the annulus healed well.	434	85

**Fig 3.11:** Sheep 1 died 4 months after surgery. Gore-Tex chordae pulled loose from the A2 segment on the vein leaflet. The vein leaflet is flexible and the 2 layers of the vein have fused completely at 4 months.

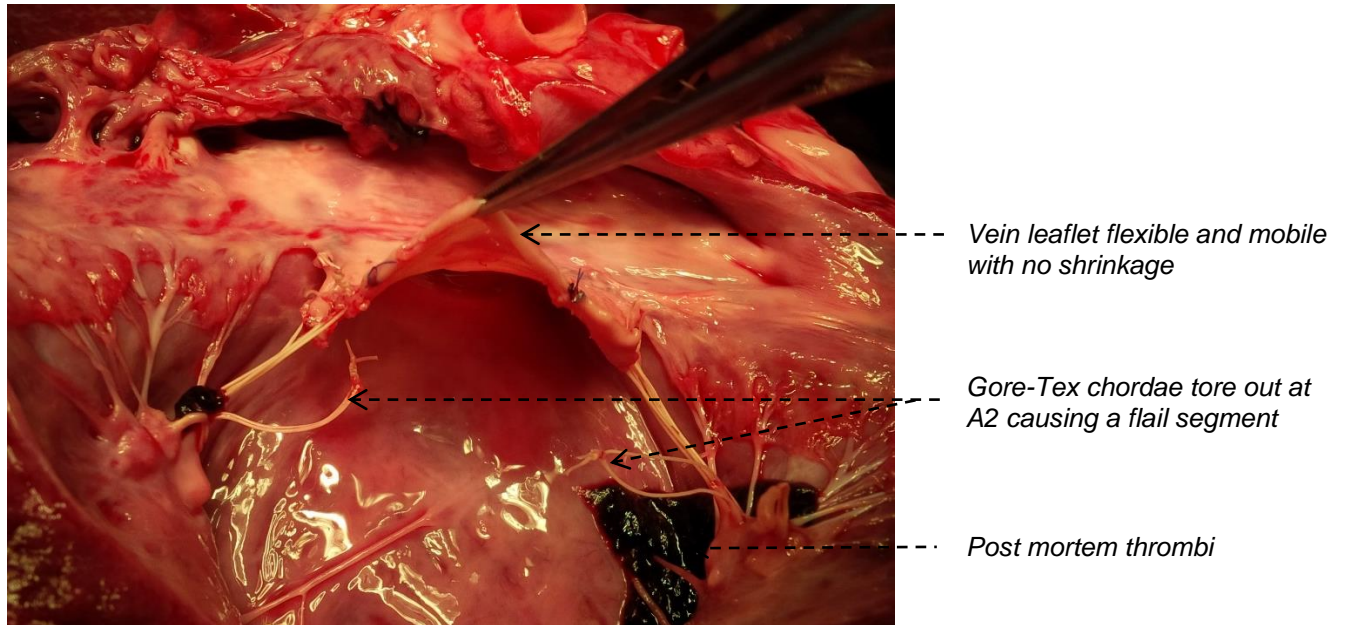
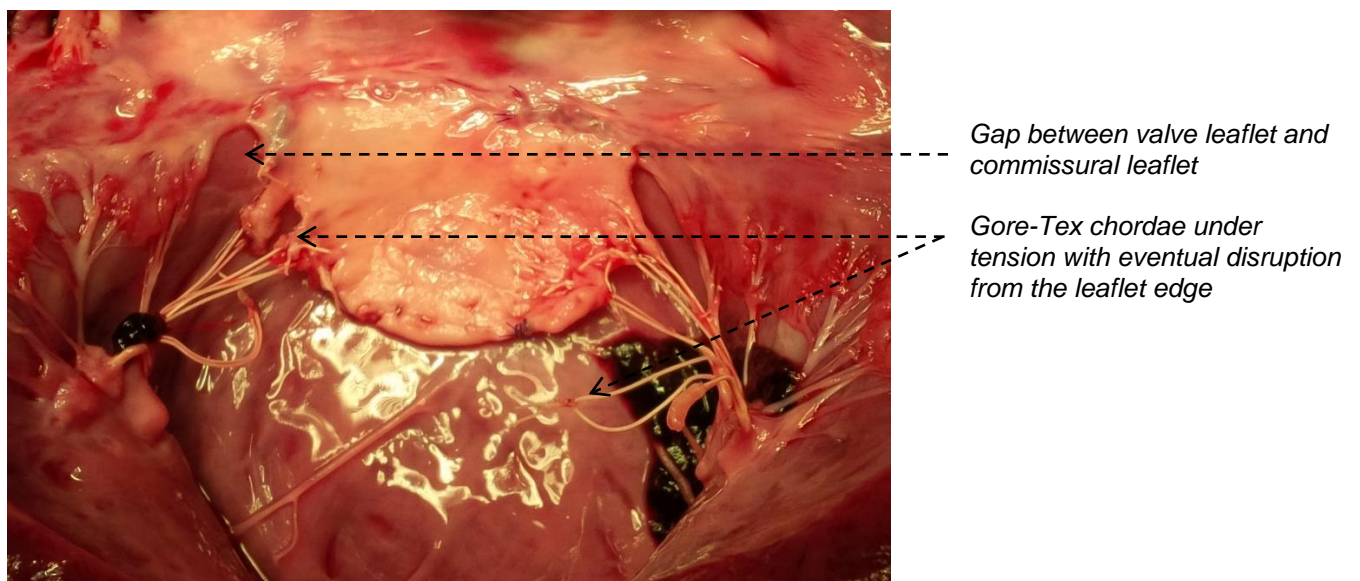


**Fig 3.12:** The same valve as Fig 3.11 (Sheep 1). Note the commissural gap at A1 and the commissural leaflet. The Gore-Tex suture (CV 8) line in the vein leaflet healed well.



Sheep 2 died 1 month after surgery from mitral regurgitation. The post mortem showed an enlarged heart and a dilated annulus. The mitral valve showed a hematoma at A3 between the 2 layers of the vein and all the Gore-Tex chords from the medial papillary muscle pulled loose from A2 and A3 creating a large flail segment (Fig 3.13).

The hematoma was fresh and was most likely caused by blood entering the ventricular side of the vein leaflet where the branches were sutured with Gore-Tex CV-8 (Fig 3.14). The suture line between the vein leaflet and the commissural native leaflet at A3 also disrupted. The vein leaflet was sutured to the annulus with 5-0 Prolene in this sheep, but we switched to Gore-Tex CV-6 for the annular suture as it would be less likely to cut through the delicate commissural leaflet. The rest of the vein leaflet, apart from the hematoma, was mobile.

**Fig 3.13:** Sheep 2 died 1 month after surgery. Hematoma formed between the 2 layers of the vein. The Gore-Tex chords from the medial papillary muscle pulled loose from the leaflet edge at A2 and A3, creating a large flail segment. The suture line between the commissural leaflet and vein leaflet also pulled loose.

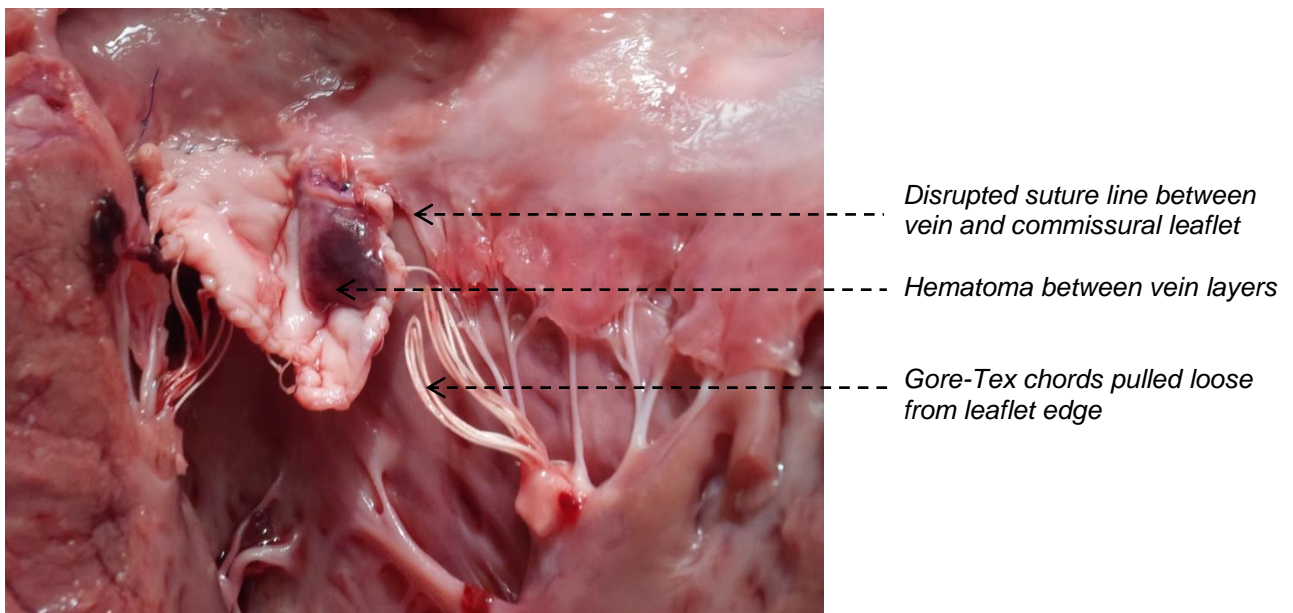
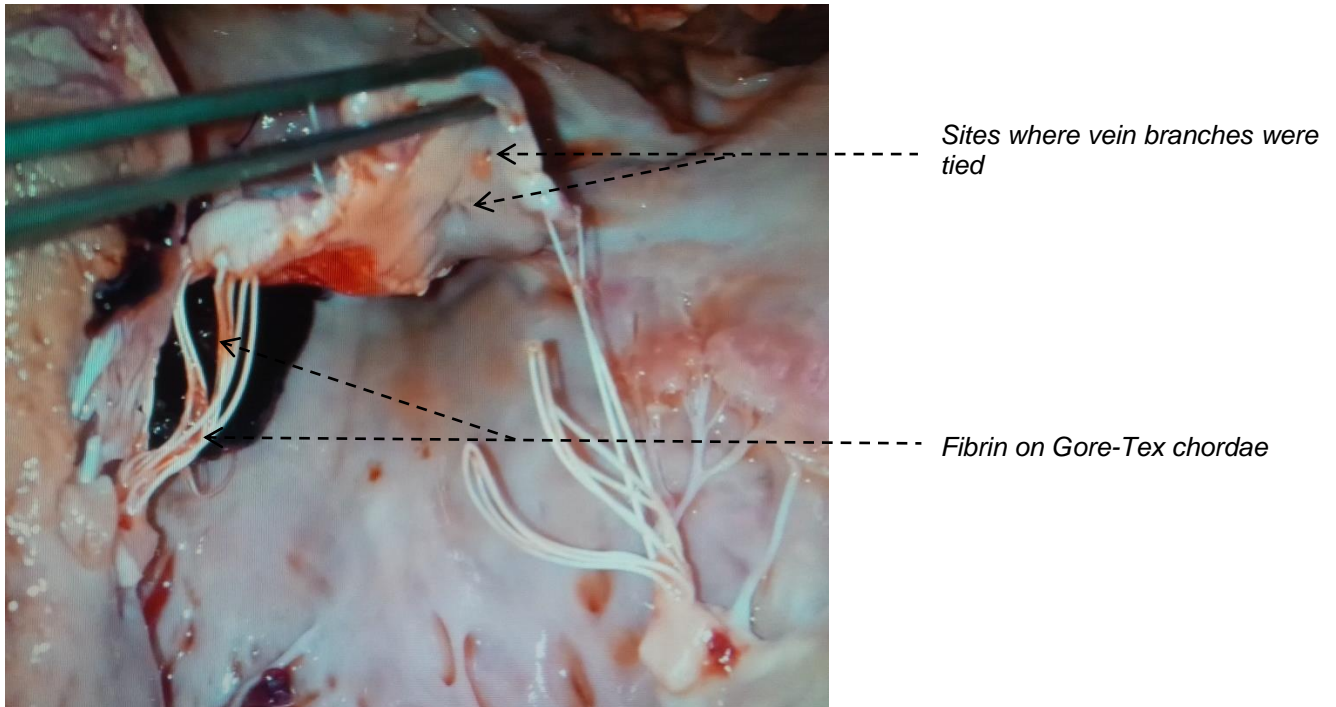


**Fig 3.14:** Sheep 2 underside of vein leaflet to show the sites where the vein branches were closed with Gore-Tex CV 8 sutures. This was the most likely entry point of blood from the left ventricle to cause the hematoma in the leaflet.



Sheep 15 died 4 months after surgery on a very hot day on the farm (43°C). The post mortem showed calcification of the Gore-Tex chords and the Gore-Tex chords from the medial papillary muscle showed a partial disruption from A2 (Figs 3.15 and 3.16). The vein leaflet showed good mobility and no calcification.

**Fig 3.15:** Mitral valve from sheep 15 (4 month implant) shows calcification of the Gore-Tex chordae and partial disruption from the A2 Gore-Tex chords from the medial papillary muscle

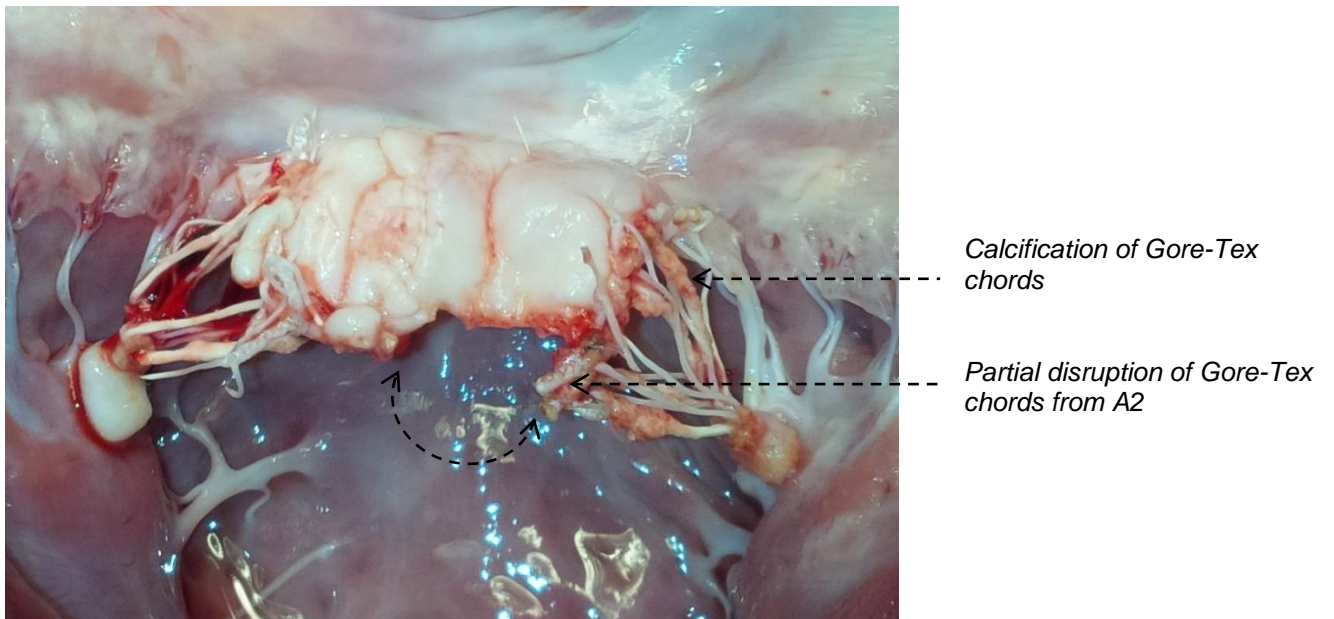
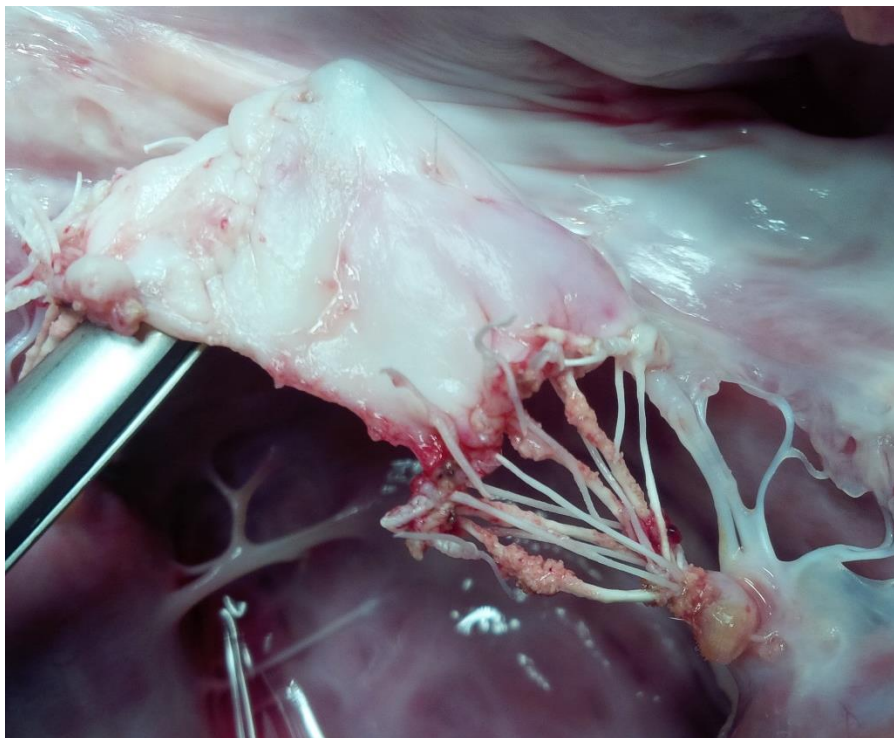
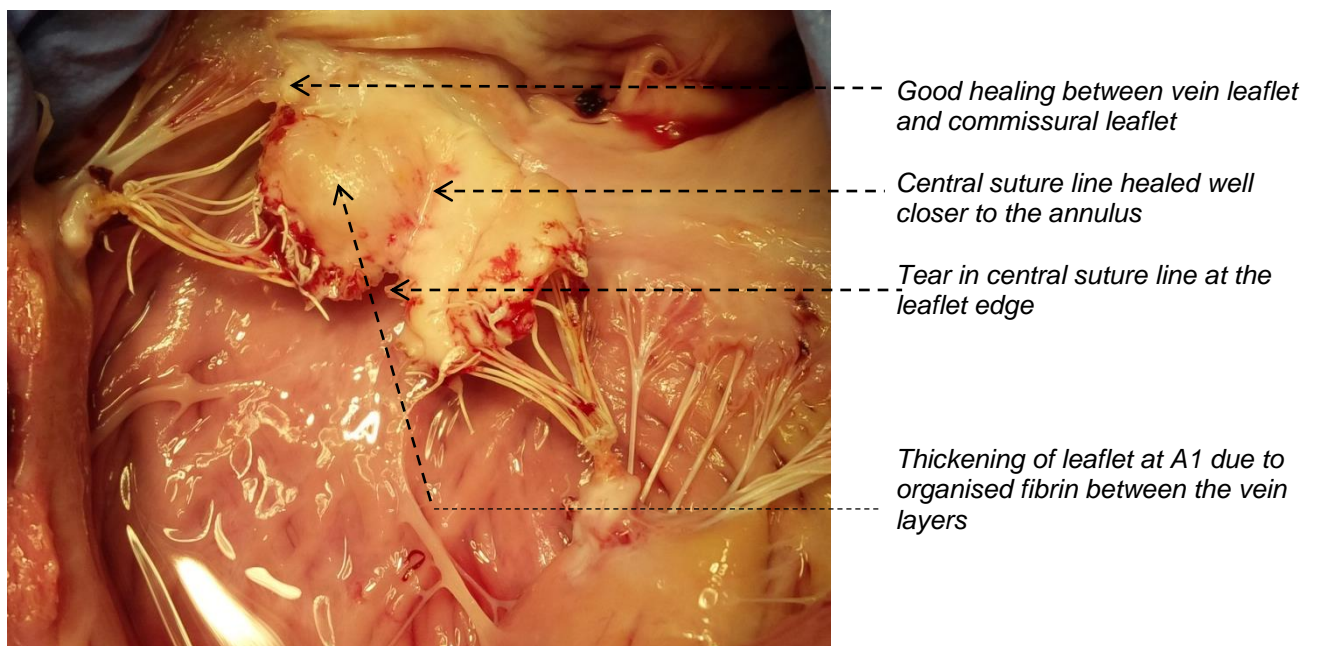


**Fig 3.16:** Mitral valve from sheep 15 (same as Fig 3.15) shows the mobility of the vein leaflet and the calcification of the Gore-Tex chords.



Sheep 20 died 3.2 months after surgery. The post mortem revealed a tear in the central suture line between the vein halves at the leaflet edge (Fig 3.17). The central suture line close to the annulus healed well. Thickening of the vein leaflet was also noted at A1 because of organised fibrin between the vein layers. The echocardiogram at 3 months showed mild to moderate MR.

**Fig 3.17:** Sheep 20 died 3.2 months after surgery. Note a tear in the central suture line between the vein halves.



Four sheep developed infective endocarditis (SBE) on the mitral valve (Sheep 8, 9, 11 and 18). Sheep 11 was euthanized at 1 month for dyspnea and moderate to severe MR on the echocardiogram. The valve looked thickened on echocardiography with possible vegetations (Fig 3.18). The post mortem showed that the vein leaflet had an organising hematoma between the vein layers at A1. (Fig 3.19) This made the leaflet restrictive in the A1 area. There was also a perforation in the leaflet at A3. Vegetations was noticed on the Gore-Tex chordae and histological examination confirmed the presence of infective vegetations with Gram negative organisms on the leaflet edge. This sheep was one of 2 sheep which had annuloplasty sutures placed to improve leaflet coaptation.

**Fig 3.18:** Echocardiogram of sheep 11 shows thickening of the vein leaflet (yellow arrow) with mild billowing and possible vegetations on the leaflet and chordae (red arrow).

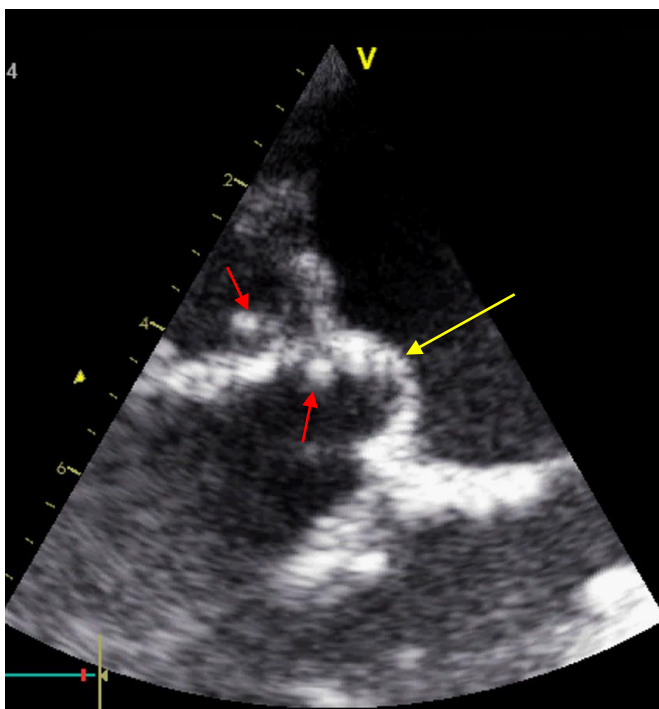
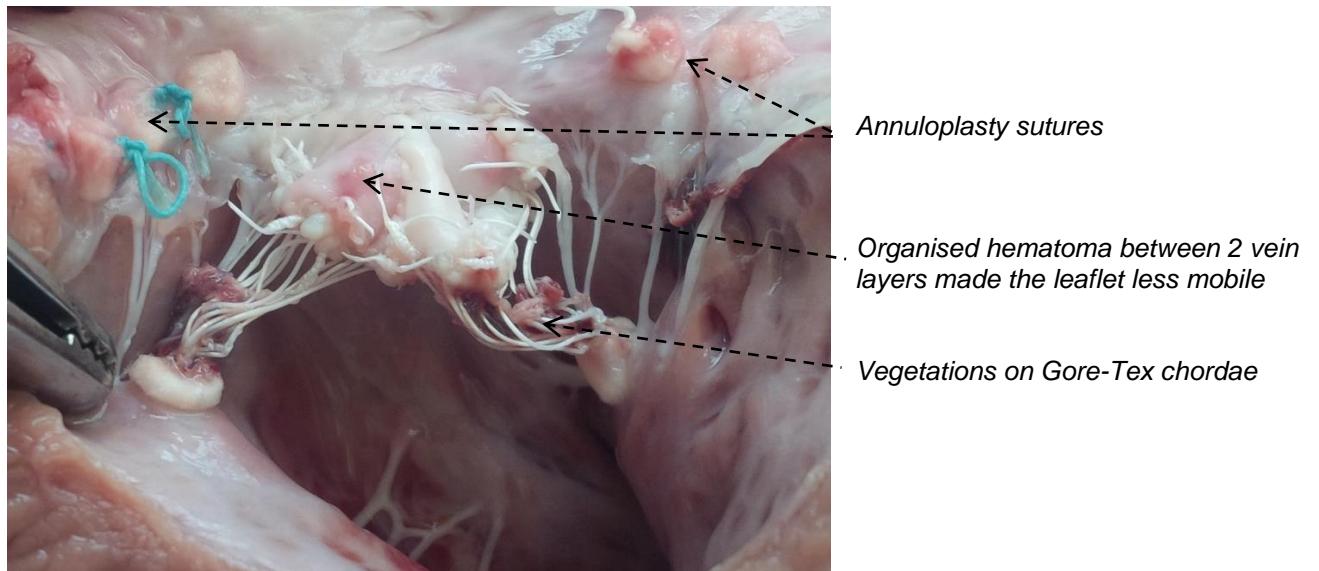


**Fig 3.19:** Sheep 11 was euthanized at 1 month for dyspnea. The vein leaflet shows an organised hematoma between the leaflets in the A1 region. Notice the vegetations on the Gore-Tex chordae



Sheep 8 was euthanized at 6 months because of dyspnea (Table 3.5). The echocardiogram showed severe mitral regurgitation with prolapse of A2 (Fig 3.20). The post mortem revealed SBE on the mitral valve with vegetations on both leaflets and loose Gore-Tex chordae at A1 and A2 (Figs 3.21 and 3.22). *Staphylococcus aureus* was cultured from the vegetations.



**Fig 3.20:** Echocardiogram with colour flow of sheep 8 at 6 months showing moderate to severe MR due to chordal rupture at A2 with A2 prolapse. The red arrows mark the vein leaflet.

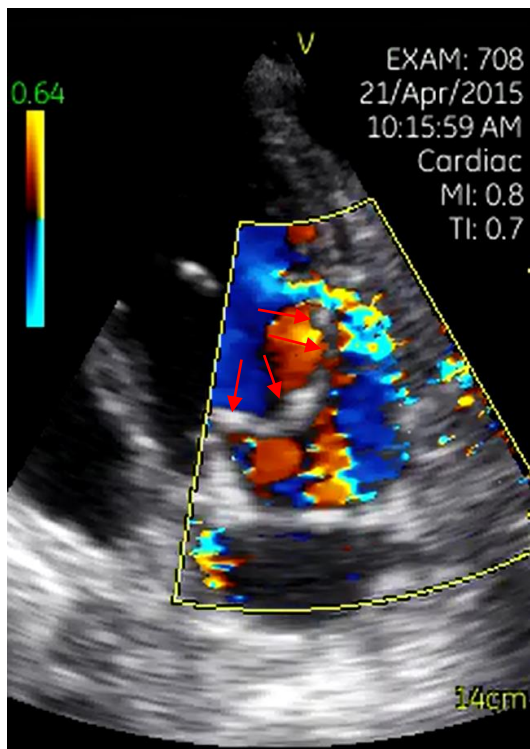


**Fig 3.21:** Sheep 8 was euthanized at 6 months for dyspnea. The post mortem showed SBE on the mitral valve with vegetations on both leaflets. Gore-Tex chordae are loose at A1 and A2.

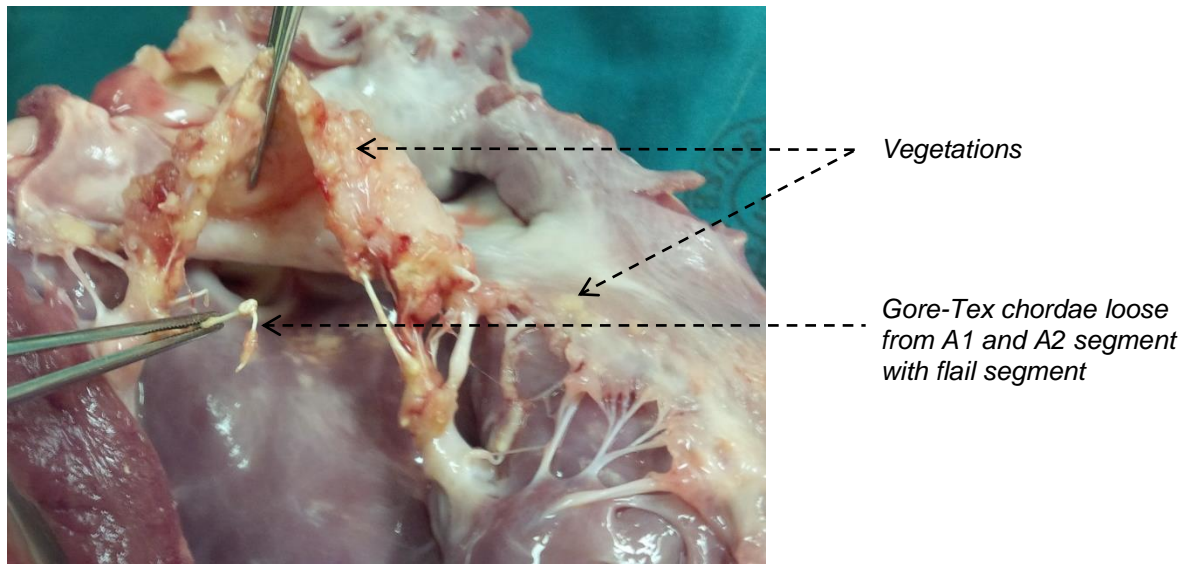
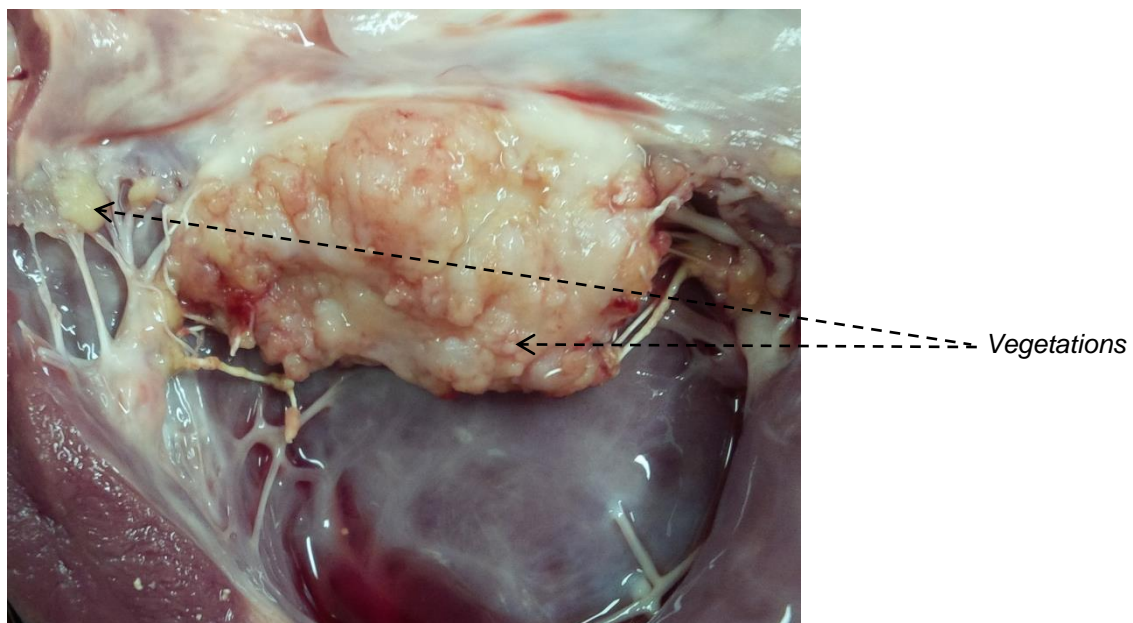


**Fig 3.22:** The atrial view of the mitral valve of sheep 8 (same as Fig 3.6) shows vegetations on the vein leaflet and the posterior leaflet.



Sheep 9 died 6.7 months after surgery from SBE. The post mortem showed vegetations on the leaflet tip at A2 and disruption of the Gore-Tex chordae from the medial papillary muscle (Figs 3.23 and 3.24). The lung histology showed pulmonary congestion and oedema.

**Fig 3.23:** Sheep 9 died 6.7 months after surgery from SBE. Note vegetations on the leaflet and disruption of the Gore-Tex chordae from the medial papillary muscle, causing a large flail segment.

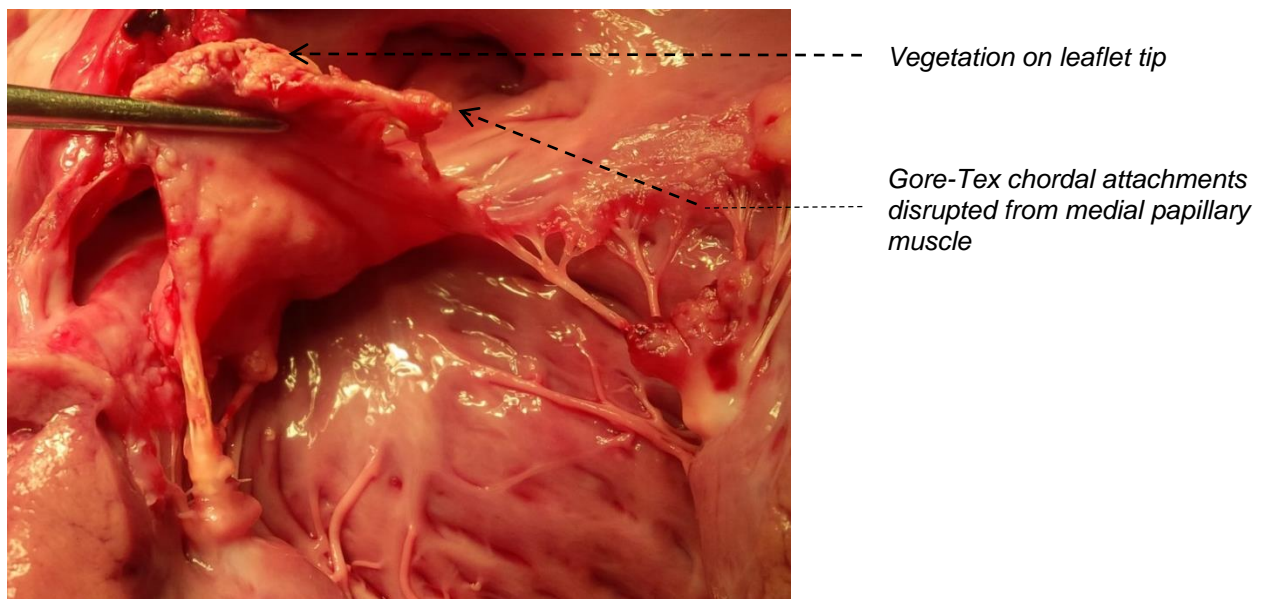
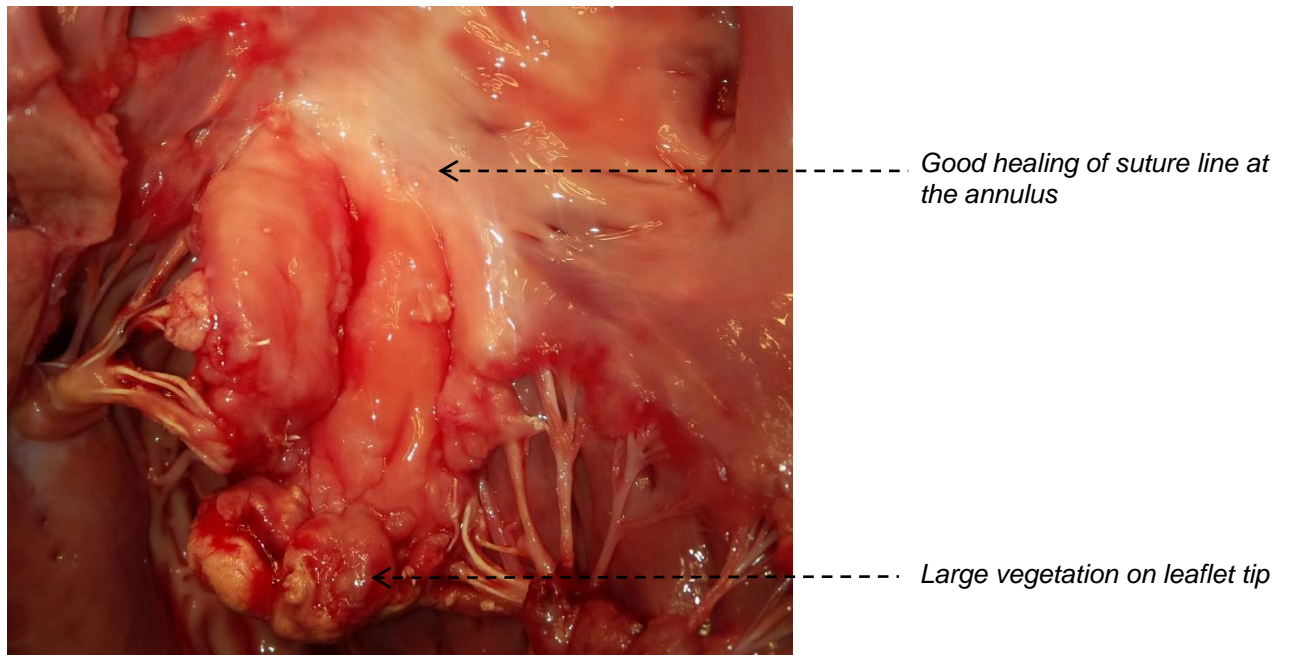
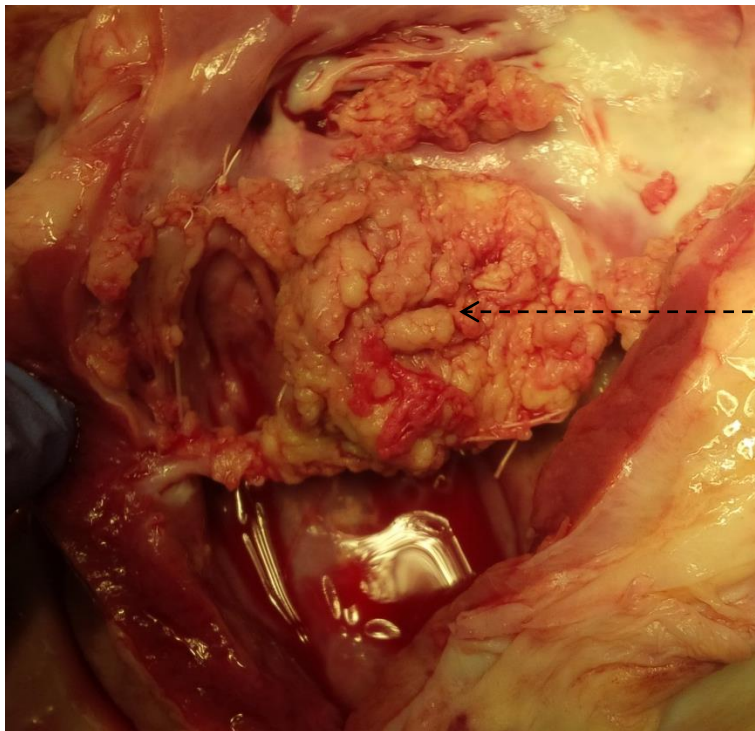


**Fig 3.24:** Atrial view of mitral valve of sheep 9 (same as Fig 3.12) shows the large vegetation on the vein leaflet edge at A2 and A3.



Sheep 18 died 4 months after surgery from SBE with disruption of all the Gore-Tex chords from the medial papillary muscle. The post mortem showed a severe infection with vegetations over the whole vein leaflet and the native leaflets (Fig 3.25). The medial papillary muscle with its attachments were destroyed.

**Fig 3.25:** Mitral valve of sheep 18 shows severe infection with vegetations over the whole valve.



*Vegetations covering the whole valve*

### 3.5 Euthanized sheep.

The rest of the sheep were euthanized between 1 to 10 months to evaluate the vein leaflet macroscopically and histologically. The echocardiographic result and macroscopic evaluation at the time of euthanasia are given in Table 3.5.

**Table 3.5:** Results of the sheep that were euthanized.

Sheep nr	Time between surgery and euthanasia	Echocardiogram at time of euthanasia	Vein leaflet morphology	Heart weight	Annulus circumference
3	10 months	Mild MR	Vein tissue mobile and intact, good healing of suture lines (Figs 3.26 to 3.28).	435	94
5	8 months	Moderate MR.  Calcium on valve edge, leaflet perforation	Perforation in central suture line, with focal calcification on the leaflet edge suture lines and central suture line (Fig 3.29). Defect between vein leaflet and medial commissure (Fig 3.30).	486	90
6	7 months	Moderate to severe MR	Vein tissue mobile and intact, good healing of suture lines. One Gore-Tex chord pulled loose from A2 (Fig 3.31).	313	85
8	6 months for dyspnea	Moderate to severe MR, prolapse A2 segment, Mass on valve, possible SBE	Vegetations on mitral valve, Infective endocarditis with flail A2 from Gore-Tex chord that pulled loose (Figs 3.21 and 3.22).	360	98
10	6 months	Mild MR, Good EF	Leaflet mobile, Good healing of suture lines. Small defect in central suture line (Figs 3.32 to 3.34)	302	80
11	1 month for dyspnea	Severe MR, Nodular mass on leaflet (Fig 3.18)	Organised hematoma at A1 between vein layers. (Fig 3.19). Histology showed infective vegetation with Gram negative organisms at perforation.	290	80
13	6.5 months	Mild to moderate MR, good EF	Good healing of suture lines and vein leaflet mobile. Fibrin on atrial surface of vein leaflet (Figs 3.35 and 3.36).	273	86
14	6 months	Moderate MR	Good healing of suture lines and vein leaflet mobile (Fig 3.37)	302	75
16	6 months	Moderate MR, poor LV	Good healing of suture lines. Gore-Tex suture partially pulled away from papillary muscle (Fig 3.38)	240	91
17	6 months	Moderate	Good healing of suture lines at the annulus. Vein leaflet mobile. Focal calcification of Gore-Tex chordae. Tear in distal central suture line (Fig 3.39 and 3.40).	301	80
21	6 months	Mild	Good healing of suture lines. Fibrin on atrial surface. Focal calcification of Gore-Tex chordae. (Fig 3.41)	354	90

Sheep 11 was euthanized for dyspnea at 1 month and Sheep 8 was euthanized for dyspnea at 6.5 months. These sheep both had infective endocarditis (SBE) and were discussed with the group of sheep with SBE.

The other 9 sheep were euthanized at 6 months (sheep 10, 13, 14, 16, 17, 21), 7 months (sheep 6) 8 months (sheep 5) and 10 months (sheep 3). Their results are summarised in Table 3.5. Three had mild MR, 3 had moderate MR and 3 had moderate to severe MR at the time of euthanasia.

**Fig 3.26:** Atrial view of mitral valve of sheep 3 at 10 months shows good healing of the annulus suture line.

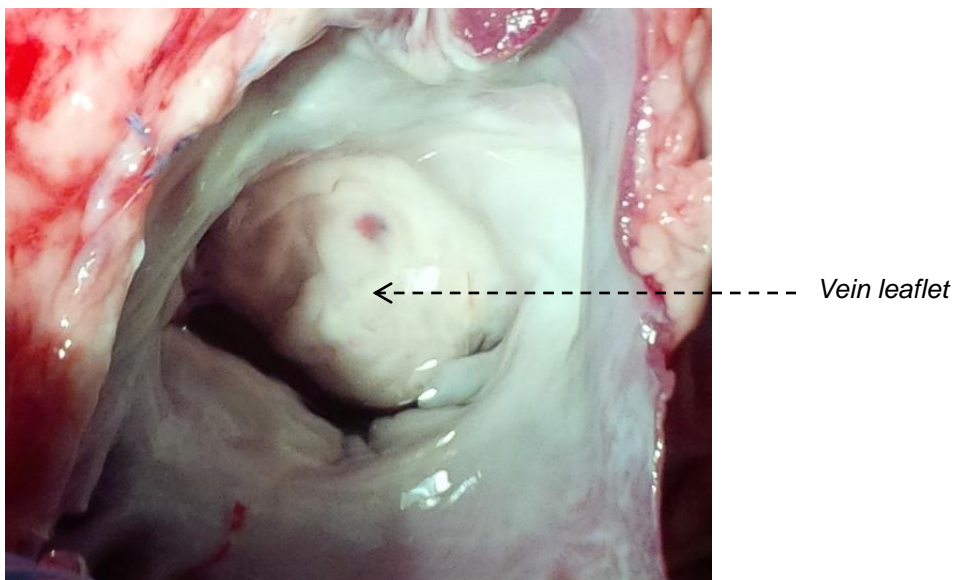
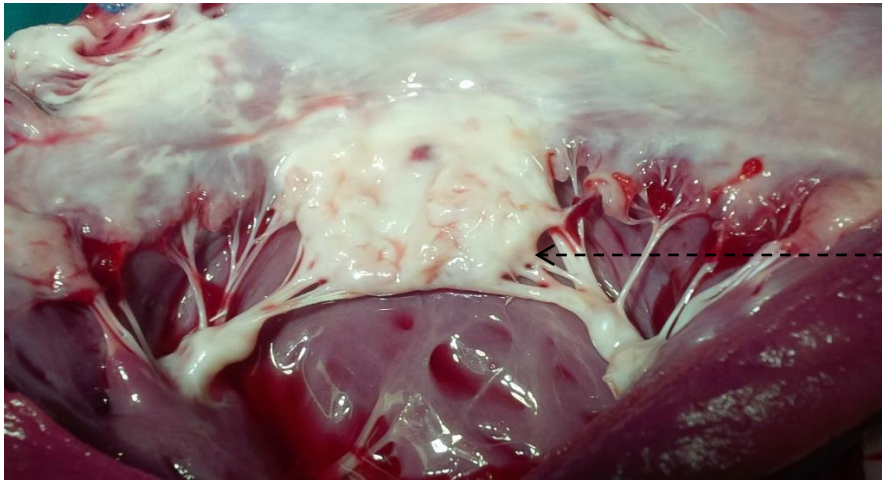


**Fig 3.27:** Mitral valve of sheep 3 at 10 months shows good healing of all suture lines of the vein leaflet and Gore-Tex sutures are covered with fibrous tissue



Gore-Tex chordae and suture knots completely covered with fibrous tissue

**Fig 3.28:** Mitral valve of Sheep 3 (same as Fig 3.26 and Fig 3.27) shows the flexibility of the vein leaflet.

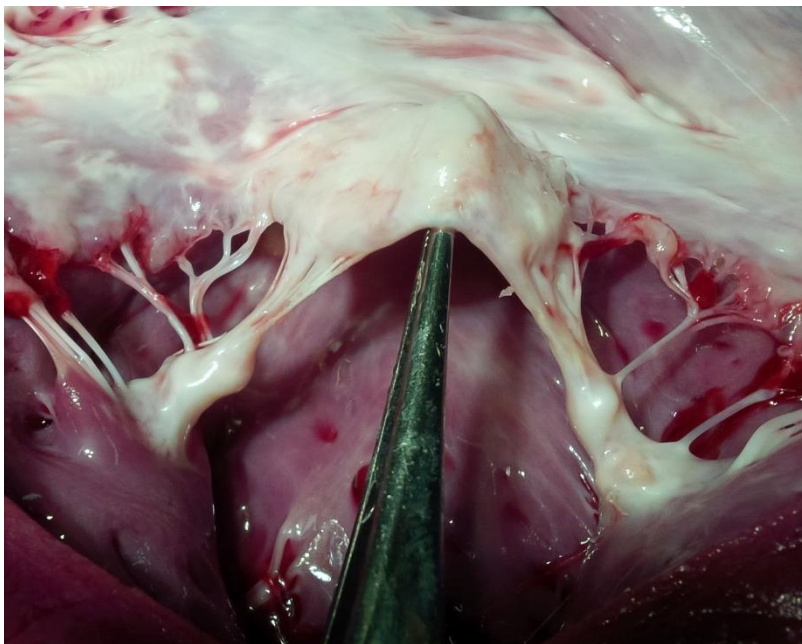




**Fig 3.29:** Mitral valve of sheep 5 at 8 months shows the perforation in the vein leaflet at the central suture line and focal calcification of the suture line and Gore-Tex chordae.

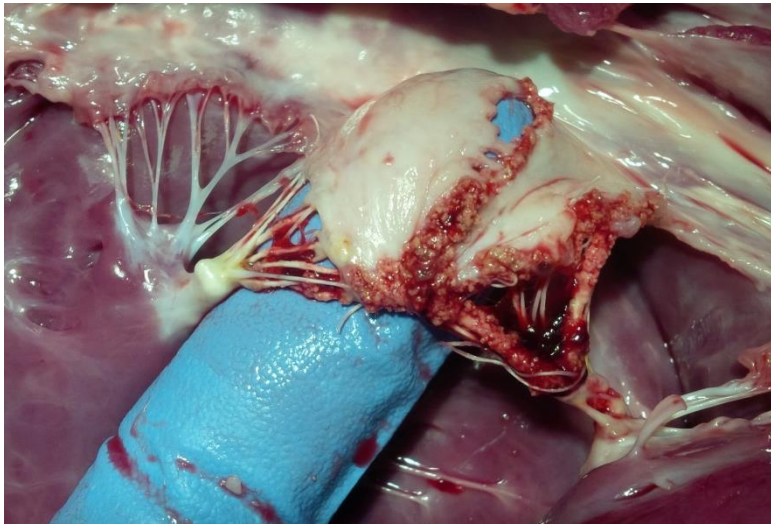


**Fig 3.30:** Sheep 5 (same as Fig 3.29) to show the large defect at the medial commissure.

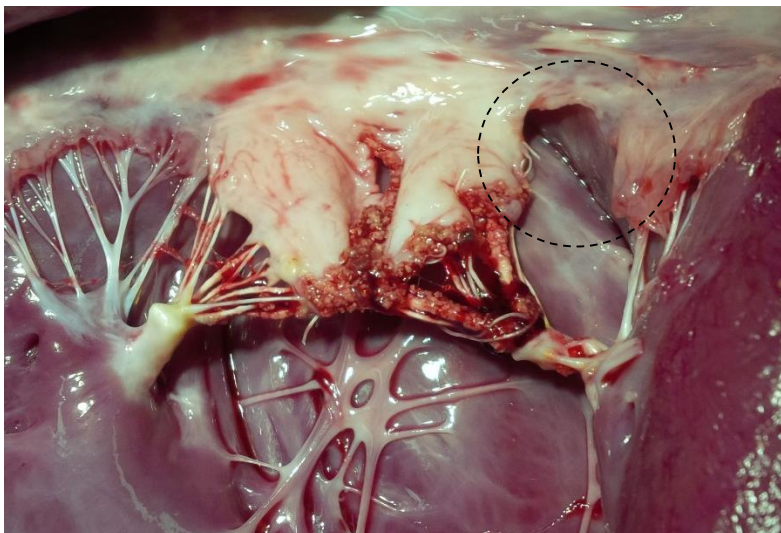
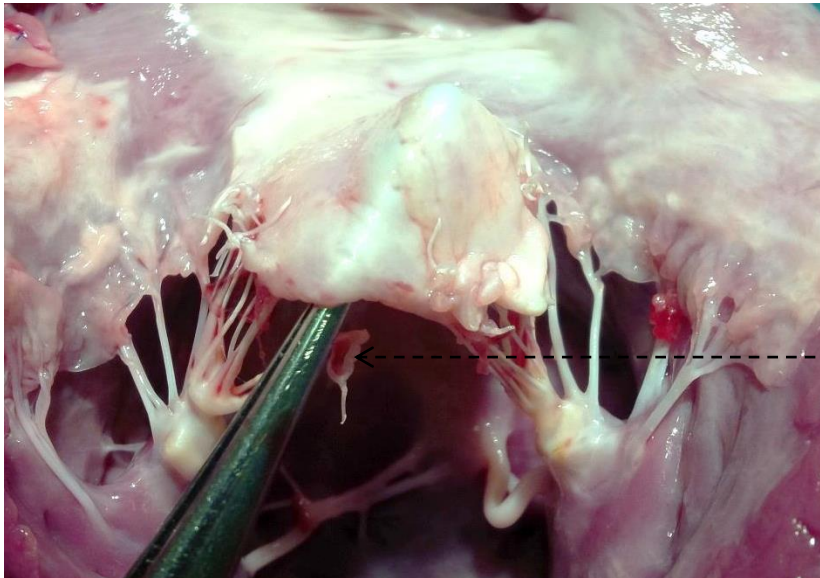
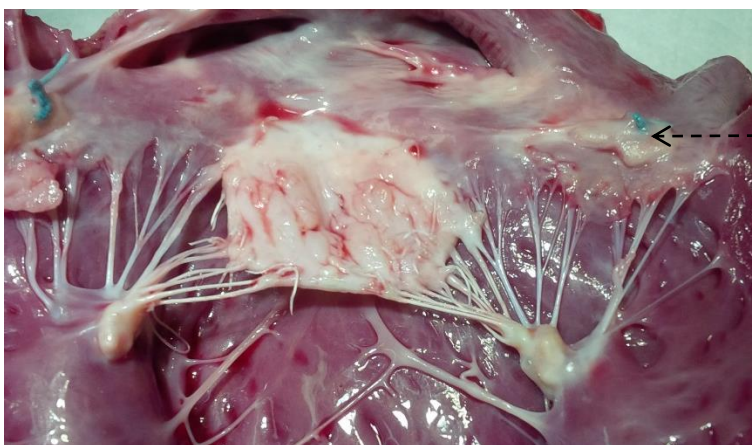


**Fig 3.31:** Mitral valve of sheep 6 at 7 months. The leaflet is mobile and suture lines have healed well. One Gore-Tex chord has pulled loose from the leaflet edge at A2.



One Gore-Tex chord pulled off the leaflet edge creating a flail segment

**Fig 3.32:** Mitral valve of sheep 10 at 6 months. The vein leaflet suture lines have healed well. The Gore-Tex chordae are partially covered with endothelium. This sheep also had 2 annuloplasty sutures placed in the annulus at the time of surgery. The annulus circumference measured 80mm.



Annuloplasty suture

**Fig 3.33:** Mitral valve of sheep 10 (same as Fig 3.32) to show ventricular aspect of valve and healing of suture line at the aortic-mitral curtain.

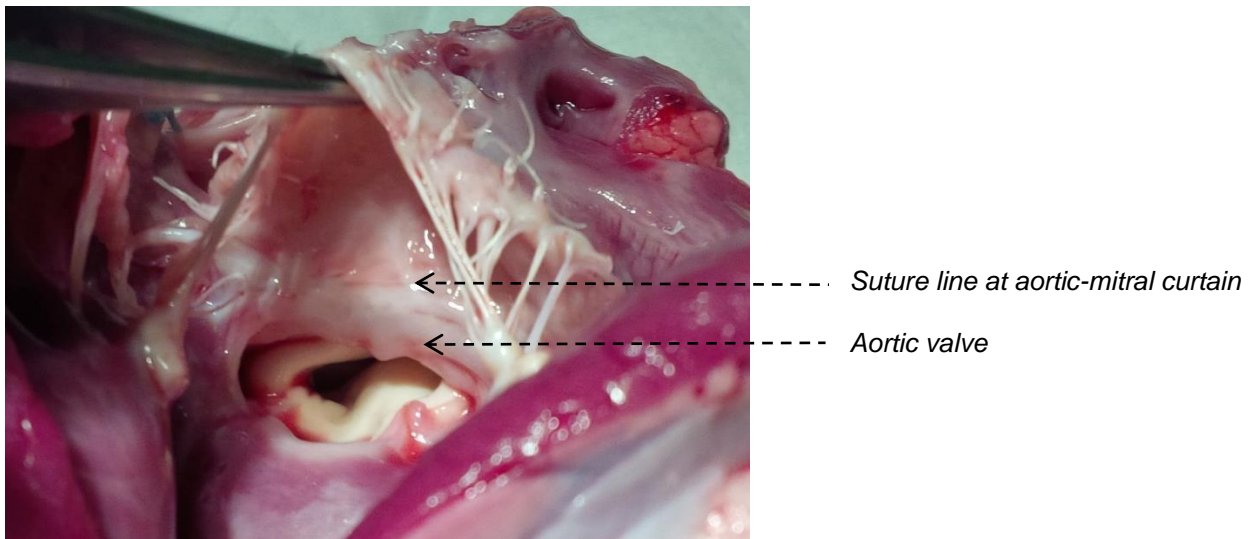


**Fig 3.34:** Mitral valve of sheep 10, with the vein leaflet stretched, show small defects in the valve leaflet at the central suture line. Area of thickening noticed on posterior leaflet because of chronic friction from Gore-Tex knot to the anterior leaflet.

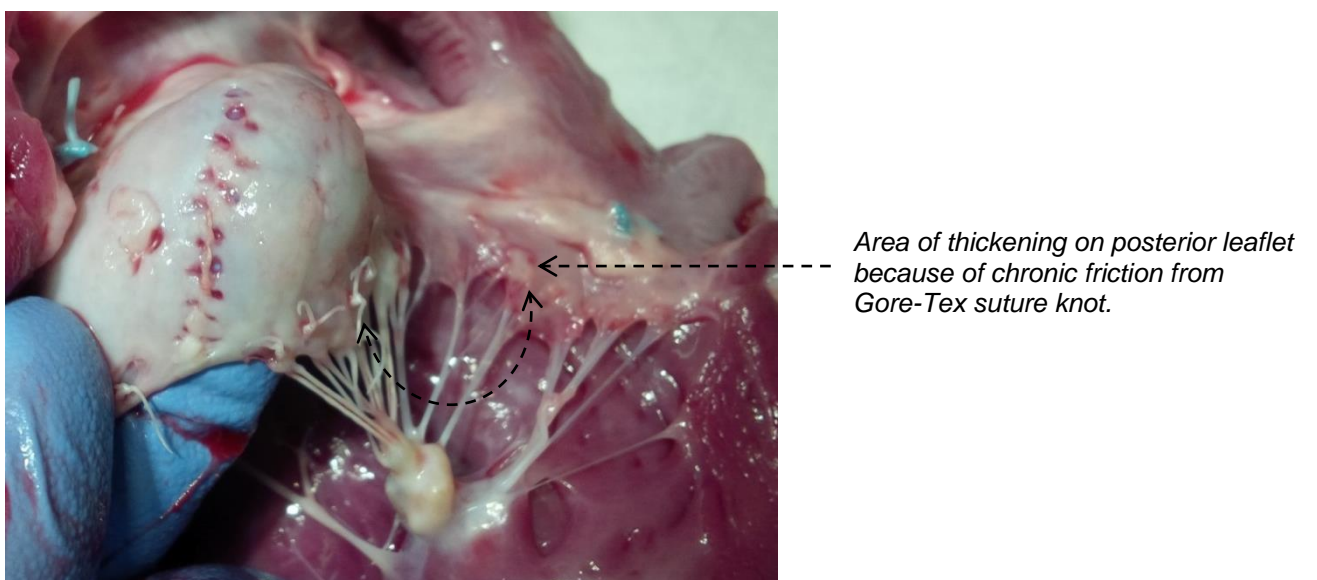


**Fig 3.35:** Sheep 13 at 6 months. The vein leaflet is mobile and suture lines have healed well. Gore-Tex sutures or partially covered with endothelium. There is some fibrin over the atrial aspect of the valve but there were no signs of infective endocarditis on histology. Note the 2 areas of billowing of the vein leaflet.

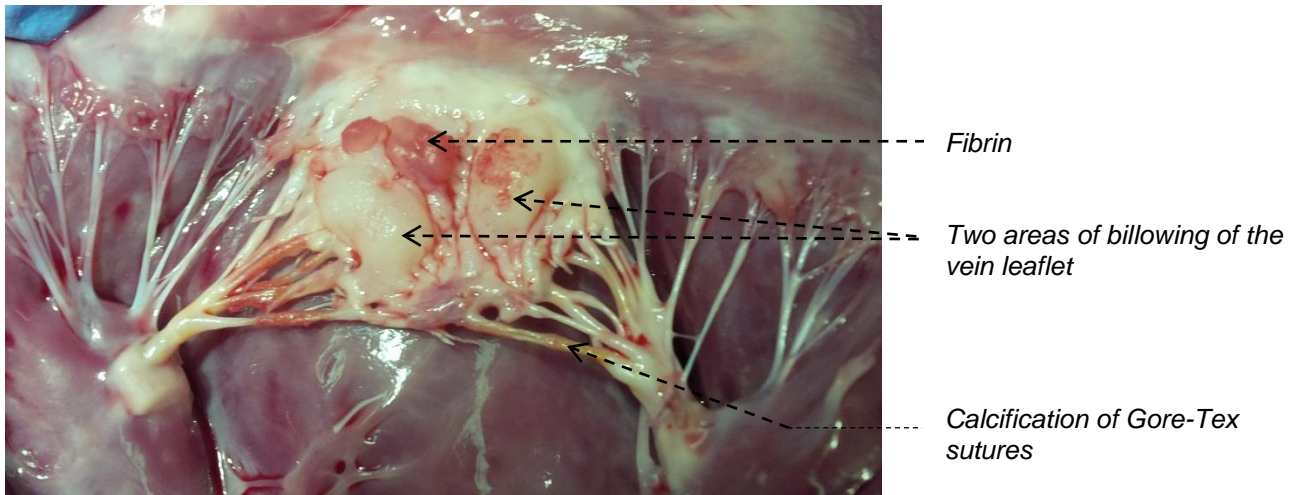


**Fig 3.36:** Sheep 13 (same as Fig 3.35), with the vein leaflet stretched, to show area of billowing.

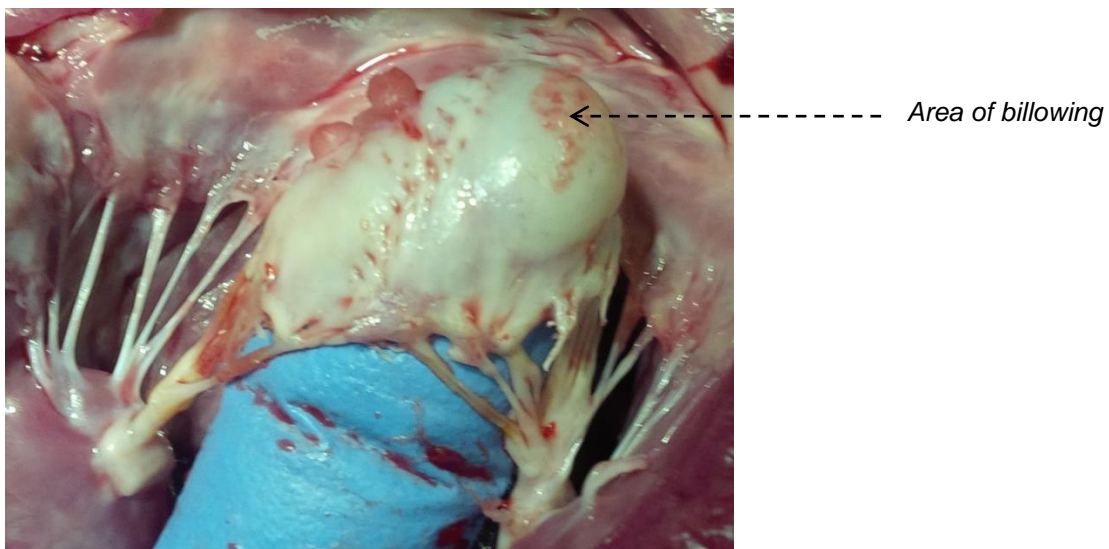
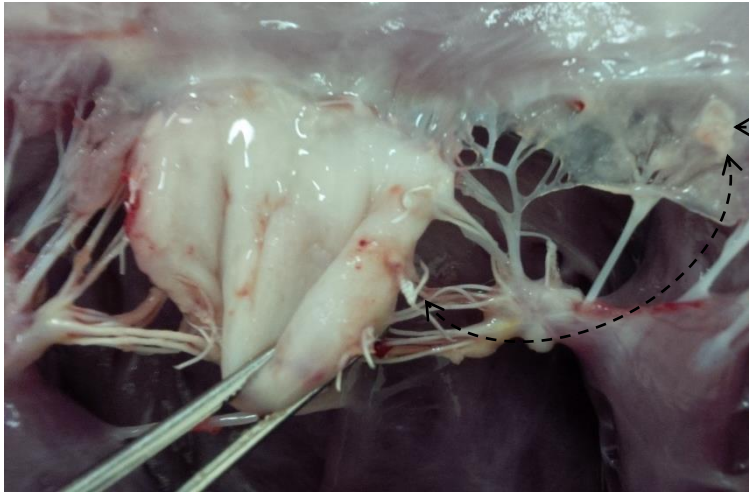
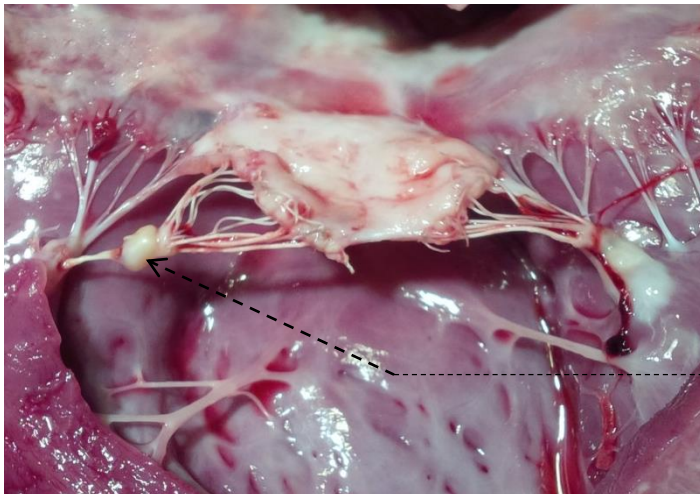


**Fig 3.37:** Mitral valve of sheep 14 at 6 months. There is good healing of all suture lines. Area of thickening noticed on the posterior leaflet from chronic friction of Gore-tex suture knot on edge of vein leaflet.



Area of thickening on posterior leaflet because of friction from Gore-Tex knot

**Fig 3.38:** Mitral valve of sheep 16 at 6 months shows good healing of suture lines. Gore-Tex suture partially pulled away from antero-lateral papillary muscle.



Gore-Tex suture partially pulled away from papillary muscle

**Fig 3.39:** Mitral valve of sheep 17 at 6 months shows good healing of suture lines at the annulus. There is focal calcification of Gore-Tex chordae and a tear in the distal central suture line (see Fig 3.40).

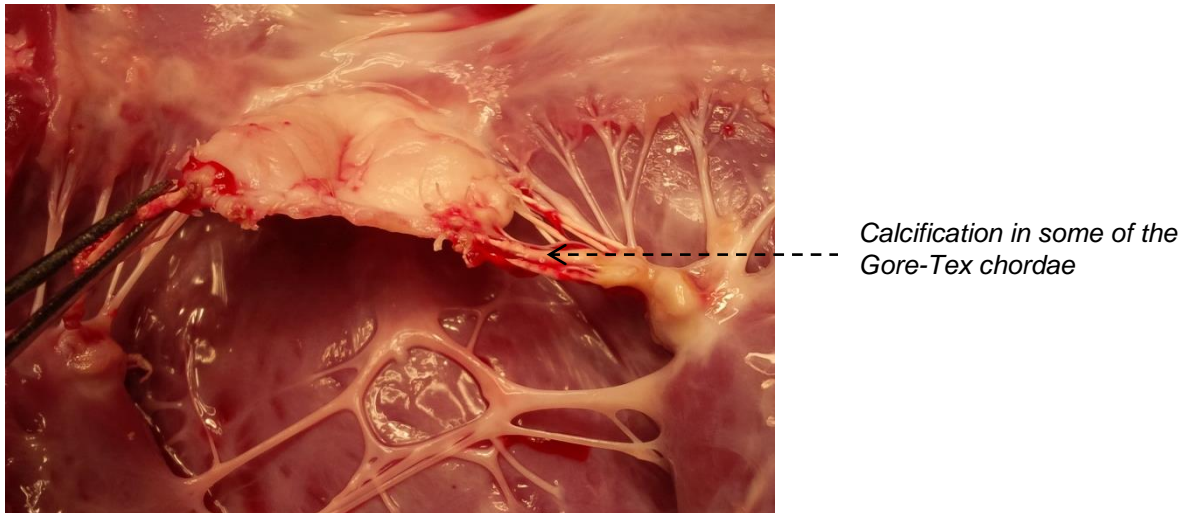


**Fig 3.40:** Mitral valve of sheep 17 to show tear in distal suture line.

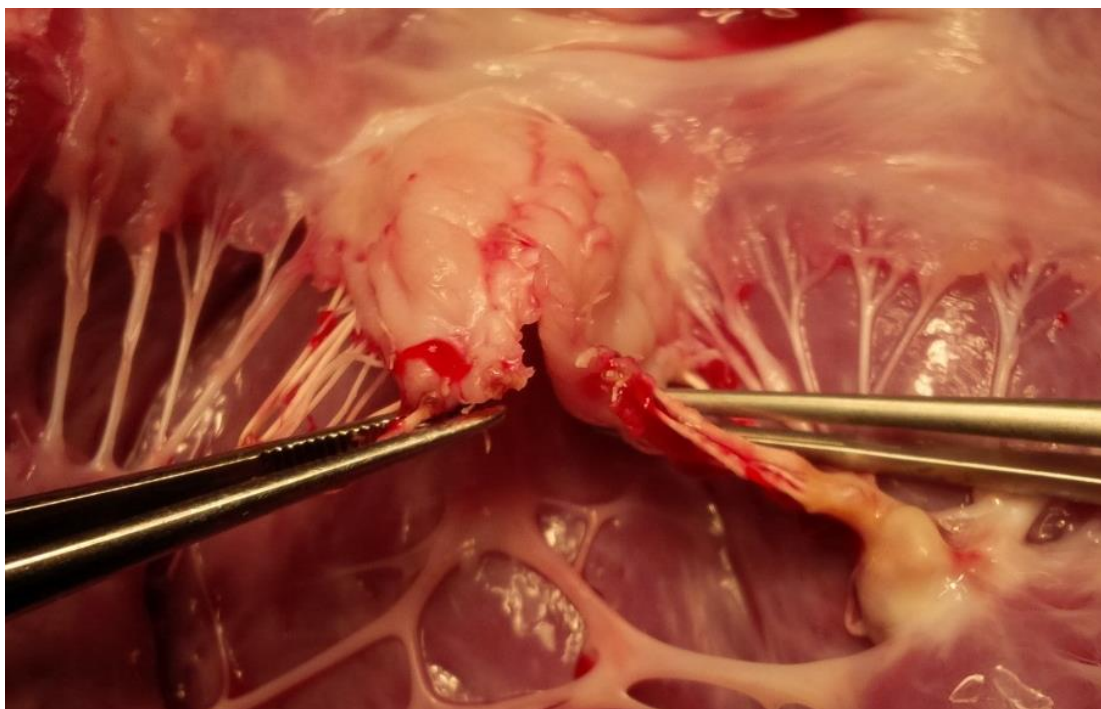
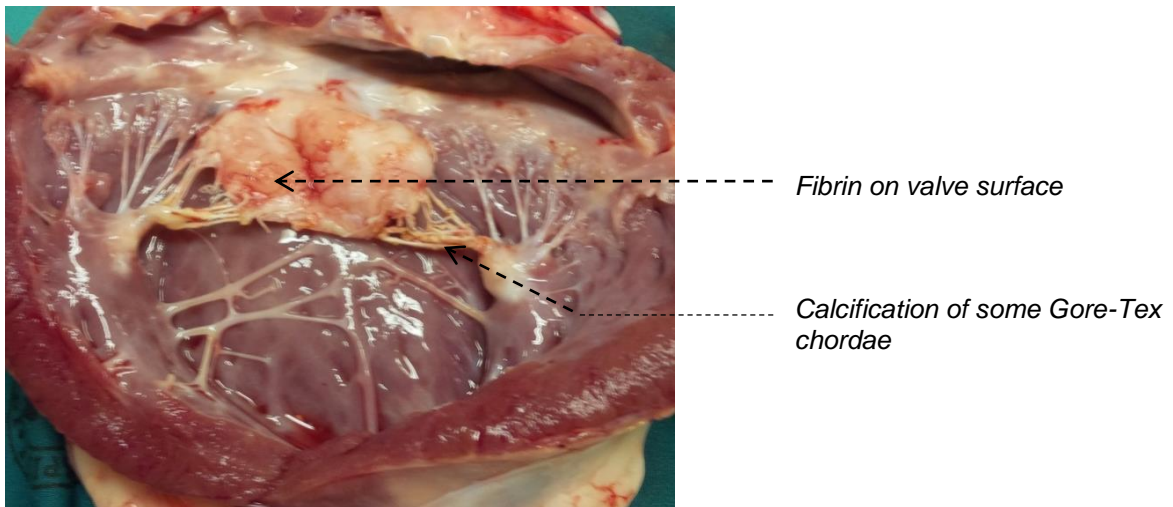


**Fig 3.41:** Mitral valve of sheep 21 shows good healing of suture lines. There is some fibrin on the valve surface with focal calcification of Gore-Tex chordae.



### 3.6 Histology results

**3.6.1** The histology of the excised **anterior mitral leaflet** showed normal valve leaflet histology with the atrialis, spongiosa, fibrosa and ventricularis layers (Fig 3.42). There are elastic fibres visible in the atrialis between the collagen fibres. The fibrosa consists of dense collagen fibres which are arranged in an orderly and parallel pattern (Fig 3.42 and Fig 3.43). The valve is more cellular (valvular interstitial cells) than human valves and the valve thickness ranges from 0.25 - 0.50 mm (Fig 3.44 and Fig 3.45).

**Fig 3.42:** Histological section of excised anterior valve leaflet with Verhoeff and Van Gieson stain (100x). Elastic fibres stain black in the atrialis and the collagen fibres stain purple:





**Fig 3.43:** Histological section of excised anterior valve leaflet with APAS stain (200x) to show the extracellular matrix. Note the orderly and parallel arrangement of the collagen fibres in the valve fibrosa (arrow):

o

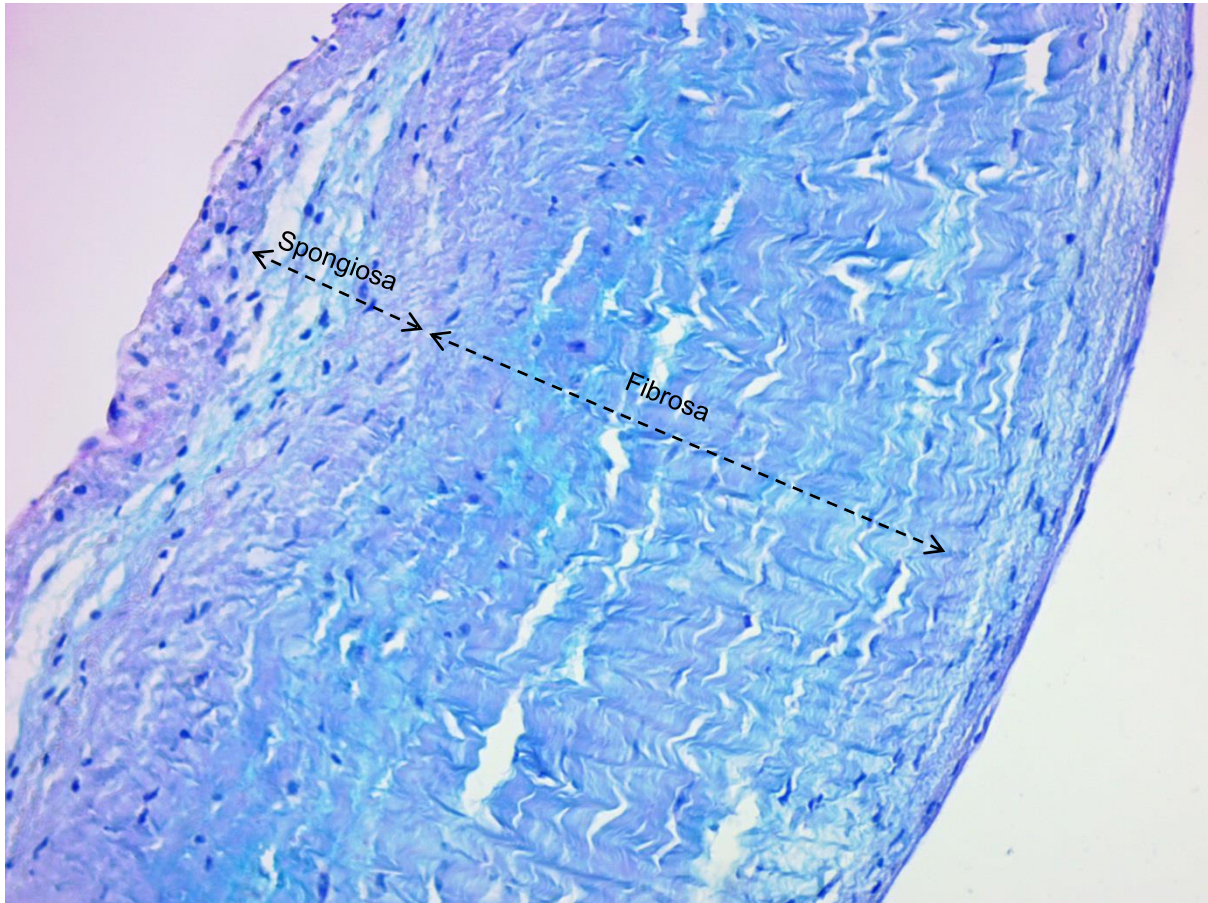
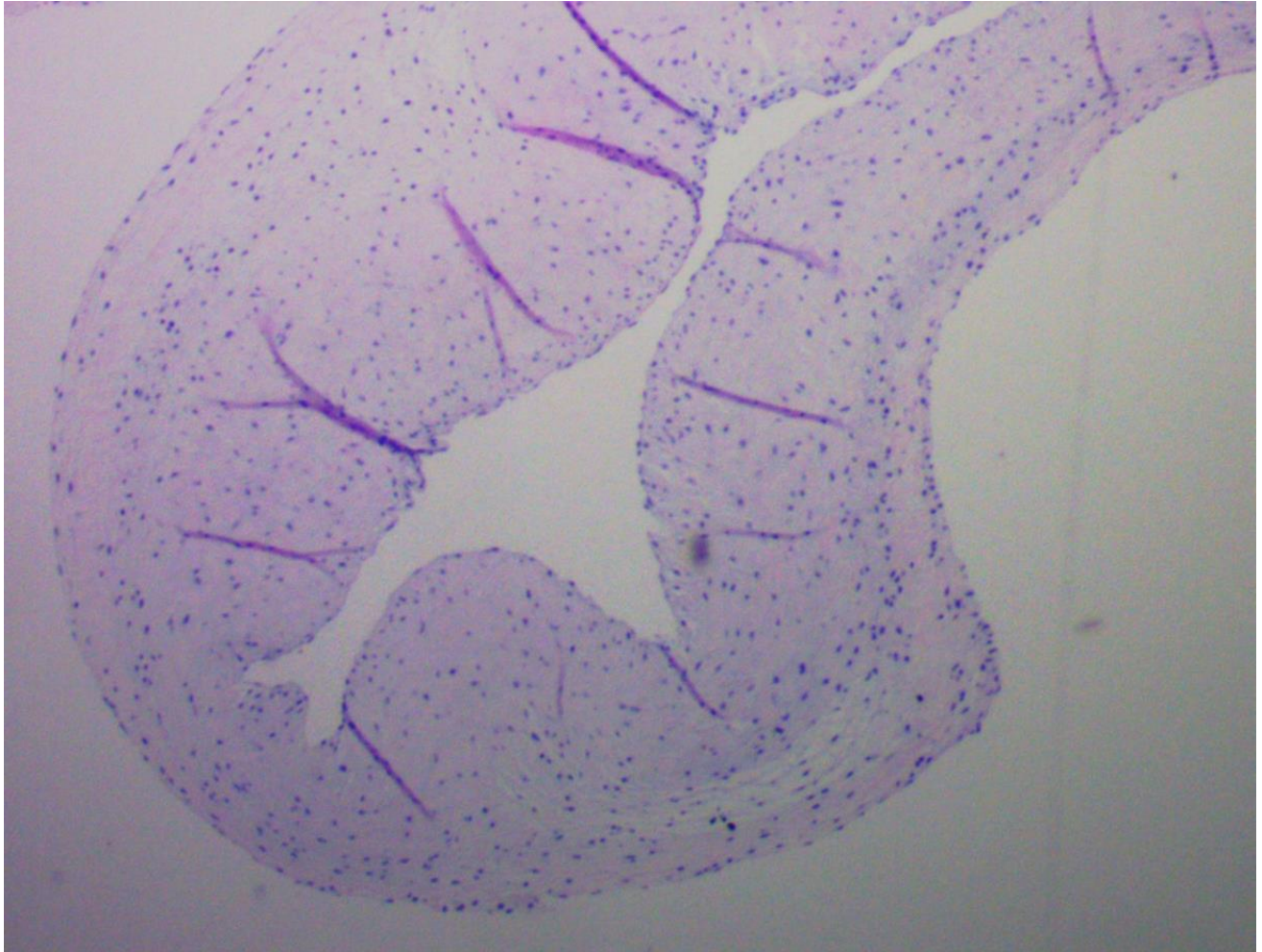


**Fig 3.44:** Histological section of excised anterior valve leaflet with Verhoeff and Van Gieson stain (40x) to show valve thickness:



**Fig 3.45:** Histological section of excised anterior valve leaflet with Haematoxylin and Eosin (H and E stain) (40x). Note the abundance of cellular nuclei in the leaflet:



**3.6.2** The histological section of the **jugular vein leaflet after preparation but before it has been implanted (control vein leaflet)** has more elastic fibres in the tunica media than the atrialis layer of the anterior mitral valve leaflet. The collagen fibres in the tunica media and tunica adventitia are more loosely arranged than in the fibrosa layer of the anterior mitral leaflet (Fig 3.46 to Fig 3.48). The vein wall thickness ranges from 0.30 - 0.5 mm, so the double layered vein leaflet thickness ranges from 0.6 - 1mm (Fig 3.49). The endothelial layer lining the tunica intima of the control vein shows a continuous endothelial lining (Fig 3.49). (The tunica intima, tunica media and tunica adventitia from here on will be referred to as intima, media and adventitia.)

**Fig 3.46:** Histological section of the jugular vein leaflet after preparation but before implant (control vein leaflet) shows the histological layers with Verhoeff and Van Gieson stain (40x). Note the tunica intima is on the outside of the vein leaflet and the tunica adventitia is in the middle. The 2 vein layers separated during the processing of the sample with a space between the layers (red arrow). The tunica media contains more elastic fibres (black) than the atrialis layer of the anterior leaflet and the collagen fibres are more loosely arranged as in the fibrosa (purple) of the anterior leaflet.

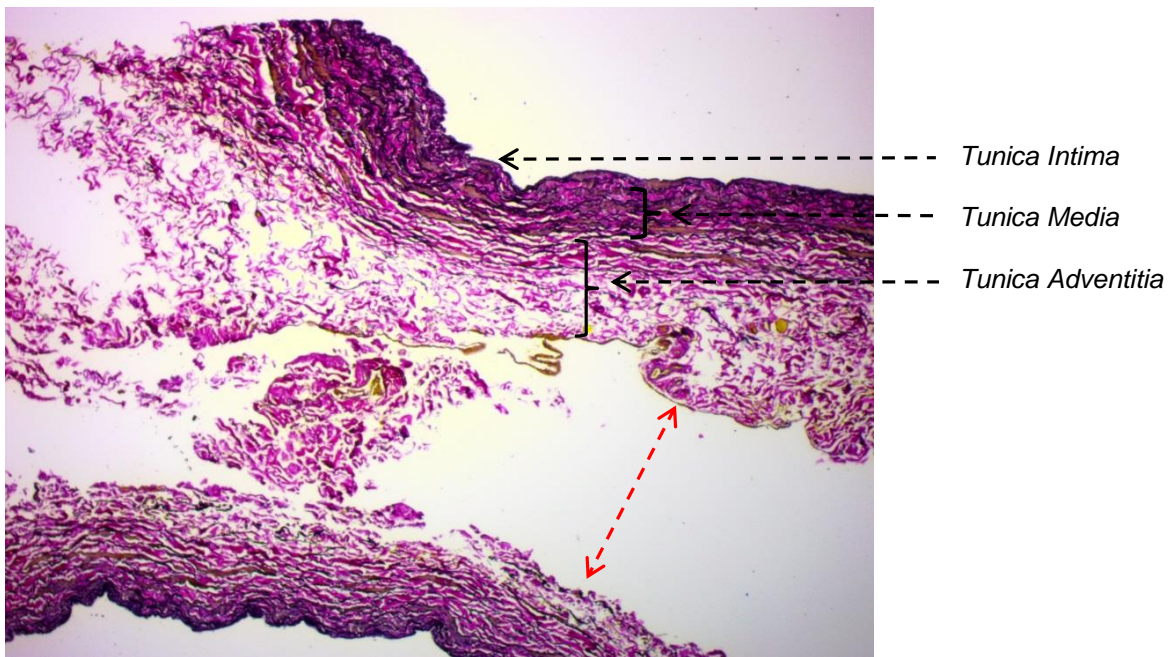


**Fig 3.47** Comparison of histological sections of the anterior mitral leaflet (left) and the internal jugular vein (right). Both were stained with Verhoeff and Von Gieson (200x) to show the elastic fibre (black) and the collagen fibre (dark pink) arrangement. The internal jugular vein contains more elastic fibres and the collagen fibres are more loosely arranged than the anterior mitral leaflet.

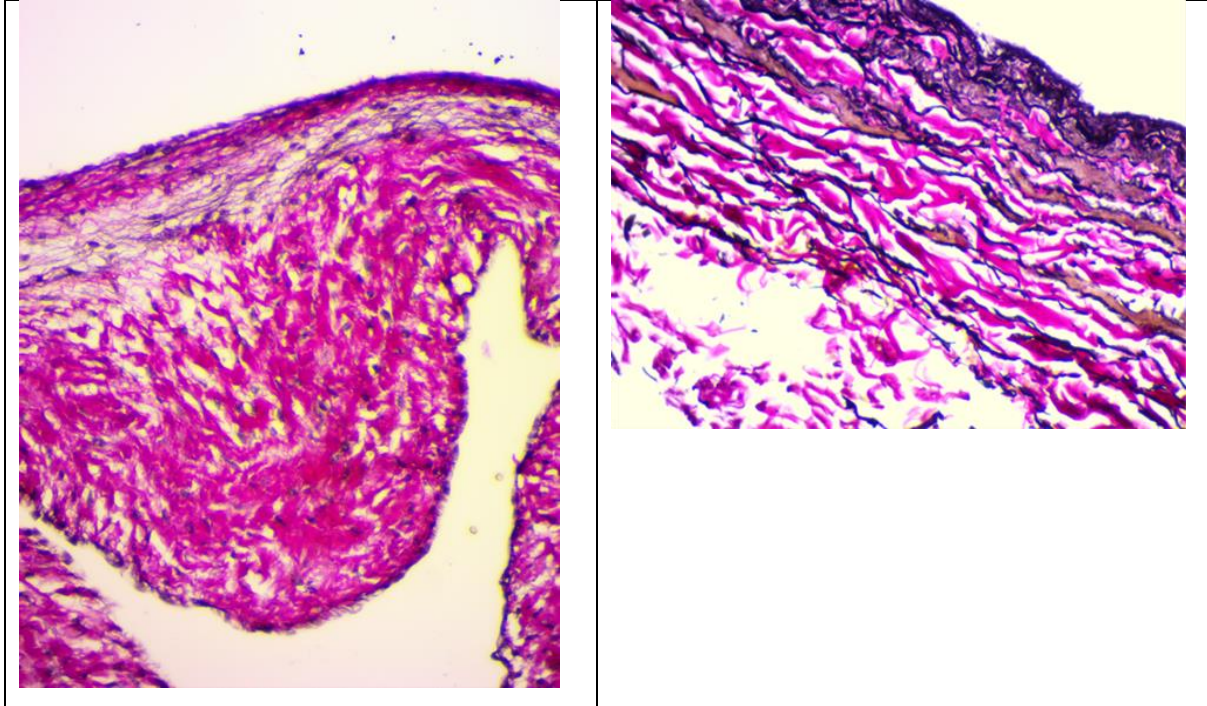


**Fig 3.48:** Histological section of the jugular vein leaflet before implant (control vein leaflet) with APAS stain (200x) to show the collagen and extracellular matrix of the vein wall.

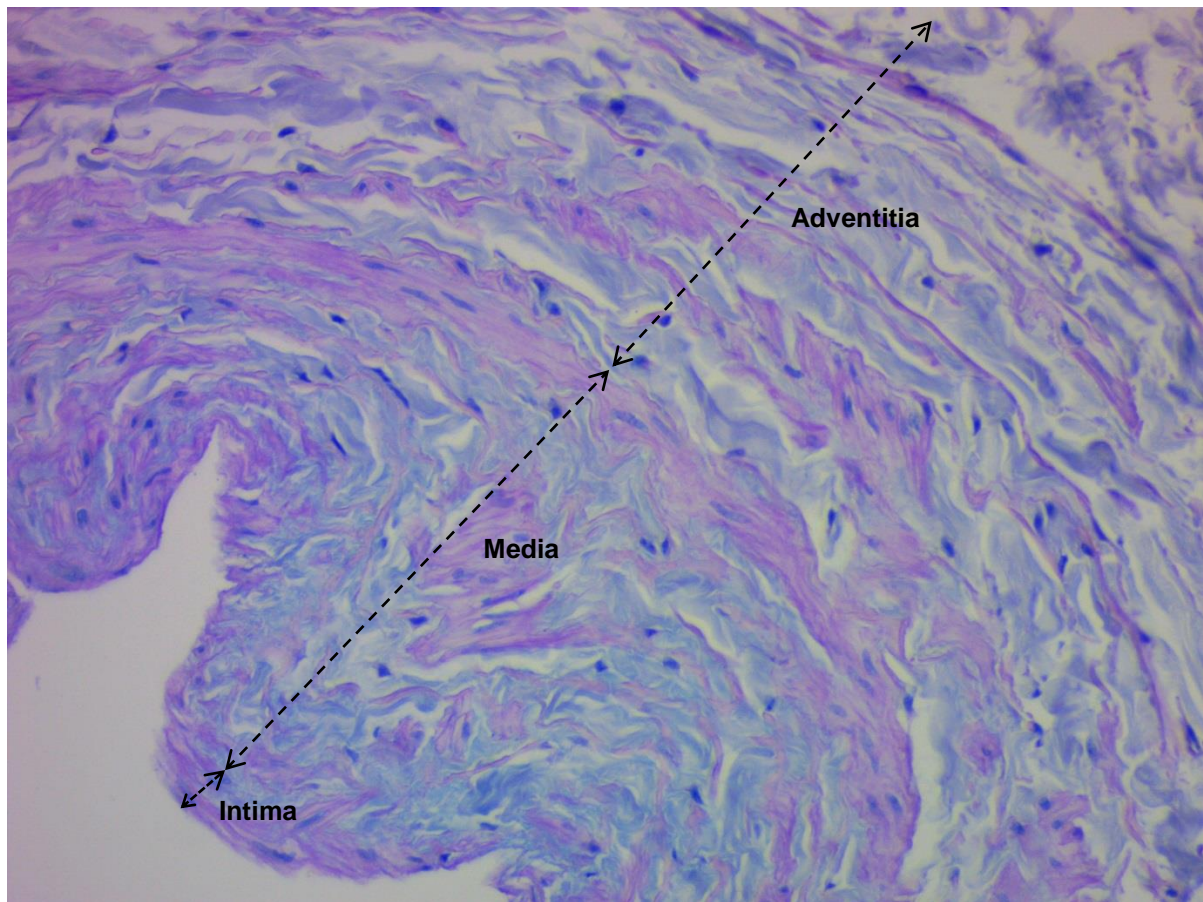


**Fig 3.49:** *Histological section of the jugular vein leaflet before implant (H and E stain 40x) shows the elastic fibres (dark pink), collagen (light pink) and the cellular nuclei of the smooth muscle cells. The intima is lined with a continuous endothelial layer. The vein wall thickness measured 0.3mm.*

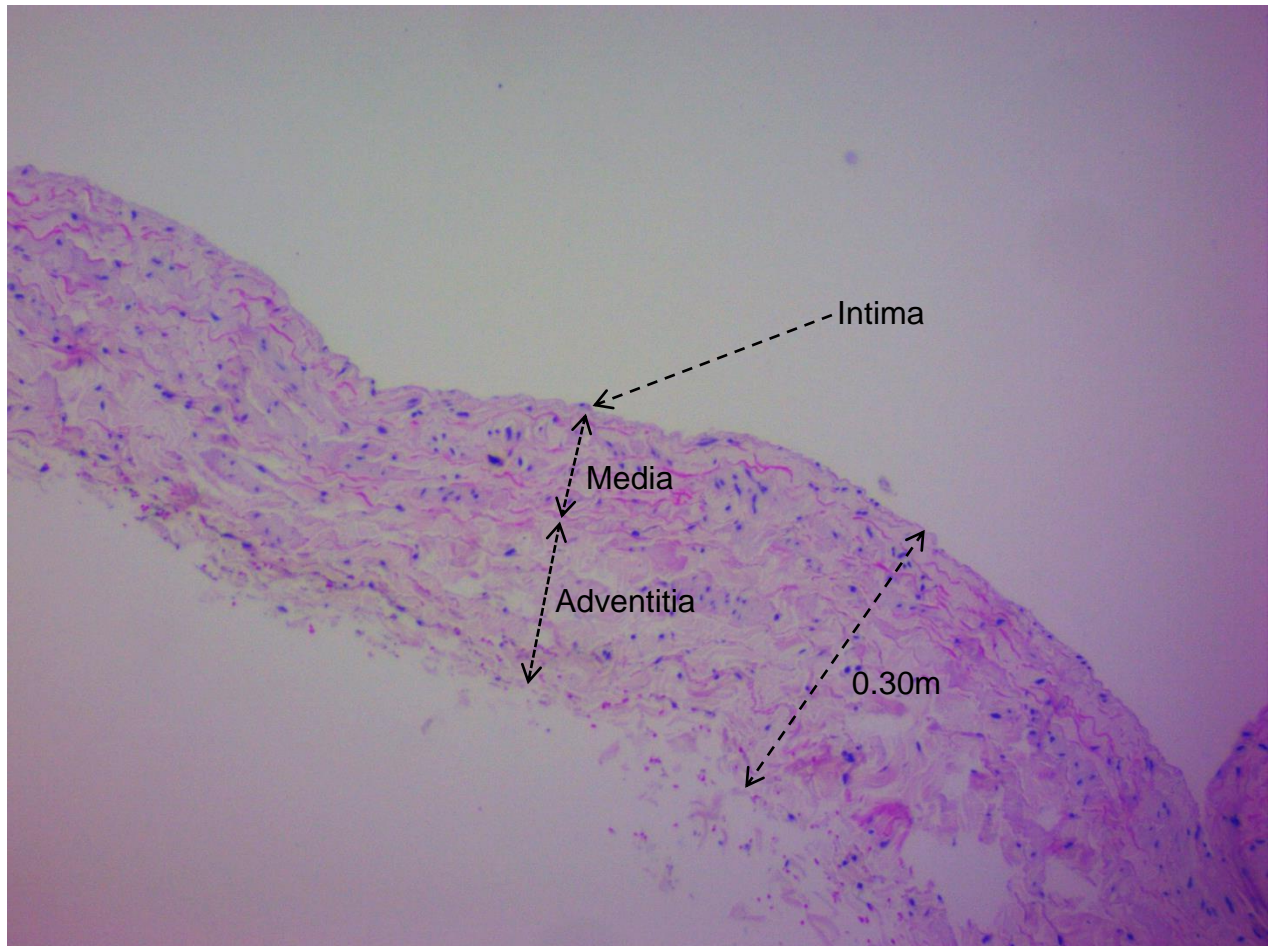


**Table 3.6:** *Histological results of the vein implants*

	Length of implant	Overlying fibrin	Infective vegetation	Endothelium	Calcification in the vein	Space obliterated between layers Nature of obliteration	Chordae tendinae	Valve annulus	Minimum valve thickness (mm)	Maximum valve thickness (mm)
1	4.1 months	Focal	Absent	Focal necrosis at A2 edge	Absent	Complete obliteration with fibrous proliferation	Normal	Normal	1.5	2
2	1 month	Absent	Absent	Normal	Absent	Focal obliteration with fibrous stroma and area of hematoma	Normal	Normal cartilage seen as part of fibrous annulus. Early calcification around sutures	2	6.5
3	9.7 months	Focal	Absent	Normal	Absent	Complete obliteration with fibrovascular proliferation	Normal, calcification at papillary muscle	Normal	2.5	6.5
4	2 days	Absent	Absent	Focal necrosis	Absent	Focal obliterated and area with hematoma	Normal	Normal	1	4.5
5	8.3 months	Absent	Absent	Normal	Focal at suture line and chordal attachment	Complete obliteration with fibrovascular proliferation	Extensive calcification	Osseous metaplasia	2	3
6	7.2 months	Absent	Absent	Normal	Focal	Complete obliteration with fibrovascular proliferation	Normal	Focal calcification Osseous metaplasia	1.75	3.5
7	2 days	Extensive Fresh fibrin	Absent	Focal necrosis 50%	Absent	Focal obliteration with fresh fibrin	Normal	Normal	0.75	3
8	6 months	Vegetations	Extensive with destruction	Necrosis	Focal	SBE	SBE	Normal	3	5



	Length of implant	Overlying fibrin	Infective vegetation	Endothelium	Calcification in the vein	Space obliterated between layers  Nature of obliteration	Chordae tendinae	Valve annulus	Minimum valve thickness (mm)	Maximum valve thickness (mm)
9	6.5 months	Absent	Extensive at leaflet edge with destruction	Normal	Extensive at Gore-Tex chordal attachment and SBE	Complete obliteration with fibrovascular proliferation	Extensive calcification	Normal	3	5.5
10	6.5 months	Absent	Absent	Normal	Absent	Complete obliteration with fibrovascular proliferation	Normal	Normal	1.5	3
11	1 month	Focal	One seen on leaflet edge	Focal necrosis 50%	Absent	Focal obliteration fibrin and organised hematoma in A3 area	Normal	Normal	1	2.5
12	2 hours	Extensive	Absent	Focal necrosis	Absent	Focal obliteration with fibrin	Normal	Normal	1.5	3.5
13	6.4 months	Focal	Absent	Normal	Absent	Complete obliteration with fibrovascular proliferation	Focal calcification	Normal	1.75	2.25
14	6 months	Absent	Absent	Normal	Focal at stitches	Complete obliteration with fibrovascular proliferation	Normal	Normal	3	5
15	4 months	Absent	Absent	Normal	Absent	Complete obliteration with fibrous proliferation	Focal calcification	Normal	1.5	3
16	6 months	Absent	Absent	normal	Absent	Complete obliteration with fibrovascular proliferation	Normal	Normal	2	4
17	6 months	Absent	Absent	Normal	Focal at free edge at chordae	Complete obliteration with fibrovascular proliferation	Focal calcification	Normal	3	3
18	4 months	Extensive	Extensive with destruction	Extensive necrosis	Focal	Complete obliteration with fibrous proliferation	Rupture	SBE	5	5
19	3 days	Focal	Absent	Focal necrosis	Absent	Separate	Normal	Normal	2.5	5
20	3 months	Focal	Absent	Focal necrosis at A1/A2	Absent	Focal obliteration with fibrous proliferation Thick layer of fibrin between layers at A1/A2	Normal	normal	3	6.5
21	6 months	Extensive	Absent	Normal	Absent	Complete obliteration with fibrovascular proliferation	Extensive calcification	Normal	3.5	4.5

**3.6.3** The vein leaflet showed progressive histological changes with the length of time it was implanted. The findings are summarised in Table 3.6.

**3.6.4** The vein leaflets that were implanted for **0-3 days** (sheep 4, 7, 12, 19) showed focal areas of endothelial necrosis which extended into the media (Fig 3.50). Fibrin was found overlying the areas of necrosis on the vein leaflets. Cell proliferation was identified by MIB-1 immunostaining. Abundant proliferation was noticed in the media and adventitia from day 2 in the transplanted vein as part of the vein wall remodeling. In the same area of focal necrosis as seen in Fig 3.50, cell proliferation was absent which suggests that these areas were not viable (Fig 3.51). Muscle specific actin (MSA) immunostaining recognizes the alpha actin from cardiac, skeletal and smooth muscle sources and was used to mark smooth muscle cells and myofibroblasts in the media and adventitia. The areas of focal necrosis in Fig 3.50 showed a notable absence of smooth muscle cells with MSA immunostaining (Fig 3.52).

The space between the layers of the vein leaflet was filled with fresh fibrin. Sheep 4 had an area of hematoma between the vein layers with areas of vein wall necrosis overlying the hematoma. (Table 3.4, Figs 3.53 and Fig 3.54).

**Fig 3.50:** Histological section of the vein leaflet of sheep 19 (H and E stain 40x) shows a focal area of necrosis (brackets) with overlying fibrin. The space between the vein layers are filled with fresh fibrin.

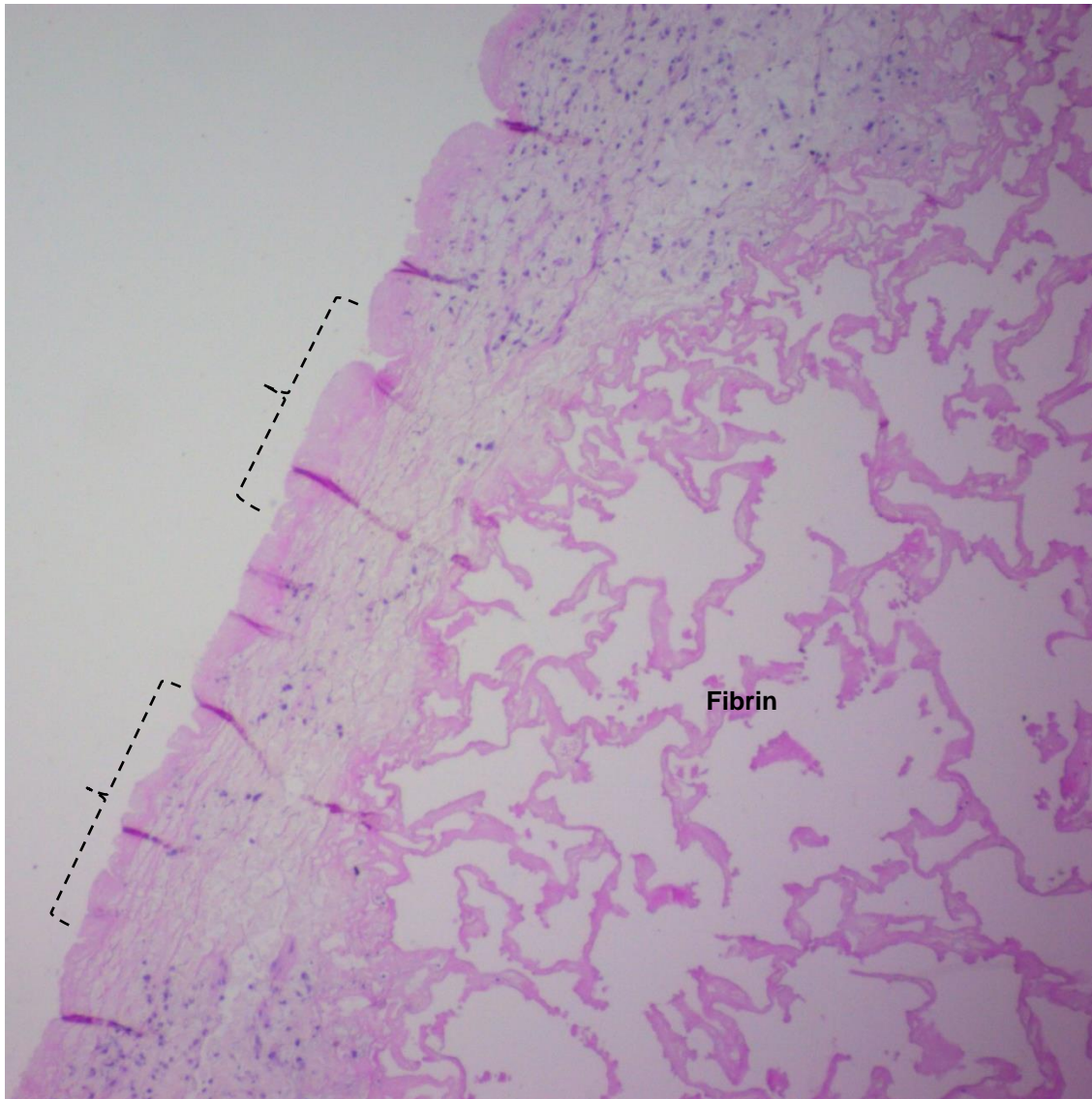


**Fig 3.51:** Cell proliferation identified by MIB-1 immunostaining of histological section of the vein leaflet of sheep 19 (same section as Fig 3.50) (20x). Note the abundant cell proliferation in the media and adventitia (cell nuclei mark brown). There is also a complete absence of proliferating cells in the areas of necrosis (brackets)

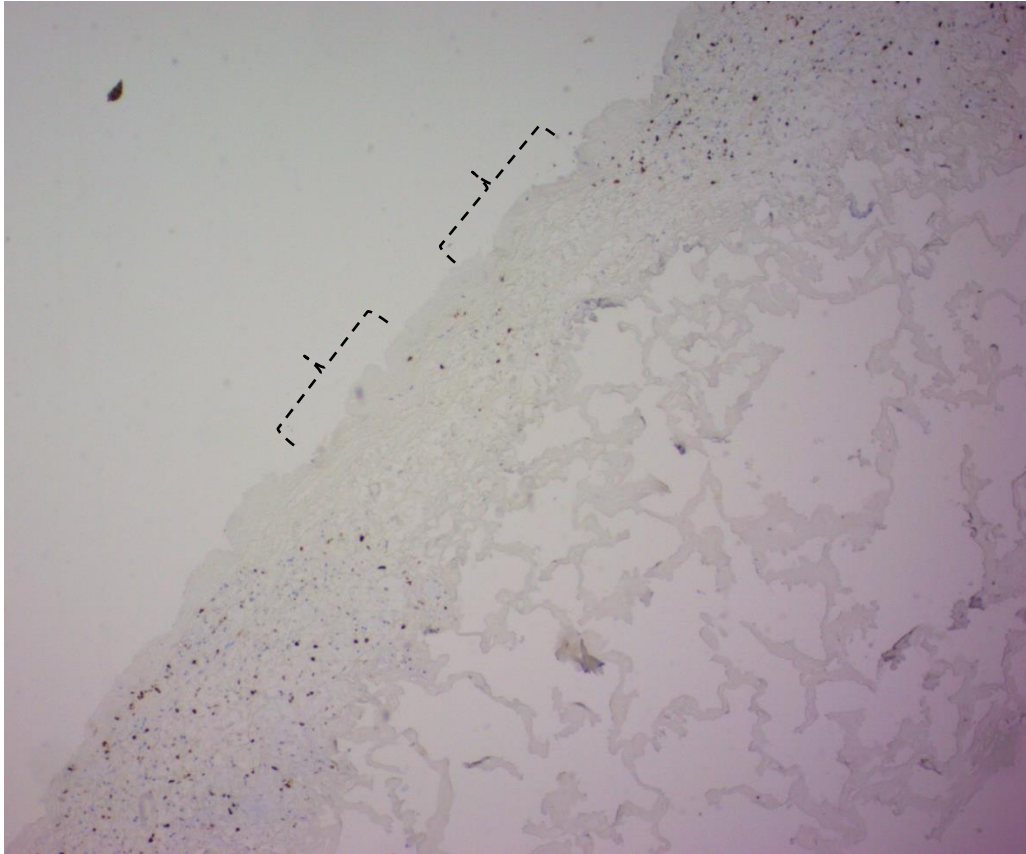


**Fig 3.52:** MSA (Muscle-specific actin) immunostaining identifies the alpha-actin in the smooth muscle cells and myofibroblasts in the media and adventitia (brown marking). Note the absence of the smooth muscle cell immunostaining in the area of necrosis (bracket) and the abundance of smooth muscle cells on the opposite side (arrows).

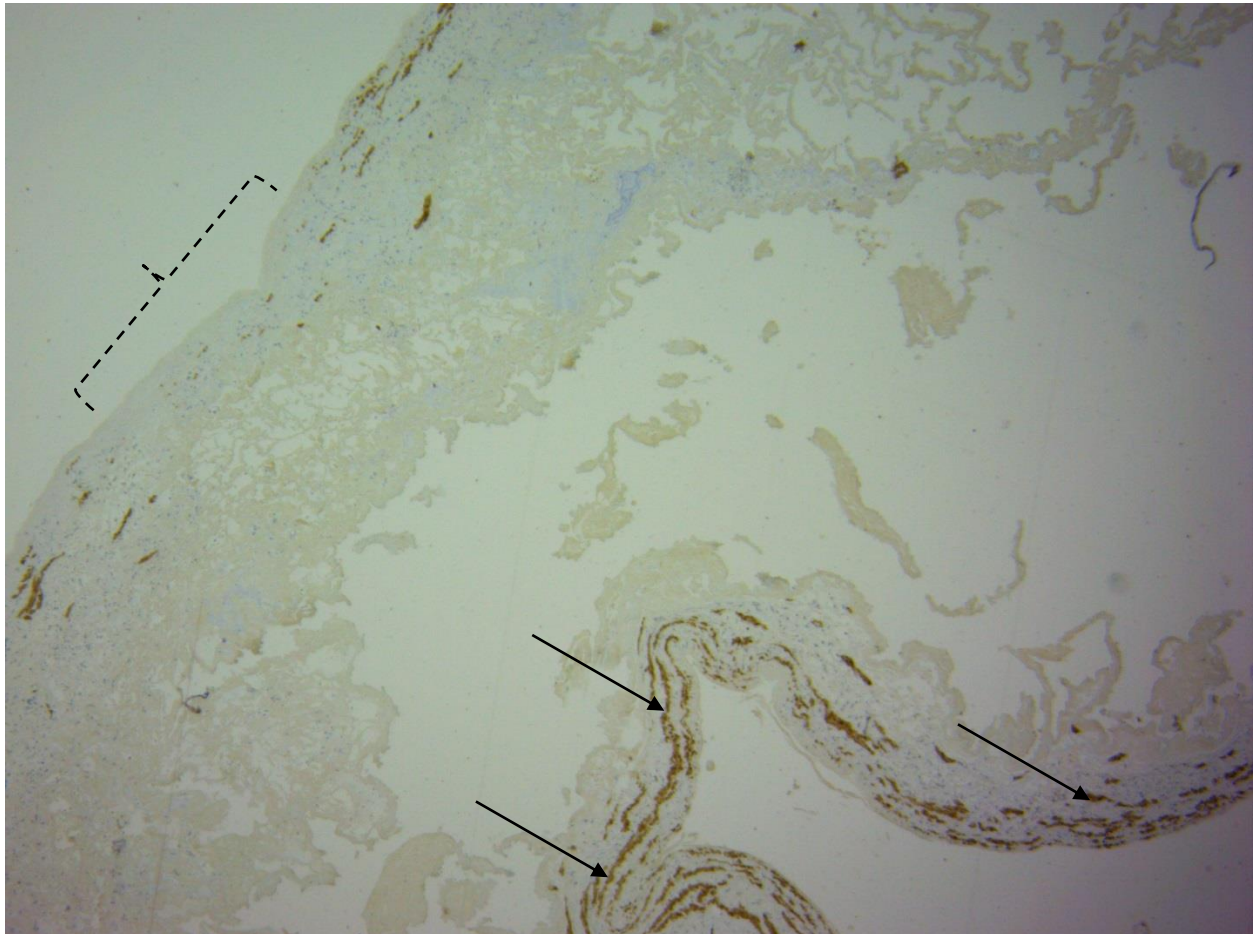


**Fig 3.53:** Histological section of the vein leaflet of sheep 4 shows a fresh hematoma which separates the 2 vein layers. Verhoeff and Van Gieson stain (20x).

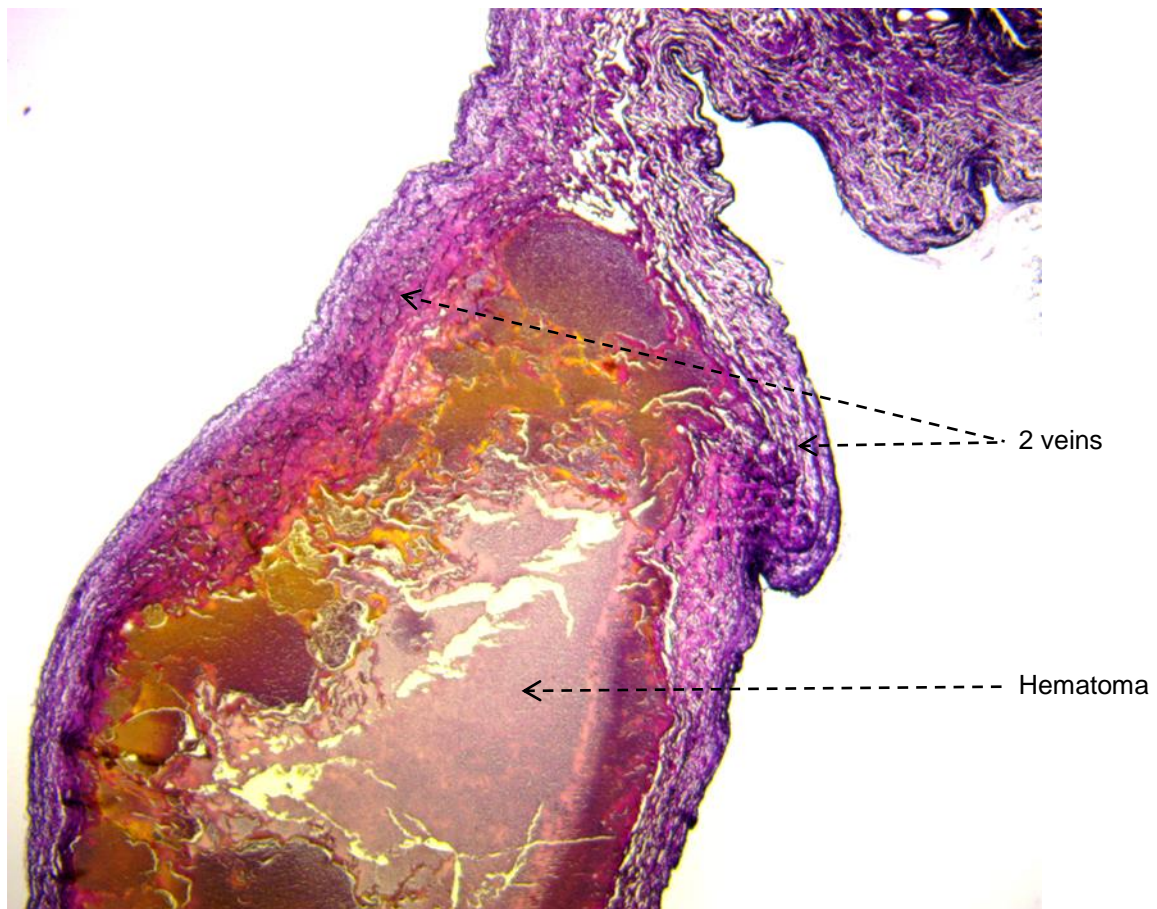
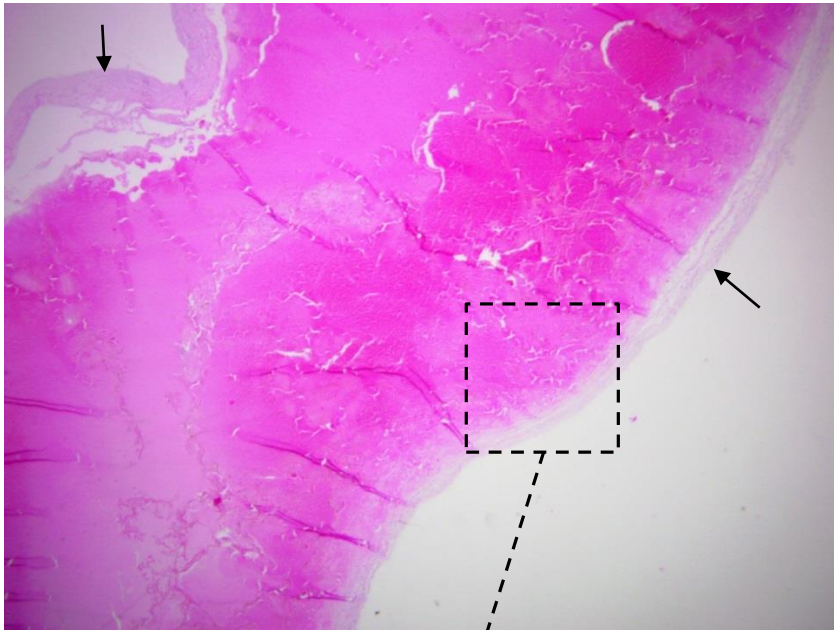
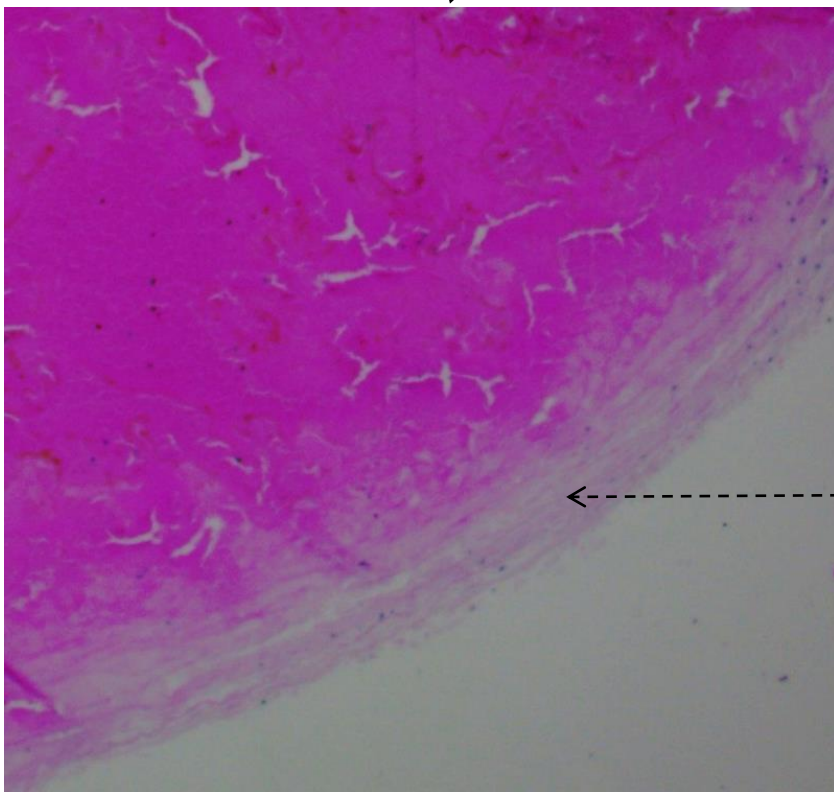


**Fig 3.54:** Histological section of the vein leaflet of sheep 4 shows a fresh hematoma which separates the 2 vein layers (arrows). Note the endothelial and media necrosis of the vein overlying the hematoma. (a) H and E stain 20x (b) H and E stain 40X

(a) H and E stain 20x



(b) H and E stain 40X



Endothelial and medial necrosis with lack of cellular structure and nuclei.

### 3.6.5 Two vein leaflets were implanted for 1 month (sheep 2 and 11).

The valve of sheep 2 showed fibrous changes in the stroma between the 2 vein leaflets with new capillary vessel formation seen as part of the granulation process. This fibrous proliferation in the adventitia part of the veins caused significant thickening of the vein leaflet (Fig 3.55). Increased fibroblastic activity was also noted where the vein leaflet was attached at the annular suture line (Prolene 5-0) with foreign body tissue reaction and early calcification around the suture material at the annulus (Fig 3.56). Cartilage was seen in the fibrous annulus which is a normal finding in sheep as part of the central fibrous body at the aortic mitral curtain (Frink and Merrick 1974). The area where the hematoma was noticed macroscopically on the vein (Fig 3.13) showed organising fibrin that caused significant thickening of the vein leaflet. (Fig 3.57). The vein endothelium appeared normal with no areas of necrosis.

The valve of sheep 11 also had an area of organised fibrin between the vein layers at A1 which caused vein leaflet thickening. The vein endothelium showed areas of necrosis overlying the organising fibrin (Fig 3.58). Other parts of the vein leaflet showed fibrous proliferation in the vein leaflet similar to sheep 2. An infective vegetation with Gram negative bacteria was seen on this leaflet and this histology is discussed further with the group of sheep with infective endocarditis.



**Fig 3.55:** Histological section of vein leaflet of sheep 2 (H and E stain 20x). Note the increased thickness of the vein leaflet because of the fibrous proliferation between the 2 veins.

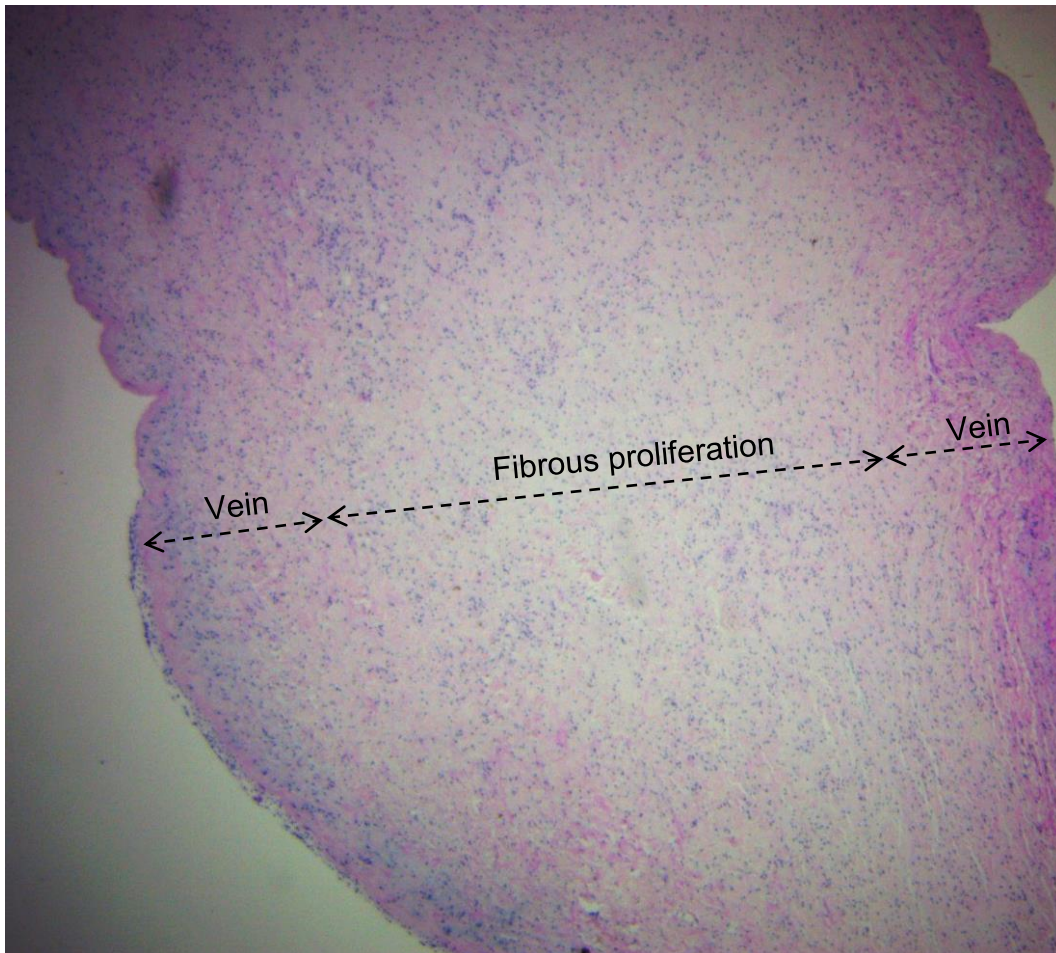


**Fig 3.56:** Histological section of the vein leaflet of sheep 2 through the annular suture line where the vein is attached to the annulus. Increased fibroblastic activity is noted in this area (black arrows) (H and E stain 20x) Early calcification is noted around the annular suture (red arrow). Prolene 5-0 was used as the annular suture in this sheep. Cartilage is seen in the fibrous annulus which is normal a normal finding in sheep.

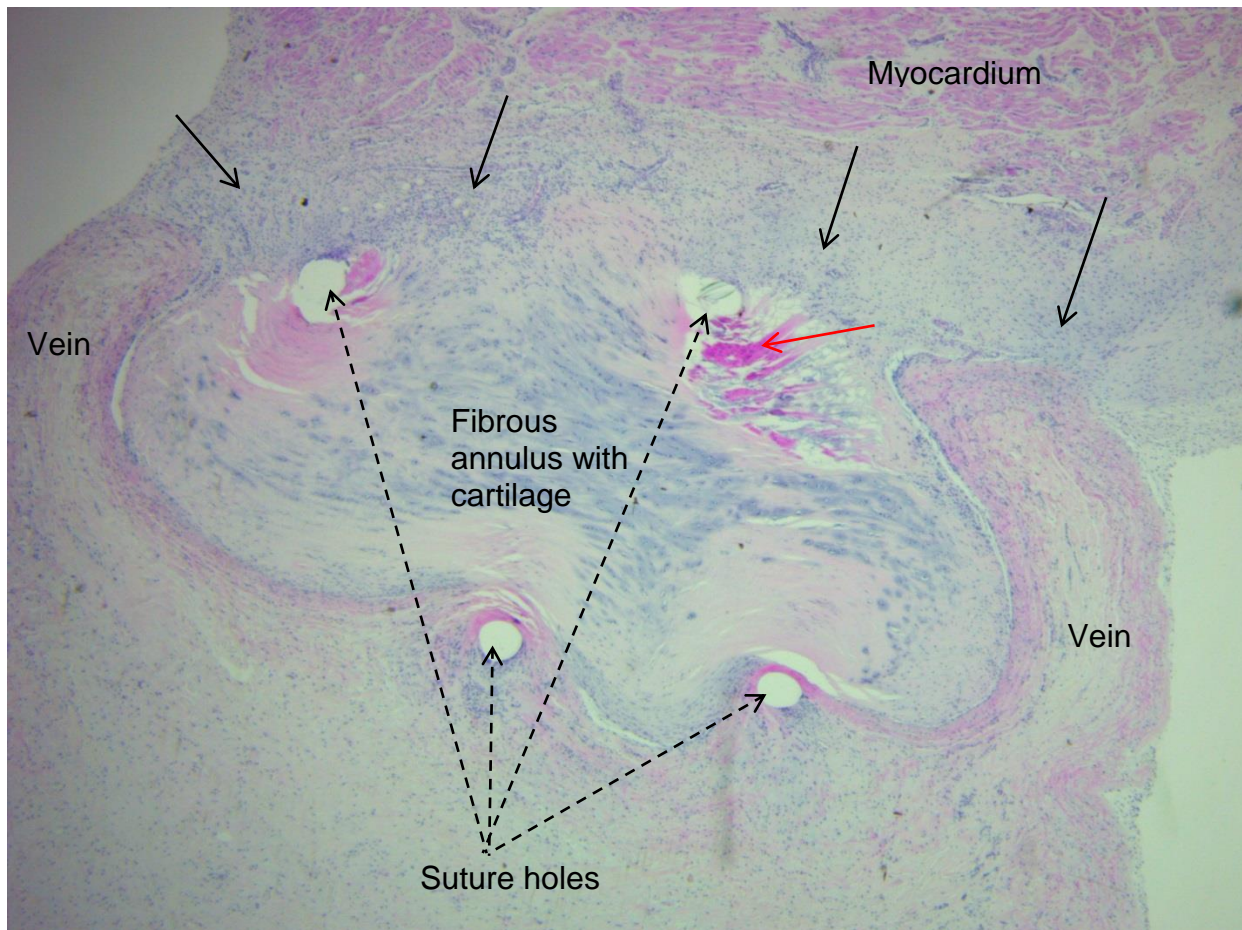


**Fig 3.57:** Histological section through the vein leaflet of sheep 2 with the organised hematoma. Organised fibrin between the vein layers causes marked thickening of the vein leaflet (6.5 mm). The endothelium looks normal with no areas of necrosis. (H and E stain 20x)

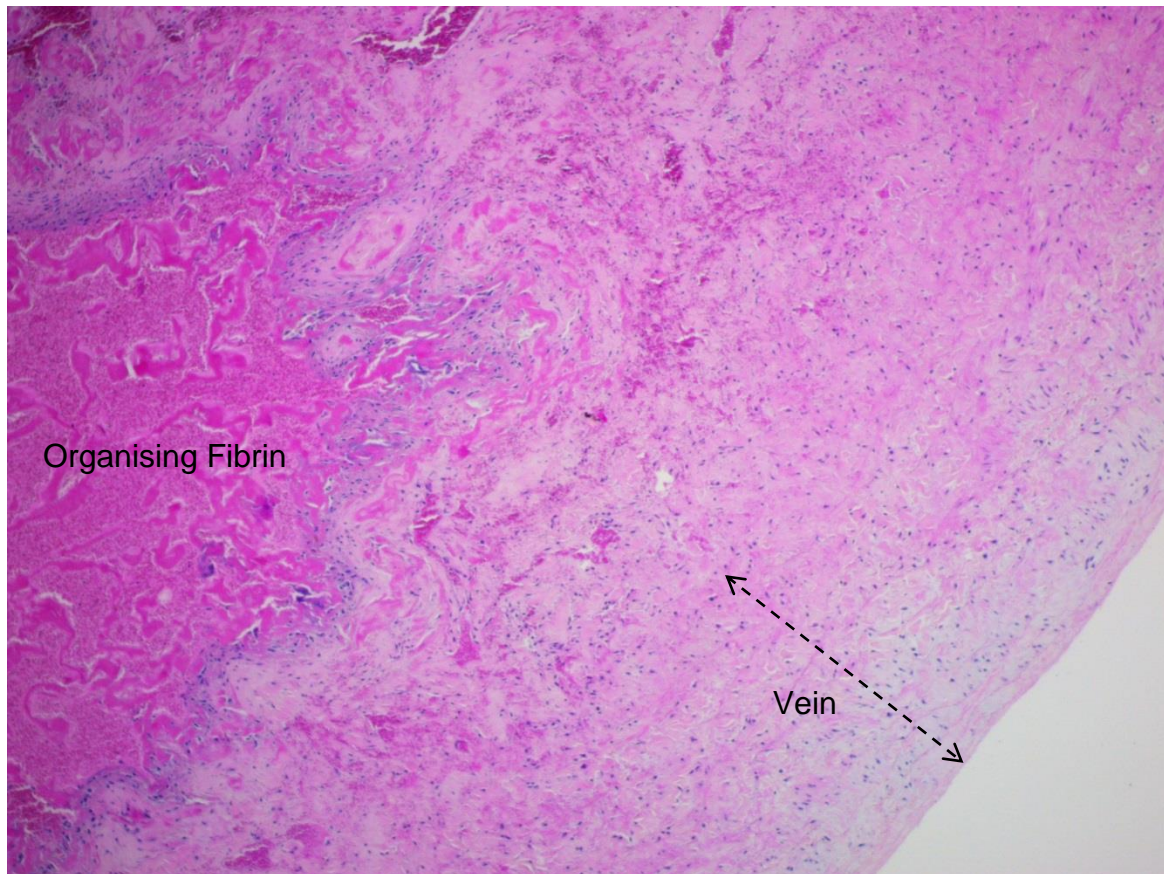
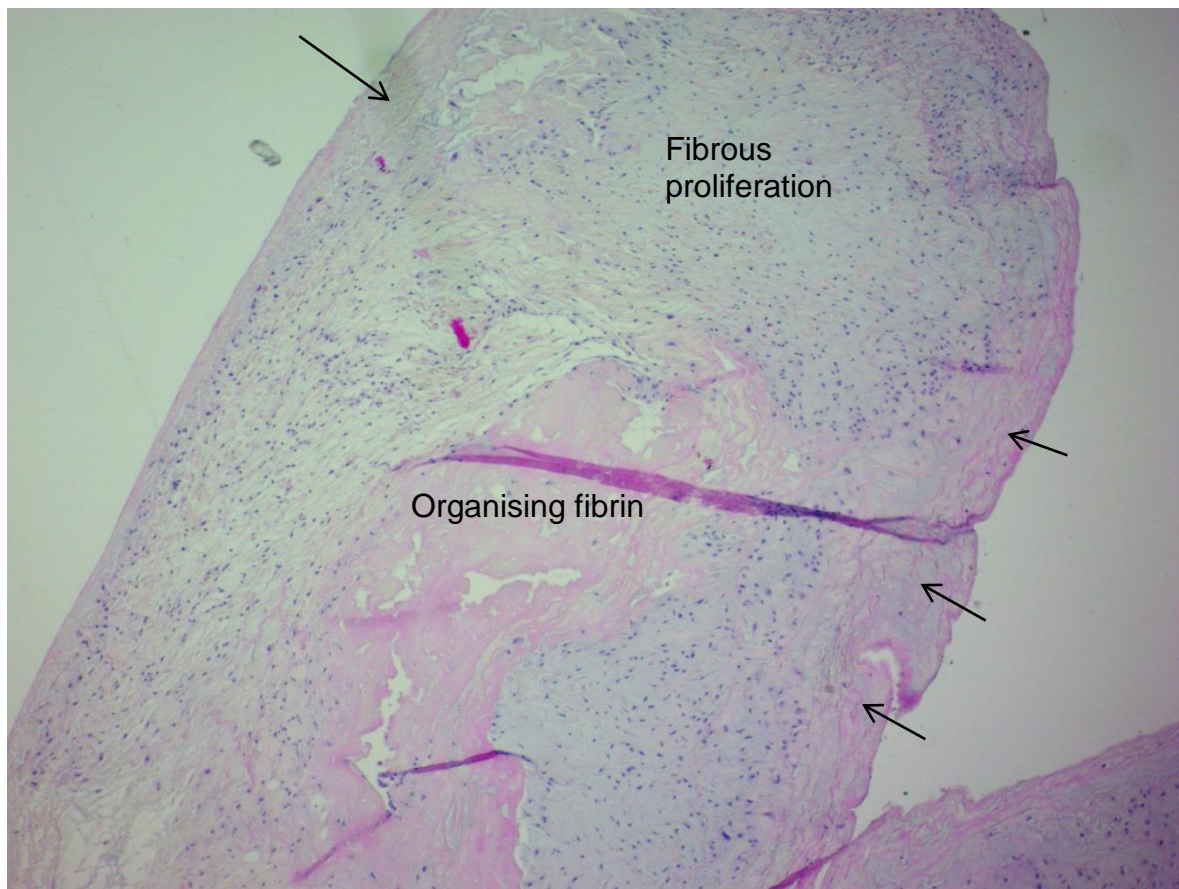


**Fig 3.58:** Histological section of sheep 11 shows organising fibrin in the vein leaflet with necrosis of parts of the vein wall overlying the fibrin (arrows) (H and E stain 40x).



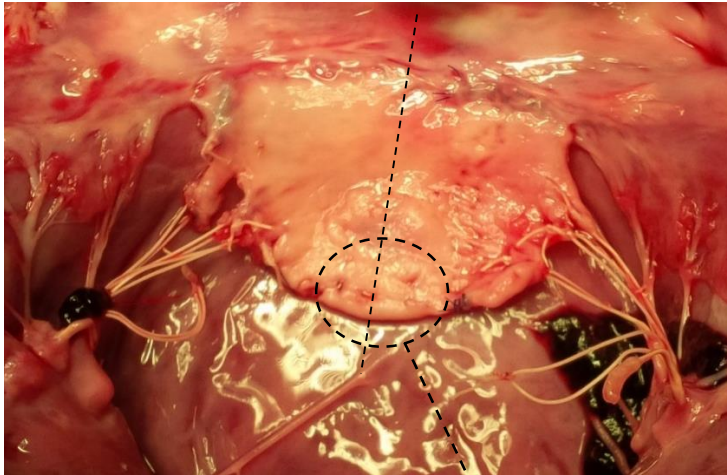
**3.6.6** Three vein leaflets were implanted for **3-4 months** (sheep 1, 15 and 20). The vein leaflet of sheep 1 showed endothelial and media necrosis in the distal part of the vein leaflet close to the leaflet edge on the atrial side. This part of the leaflet (A2) was under severe tension from the Gore-Tex chordae because of ventricular enlargement and annular dilatation (Table 3.4). The left ventricular and annular dilatation put the Gore-Tex chordae under increased tension with eventual disruption of the chordae from the leaflet edge (Fig 3.59). The ventricular side of the vein leaflet showed a viable vein and endothelium. Fibrin was noticed overlying the endothelium on the atrial side and intimal hyperplasia was noticed on the ventricular side. The space between the veins was obliterated with fibrous proliferation.

The vein leaflet of sheep 20 also showed a focal area of vein necrosis. The area of vein necrosis was on the ventricular side of the vein leaflet overlying the thickened part of the leaflet which contained a large amount of organised fibrin (Fig 3.60 and Fig 3.61). The large amount of fibrin could have been caused by blood that entered between the 2 vein layers during systole where the central suture line disrupted (Fig 3.60). The rest of the leaflet showed obliteration of the space between the 2 veins with fibrous proliferation with normal endothelium.

The vein leaflet of sheep 15 showed normal endothelial covering of the vein leaflet at 4 months with no necrosis. The space between the 2 veins were completely obliterated with fibrous proliferation (Fig 3.46). Some of the Gore-Tex chordae showed focal calcification.

**Fig 3.59:** (a) Vein implant of sheep 1 showing the section line of the histological sample (dashed line) and the area of necrosis (circle). (b) Histological section shows the area of endothelial and media necrosis and fibrin overlying the endothelium on the atrial side. Intimal hyperplasia is seen on the ventricular side (H and E stain 20x).

(a)



(b)

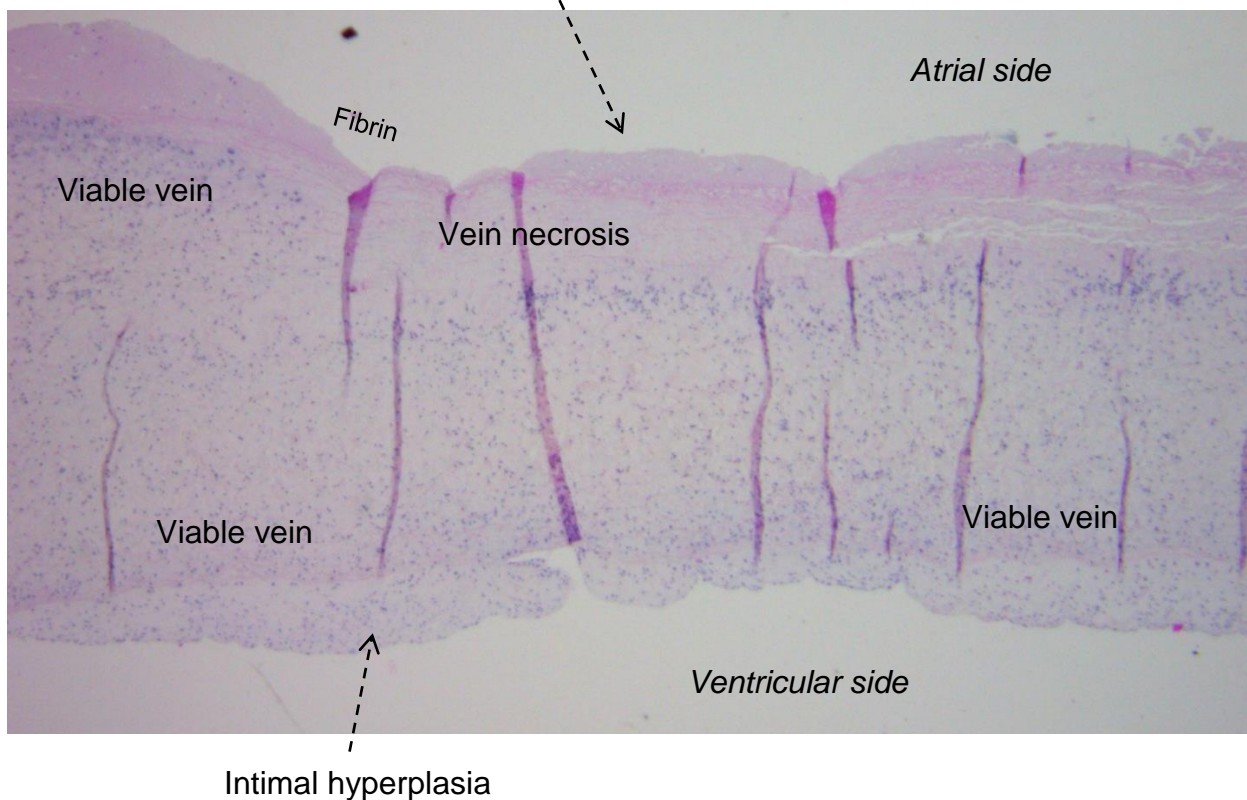
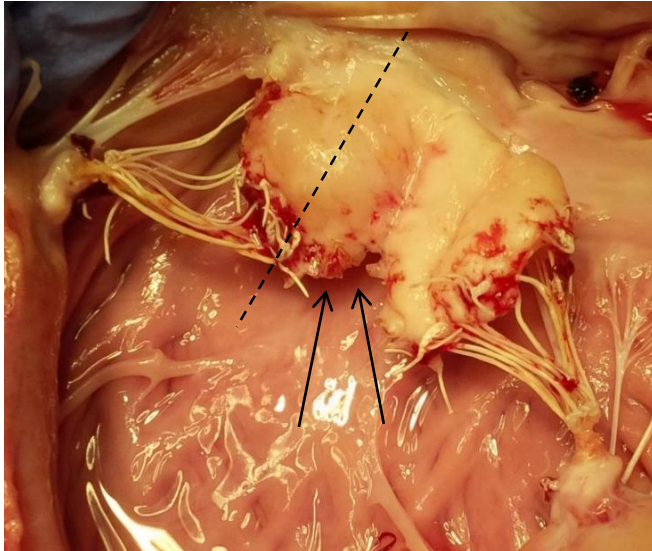


**Fig.3.60:** (a) Valve leaflet of sheep 20 implanted for 3 months. A thickened part of the leaflet is noticed in the A1/A2 area where the 2 layers were separated by a large amount of fibrin. The large amount of fibrin could have been caused by blood that entered between the 2 vein layers during systole (arrows) where the central suture line disrupted.



(b) Section through the thick part of the vein leaflet in (a) on the dashed line shows the large amount of fibrin between the vein layers (circle) and the partial destruction of the ventricular side of the vein (solid arrow)

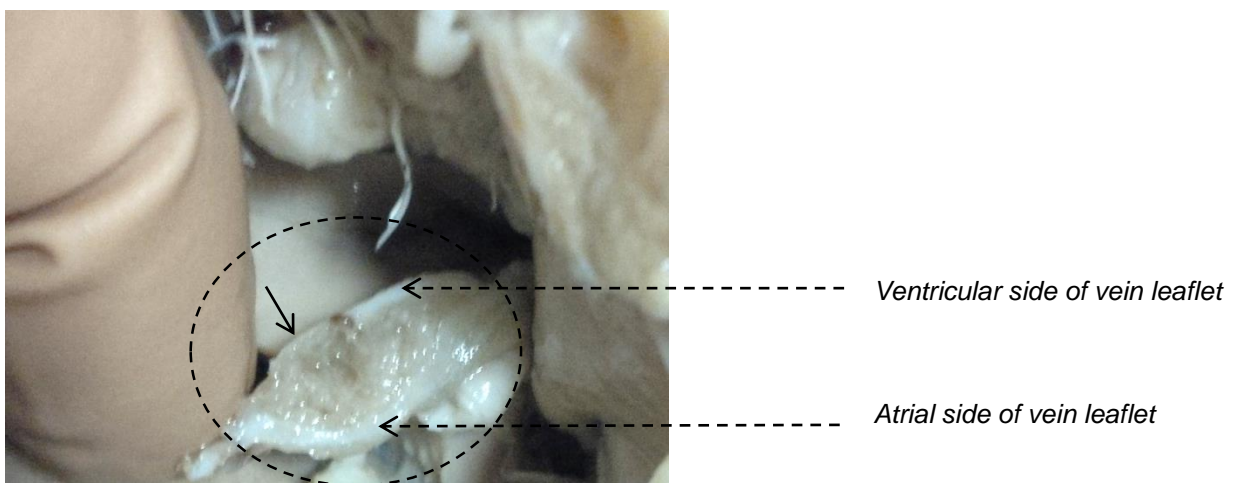


**Fig 3.61:** Histological section through the thick part of the vein leaflet in Fig 3.60 with organised fibrin between the vein leaflets and overlying vein wall. Note the transition between viable vein and necrosis (arrows) on the ventricular side

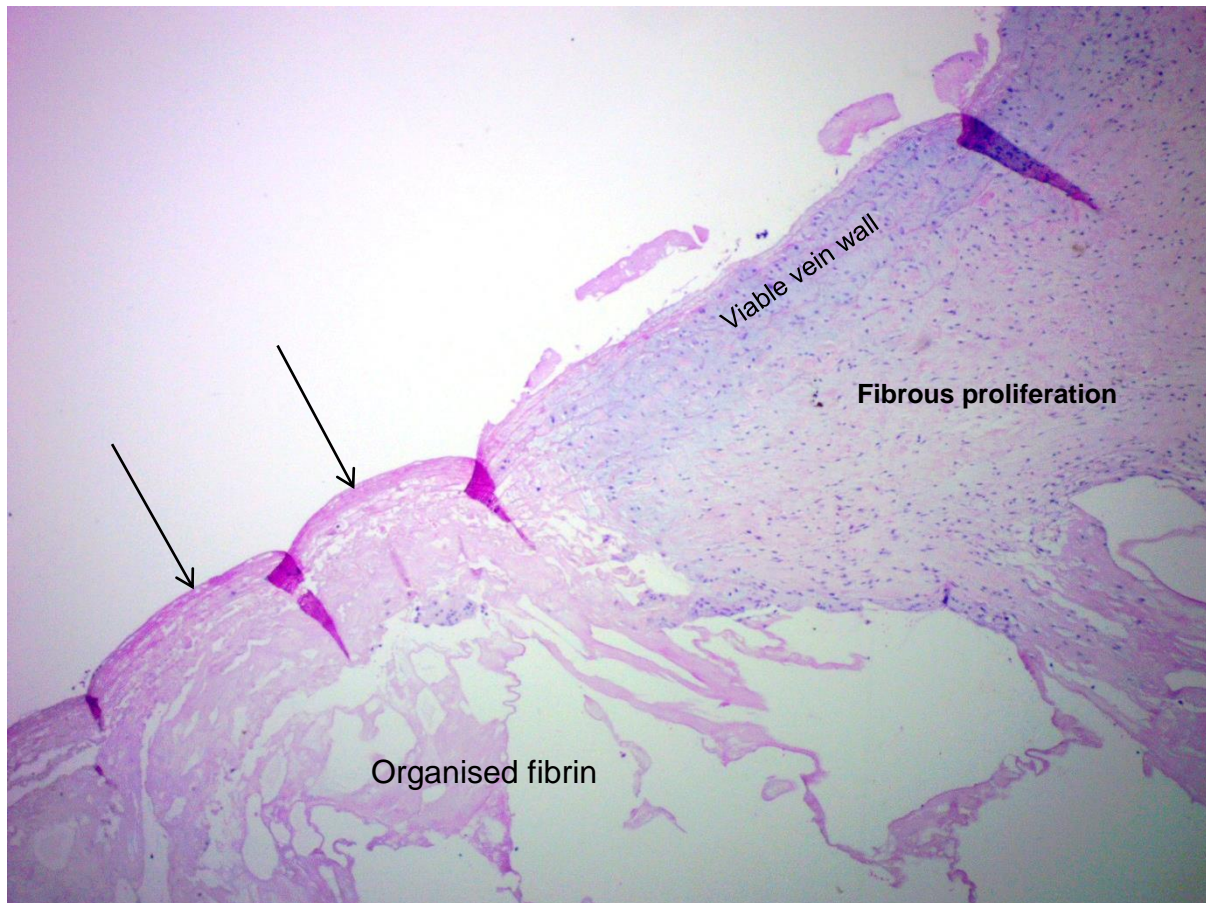
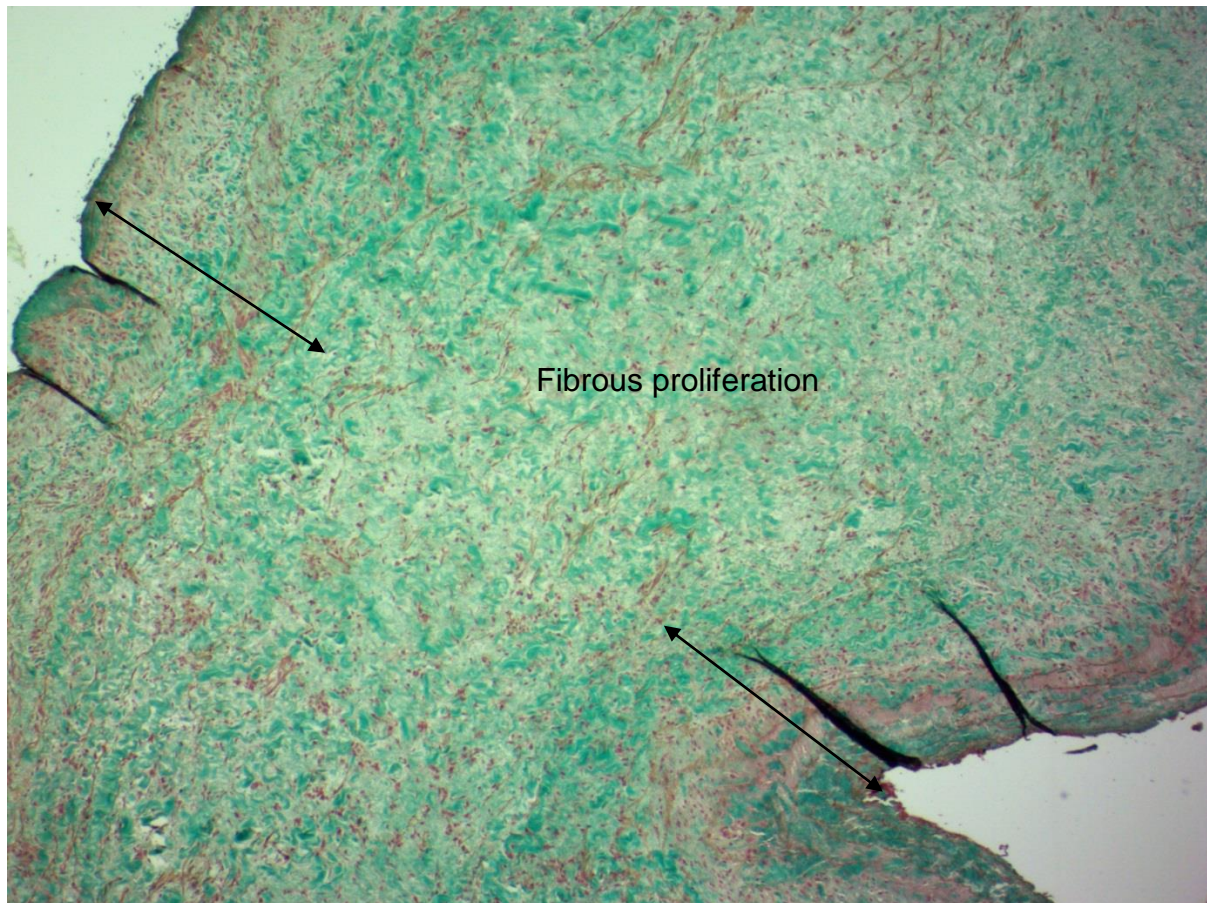




**Fig 3.62:** Histological section of vein leaflet of sheep 15 shows the 2 vein layers (black arrows) and the fibrous proliferation in-between. Masson's Trichrome staining technique was used which colours the collagen fibres green (40x).



**3.6.7** The valves of the 4 sheep with infective endocarditis (SBE) (sheep 8, 9, 11, 18) showed infective vegetations with varying degree of leaflet destruction and necrosis.

Sheep 11 had the leaflet implant for 1 month. The histology showed an infective vegetation with Gram negative bacteria at the leaflet edge where the Gore-Tex chordae implanted. There was an organised hematoma in this leaflet that caused necrosis of parts of the vein wall (Fig 3.58).

Sheep 8 had the implant for 6 months and the histology showed extensive vegetations with destruction of the vein leaflet and inflammatory cell infiltration (Fig 3.63). *Staphylococcus aureus* was cultured from the vegetations. The fibrous proliferation between the veins showed new capillary formation (neovascularization).

Sheep 9 had the implant for **6.5 months** and the histology showed a large vegetation on the leaflet edge with necrosis and inflammatory cell infiltration (Fig 3.64). There was calcification in the vegetation and also on some of the Gore-Tex chordae. The area of the leaflet away from the vegetation was spared and showed normal endothelium and the space between the 2 veins was obliterated with fibrous proliferation (Fig 3.65). Blood vessel formation (neovascularization) was noticed in the fibrous portion of the leaflet. The endothelium also showed intimal fibroplasia (Fig 3.65)

Sheep 18 had the implant for 4 months and had severe SBE on the valve. The histology showed extensive vegetations with fibrin and destruction of the vein leaflet (Fig 3.66 and Fig 3.67). Bacterial clusters and inflammatory cells were seen in the vegetations and focal areas of calcification were noted in the vegetations. Gram stain of the vegetations showed gram negative bacilli (Fig 3.68).

**Fig 3.63:** Histological section of the fibrous part of the vein leaflet of sheep 8 shows an infective vegetation with clusters of bacteria (solid black arrows) surrounded by cell necrosis (pale area without cell nuclei) and neutrophils and monocytes (red arrows) (H and E stain 100x). Neovascularization is also seen in the fibrous proliferation.

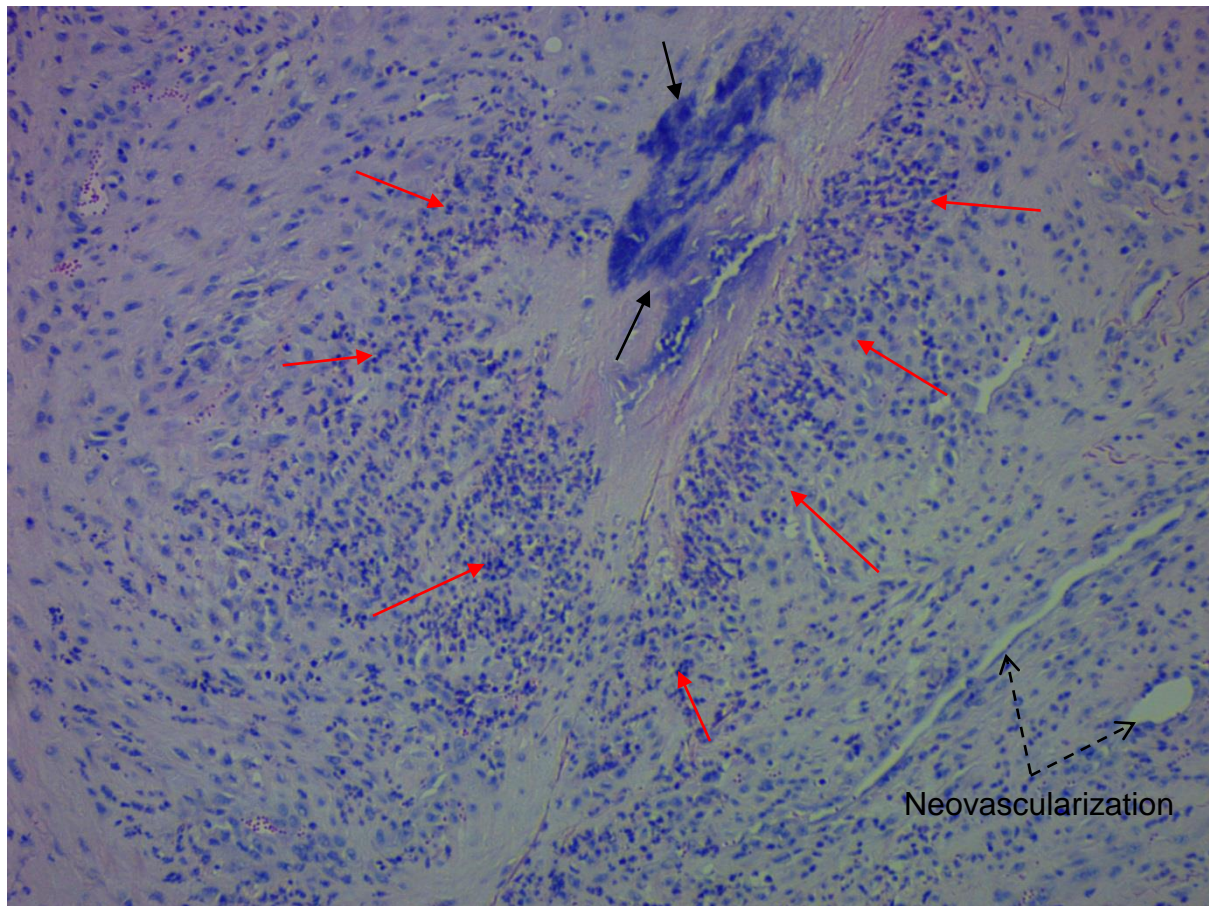


**Fig 3.64:** Histological section of vein leaflet of sheep 9 shows a large vegetation on the leaflet edge (circle) with colonies of bacteria (black arrows), inflammatory cell infiltration (red arrows), necrosis and focal calcification (dark purple) (H and E stain 40x).

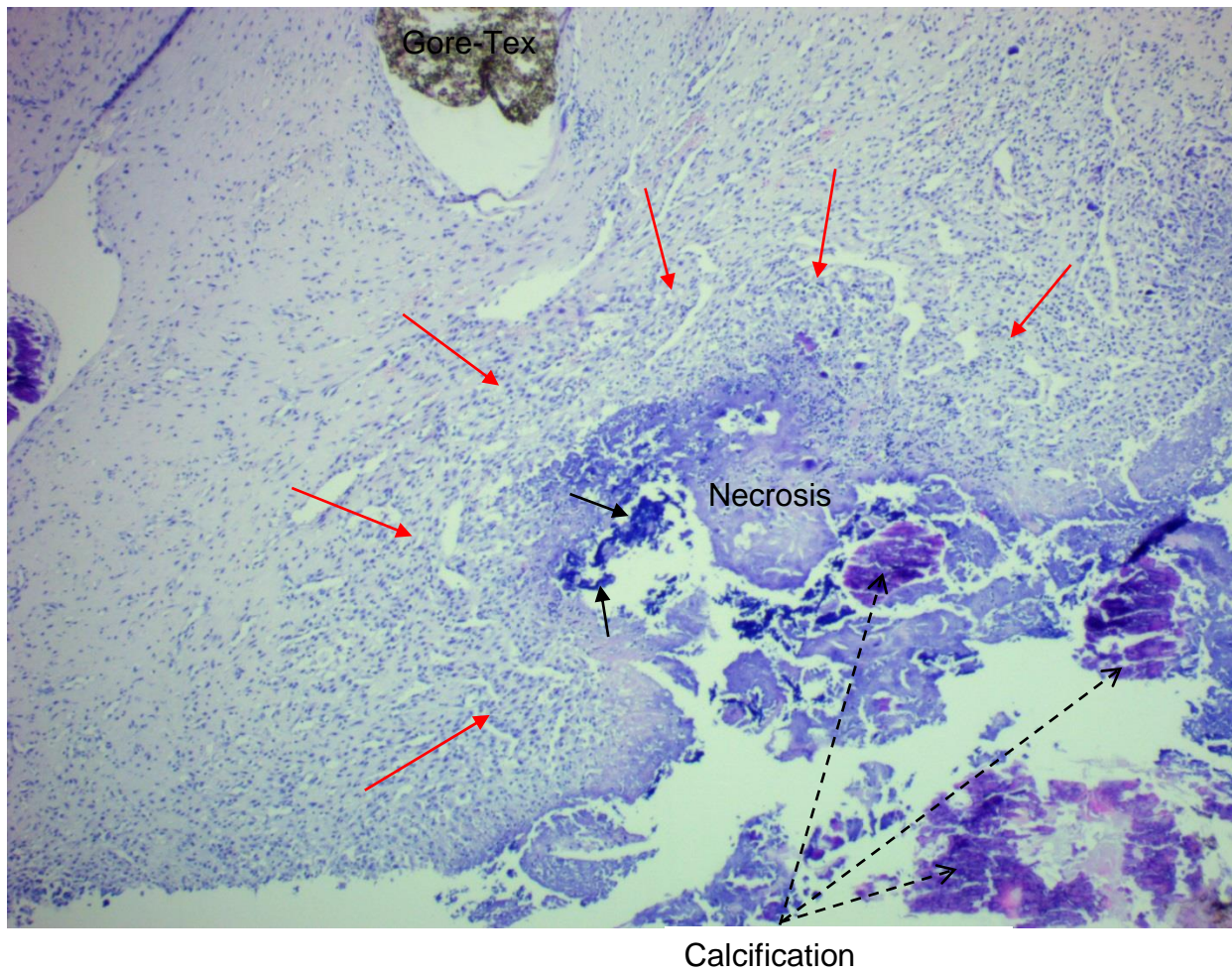


**Fig 3.65:** Histological section of the vein implant of sheep 9 away from the vegetation shows the typical architecture that was seen after 6 months with a fibrovascular proliferation in the space between the 2 vein leaflets. The vein architecture is still recognised with overlying intimal fibroplasia. (H and E stain 40x).

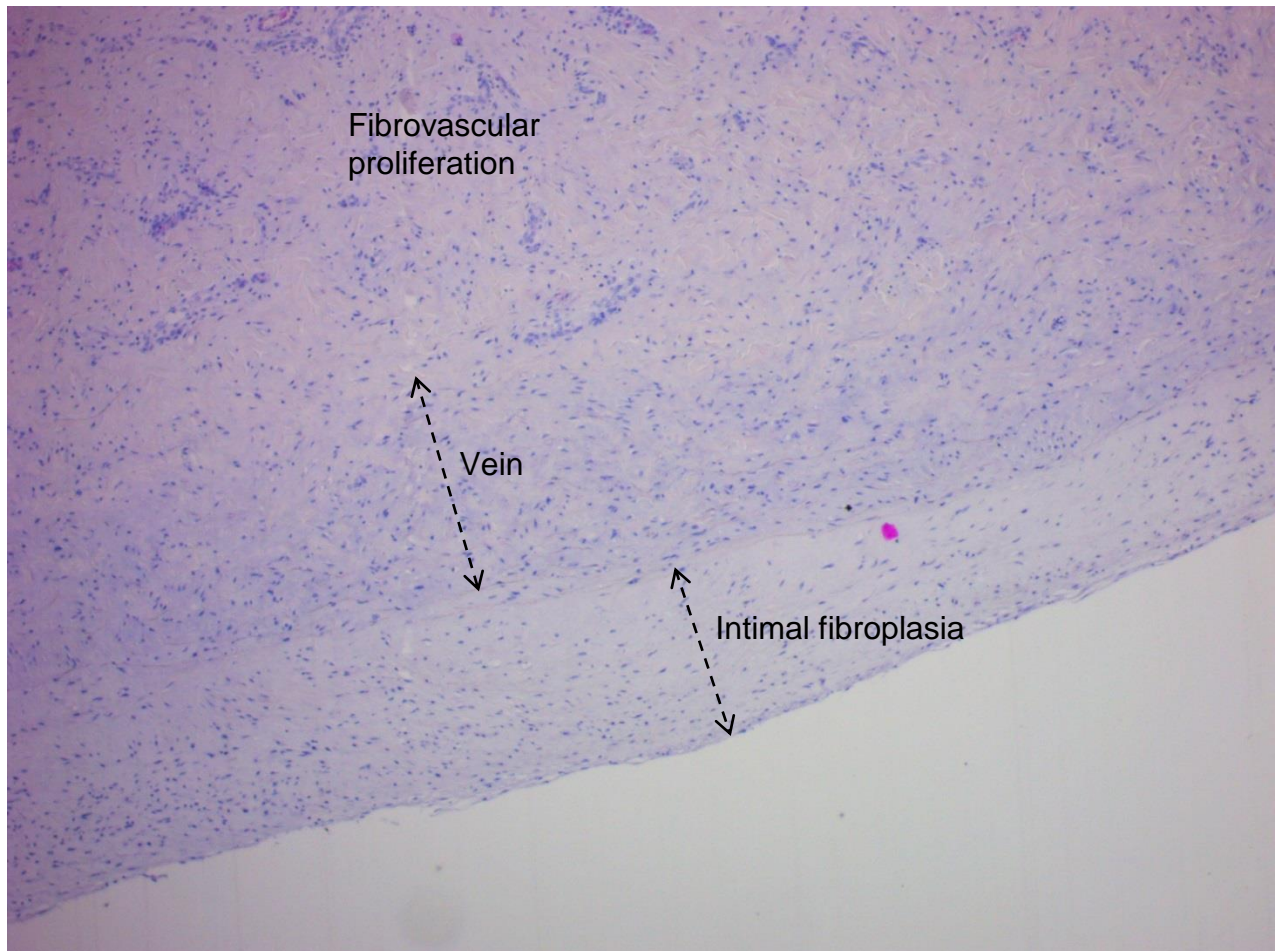


**Fig 3.66:** Histological section of sheep 18 showed extensive vegetations with vein leaflet destruction and necrosis (H and E 20x).

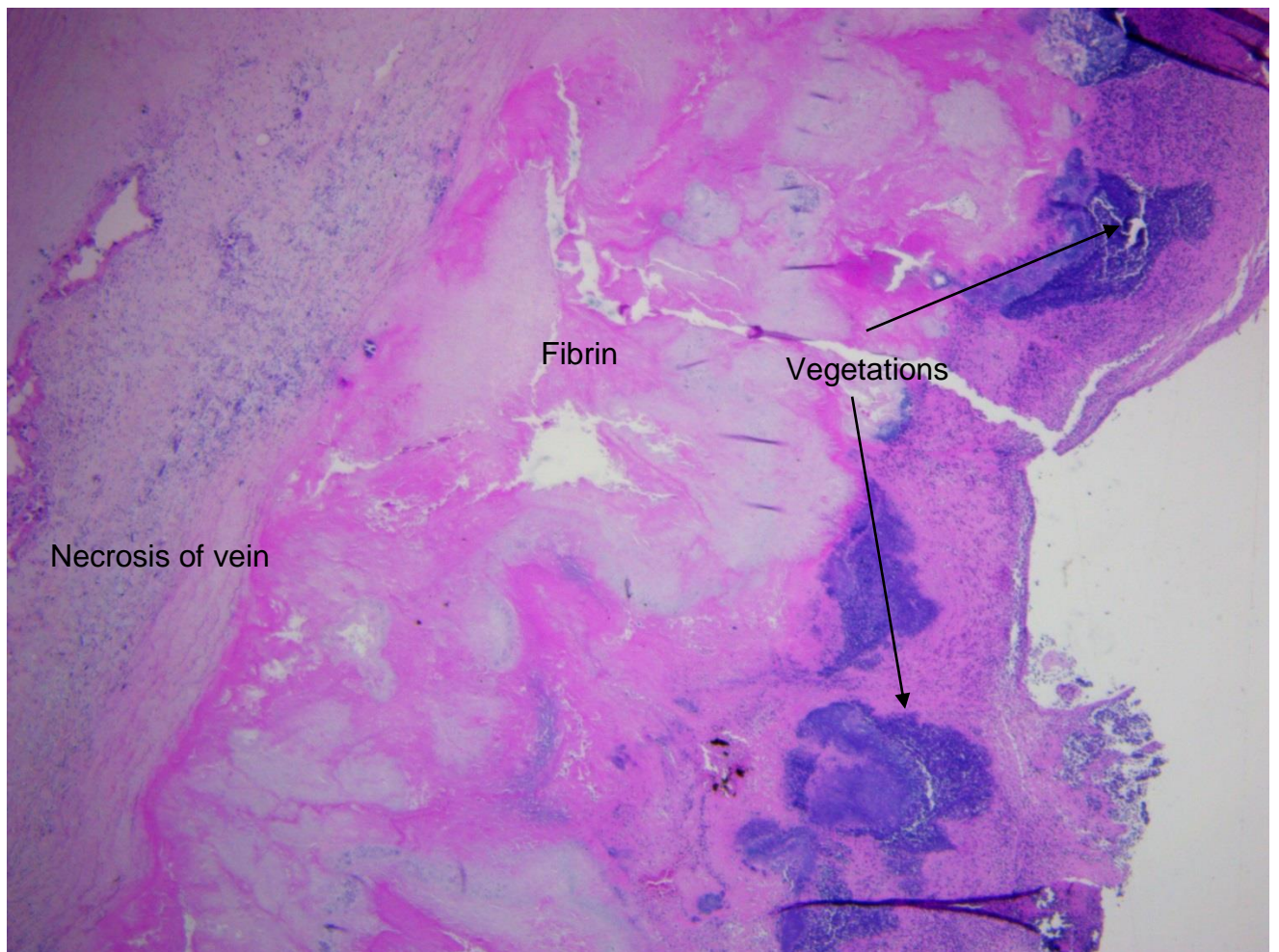


**Fig 3.67:** Bacterial clusters (arrows) and inflammatory cells can be seen in the vegetations on the vein implant in sheep 18 (H and E stain 400x)

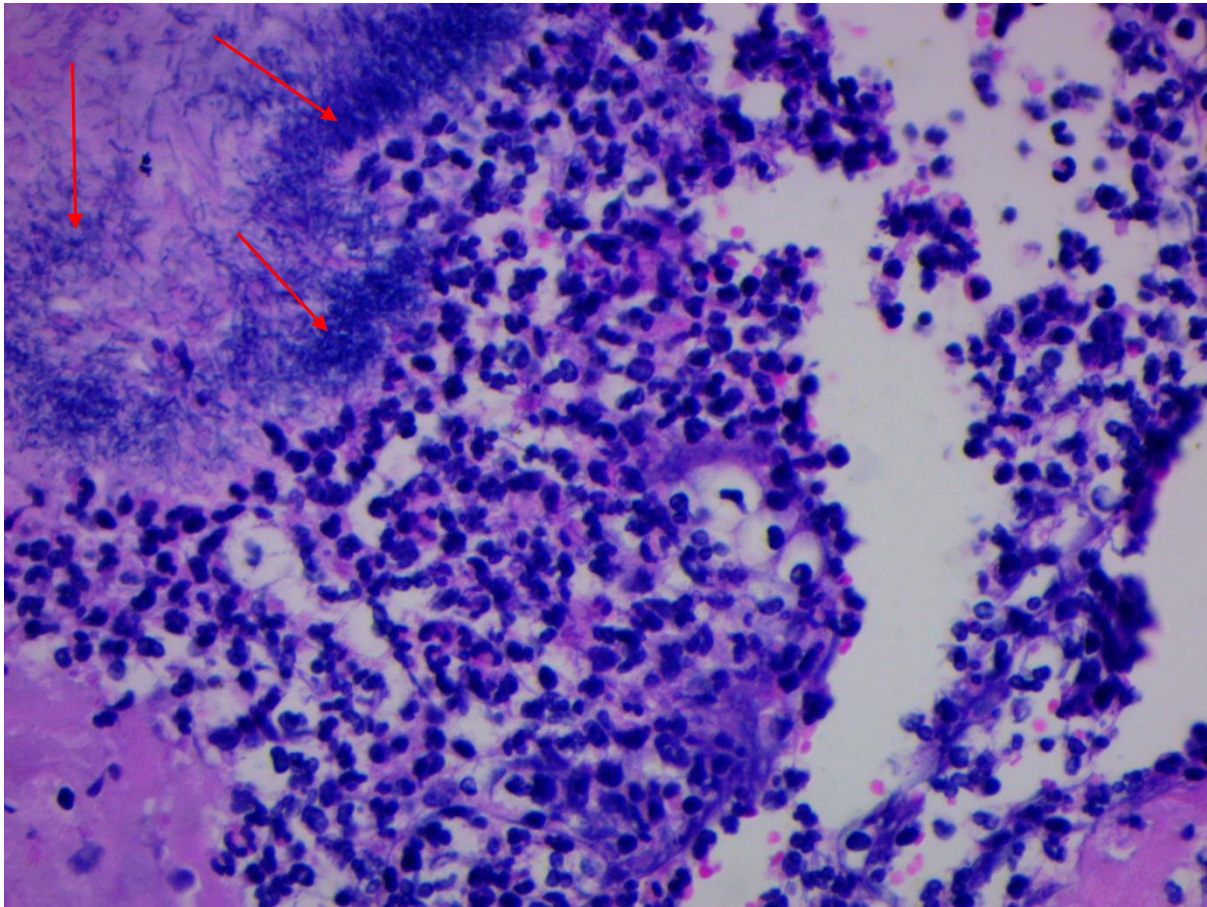
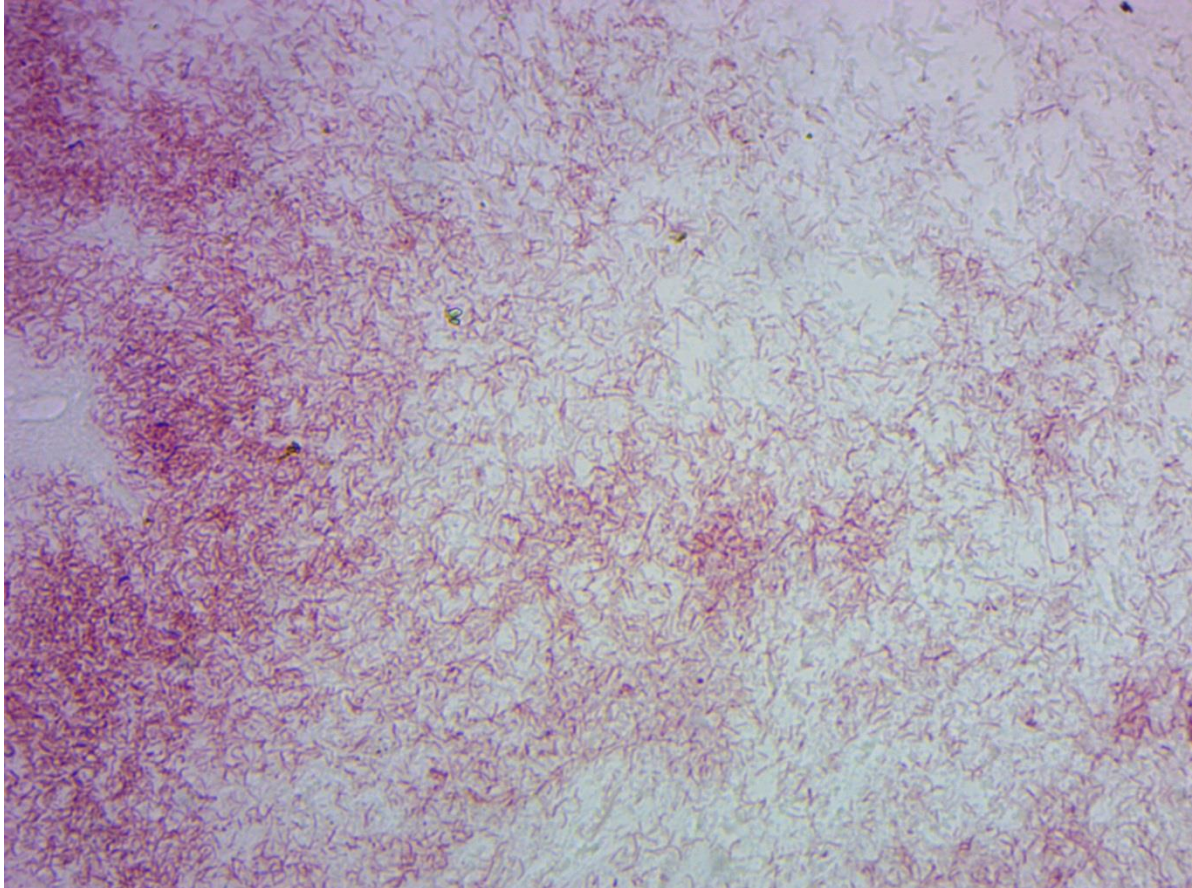


**Fig 3.68:** Gram stain of a vegetation from the mitral valve of sheep 18 showed Gram negative bacilli. (Gram stain 400x)





**3.6.8** Nine other sheep had the implant for **6 to 10 months** (sheep 3, 5, 6, 10, 13, 14, 16, 17, 21), after excluding sheep 8 and 9 which had SBE. Interesting changes were noted at this stage. Three sheep (3, 13 and 21) had areas of fibrin overlying the endothelium on the valve while there was none seen in the others. The endothelial layer looked normal in all the valves with no areas of necrosis as seen in some of the earlier specimens, so it seems as if the areas of endothelial necrosis either recovered or these valves did not have endothelial necrosis. The original vein layers could still be identified in the vein leaflet with cellular nuclei, elastic fibres and collagen in the media (Fig 3.69 and Fig 3.70). Significant intimal fibroplasia was seen in the vein (Fig 3.69 and Fig 3.70).

The space between the vein layers was completely obliterated by granulation tissue consisting of fibrovascular proliferation (Fig 3.69 and Fig 3.70). The neovascularisation in the fibrous tissue between the 2 vein layers was more prominently seen in the vein leaflets that were implanted for 6 months and more. It could be seen that blood vessels enter the vein leaflet from the annulus side (Fig 3.71 and Fig 3.72). This fibrous proliferation caused significant thickening in the leaflets with the maximum thickness varying between 3 and 6.5 mm (Table 3.5) (Fig 3.73). The orientation of the fibrous proliferation seemed more random and disorganised than the organised layers of collagen in the media of the vein or the native valve leaflet (Fig 3.70 and Fig 3.74).

The central suture line at A2 showed good healing in 7 of the 9 implants (Fig 3.75). Sheep 5 had a proximal defect in the central suture line with calcification on the central suture line and on the leaflet edge where the Gore-Tex chordae implanted (Fig 3.80). Sheep 10 showed very small defects at the suture line with no calcification.

A foreign body tissue response was noted around the Gore-Tex sutures (Fig 3.76). The fibroblasts and collagen fibres were laid down orderly and parallel to the Gore-Tex chordae in line with the strain that the chord endures and is covered with an endothelial layer (Fig 3.77). The fibrous covering of the Gore-Tex sutures started forming from both ends, the papillary muscle side and the leaflet edge side, and then gradually covered the Gore-Tex chordae towards the middle of the chordae. The vein implant of sheep 10 (6.5 month implant) shows partially covered Gore-Tex chordae and it can be seen how the fibrous covering started from the leaflet edge and the papillary muscle (Fig 3.78). It is also interesting to see how the one Gore-Tex chordae that has torn loose from the leaflet edge at A1 only has a fibrous covering starting from the papillary muscle side, since the leaflet edge could not contribute fibroblasts

for the fibrous reaction (Fig 3.78). Sheep 3 (10 month implant) shows complete covering of the Gore-Tex chordae with a layer of fibrous tissue (Fig 3.79)

The pledgets on the Gore-Tex suture also stimulated a foreign body tissue response at the papillary muscle (Fig 3.80).

Calcification was noticed around the Gore-Tex chordae and sutures in 7 of the implants. In 6 implants, the calcification was limited to some of the Gore-Tex chordae and 4 had calcification on the Gore-Tex chordae and where the Gore-Tex sutures were tied to the leaflet (Fig 3.81 – Fig 3.86). Sheep 3 (10 month implant) only had focal calcification where the Gore-Tex was sutured to the papillary muscle and sheep 10 (6.5 month implant) and 13 (6.4 month implant) showed no signs of calcification on histology (Table 3.5).

Cartilaginous metaplasia was seen in sheep 21 around the Gore-Tex sutures (Fig 3.87).

Sheep 5 and 6 had osseous metaplasia seen at the valve annulus next to the Gore-Tex sutures (Fig 3.88). This is different to the bone formation that can be found in the central fibrous body of sheep as part of the os cordis (Frink and Merrick 1974).

There was no calcification noted in the vein leaflets itself apart from the calcification around the Gore-Tex sutures.

The posterior leaflets (native leaflets) of these sheep also showed some degree of leaflet thickening with areas of intimal hyperplasia, presumably because of friction from the Gore-Tex sutures or from increased shear stress from regurgitation (Fig 3.89).

**Fig 3.69:** Histological section of the vein implant in sheep 16 (6 month implant) shows the original vein between the intimal fibroplasia and underlying fibrous proliferation with neovascularization (H and E stain 40x). There is preserved cells, collagen and elastic fibres in the original vein wall.

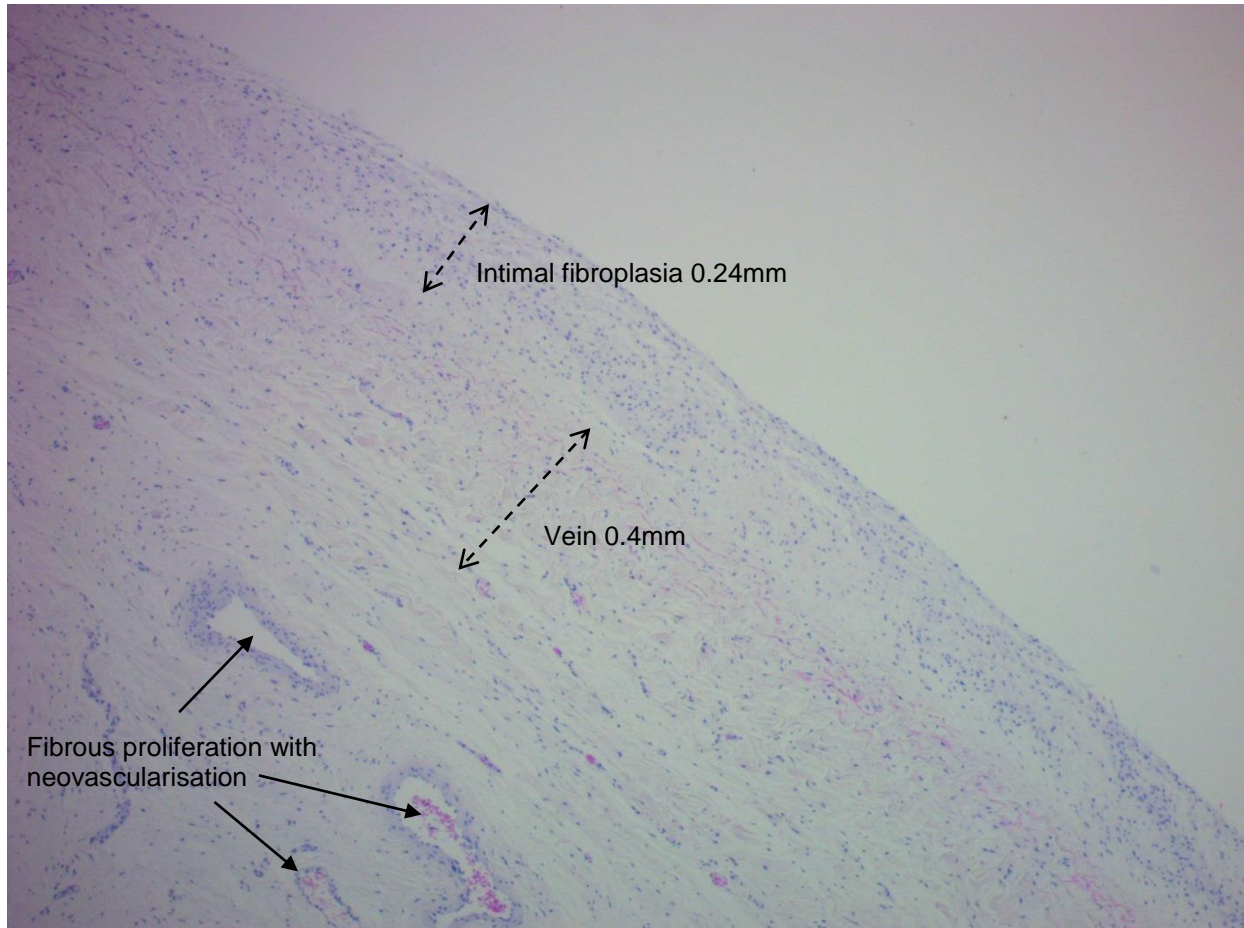


**Fig 3.70:** Histological section of vein leaflet of sheep 3 (10 month implant) (Verhoeff and Van Gieson stain 40x). The original vein (black arrow) can be identified between the intimal fibroplasia (red arrow) and the fibrous proliferation with neovascularization (yellow arrow). Note the preserved layers of elastic fibres (stain black) and the collagen (stain dark purple) in the vein wall. The collagen fibres in the fibrous stroma (yellow arrow) show a random, disorganised distribution.

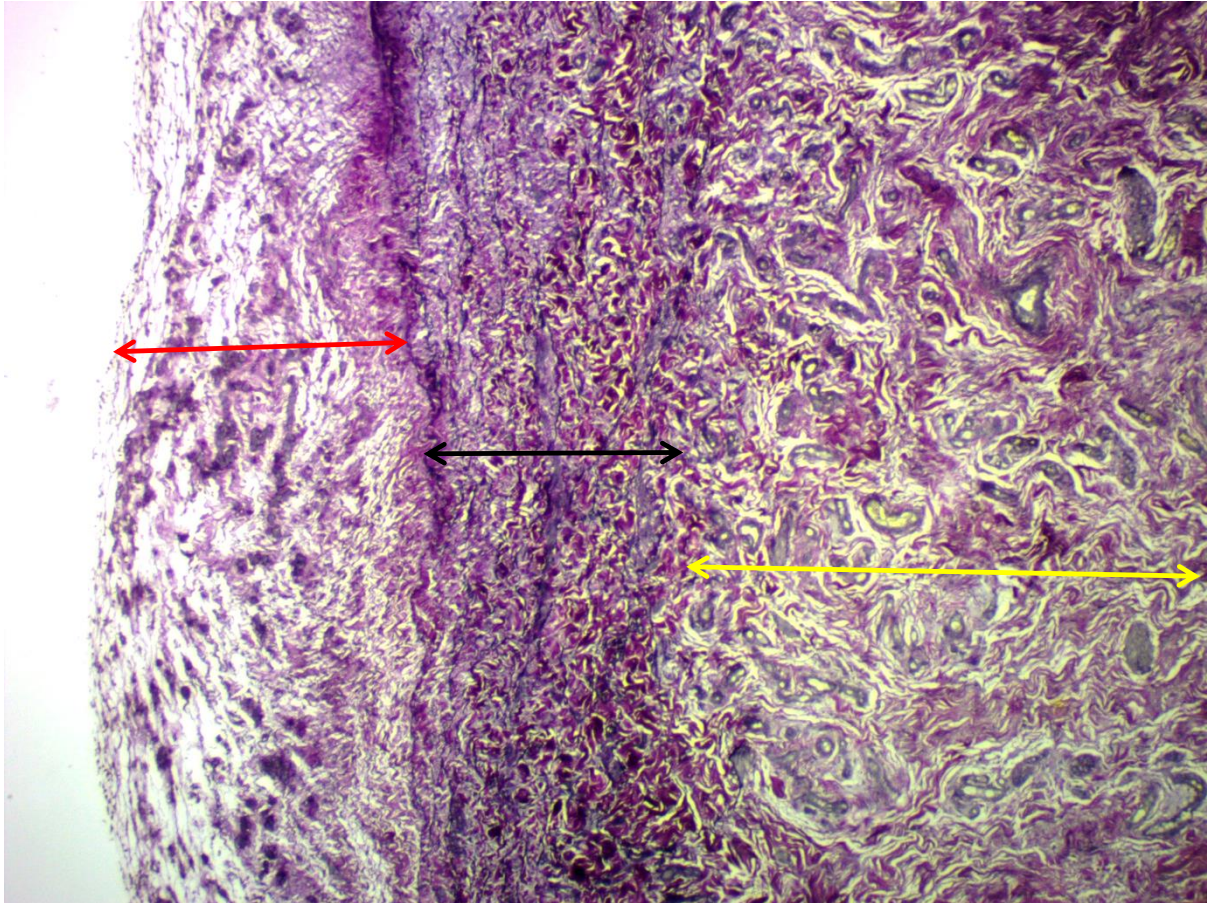


**Fig 3.71:** Histological section of the vein leaflet of sheep 16 (6 month implant) at the annular suture line shows new blood vessels running between the Gore-Tex sutures (G) from the annulus to vein leaflet (black arrows). A foreign body tissue reaction is seen around the Gore-Tex suture (red arrow) (H and E stain 40x).

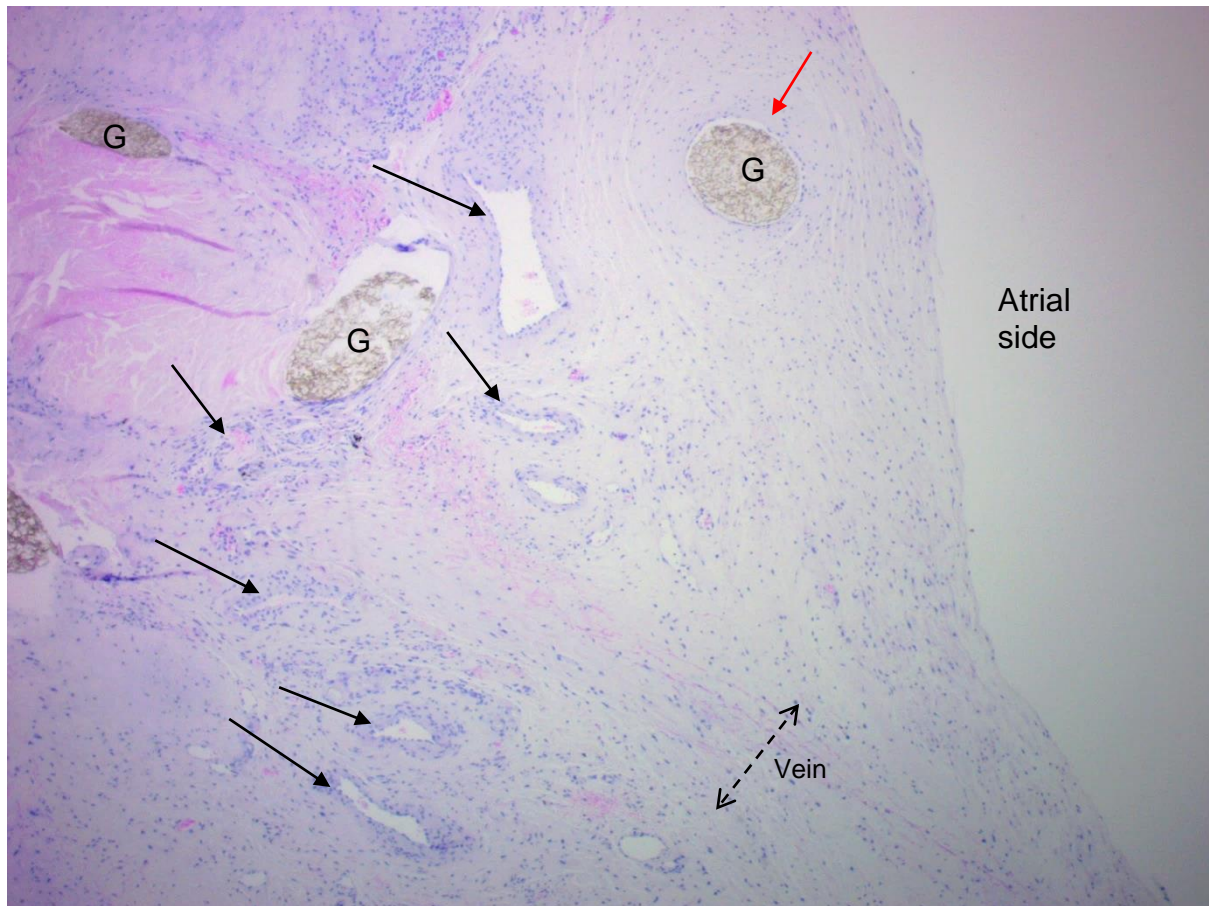


**Fig 3.72:** The same section as Fig 3.53 to show both vein walls and the fibrous proliferation inbetween (H and E stain 40x). The neovascularization can be seen between the 2 veins and on the atrial side of the vein (black arrows). Note intimal fibroplasia on both sides of the leaflet (red arrows)

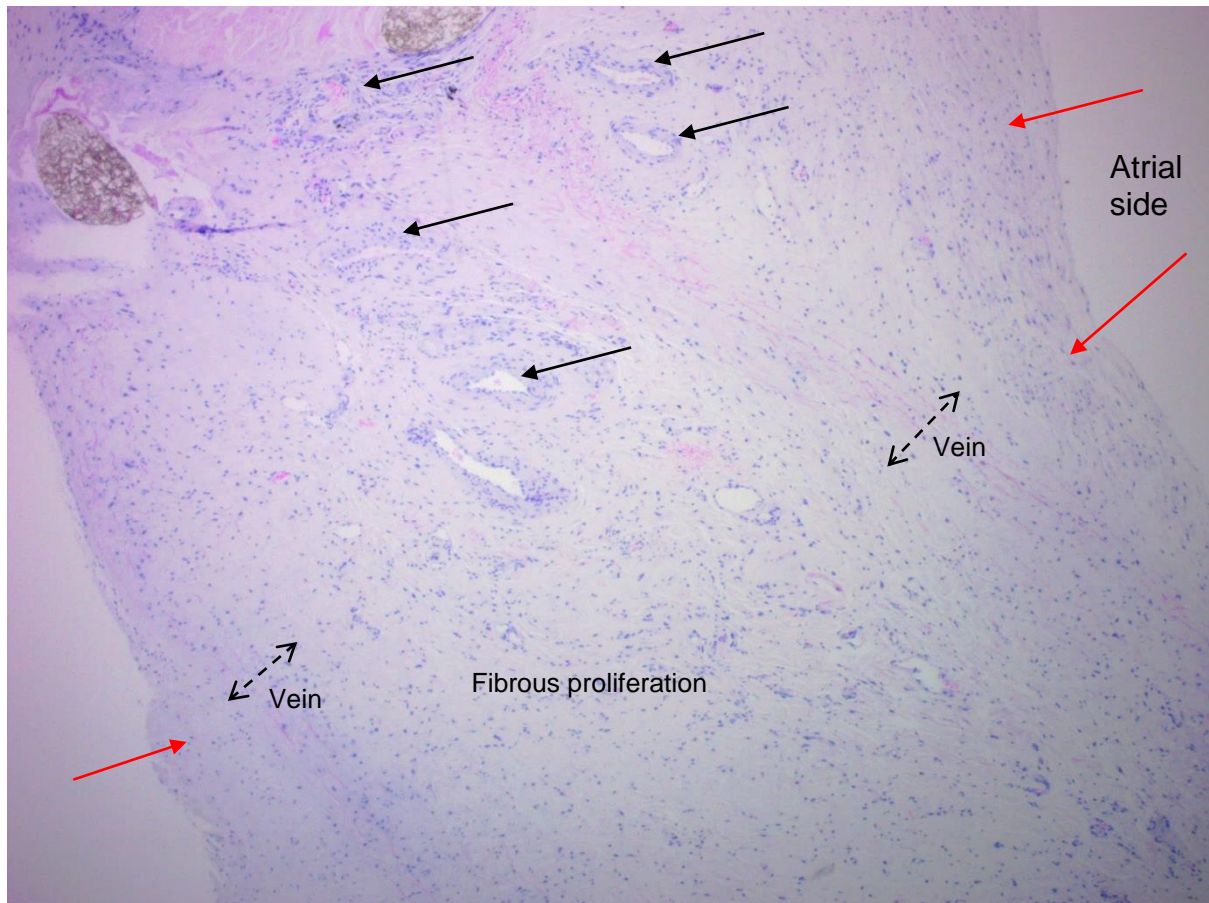


**Fig 3.73:** Histological section of sheep 3 (10 month implant) (Verhoeff and Van Gieson 20x) showing the vein attachment site at the annulus. The 2 vein layers can be seen (black arrow) and the fibrous stroma with blood vessels cause significant thickening of the vein (yellow arrow).

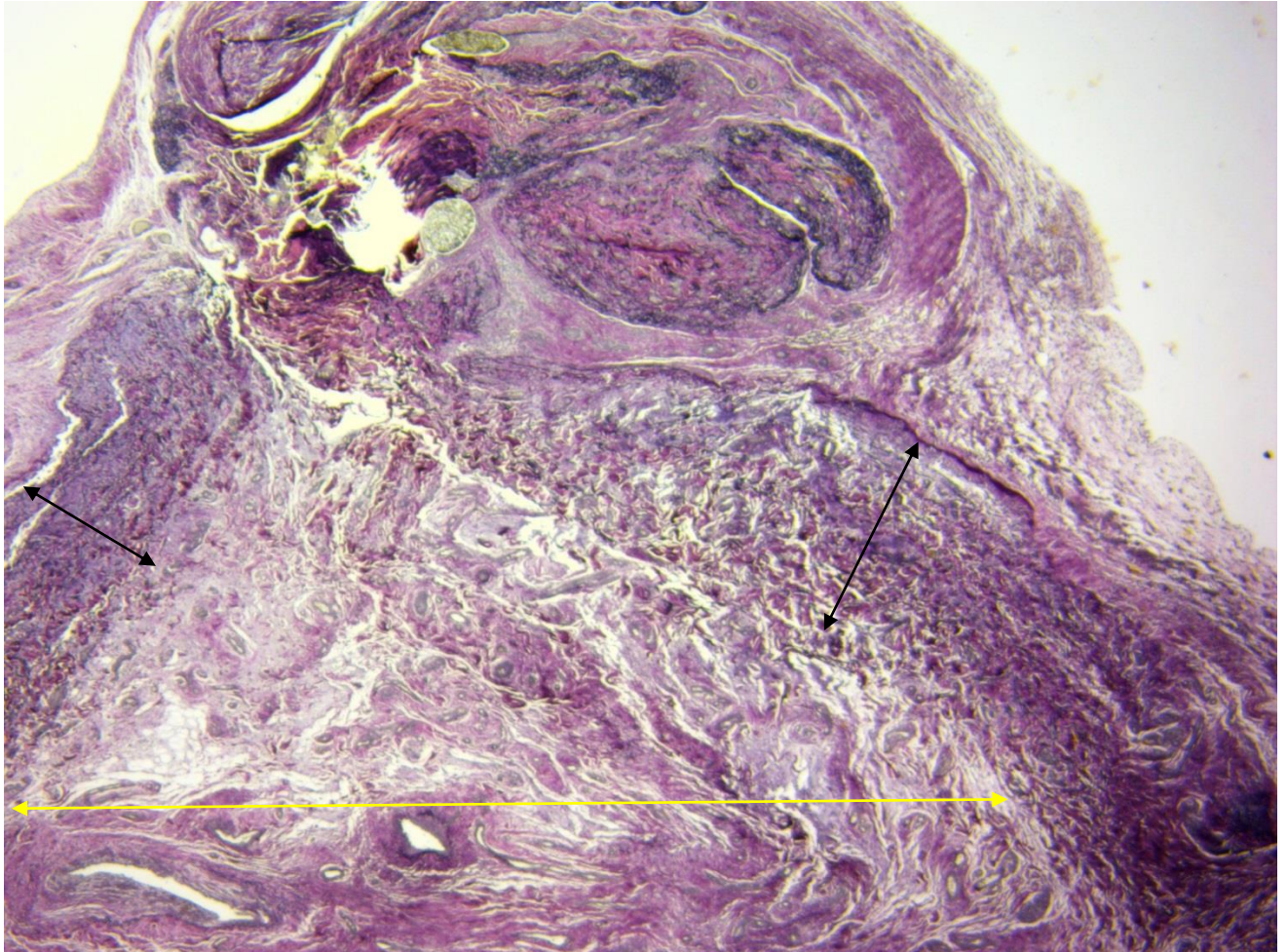


**Fig 3.74:** *Histological section of the vein leaflet of sheep 16 (6 month implant) to show the fibrous proliferation and neovascularization between the vein layers in more detail (H and E 100x). The capillaries, fibroblasts and collagen fibres are not orderly arranged in a single plane, but are arranged randomly in different directions.*

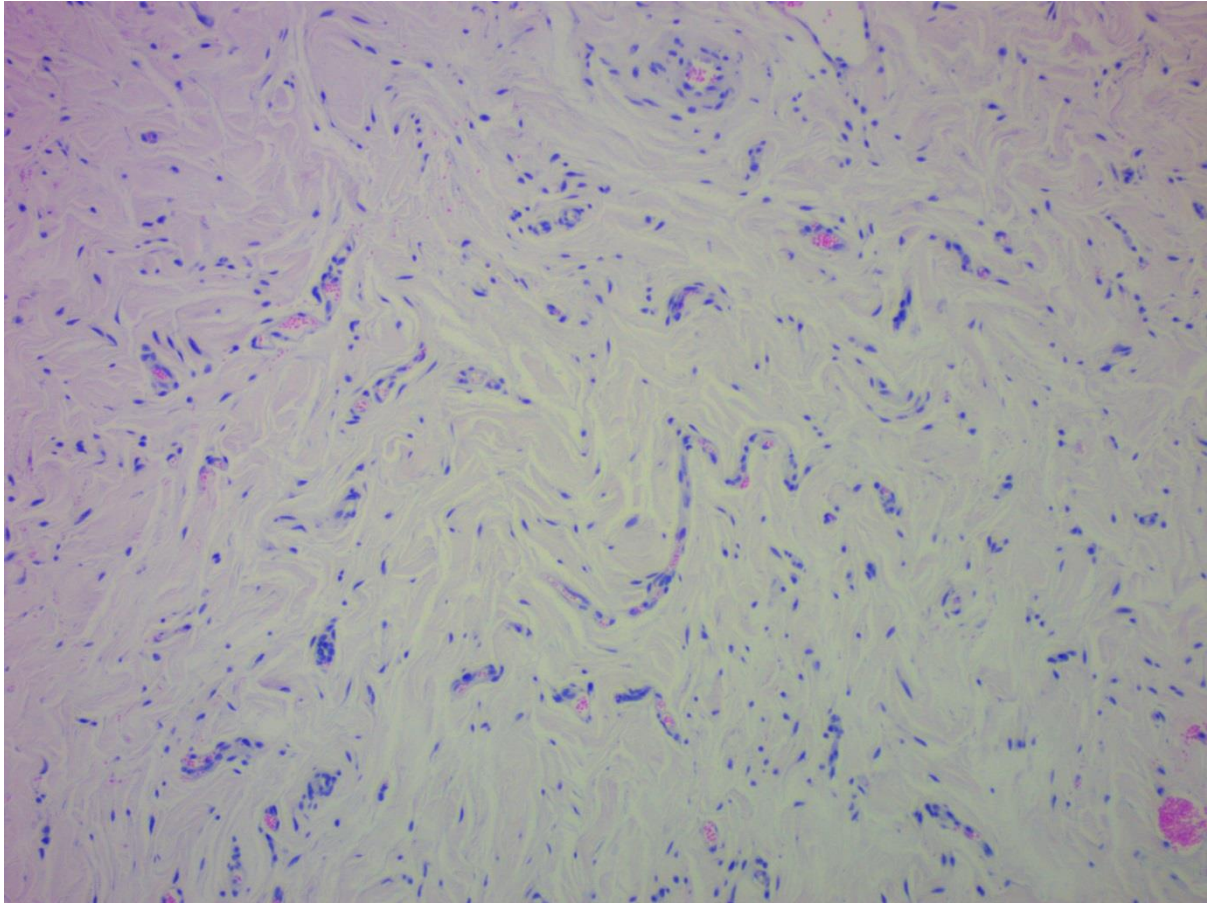




**Fig 3.75:** Histological section of the vein leaflet of sheep 14 (6 month implant) shows good healing of the central suture line in the A2 part of the anterior leaflet (H and E stain 40x). Two Gore-Tex sutures CV 8 are visible that was used as a running suture to join the 2 veins together.

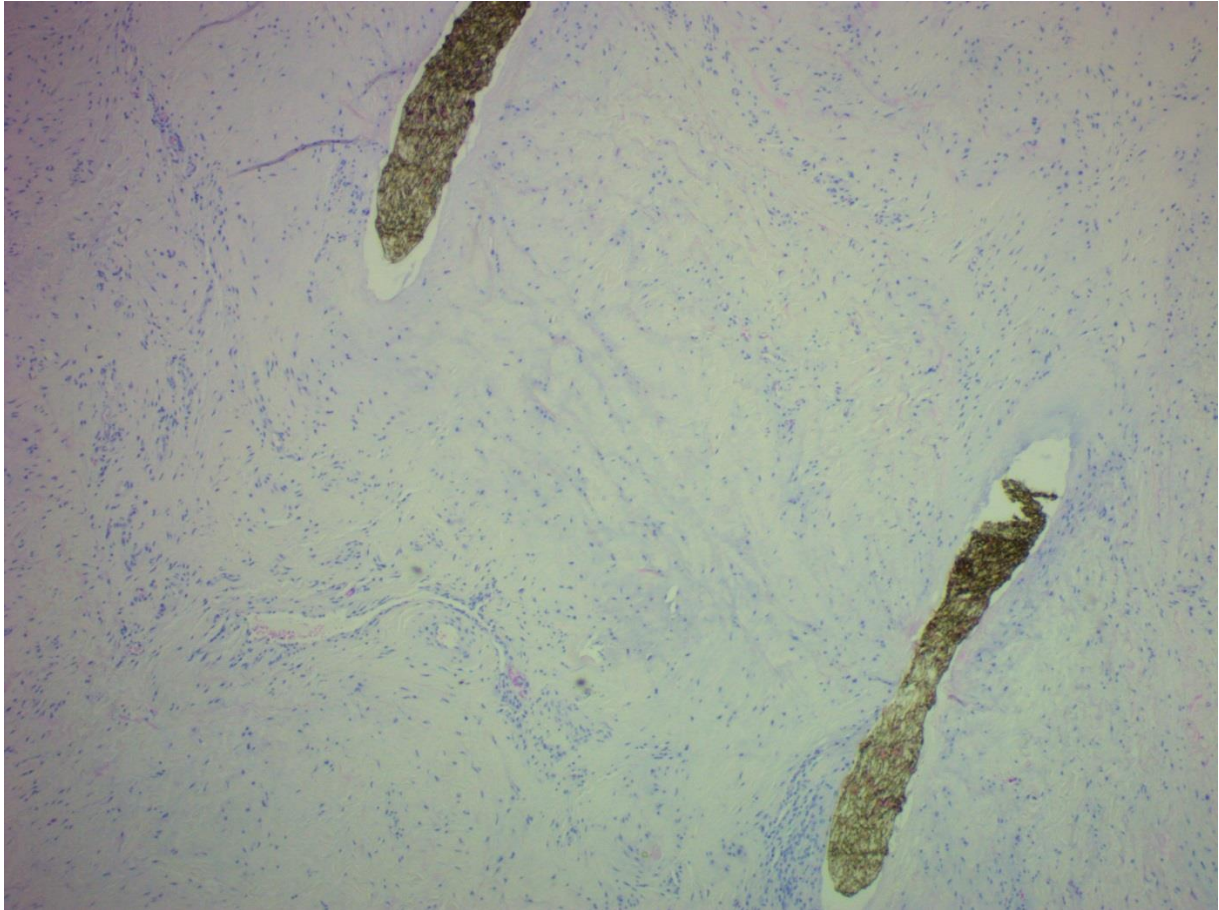


**Fig 3.76:** Histological section of Gore-Tex chordae of sheep 13 (H and E stain 200x) shows a foreign body reaction to Gore-Tex with macrophage activation, giant cell formation, fibroblast activation and fibrosis.

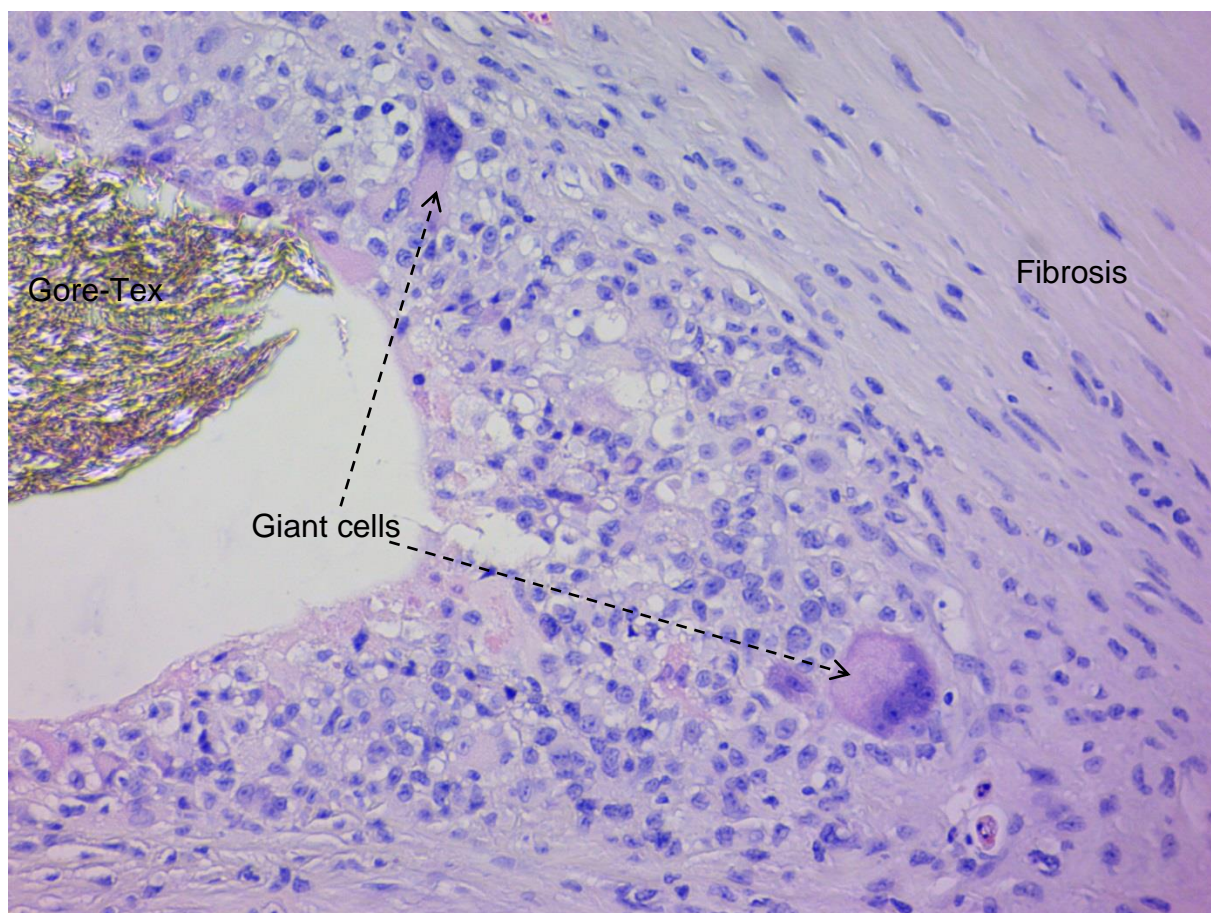


**Fig 3.77:** *Histological section of Gore-Tex chordae of sheep 13 (H and E stain 40x) shows the endothelial covering of the fibrous tissue around the Gore-Tex chord. Note the arrangement of the collagen fibres which are parallel to the Gore-Tex chords and in line with the strain that the chord endures. The fibrous tissue is covered with an endothelial layer.*

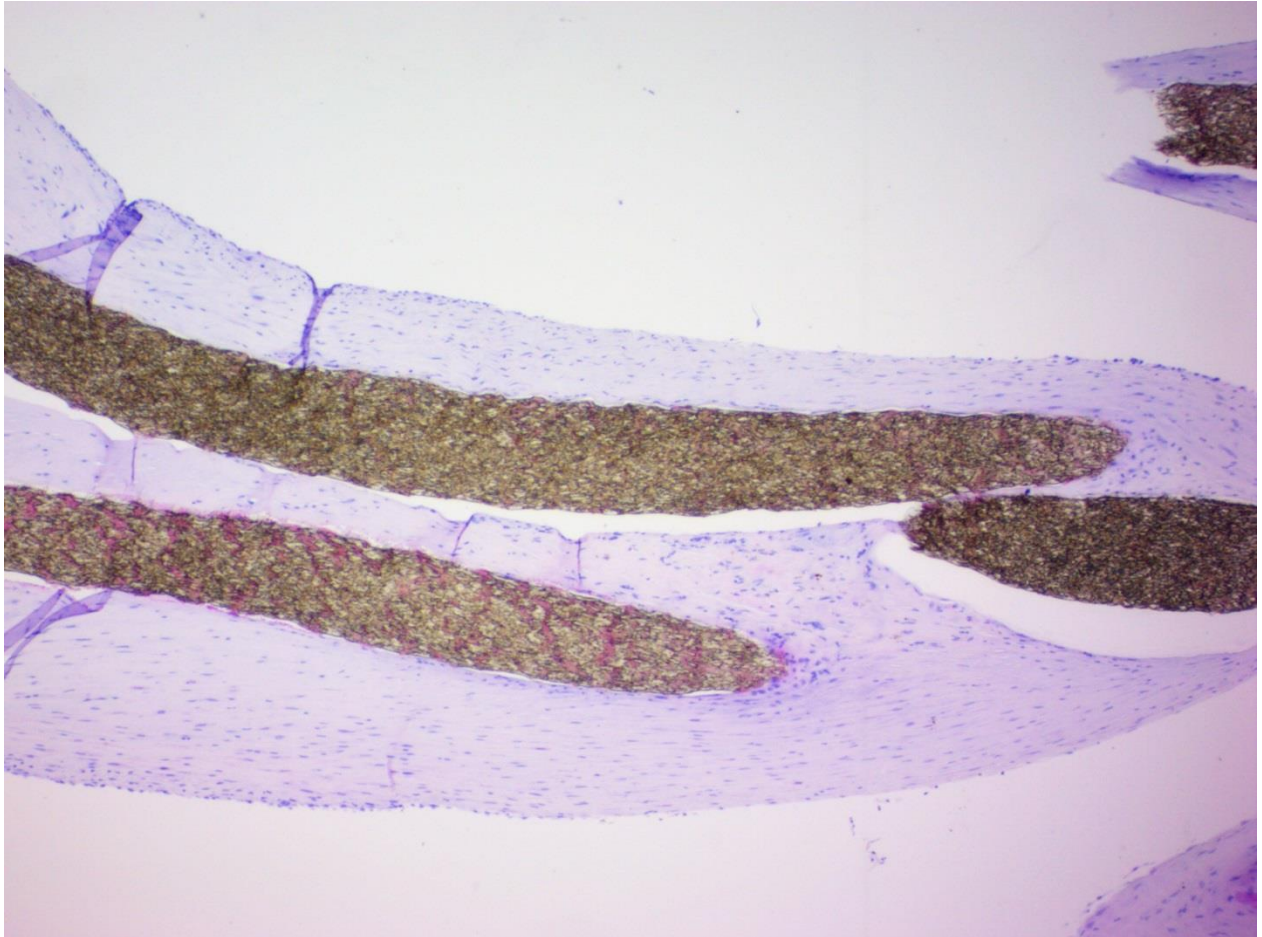
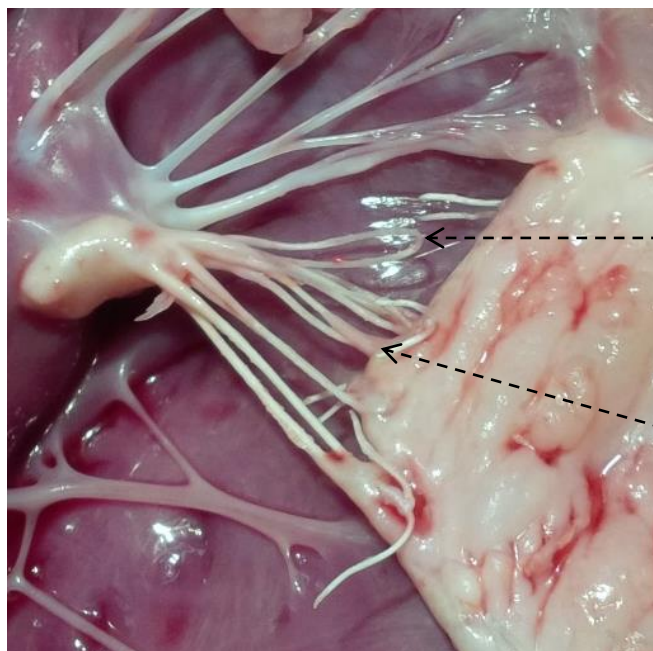


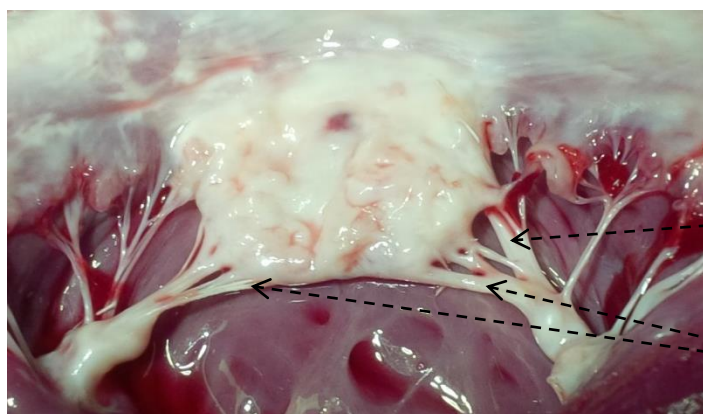
**Fig 3.78:** Mitral valve of sheep 10 (6.5 month implant) shows that the Gore-Tex chordae are partially covered with fibrous tissue. The last loop to A1 has torn loose from the leaflet edge and is only covered with fibrous tissue from the papillary muscle side.



Gore-Tex chordal loop to A1 tore loose from leaflet edge. Notice how this chord is only covered with fibrous tissue from the papillary muscle side

This Gore-Tex loop is partially covered with fibrous tissue on the leaflet edge side and the papillary muscle side, but not in the centre

**Fig 3.79:** Mitral valve of sheep 3 (10 month implant) shows that the Gore-Tex chordae are completely covered with fibrous tissue.



Gore-Tex chordae to A3

Gore-Tex chordae to A2

**Fig 3.80:** Histological section of the felt pledget material (P) at the papillary muscle of sheep 13 (H and E stain 200x) shows a foreign body reaction to the felt pledget with fibroblast and macrophage activation and giant cell formation (arrows).

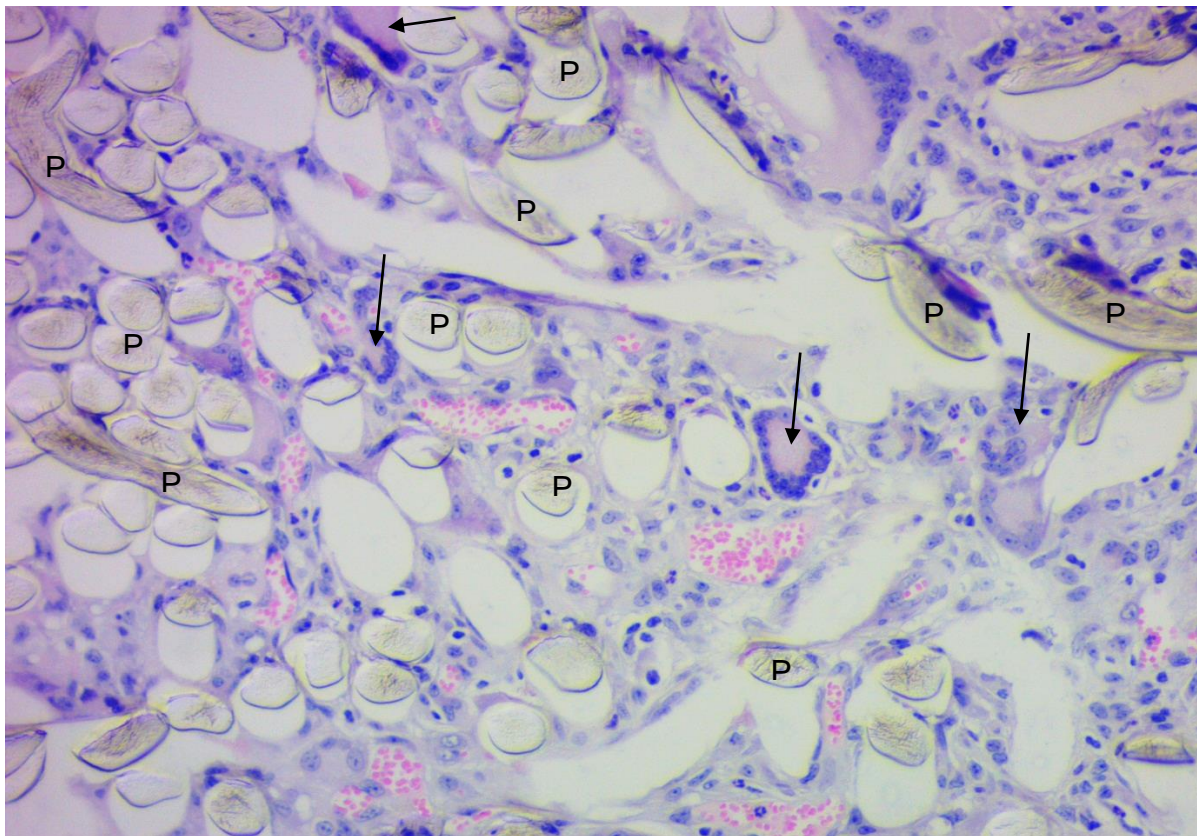


**Fig 3.81:** *Histological section of a Gore-Tex chordae of sheep 13 shows the fibrous proliferation around the Gore-Tex with fibres running parallel to the chord. Calcification is also noted in the Gore-Tex suture (dark purple) (H and E stain 100x).*

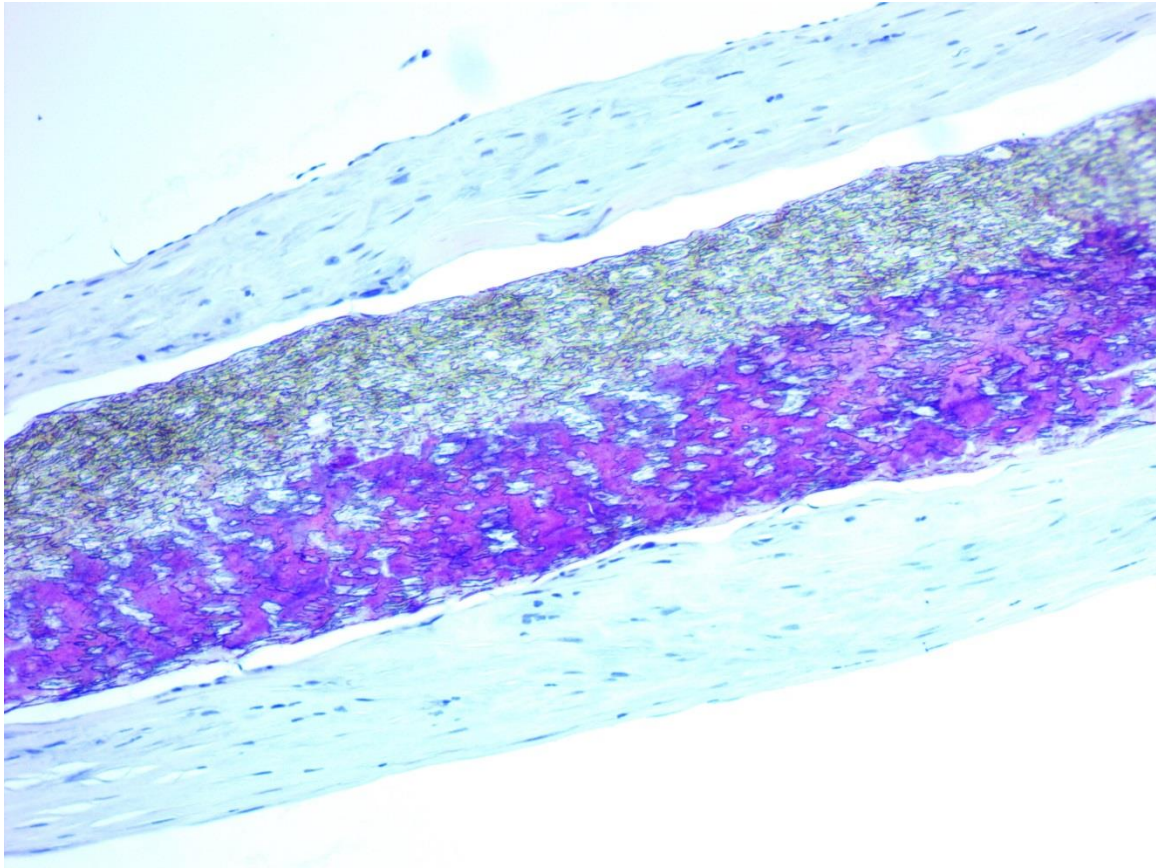


**Fig 3.82:** Histological section of the Gore-Tex chordae of sheep 21 shows extensive calcification (dark purple) in the Gore-Tex (arrows) (H and E 20x).

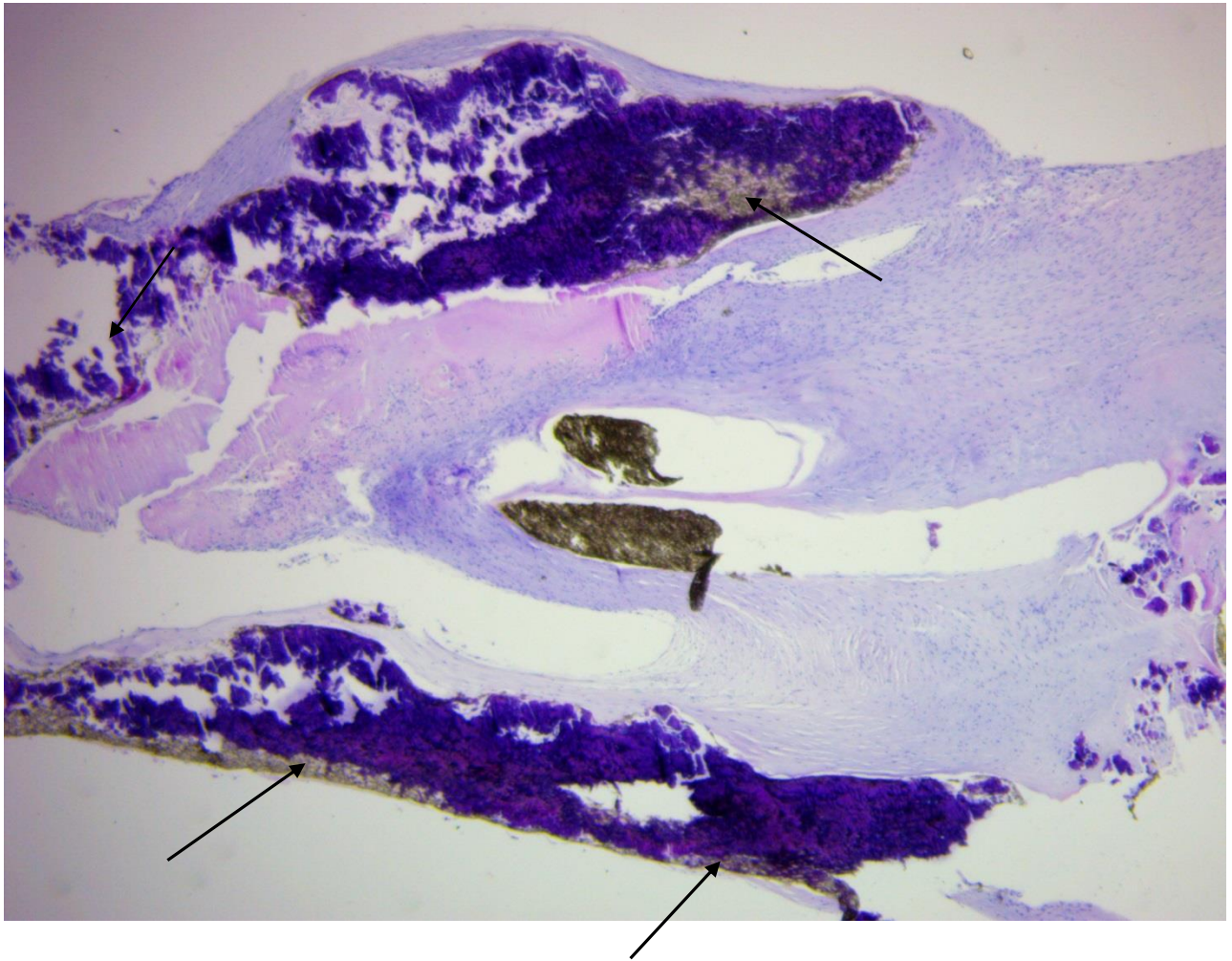


**Fig 3.83:** Vein leaflet of sheep 5 (implant for 8 months) with a central suture line defect and calcification on the leaflet edge where Gore-Tex sutures were placed. There is quite extensive calcification of the Gore-Tex chordae. All the calcification is limited to areas on the vein where Gore-Tex sutures were placed. This photograph helps to orientate where histological samples were taken for Fig 3.84 – Fig 3.86

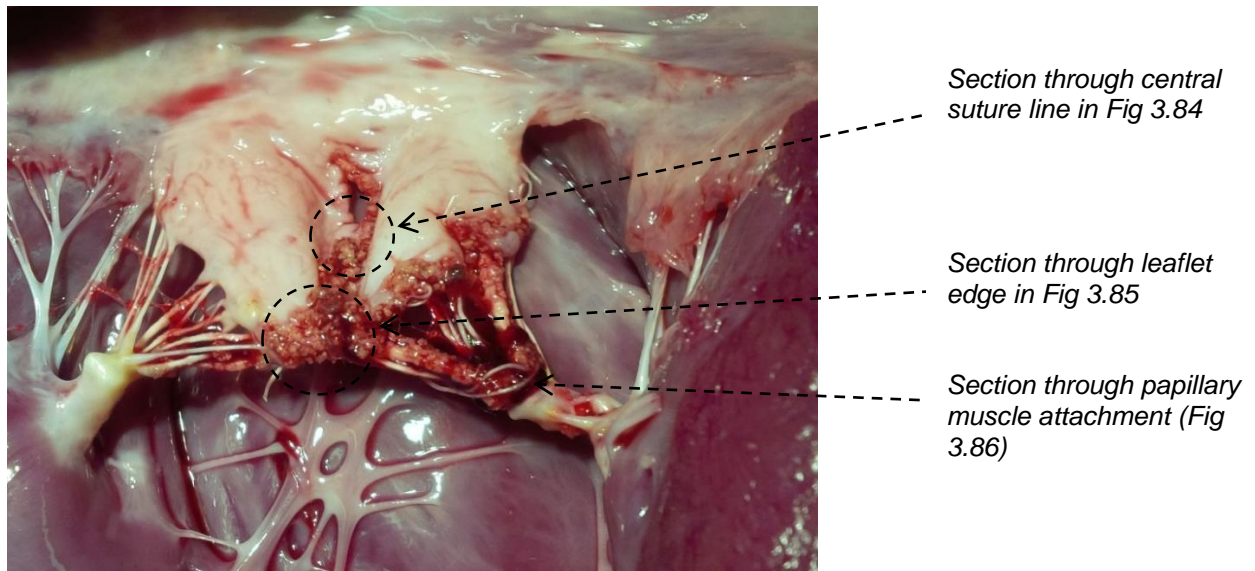


**Fig 3.84:** Histological section of vein leaflet of sheep 5 through the central suture line shows calcification (dark purple) around the Gore-Tex suture line (H and E stain 20x). The Gore-Tex sutures came out during sectioning of the specimen and the open spaces remain.

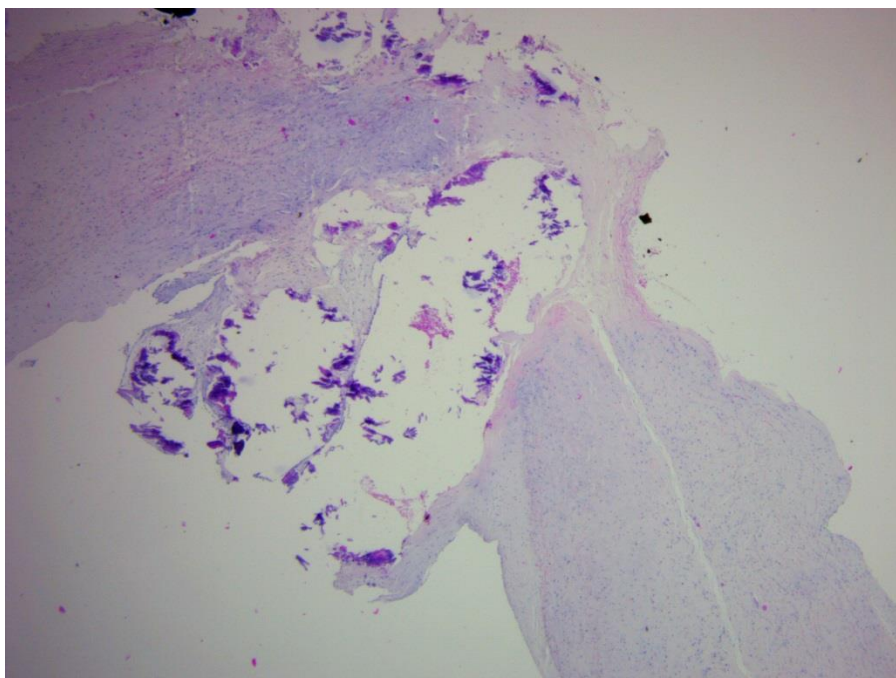




**Fig 3.85:** Histological section of vein leaflet of sheep 5 where the Gore-Tex chordae was tied to the vein leaflet edge (H and E stain 40x). Osseous metaplasia with calcification is noted (dark purple). The Gore-Tex sutures came out during sectioning of the specimen and the open spaces remain.

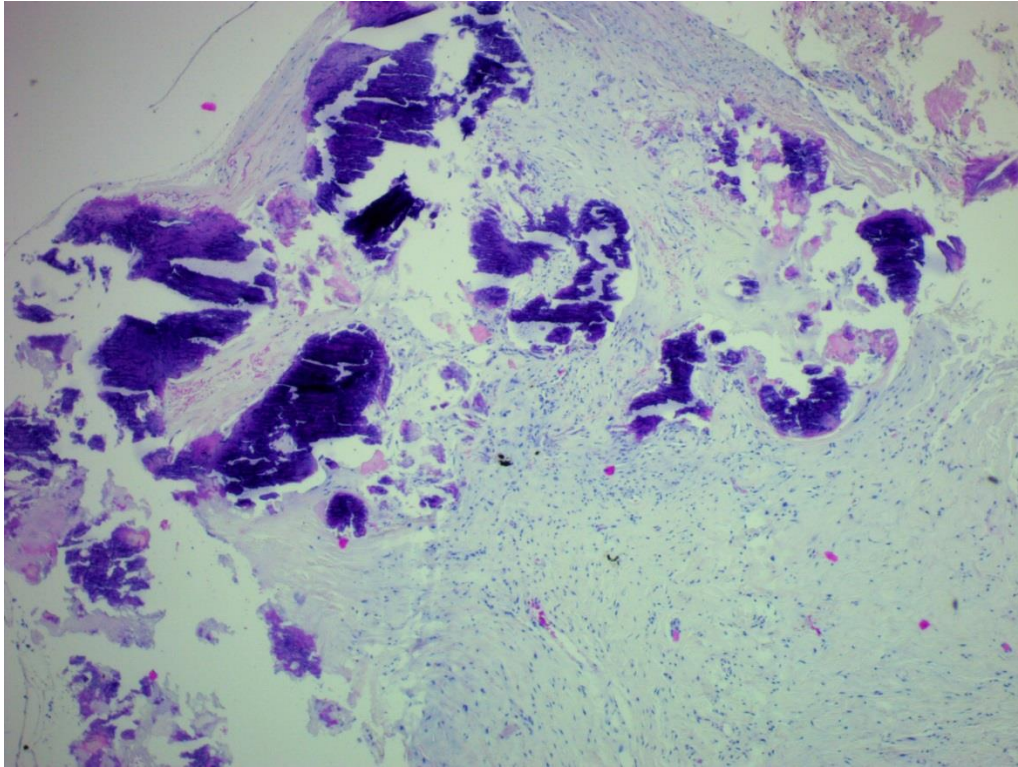


**Fig 3.86:** Histological section of the Gore-Tex attachment at the papillary muscle of sheep 5 shows extensive calcification (dark purple) around the Gore-Tex suture (H and E stain 40 x).

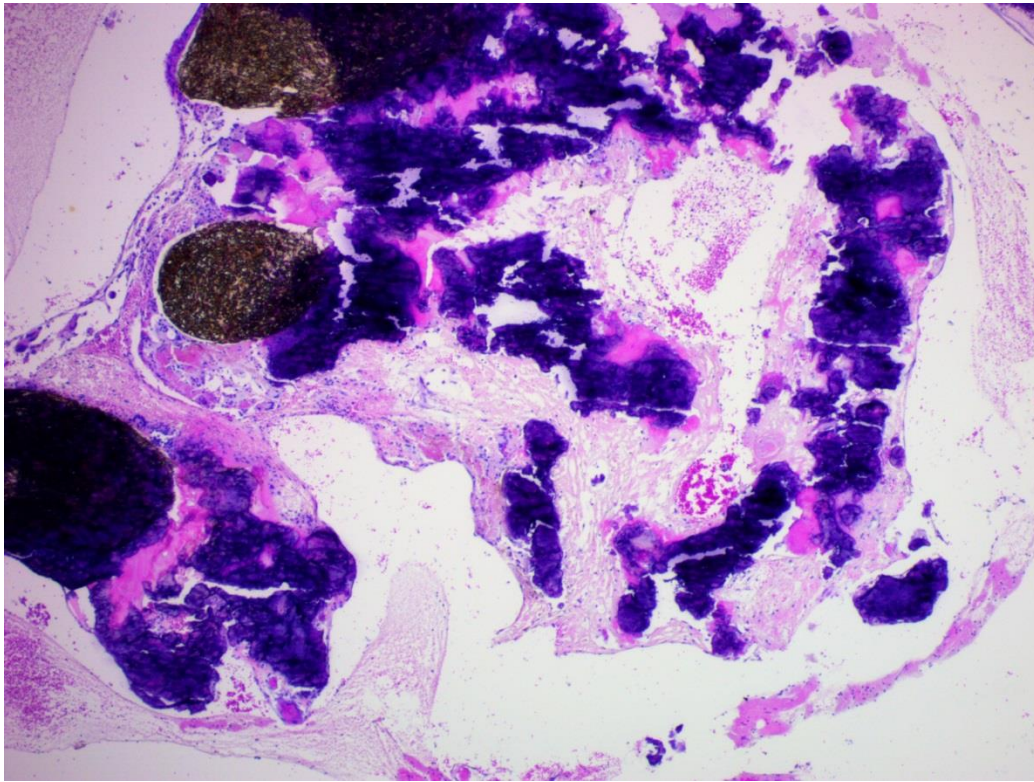


**Fig 3.87:** Histological section of the vein leaflet of sheep 21 at the annulus suture line shows cartilaginous metaplasia around the Gore-Tex sutures (H and E stain 100x).

□

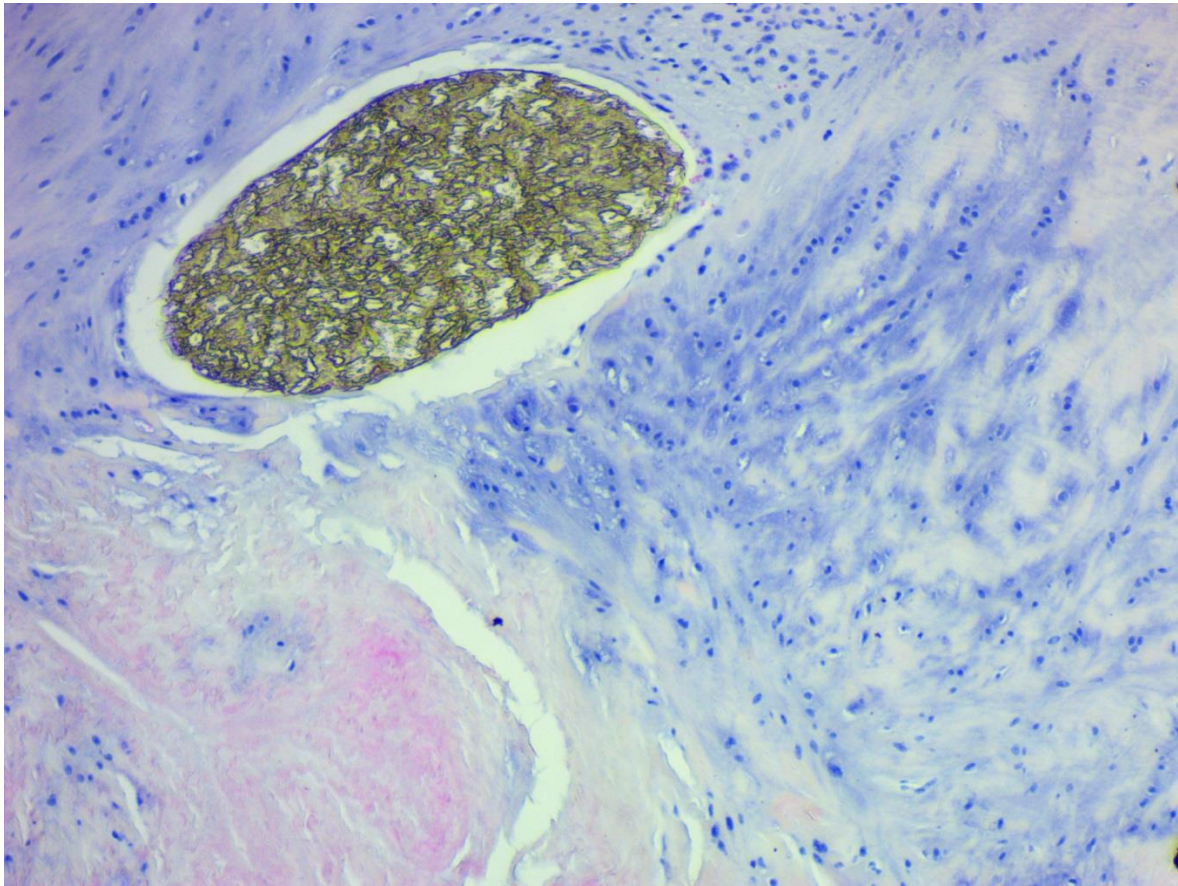


**Fig 3.88:** *Histological section of vein leaflet of sheep 6 shows calcified osseous metaplasia (dark purple) with bone marrow (arrows) at the annular suture line around the Gore-Tex sutures (H and E stain 20x).*

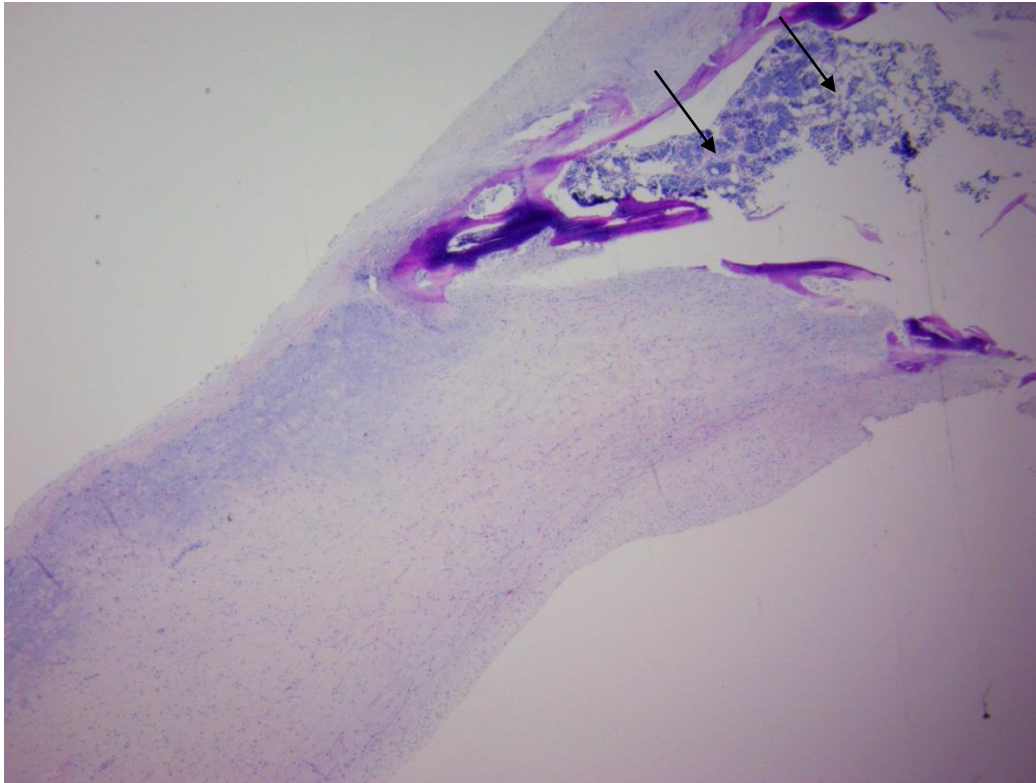
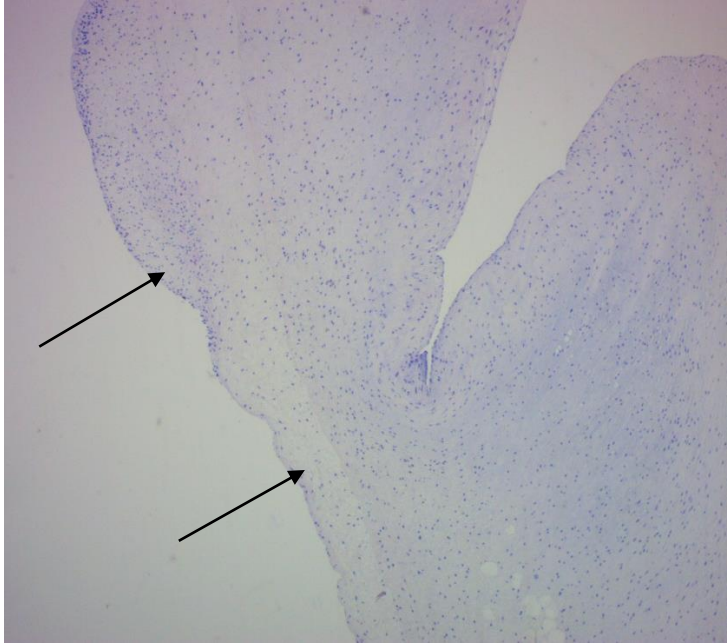
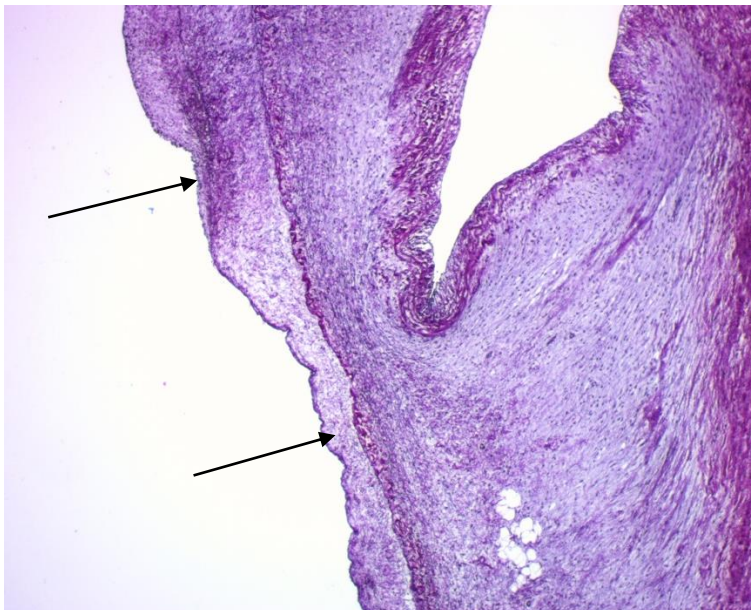


**Fig 3.89:** Histological section of the posterior (native) leaflet of sheep 6 shows intimal hyperplasia (black arrows) on the atrial side of the leaflet.

**(a)** H and E stain (40x)



**(b)** Verhoeff and Van Gieson stain (40x).



#### 4. Discussion:

The ideal prosthetic heart valve should have the following characteristics (Davila 1989, Harken 1989):

1. It must be safely and easily implantable and the procedure must be reproducible.
2. Implantation should be secure with a permanent linkage between the prosthesis and the host.
3. It must be a unidirectional valve that, within a physiological flow range, offers minimal opening resistance and minimal resistance to forward flow without turbulence.
4. It must close without regurgitation.
5. It must not activate the coagulation system.
6. It must be chemically inert and not damage blood elements.
7. It must be durable and function normally for the rest of the patient's life.

The **autologous jugular vein** of the sheep must be tested against these criteria to see how it performed as a **heart valve prosthesis**. Each of the 7 characteristics tabulated above will be discussed in sections 4.1 to 4.7.

##### 4.1 Technical aspects of vein implantation and the reproducibility of the procedure:

Creating a valve leaflet from the jugular vein has a learning curve. It is not easy to implant and the technique needs to be refined to make it easier and more reproducible. There is a time constraint when making the valve, because the valve must be made intra-operatively after the vein is harvested. Unlike valves off the shelf, the valve function cannot be tested before implantation, but only afterwards with a saline test and with post-bypass echocardiography. This puts the surgeon under pressure, because the final valve function is only known after the procedure. Many of the principles of mitral valve repair are used when doing a vein implant and, as with repair, the valve must function well with good coaptation on echocardiography before leaving the operating room. A poor functioning valve cannot be accepted and will either need to be corrected or replaced with a conventional valve prosthesis. Reproducing a

competent valve each time is dependent on the surgeon's expertise and skill and has a learning curve, much like mitral valve repair. This makes reproducibility difficult and the only way to overcome this would be to standardize each step of the valve preparation and implantation. The implantation of the chordal support also needs to be standardized to ensure reproducibility.

The vein ischemic time from harvesting to implantation needs to be as short as possible. In our study the vein ischemic time was about 3-4 hours. When the ischemic time of the vein is longer than 90 minutes before transplant, there is significant endothelial cell loss with exposed subendothelial collagen fibers that may aggregate and activate platelets and trigger vascular inflammation (Zou et al 2012). It is important to handle the vein graft with care during harvesting with minimal instrument contact to the vein wall to avoid mechanical injury. (Davies and Hagan 1995, Owens 2010). Optimal vein procurement in an appropriate physiological storage solution will minimize chemical injury and hypothermia at 20°C may reduce ischemic injury. (Davies and Hagan 1995, Rosenfeldt et al 1999, Zou et al 2012).

Harvesting of the left internal jugular vein gives enough tissue for 2 layers of vein leaflet which is large enough for an anterior mitral leaflet. A template with the shape of a normal mitral leaflet will help with the shaping of the leaflet. In this study a 28mm mitral ring sizer was used to make sure the vein leaflet was large enough to replace the anterior leaflet. It is important to suture the edges of the 2 layers together meticulously and to make sure all vein branches are closed with a suture to avoid any hematoma formation between the layers which was seen in 4 sheep. Gore-Tex CV-8 was used in this study because Gore-Tex sutures have been used successfully on the aortic valve leaflet to strengthen the leaflet free edge during aortic valve sparing surgery (David and Armstrong 2010).

The vein leaflet is sutured to the annulus with a continuous suture and care must be taken to avoid injuring the aortic leaflet on the ventricular side. The free edge of the leaflet needs to be supported with chordae and we used artificial Gore-Tex chordae. The Gore-Tex chordae must have the correct length to avoid either prolapse or tethering of the leaflet. It is not easy to reproduce the correct chordal length for each valve. We used 6 Gore-Tex loops to support the leaflet edge from each papillary muscle and used the measured chordal distance of the native valve, before excision, as a guide. The Gore-Tex loops should be fashioned so that the loops on the outside are longer than the middle loops otherwise the leaflet edge will not be supported

in one plane (Fig 4.1). If the Gore-Tex loops are of equal length and the distance of the first and last loops are far apart, the leaflet edge will be curved. This may create a central segment that is prolapsing or a peripheral segment that is tethered (Fig 4.2). This could be a reason why some of the chordae tore loose from the leaflet edge in this study (Fig 4.3). It could also explain the mitral regurgitation (MR) at the commissures because of leaflet tethering. We attempted to tailor the length of the loops for each valve, but did not get it right each time. Sheep 3 is an example of an implant where the chordal lengths were tailored well (Fig 4.4).

**Fig 4.1:** Gore-Tex loops of **equal** length (in this case 15mm) cannot support the leaflet edge in one plane if the distance between the first and last loops are too far apart. The central part may either be prolapsing or the tension on the furthest loops will be too much, creating tethering and possible rupture of the chord or leaflet edge.

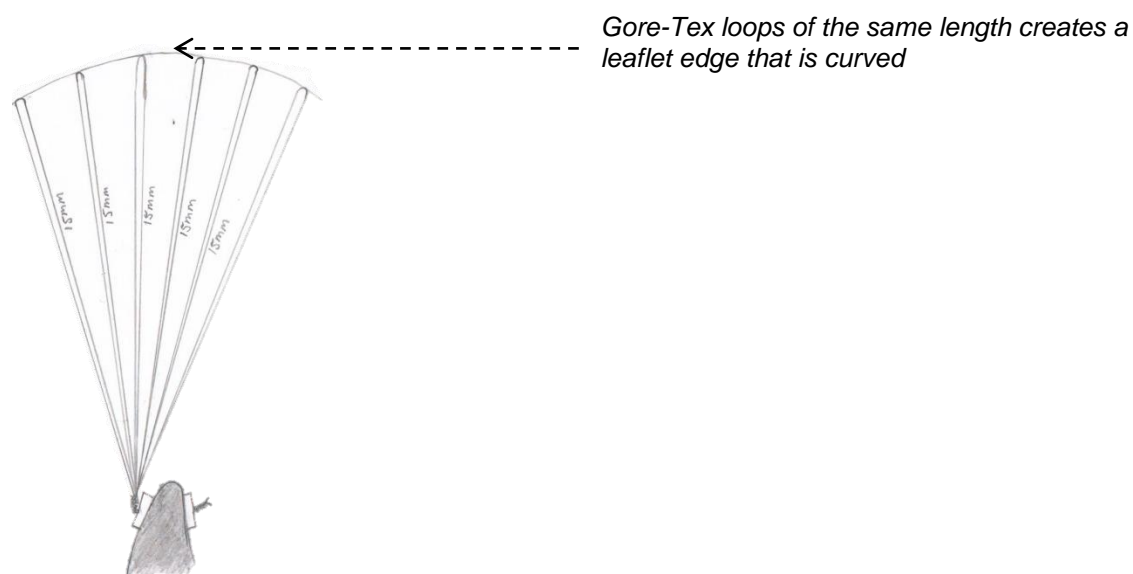




**Fig 4.2:** Part of the vein anterior leaflet is prolapsing because the Gore-Tex chordal length from the posterior papillary muscle is incorrect. The chordae from the anterior papillary muscle is correct with good leaflet coaptation.

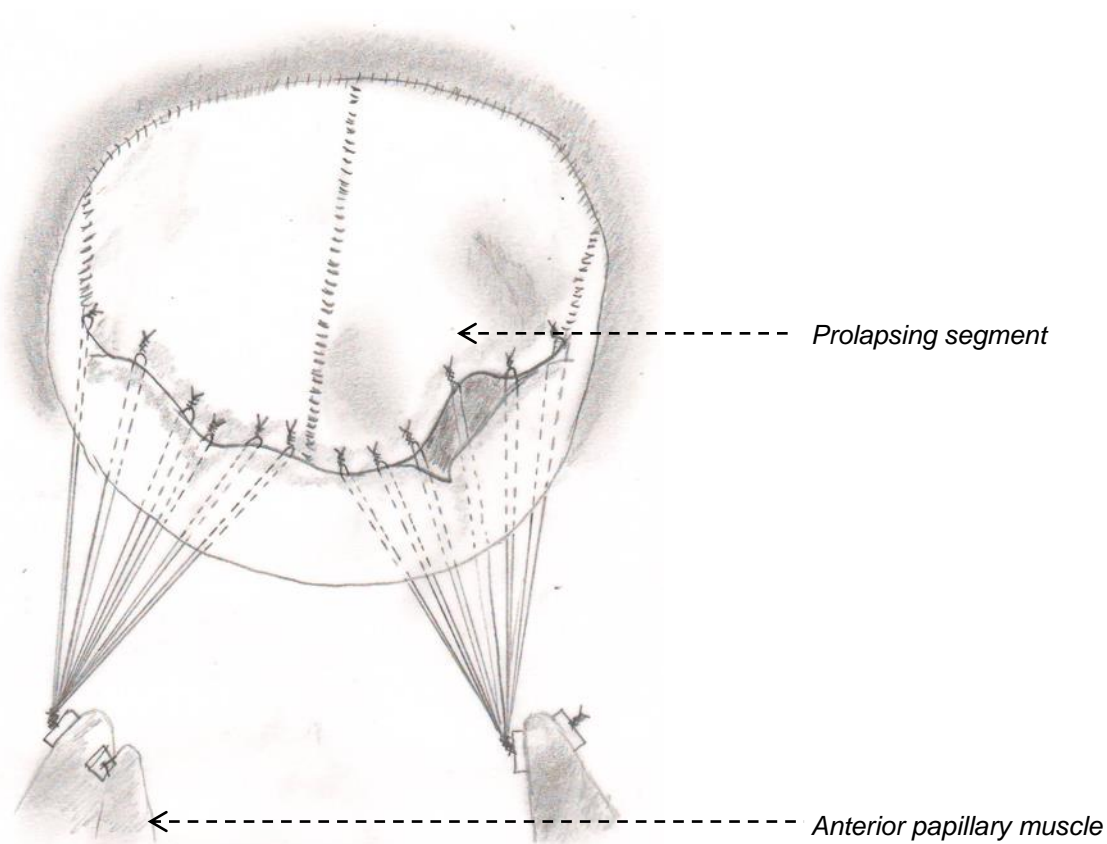


**Fig 4.3:** Mitral valve of sheep 10 (6.5 month implant) shows that the Gore-Tex chordae to A2 are under tension. The last loop to A1 has torn loose from the leaflet edge from increased tension.

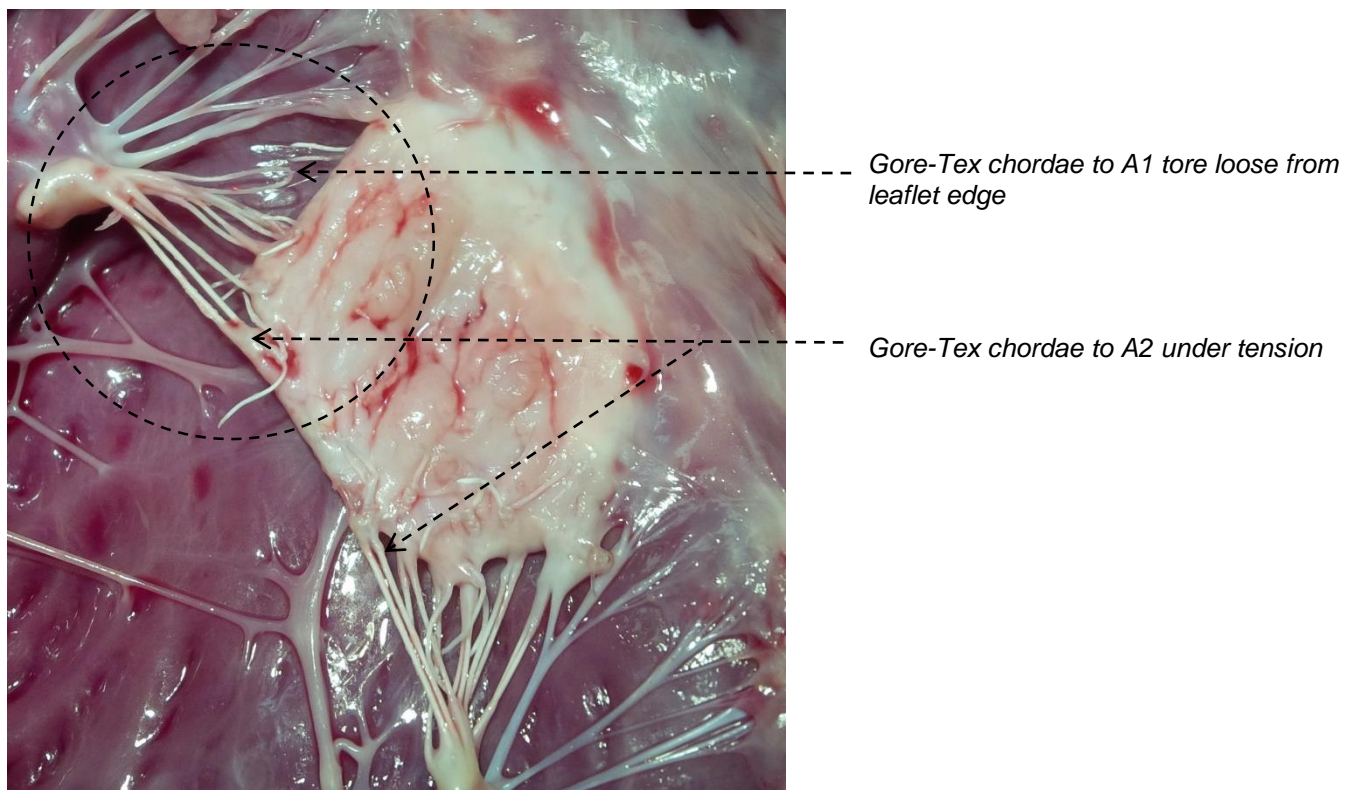
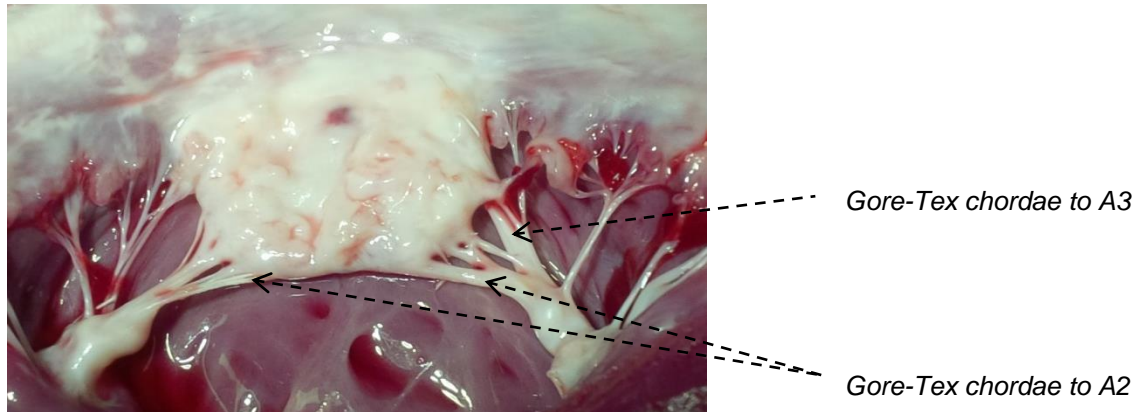


**Fig 4.4:** Mitral valve of sheep 3 (10 month implant) shows that the Gore-Tex chordal lengths were tailored well with no increased tension noted on any particular chords. Most of the chordae are covered with fibrous tissue and endothelium.



The outer loops must be made longer to overcome the problem of possible tethering. The length that is needed can be worked out by Pythagoras' theory: In a right angled triangle the square of the longest side is equal to the squares of the other 2 sides (Fig 4.4). Therefore, if the length of the middle chordae is 15mm and the distance to the furthest chordae is 10mm, the length of the furthest chordae should be 18mm (Fig 4.5). To ensure the accuracy of this measurement it is important that the middle chordal loop is perpendicular from the leaflet edge of the papillary muscle.

**Fig 4.4:** The theory of Pythagoras states that  $a^2 + b^2 = c^2$

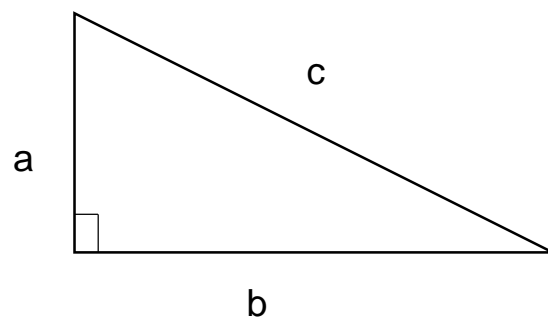
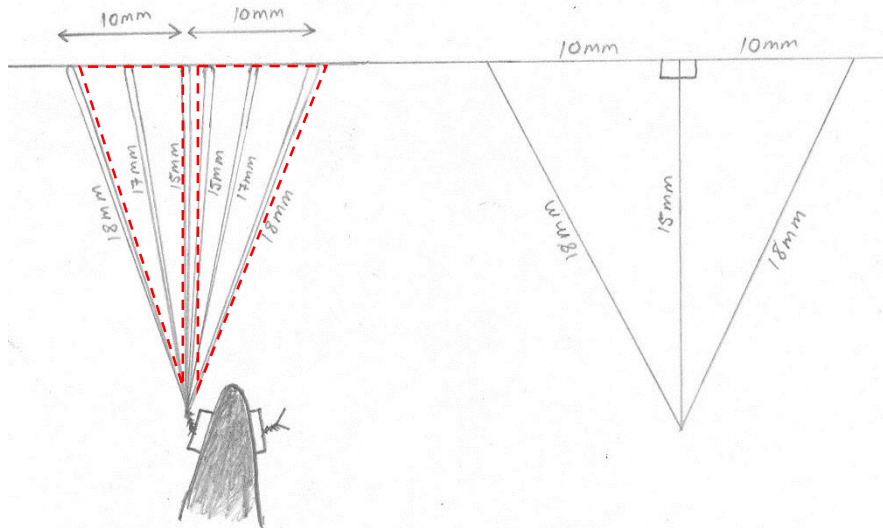
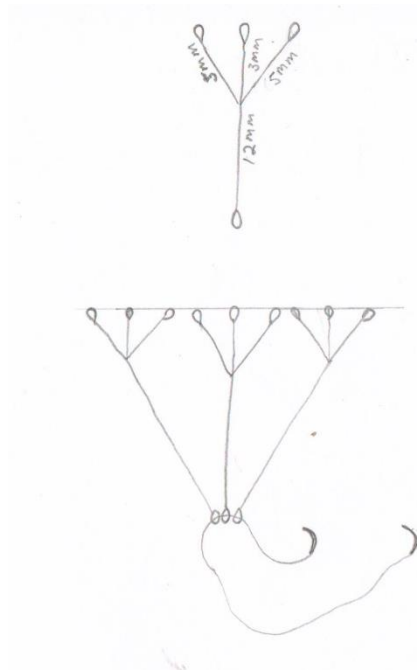


**Fig 4.5:** The length of the end loops can be worked out from the middle loop if the distance between the loops is known. Note the 2 right angled triangles in the diagram. In reality the triangles might not be an exact right triangle, but should be very close if the middle chord is perpendicular to the leaflet edge. This should create a leaflet edge that is supported in one plane with no areas of tethering or prolapse.



One way to make the attachment of chordal support quicker, more uniform and reproducible would be to have ready-made Gore-Tex chordal loops of different lengths and a range of lengths in the same loop set as in Fig 4.5. It is possible to have more than one set of loops on each papillary muscle, but space is limited on the papillary muscle and attaching more loops increases the risk of damaging the papillary muscle. If a complete valve is implanted in this way with anterior and posterior leaflets, it would be preferable to have just 4 Gore-Tex loops attached, 2 from the anterior papillary muscle heads and 2 from the posterior papillary muscle heads. If it is possible to manufacture Gore-Tex chords that divide into 3 chords that fan out at the distal end, it would be much easier to support the leaflet edge in one plane (Fig 4.6). This configuration would mimic the native mitral valve chordae and with only 3 chords it would be possible to have 9 attachment sites to the leaflet edge. It would then be possible to support half of the anterior leaflet and the commissural leaflet from one set of chordae (Fig 4.6).

**Fig 4.6:** *If Gore-Tex chordae can be manufactured to split into 3 distal segments that fan out, it would mimic the native mitral valve chordae. Three chordae can have 9 attachment sites on the free edge of the valve.*



The Gore-Tex sutures that was used to tie the Gore-Tex loops to the leaflet edge leaves a knot on the leaflet edge. This knot can cause friction to the opposite leaflet, as was found in some cases of our study (Figs 3.23 and 3.26). It can also cause an area of mitral regurgitation if the knot interferes with proper coaptation between the leaflets. One way to avoid this is to always leave the knot on the ventricular side of the leaflet.

When we removed the native anterior mitral valve leaflet, we had to cut and remove the secondary chordae. Sectioning of secondary chordae does not produce mitral regurgitation, but they do serve an important function in maintaining left ventricular size, geometry and function (Silbiger and Bazaz 2009). The strut chordae also connects the musculature of the left ventricle (at the papillary muscles) to the mitral annulus (at the fibrous trigones) and maintains papillary-annular continuity (David 1994). This helps to maintain the D-shaped annulus during systole which increases the coaptation area of the leaflets. Without secondary chordae to support the annulus shape, the annulus dilates and tension increases on the primary chordae. Fig 4.7 shows secondary chordae on the native mitral valve supporting the

central part of the anterior mitral valve leaflet up to the annulus. This secondary chordae is connected with the strong network of collagen fibres in the fibrosa layer of the leaflet which transmits the tension to the whole leaflet (Fenoglio et al 1972). In contrast, the vein implants in this study had no secondary chordal support (Fig 4.8). This caused billowing of the central part of the leaflet and the D-shape of the mitral annulus is lost during systole with less coaptation surface between the anterior and posterior leaflets (Fig 4.9). All the tension is transferred to the primary chordae, with more chance of primary chordal rupture or dehiscence from the leaflet edge. Secondary chordae in the sheep implants would have helped to take tension off the primary chordae and might have resulted in less primary chordal failure.

We considered and tried to place secondary chordae to the belly of the leaflet, but there was a risk that these sutures would pull out and create a perforation in the central part of the leaflet. This is because the Gore-Tex sutures puts all the tension on the attachment site of the leaflet and does not distribute the tension evenly throughout the fibrosa layer like native chordae would. A possible way to support the vein leaflet with secondary chordae would be to place a row of 3 chordal loops on each side of the central part of the vein leaflet body. This could help to distribute tension evenly throughout the leaflet with less chance of leaflet perforation (Fig 4.10). It will complicate the implant procedure, but it is clear from this study that secondary chordae serve an important function to decrease tension on the primary chordae, prevent billowing of the leaflet and maintain papillary-annular continuity in the long term.

An annuloplasty ring during mitral valve repair helps to maintain the systolic annular size and shape and prevents annular dilatation (Carpentier 1983, Carpentier et al 1995). It increases the coaptation surface of both leaflets and helps to decrease tension on the primary chordae, secondary chordae and the anterior leaflet belly (Jimenez et al 2005, Nielsen et al 2011). We elected not to place an annuloplasty ring with the implants to minimize foreign tissue and to allow for growth of the annulus. We wanted to see what the host response would be to the vein leaflet without the possible reaction to the annuloplasty ring. The disadvantage of a ring is that you fix the mitral annulus in a systolic position and you lose the diastolic enlargement of the mitral annulus during ventricular filling (Ormiston et al 1981, Lansac et al. 2001, Timek et al. 2003).

Secondary Gore-Tex chordae and an annuloplasty ring may help to improve the durability of the vein leaflet by decreasing the tension on the primary chordae and leaflet belly. It will also

improve the coaptation surface and prevent billowing of the vein leaflet. It may be necessary to add one of these techniques, maybe both, to improve long term function of the vein leaflet. This will have to be evaluated further.

**Fig 4.7:** Ventricular surface of the native anterior mitral valve leaflet showing secondary chordae implanting into the belly of the anterior mitral valve leaflet (Lam et al 1970). The whole anterior leaflet is supported by chordae tendinae from the annulus to the leaflet edge.

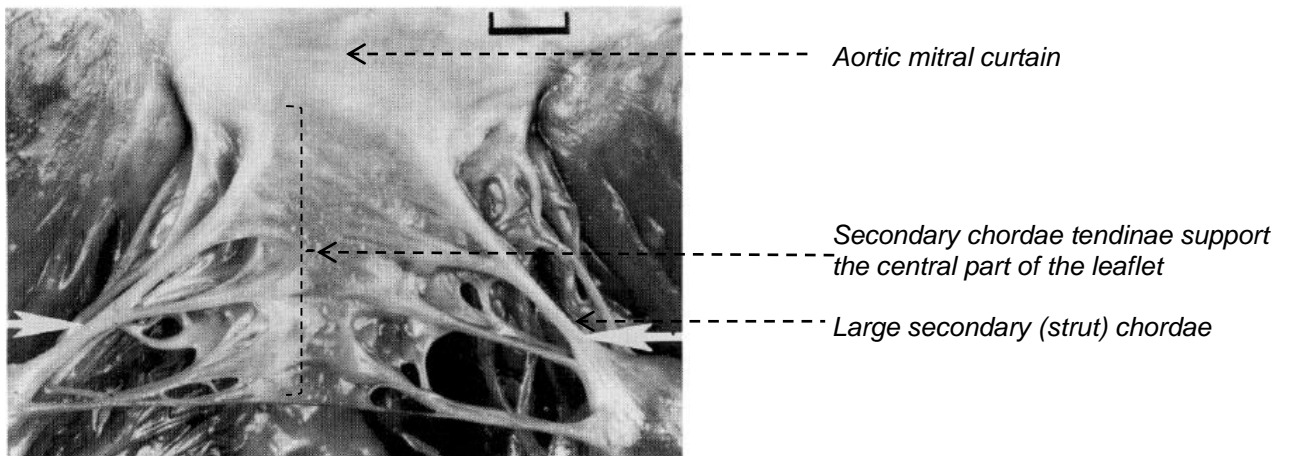


**Fig 4.8:** Ventricular view of vein implant shows no secondary chordae supporting the central part of the leaflet and the anterior annulus. This causes billowing of the leaflet and the D-shape of the mitral annulus is lost during systole.

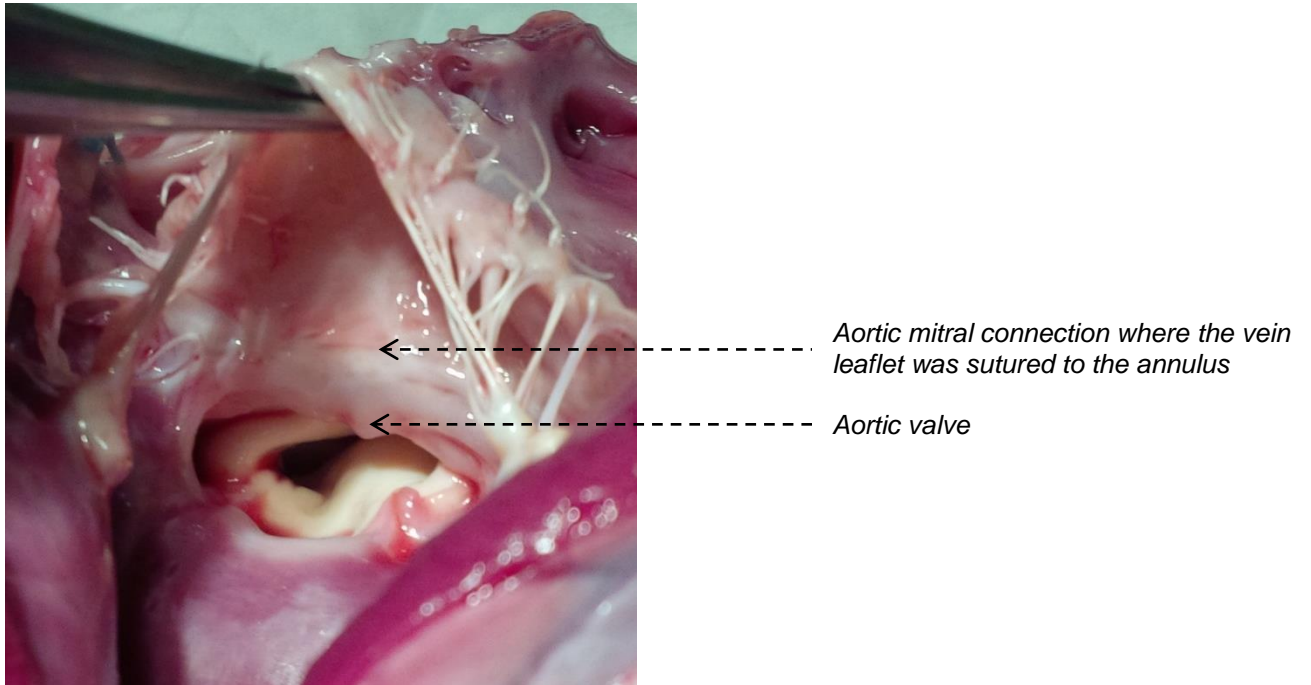


**Fig 4.9:** Billowing of vein leaflet without support from secondary chordae.

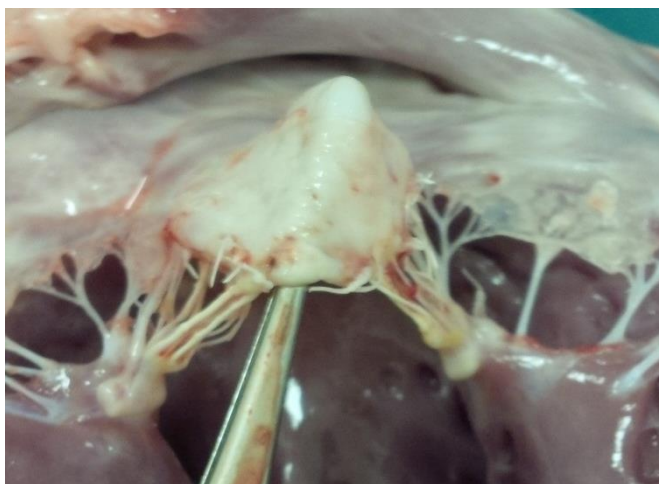
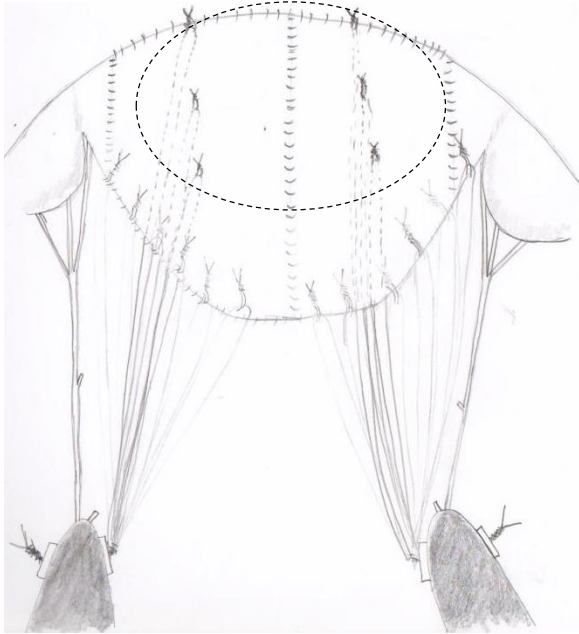




**Fig 4.10:** A possible way to support the vein leaflet with secondary chordae. Three Gore-Tex chordae are placed on each half of the leaflet from the annulus to the midportion.



Only the anterior mitral leaflet was replaced in this study, but when a complete mitral valve is replaced it will be necessary to create anterior, commissural and posterior leaflets from vein tissue. The native mitral valve leaflets actually consist of a single continuous structure which hangs into the left ventricle like a veil with indentations at the commissures (Fig 4.11 and Fig 4.12). The height of the different leaflets and the insertion length of each leaflet at the annulus is known from anatomical studies and is shown in Table 4.1 (Carpentier 2010). One can create a mitral valve from a continuous length of vein by using a template with the measurements of a normal mitral valve (Fig 4.13). To illustrate the feasibility of this concept, a standard valve size is used (32mm annuloplasty), but the templates can be adapted to accommodate different valve sizes from a 26 mm to a 34 mm annuloplasty ring, depending on the patient's size.

**Fig 4.11:** Left ventricular view of the mitral valve which is opened up to show the continuity of the mitral valve leaflets (Carpentier et al 2010). P1, P2 and P3 of the posterior leaflet are shown.

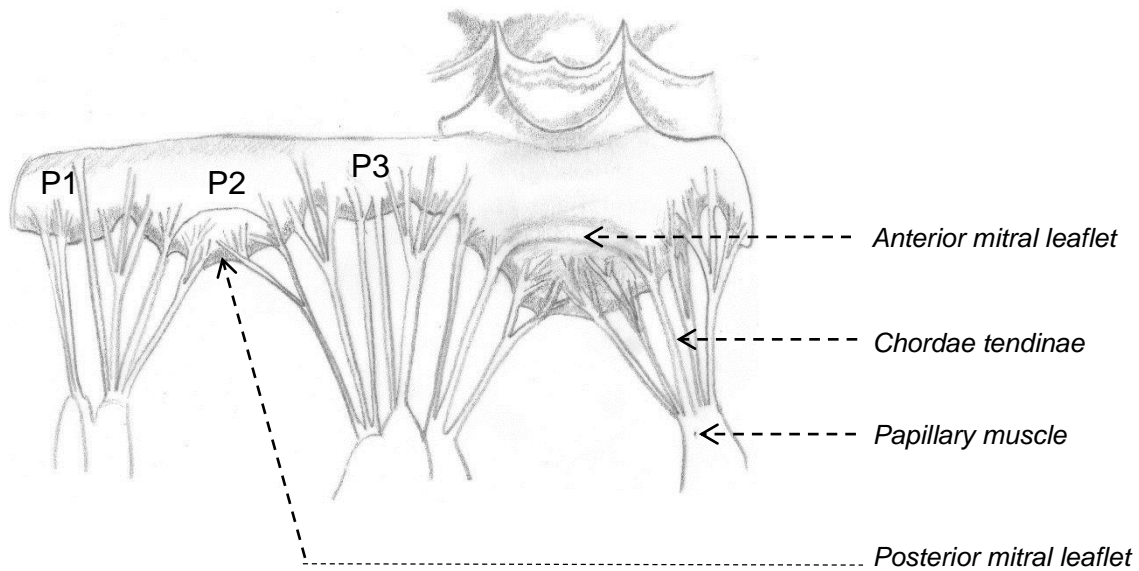


**Fig 4.12:** The ventricular side of a porcine mitral valve, highlighting the mitral leaflets, chordae tendinae, and papillary muscles. The valve was excised from an explanted heart and cut in half at the P2 scallop of the posterior leaflet (Rabbah et al 2013). Notice how the mitral valve leaflets hangs from the annulus as a continuous curtain. The leaflet height increases at the anterior and posterior leaflets and are smallest at the commissures.

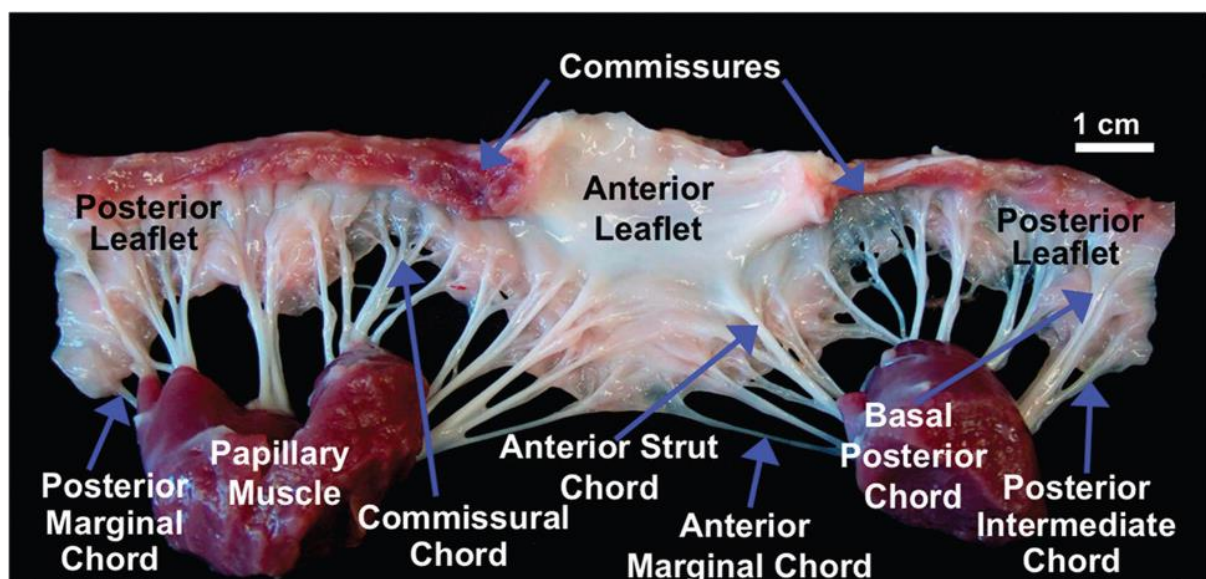
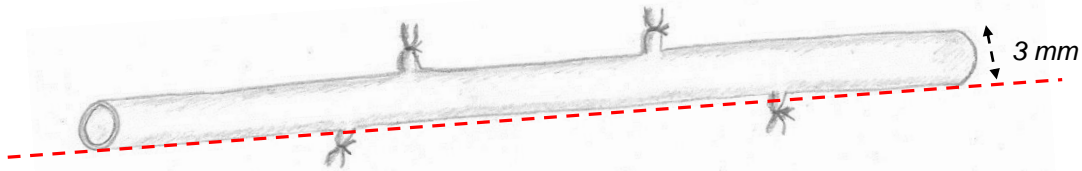


**Table 4.1:** The normal dimensions of mitral valve leaflets (Carpentier 2010).

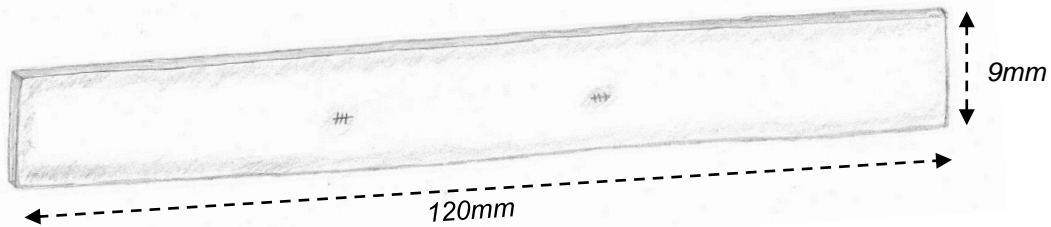
	<b>Antero-lateral Commissural leaflet</b>	<b>Anterior leaflet</b>	<b>Posteromedial Commissural leaflet</b>	<b>Posterior leaflet</b>
<b>Insertion length at the annulus (mm)</b>	12	32	17	55
<b>Leaflet height (mm)</b>	8-9	23	8-9	P1: 10 P2: 14 P3: 10

**Fig 4.13:** A concept to shape a complete mitral valve leaflet from a saphenous vein

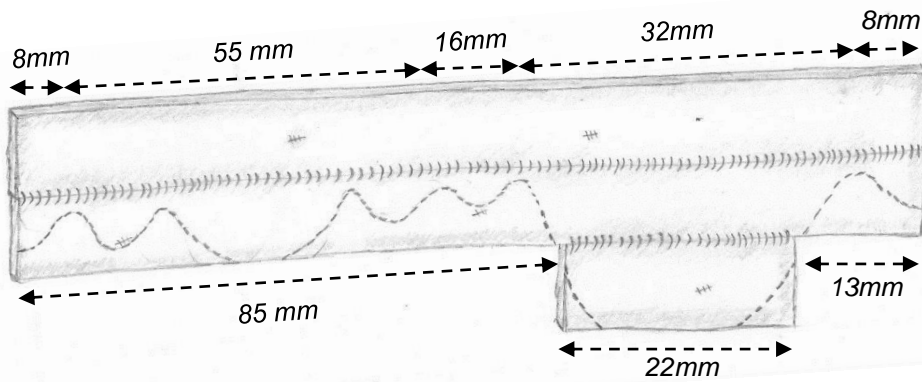
Saphenous vein of 3mm diameter cut open lengthwise through the side branches on one side (red line) to have fewer branches in the middle of the vein leaflet that need to be sutured.



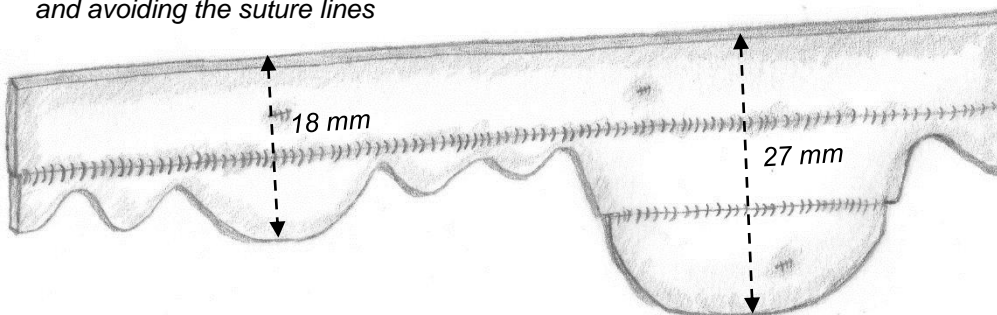
The vein opened lengthwise with its side branches sutured.



Three pieces of vein opened up and sutured together.



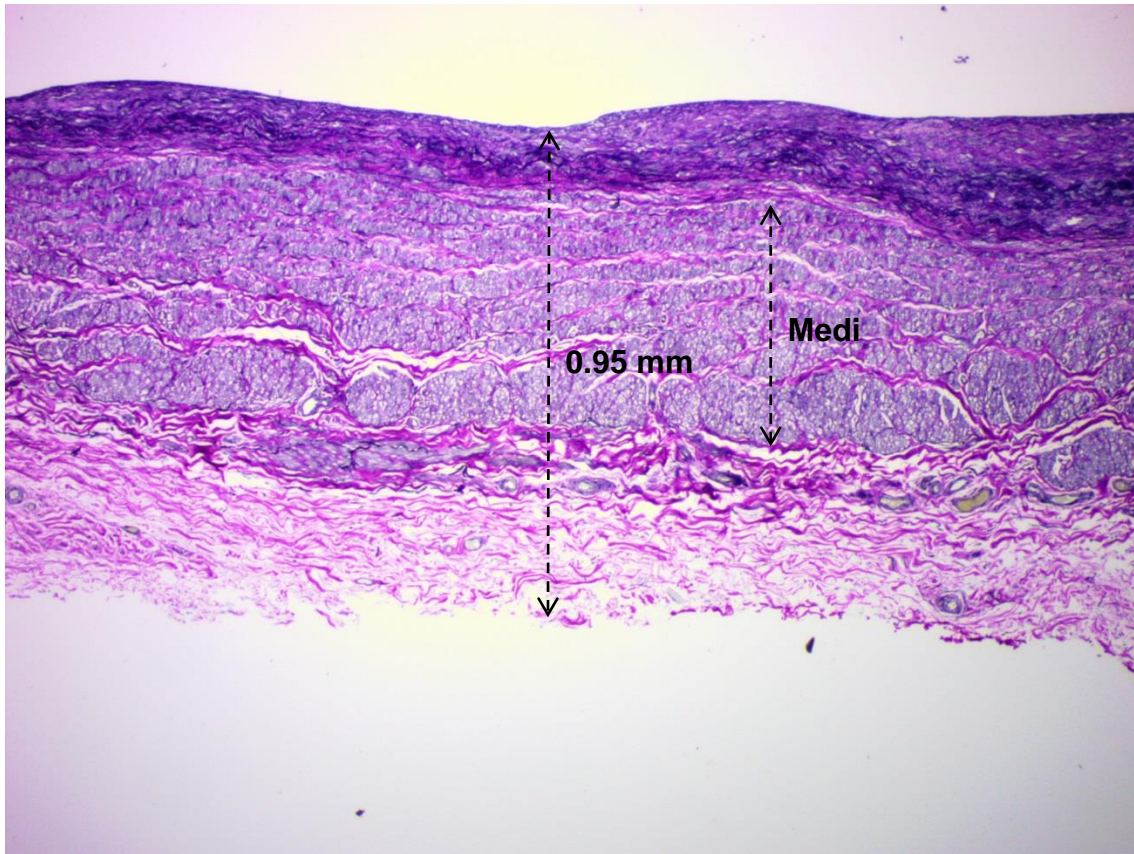
Shape of leaflets cut out with a template and avoiding the suture lines



In humans, the saphenous vein of one upper and lower leg will give sufficient surface area to create a whole mitral valve. The diameter of saphenous veins vary between 3 mm and 5.5 mm depending on the dilatation of the vein (Stooker et al 2003). The circumference of a 3mm vein would be about 9 mm ( $3 \times \pi$ ) so after opening the vein lengthwise, the width will be 9 mm. A normal anterior mitral leaflet height measures 23mm, hence 3 veins ( $3 \times 9 = 27$  mm) would give enough surface area for the anterior leaflet. The normal posterior leaflet height measures 14 mm and 2 veins ( $2 \times 9 = 18$ mm) would be sufficient for the posterior leaflet. The commissural leaflet height is 8mm. After suturing the vein together and closing the vein branches, the new vein leaflet can be tailored according to the template. Care must be taken to not cut over any suture lines (Fig 4.13).

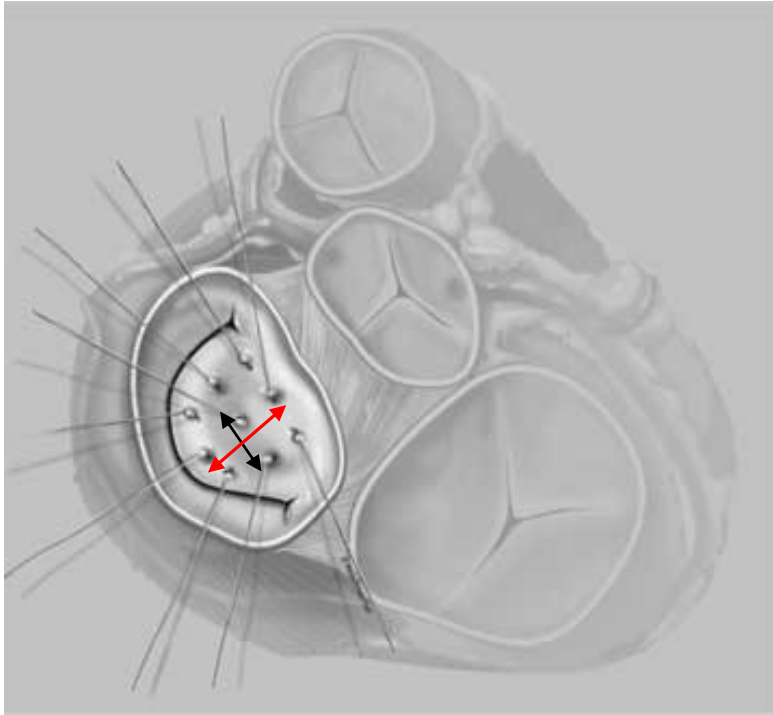
The saphenous vein in an adult has a thicker wall than the jugular vein of sheep because the vein has adapted to the hydrostatic pressure in the legs. The jugular vein in our study measured 0.3-0.4 mm and the saphenous vein wall normally measures twice as much from 0.6-0.9 mm (Fig 4.14) (Golbasi et al 2005). The saphenous vein may have sufficient strength to use as a single layer when creating a valve leaflet. This would simplify the procedure if one can create a valve from a single layer of vein tissue, but only one side of the leaflet will be covered by endothelium with implantation.

**Fig 4.14:** Histological section of a saphenous vein to show the thickness of the vein wall (Verhoeff and Van Giesen 40x). The media of the saphenous vein is much thicker than the media of the jugular vein in sheep and consists of smooth muscle cells, interlaced with collagen and some elastic fibres.



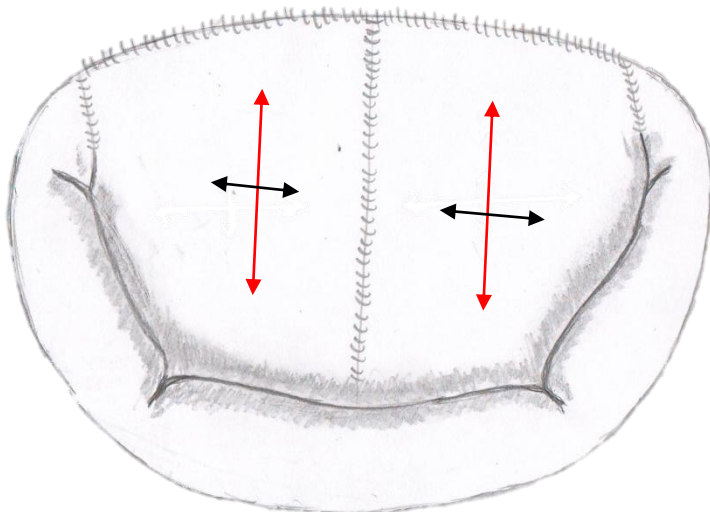
The interconnected sheets of collagen and layers and tubes of elastin give normal valve tissue viscoelasticity, anisotropy and highly non-linear mechanics. Anisotropy describes the direction-dependent properties of materials and valve tissue show a larger strain in the radial direction than in the circumferential direction (Sacks and Yoganathan 2007). The strain on the anterior mitral leaflet is 3 to 4 times more in the radial direction than in the circumferential direction (Fig 4.15) (Sacks et al 2006).

**Fig 4.15:** Mitral valve strain measured with piezo-electric transducers on the anterior mitral valve leaflet during the cardiac cycle. Peak radial strain is 16-22% (red arrow) and peak circumferential strain is 2.5-3.3% (black arrow) (Sacks et al 2006).



Jugular vein tissue also shows anisotropy and has a larger longitudinal strain (extension ratio) than circumferential strain (Wesly et al 1975). This may be an important observation when using the vein as a valve leaflet. The jugular vein in this study was used lengthwise in the radial direction when the valve leaflet was fashioned, so it was more likely to deform in the radial direction when subjected to systolic pressure (Fig 4.16). This mimics the anisotropy which is seen in the mitral leaflet (May-Newman and Yin 1995, Sacks et al 2006).

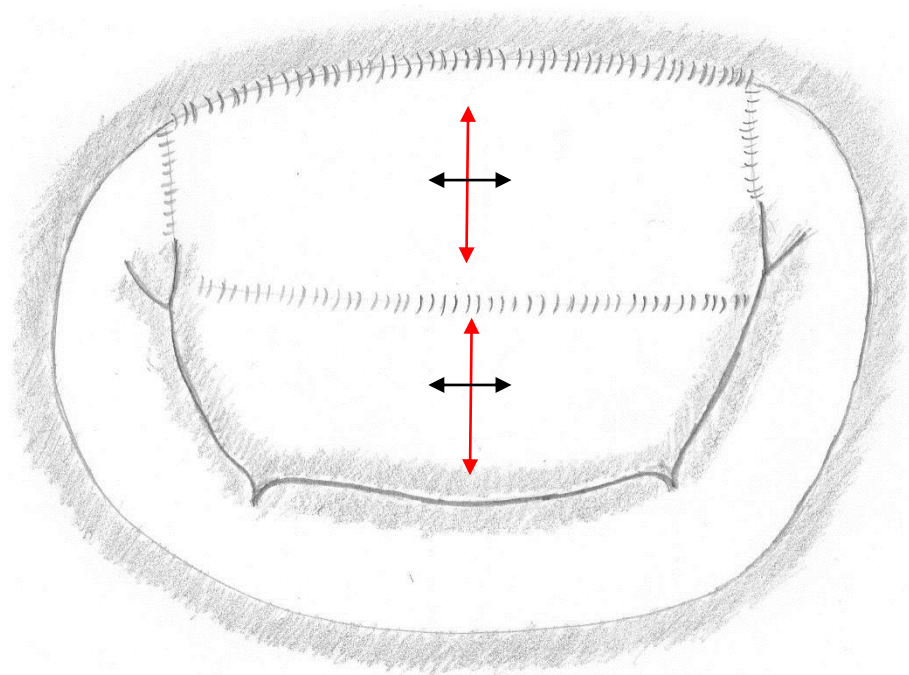
**Fig 4.16:** *The jugular vein has a larger longitudinal strain (extension ratio) than circumferential strain (Fig 4.18) and was sutured lengthwise to the annulus when creating the leaflet. The vein leaflet stretched more in the radial direction (red arrow) than the circumferential direction (black arrow), mimicking the anisotropy of the anterior mitral valve leaflet.*





In contrast to the internal jugular vein, the saphenous vein shows more circumferential strain than longitudinal strain (Wesly 1975). When the saphenous vein is used to shape a mitral valve it would be better to use it lengthwise in the circumferential direction to mimic the mitral valve anterior leaflet. This would also be more practical and require less suture lines (Fig 4.17)

**Fig 4.17:** *In contrast to the jugular vein, the saphenous vein has more circumferential strain (red arrow) than longitudinal strain (black arrow) (Fig 4.18). When creating a mitral leaflet from a saphenous vein it would be better to suture it lengthwise in the circumferential direction to mimic the anisotropy of the anterior mitral valve leaflet. It would also be more practical to suture a saphenous vein in this direction because the vein has a smaller diameter than the internal jugular vein and if sutured circumferentially it would result in fewer suture lines.*



Vein tissue loses most of its elasticity at arterial pressure (40 cm H<sub>2</sub>O for jugular veins and 120cm H<sub>2</sub>O for saphenous veins) when used as an arterial graft, because its elastic fibres are stretched to the maximum and the inextensible collagen fibres come into play (Wesly et al

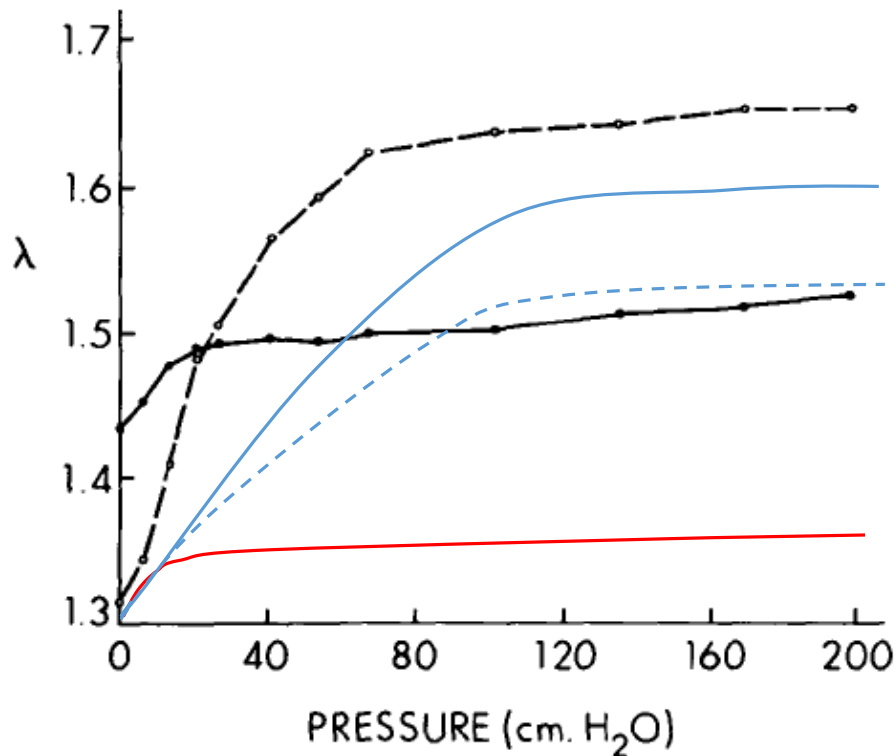
1975). Mitral valve tissue has exceptionally high strain because the tissue cycles from a completely unloaded state in diastole to the high tension during left ventricular systole (Sacks and Yoganathan 2007). When using a vein graft as a valve leaflet the pressure that the leaflet is subjected to vary from 0-150 mm Hg in the normal human, which is very different from when it is used as an arterial graft where the pressure in the vein would be 80–120 mm Hg. At the lower pressure, from 0-120 mm Hg, the elastic properties of venous tissue could affect the way the vein performs as a valve leaflet.

The mechanical properties of the jugular vein, saphenous vein and the anterior mitral leaflet all show stress-strain relations that are highly nonlinear, as is characteristic of most soft biological tissues (Wesly et al 1975, May-Newman and Yin 1995, Stoker et al 2003, Sacks et al 2006, Martinez et al 2010). The stress-strain curves all show the same pattern with a transition zone where the curves plateau (Fig 4.18). Jugular veins reach this transition zone at a pressure of 40 cm H<sub>2</sub>O and saphenous veins reach the transition zone at 120cm H<sub>2</sub>O. The maximum strain or extension ratio of the 3 tissues differ with jugular vein having the highest extension ratio and anterior mitral valve leaflet the lowest extension ratio (Fig 4.18). The maximum jugular vein extension ratio is about 1.65 in the longitudinal direction and 1.5 in the circumferential direction (Wesly et al 1975). The maximum saphenous vein extension ratio is about 1.5 in the longitudinal direction and 1.6 in the circumferential direction (Wesly et al 1975). The maximum anterior mitral valve leaflet extension ratio is 1.18 in the circumferential direction and 1.34 in the radial direction (May-Newman and Yin 1995).

The increased elasticity of venous tissue needs to be taken into account when creating a valve leaflet from a vein. An anterior mitral leaflet with a leaflet height of 23 mm would have a maximal length of 30 mm (23 x 1.3) under strain. A jugular vein of 23 mm height would stretch to 38 mm (23 x 1.65) under the same strain according to its mechanical properties, and a saphenous vein would stretch to about 37 mm (23 x 1.6). Under strain, the vein leaflet stretches about 8 mm more than the anterior mitral valve leaflet. This can be an advantage when the extra length of the leaflet gives redundant length at the coaptation zone and increases the coaptation area, but it is a drawback when the extra vein length is billowing into the atrium. We did not compensate for vein leaflet stretch when creating the size of the leaflet but hoped that the stretch would increase the leaflet area and help with coaptation. The elasticity of the vein was seen with echocardiography. In diastole it retracts and shortens and during systole, with increasing pressure, the vein stretches, which helps with better coaptation, but also resulted in billowing of the vein leaflet. Secondary chordae could prevent excess

billowing of the vein leaflet by supporting the leaflet belly and in effect would pull more of the vein leaflet into the coaptation zone. An annuloplasty ring would decrease the antero-posterior dimension of the annulus which would place more vein leaflet into the coaptation area if the primary chordal length is correct (Jimenez et al 2005, Nielsen et al 2011).

**Fig 4.18:** The stress-strain relationship of the jugular vein, saphenous vein and the anterior mitral leaflet is demonstrated with pressure (cm H<sub>2</sub>O) on the x-axis and extension ratio or strain ( $\lambda$ ) on the y-axis. Note the non-linear stress-strain relationship up to the maximal strain. The anterior mitral valve leaflet extension ratio is less than the saphenous vein and jugular vein (Wesly et al 1975, May-Newman and Yin 1995, Sacks et al 2006).



Jugular vein circumferential strain = —————

Jugular vein longitudinal strain = - - - - -

Saphenous vein circumferential strain = —————

Saphenous vein longitudinal strain = - - - - -

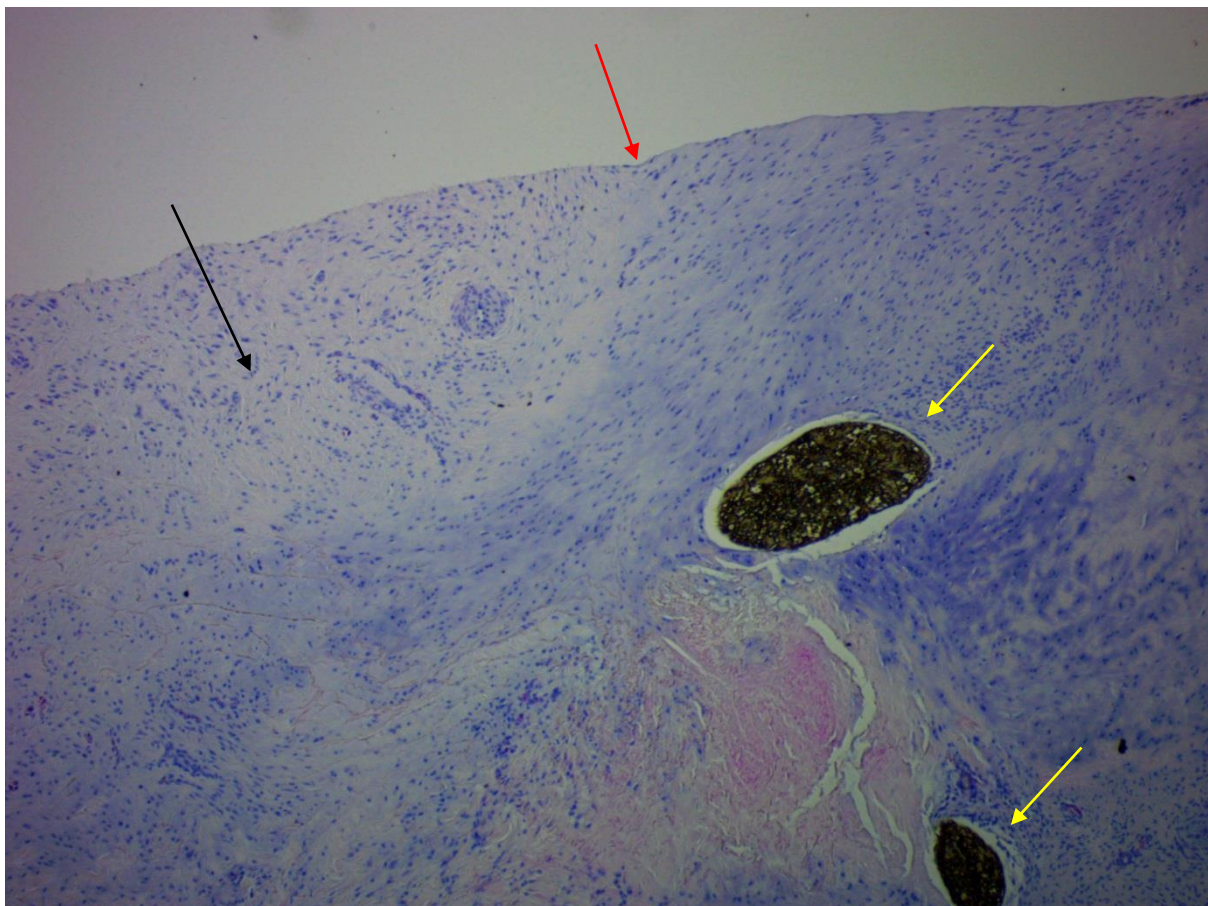
Anterior mitral valve leaflet radial strain = —————

Anterior mitral valve leaflet circumferential strain = 1.18 (not on chart)

#### 4.2 The nature of the linkage between the vein leaflet and the host.

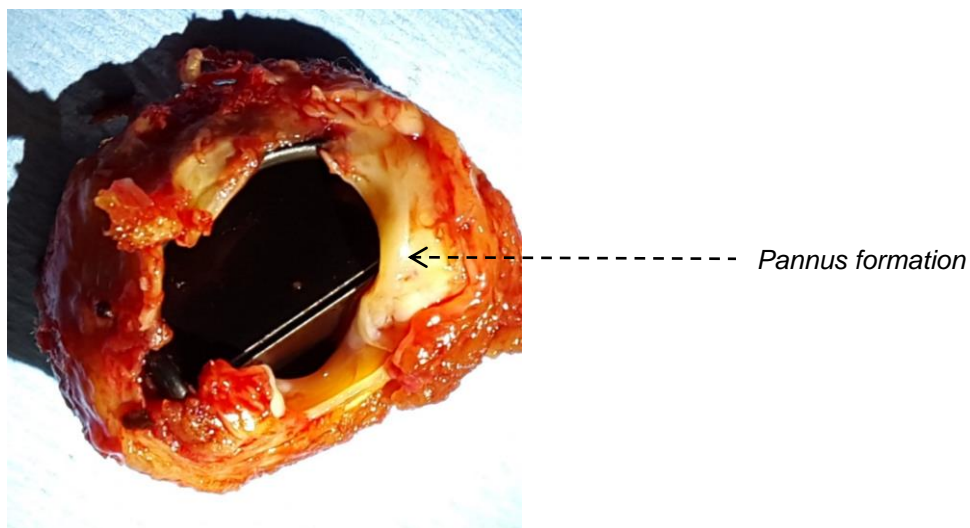
The vein is autologous living tissue and showed healing at the annulus suture line with formation of normal granulation tissue and vascular ingrowth into the vein tissue. There was no inflammatory response noted at the vein-host interface and the endothelial layer of the vein was in continuity with the endocardial cells at the suture line. A foreign body response was noted around the Gore-Tex sutures (Fig 4.19).

**Fig 4.19:** Sheep 21 (6 month implant) shows endothelial continuity at the vein-annulus interface (red arrow) with normal granulation tissue with vascularisation over the vein (black arrow). A foreign body tissue reaction is noted around the Gore-Tex sutures (yellow arrows) (H and E stain 40x).



This healing process differs from the healing process that is normally seen between a valve prosthesis and the host annulus which shows a foreign body tissue response. The Dacron ring of a mechanical or tissue valve becomes encapsulated by healthy scar tissue from infiltrating fibroblasts that links the prosthesis to the host (Braunwald and Morrow 1969, Davila 1989). Homografts and stentless porcine valves show a host cellular response at the host-graft interface with mild chronic inflammation and gradual infiltration of the prosthetic aortic root by poorly cellular organizing granulation tissue (scar or pannus) (Smith 1967, Siddiqui et al 2009). This granulation tissue formation or pannus is due to a persistent neointimal development from a chronic inflammatory response which provokes proliferation of myofibroblasts and extracellular matrix and can extend onto the valve leaflets and cause stiffening of the leaflets and even obstruction of mechanical valves (Fig 4.20) (Teshima et al 2003). The aortic root part of the prosthesis can also calcify and stiffen (Siddiqui et al 2009). In contrast, the vein leaflet in this study healed with minimal scar tissue and fibrosis at the suture line for up to 10 month follow up.

**Fig 4.20:** Pannus formation under a mechanical aortic valve caused obstruction of one leaflet and increased gradients over the valve. The valve was implanted for 23 years.



The leaflet edge is supported by Gore-Tex chords which are attached to the papillary muscles and this is an advantage over other mitral prosthetic devices which are only connected to the host at the mitral annulus. Studies have shown that mitral valve replacement with chordal

preservation has a beneficial effect on postoperative left ventricular performance and survival by maintaining continuity between the mitral annulus and the papillary muscle (David et al 1995, Okita et al 1995, Straub et al 1997).

The normal mitral valve can only function well if all the parts of the mitral complex are working together: the left atrium, the mitral annulus, mitral leaflets, chordae tendinae, papillary muscle and the left ventricle. Mitral valve tissue has exceptionally high strain, more than any of the other heart valves, because the tissue cycles from a completely unloaded state in diastole to high tension during left ventricular systole (Sacks and Yoganathan 2007). The normal mitral valve leaflets need support from chordae tendinae which are attached to the papillary muscles to maintain ventricular annular continuity, left ventricular geometry and to support the leaflets during valve closure (David 1994, Nielsen 2003, Silbiger and Bazaz 2009). The papillary muscles shorten during systole and this maintains a constant distance between the papillary muscle tips and the mitral annulus as the ventricle contracts. The papillary muscles act as a shock absorber of the mitral valve complex, keeping the tension on the chordae tendinae constant. (Joudinaud et al 2007).

In this study Gore-Tex chordae were placed to support the leaflet edge during systole. Secondary chordae were not placed, but could help to maintain ventricular-annular continuity and left ventricular geometry. Current porcine and pericardial valves that are placed in the mitral position do not last as well as in the aortic position, because the leaflets are unsupported, experience much larger strain during left ventricular systole and degenerate earlier (Burdon et al 1992, Vongpatanasin et al 1996). The Gore-Tex chordae mimic the chordae tendinae of the normal mitral valve and are needed for normal valve function. If the length of the Gore-Tex chordae are correct with good valve coaptation, the stress on the leaflets is reduced.

#### **4.3 Opening resistance and forward flow across the valve**

The vein leaflet has minimal opening resistance and showed good diastolic flow without turbulence on colour flow. The opening valve area was 2.8 cm<sup>2</sup> on average, the same as the native valve. If an annuloplasty ring has to be implanted to improve valve coaptation, the

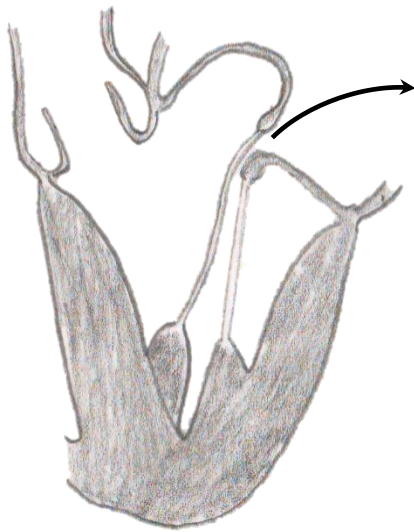
diastolic gradient will increase because the diastolic mitral annular area is then effectively reduced to the systolic mitral annular area. (Timek and Miller 2001). A 30 mm Carpentier-Edwards annuloplasty ring reduces the mitral annular area down to 3.3 cm<sup>2</sup> in humans from a normal area of 6.5 cm<sup>2</sup> (Yamaura et al 1995). The effective orifice area of a 31 mm St Jude mechanical valve is 2.02 cm<sup>2</sup> (Magni et al 2007), therefore even if an annuloplasty ring has to be implanted with the vein implant, it would still give a larger mitral valve orifice area with better diastolic flow than any currently available mitral valve prosthesis.

#### **4.4 Valve closure and competence.**

It was possible to create a competent valve in this study by replacing the anterior leaflet with a vein leaflet. Out of 20 sheep the post-operative echocardiography showed 14 had trace to mild mitral regurgitation (MR), 2 had mild to moderate MR, 3 had moderate MR and 1 had moderate to severe MR.

The MR was almost always at one or both commissures. At the commissures the surface area of leaflet coaptation is the smallest between the vein leaflet and the commissural leaflet and the margin for error in chordal length is small. The MR could have been from incorrect Gore-Tex chordal length at the commissure with leaflet restriction if the chordae were too short or leaflet prolapse if the chordae were too long (Fig 4.21). It may also have been from the change in shape of the anterior mitral annulus during systole without the support of the secondary chordae. Normally the anterior mitral annulus would move closer to the posterior mitral annulus during systole, but without the support of the secondary chordae, this movement is less (David 1994, Lansac et al. 2001; Timek et al. 2003).

**Fig 4.21:** Billowing of anterior vein leaflet and Gore-Tex chords that are too long causes prolapse of the leaflet with mitral regurgitation.



If there is only a small area of coaptation between the leaflets, the tension on the primary chordae is increased (Fig 4.22) (Rabbah et al 2013). It is tempting to increase the size of the leaflet to create a larger area of coaptation, but this will not help if the excess leaflet billows into the left atrium (Fig 4.23). The belly of the leaflet needs support to prevent prolapse and to pull more leaflet into the coaptation zone. Secondary chordae will help to achieve this and also support the anterior annulus (Fig 4.23). A mitral annuloplasty will also support the anterior annulus and the leaflet belly (Jimenez et al 2005, Nielsen et al 2011).



**Fig 4.22:** With a small area of coaptation between the leaflets, the tension on the primary chordae is increased.

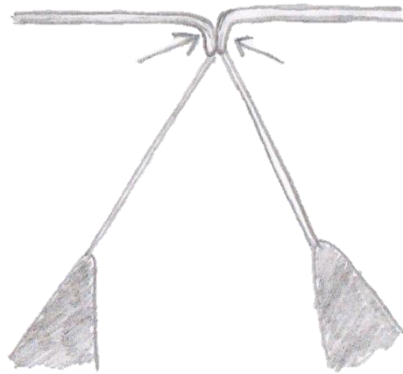
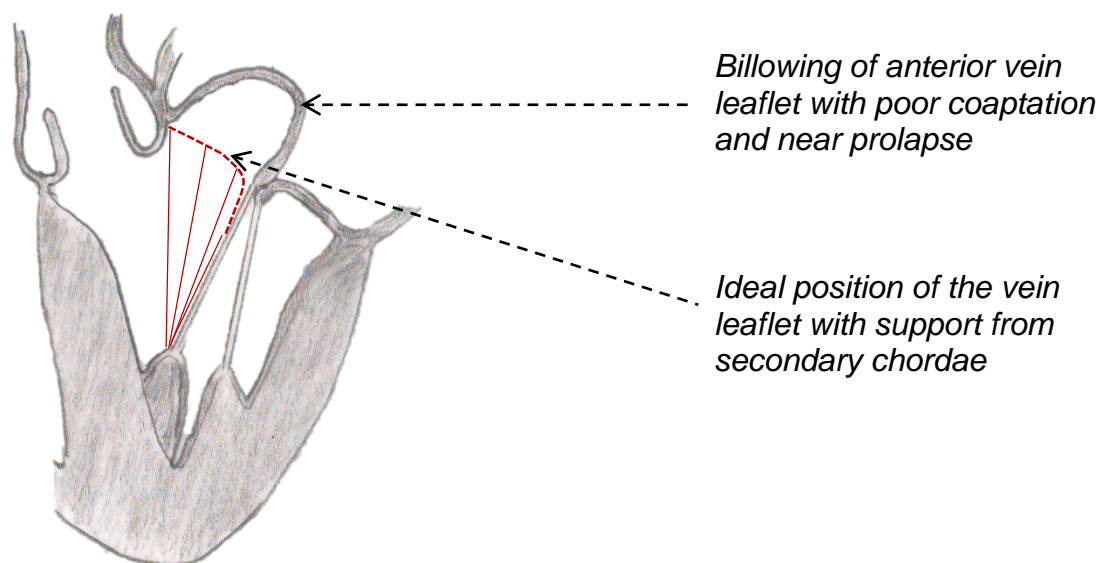


**Fig 4.23:** Billowing of the anterior vein leaflet with poor coaptation between the vein and posterior leaflet causing near prolapse. Notice how secondary chordae could support the vein leaflet, prevent billowing and pull more vein leaflet into the coaptation zone.

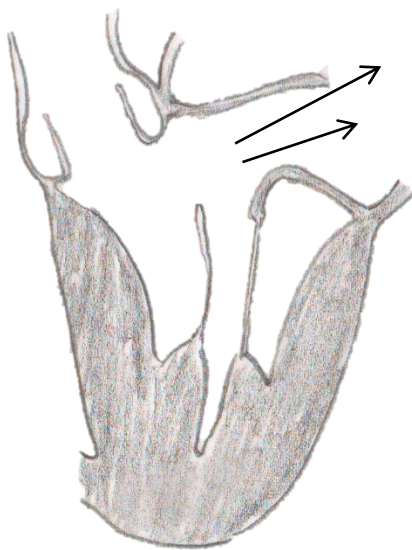


*Billowing of anterior vein leaflet with poor coaptation and near prolapse*

*Ideal position of the vein leaflet with support from secondary chordae*

The initial mild MR can lead to annular dilatation, which decreases the coaptation between leaflets further and increases primary chordal tension (Kunzelman et al 1997). This will lead to progression of the MR which was seen in our study at the 6 month post-implant echocardiography. Out of 11 sheep, 3 had mild MR, 1 had mild to moderate MR, 4 had moderate MR and 3 had moderate to severe MR. When the tension on the chordae becomes too much, the chordae tears out of the leaflet, resulting in leaflet prolapse (Fig 4.24). This was noticed in 7 sheep, but 2 of these had infective endocarditis.

**Fig 4.24:** Gore-Tex suture tearing out of vein leaflet edge causing severe prolapse and regurgitation.



It is important to make sure that each valve that is implanted has no regurgitation with a large surface of coaptation between the leaflets. With good coaptation between the leaflets, the tension on the primary chordae would be less and the valve would be more durable. (Fig 4.24 and Fig 4.25) (Rabbah et al 2013). In mitral and aortic valve repairs it has been shown that good leaflet coaptation height after valve repair results in better long term outcome. (Yamauchi et al 2005, Aicher et al 2011)

**Fig 4.25:** Optimal leaflet coaptation between leaflets reduces tension on the primary chordae.

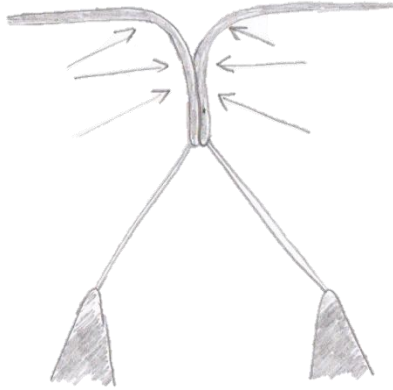
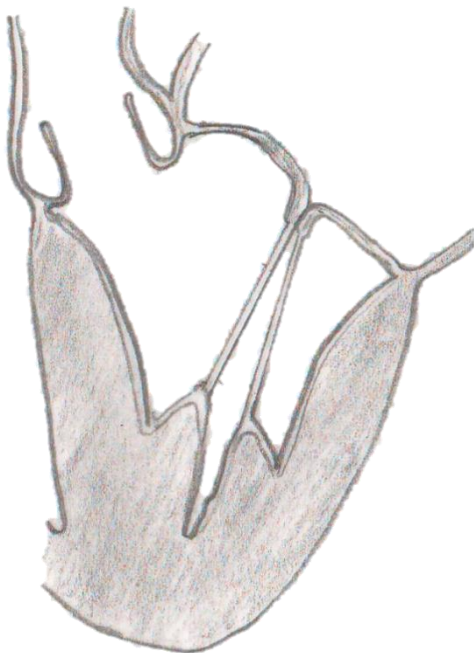


**Fig 4.26:** A valve with a good coaptation length between leaflets will be more durable.



#### 4.5 Activation of the coagulation system.

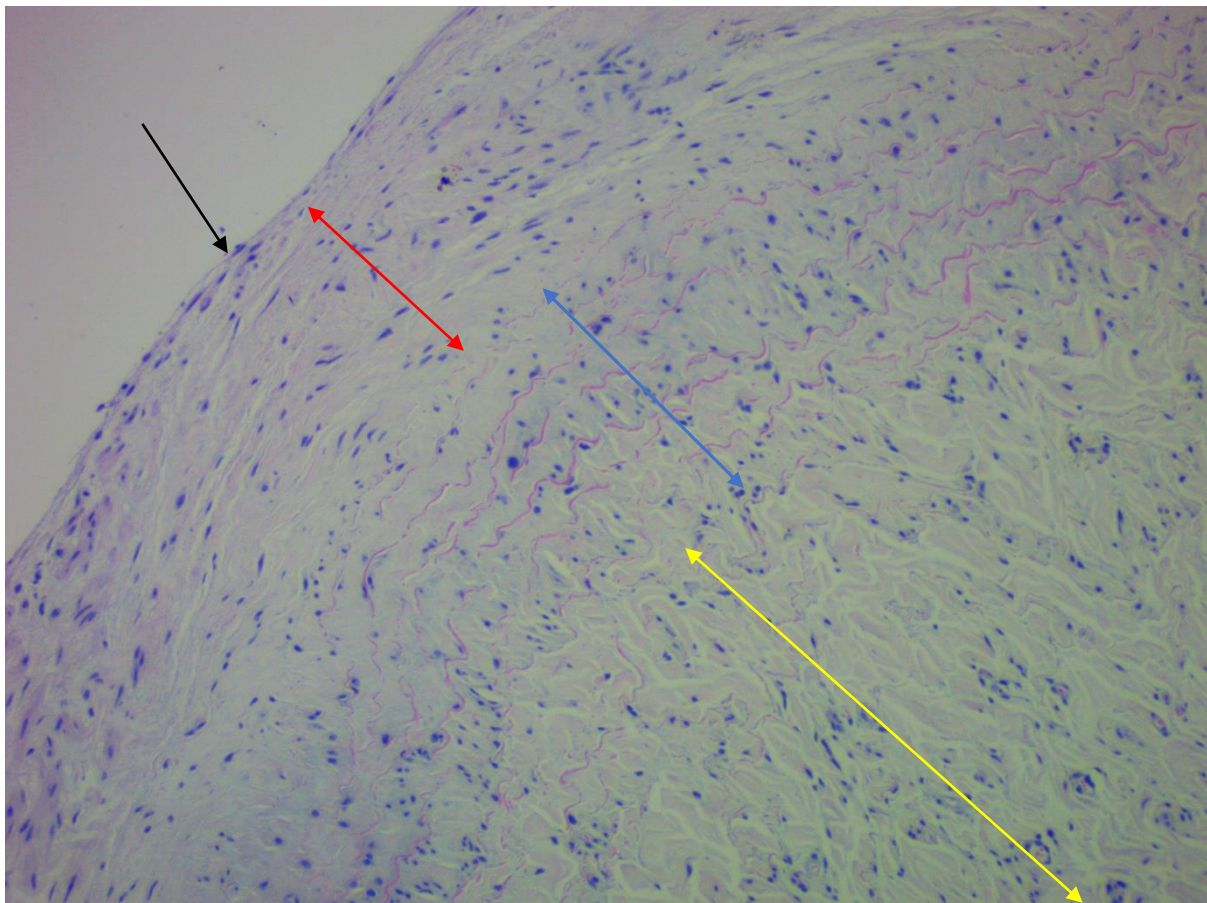
The vein leaflet is covered with endothelium which protects the leaflet against thrombus formation since normal vascular endothelial cells exhibit anticoagulant and antithrombotic properties (Underwood et al 1993). Intimal fibroplasia was seen in the vein leaflets but the intima was covered with endothelium (Fig 4.27). Potential areas for thrombus formation would be the suture lines and the Gore-Tex suture material and knots. In our study, all the early vein implants (0-3 days) showed focal areas of endothelial necrosis with overlying fibrin. These early endothelial changes are also seen when veins are transplanted as arterial grafts (Davies and Hagan 1995, Cavallari et al 1997, Kalra and Miller 2000). These areas could be potential sites of thrombus formation because the underlying collagen and smooth muscle cells are exposed. Twelve out of 17 vein implants implanted for longer than a month showed a normal endothelial lining, so it seems like the focal areas of necrosis recovered in the implants with time. The 5 implants that had areas of intimal necrosis after a month had an underlying cause such as infective endocarditis (SBE) (3 cases), a large hematoma between the vein layers (1 case), a hematoma and SBE (1 case) and a leaflet edge that was under severe tension from annular and left ventricular dilatation (1 case).

The sheep in this study did not receive any anticoagulation therapy after surgery and thrombo-embolic events were not observed postoperatively. No organised thrombi were observed on any of the valves at post mortem, but focal areas of fibrin were seen on 4 of the long term implants. The sheep's brain, spleen and kidneys were not examined for signs of distal emboli and infarcts.

If a human trial is done, it would be advisable to give anti-coagulation therapy for 3 months until the sutures endothelialize and the areas of focal necrosis heal. The European Society of Cardiology (ECS) and the European Society of Cardiothoracic Surgery (EACTS) recommend that patients with a bioprosthetic mitral valve or mitral valve repair receive 3 months anti-coagulation therapy after surgery (Vahanian and Lung 2012). The 2014 American Heart Association (AHA) and the American College of Cardiology (ACC) guideline for the management of patients with valvular heart disease also recommend 3 months anti-coagulation therapy after a bioprosthetic mitral valve replacement or mitral valve repair (Guyton et al 2014). These guidelines are based on studies that have shown the risk of thrombo-embolic events is highest in the first 3 months after all types of mitral valve surgery

with the highest incidence in the first month (2% at 30 days and 3% at 180 days). This data includes mechanical valves and the rate is generally lower for mitral valve repair and bioprosthetic valves. There are no randomized trials to show the safety of omitting warfarin in the first 3 months for mitral valve repair, but there is evidence from retrospective studies that show no difference in thrombo-embolic events after mitral valve repair or biological mitral valve replacement when patients are given Warfarin or only aspirin in the first 3 months (Colli et al 2010, Schwann et al 2013). Many centres do not adhere to the current guidelines and omit warfarin therapy in the first 3 months for mitral valve repair or biological mitral valve replacements in patients with sinus rhythm (Ruel et al 2004, Schwann et al 2013). Our own policy is to give aspirin to all mitral valve repairs and only warfarin without aspirin for those patients in atrial fibrillation. We do not give warfarin routinely to all mitral valve repairs in the first 3 months, but will weigh up the risk of thrombo-embolism, bleeding and the patients' socio-economic background, compliance and ability to manage warfarin therapy safely.

**Fig 4.27:** Histological section of sheep 5 (8.3 month implant) shows intimal fibroplasia (red arrow) with overlying endothelium (black arrow). The vein (blue arrow) and underlying fibrous stroma (yellow arrow) is also seen (H and E stain 100x).



One of the major benefits of an autologous vein as a mitral valve bioprosthesis would be the ability to omit long term anticoagulation therapy because of a low thrombo-embolic risk. The risk of thrombo-emboli should be no more than a mitral valve repair or a biological mitral valve prosthesis. Patients with rheumatic heart disease who need valve surgery are younger patients (under 40 years) and often live in poor socio-economic conditions where good control of warfarin therapy may not be available or easily accessible (Marijon et al 2007, Nkomo 2007). These patients would benefit most from a biological valve that does not need anticoagulation therapy and does not develop structural valve failure like current biological valves in young patients (Vongpatanasin et al 1996, Une et al 2014).

#### **4.6 Tissue response to the vein leaflet and Gore-Tex chordae and effect on blood elements.**

The vein leaflet is living autologous tissue and does not stimulate an immune response. The host sees the vein as its own tissue and incorporates it with a normal healing pattern.

Gore-Tex or expanded polytetrafluoroethylene (ePTFE) sutures are known to function well as artificial chordae for mitral valve repair with good long term function of up to 20 and 25 years (Salvato et al 2008, David et al 2013). Experimental work with ePTFE artificial chordae was started in the 1980's in search of a suitable material to replace elongated or ruptured chordae tendinae (Revuelta et al 1989, Zussa et al 1990).

Expanded polytetrafluoroethylene (ePTFE) or Gore-Tex is a thermoplastic polymer and has outstanding physical, chemical, mechanical and thermal properties. It is flexible, has high tensile strength, and shows resistance to fatigue (Bortolotti 2012). It is known to be resistant to degradation and has been used for many years as a biomaterial in vascular grafts and heart valves with good biocompatibility. (Williams 2008). Biocompatibility is the ability of a biomaterial to perform its desired function with respect to a medical therapy without eliciting any undesirable local or systemic effects in the recipient, but generating the most appropriate

beneficial cellular or tissue response in that specific situation (Williams 2008). Gore-Tex is not inert but elicits a foreign body tissue response with macrophage activation, foreign body giant cell production and fibrous tissue formation around the Gore-Tex (Fig 4.28) (Williams 2008). This reaction is beneficial to give strong, durable anchorage of the Gore-Tex sutures to the papillary muscle and the leaflet edge. The fibrous tissue that covers the Gore-Tex suture is covered with endothelium which prevents thrombus formation. (Fig 4.29) The fibrous tissue around the Gore-Tex shows an organised arrangement of the collagen fibres which run parallel to the suture and is in line with the mechanical strain that the chord endures (Fig 4.29). This arrangement mimics the collagen fibres in the native chordae tendinae and other load bearing organs such as ligaments, tendons, cartilage and bone where the load bearing fibrils are laid down in the path of the applied mechanical strain (Fenoglio et al 1972, Wang and Thampatty 2005, Flynn et al 2010). This helps to strengthen the Gore-Tex chord.

The initial experimental results using ePTFE sutures as artificial chordae in sheep and dogs in the 1980's showed that the microporous, nonabsorbable, monofilament suture healed well at the papillary muscle connection and at the anterior leaflet edge. The histology showed that the sutures were progressively and uniformly covered with fibrous tissue and a neointimal cellular sheath without signs of calcification up to 13 months of implantation (Revuelta et al 1989, Bortolotti et al 2012). These experimental results led to the clinical application of ePTFE sutures to repair elongated or ruptured chordae tendinae with good early and long term results (David et al 1989, Zussa et al 1990, Salvato et al 2008, David et al 2013). The sutures are durable in most cases, but there have been a few reported cases of calcification and rupture of ePTFE sutures from 6 to 14 years after implant (Butany et al 2004, Bortolotti et al 2012).

**Fig 4.28:** Histological section of Gore-Tex chordae of sheep 13 (H and E stain 200x) shows a foreign body reaction to Gore-Tex with macrophage activation, giant cell production, fibroblast activation and fibrosis.

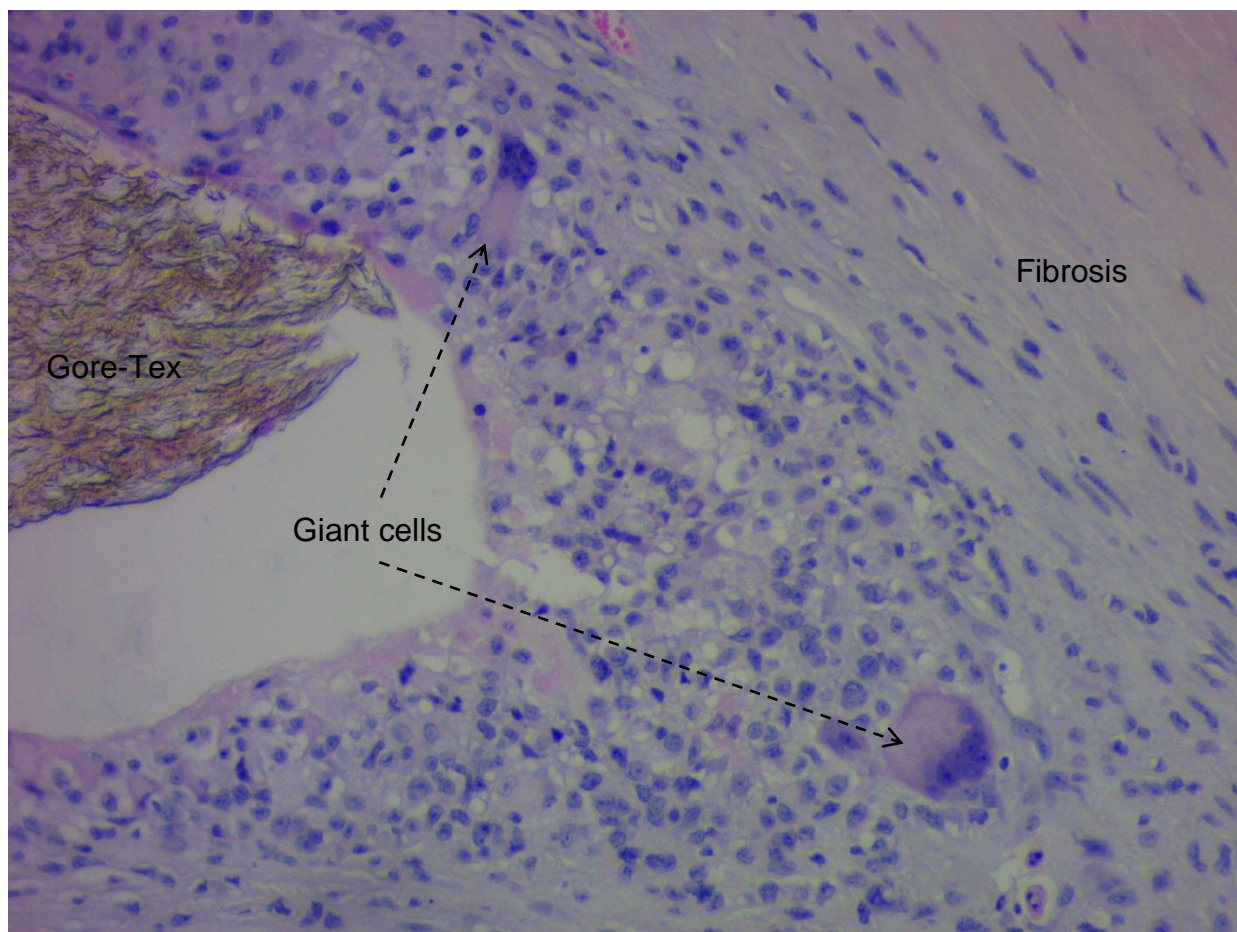
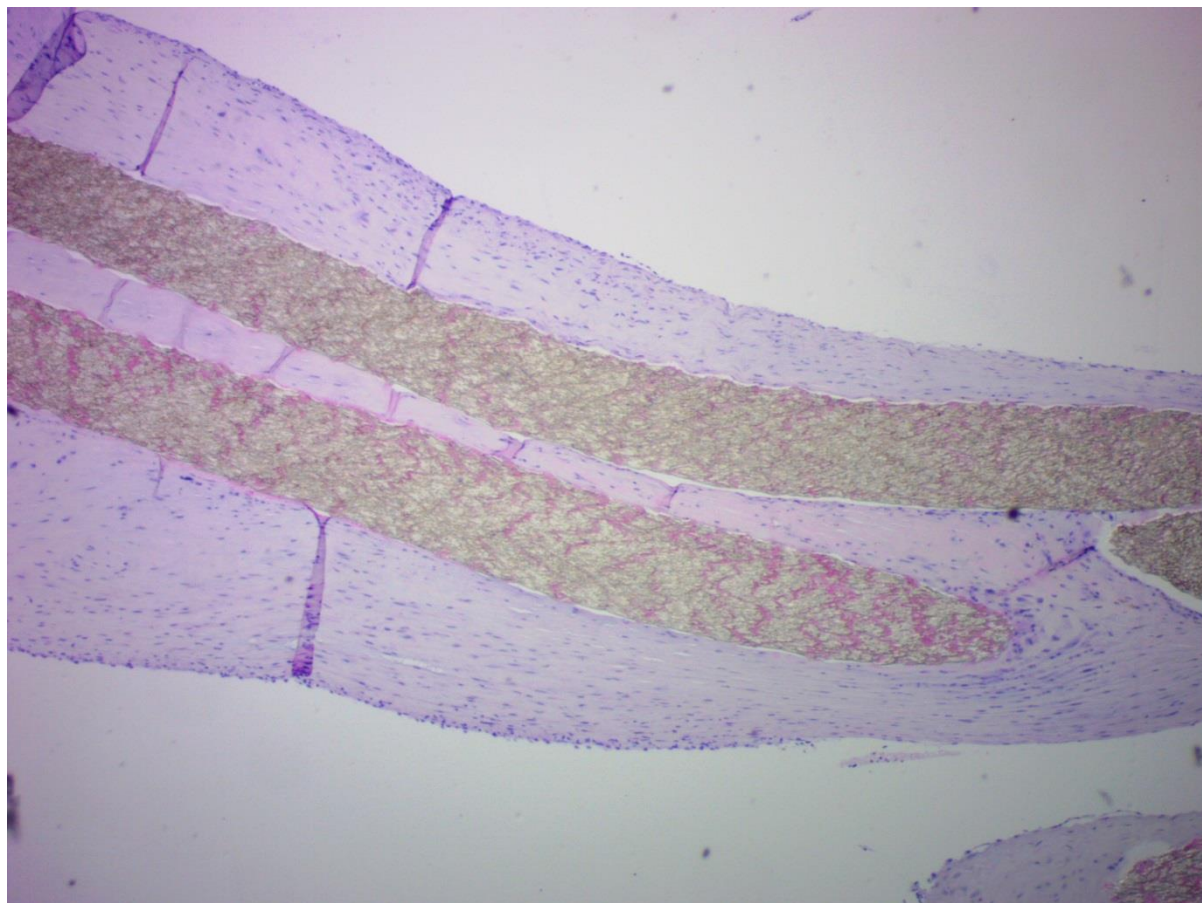




**Fig 4.29:** Histological section of Gore-Tex chordae of sheep 13 (H and E stain 40x) shows the endothelial covering of the fibrous tissue around the Gore-Tex chord. Note the arrangement of the collagen fibres which are parallel to the Gore-Tex chords and in line with the mechanical strain that the chord endures.



Seven implants showed areas of dystrophic calcification on and around the Gore-Tex sutures and chordae. The calcification was seen from as early as 4 months and calcification was also noticed in some of the vegetations in the valves with infective endocarditis. We were surprised to find dystrophic calcification in and around the Gore-Tex sutures in so many implants, because calcification was not described in the initial experiments with ePTFE artificial chordae in sheep and dogs for up to 13 months implantation (Revuelta et al 1989, Bortolotti 2012). We are unsure why some Gore-Tex chordae in our study showed none or very little calcification while others showed quite extensive calcification. One possible explanation is that thrombi, fibrin and infective vegetations attach to the Gore-Tex which then calcify. Devitalized cells and

cell remnants are important foci for calcification (Valente et al 1985, Tamura et al 1995, Flameng et al 2005, Schoen and Levy 2005). This theory is supported by the fact that in some specimens the calcification is seen more in areas of turbulence where high shear stress could cause platelet activation and aggregation which leads to fibrin and foci of cell debris on the chordae which then calcify (Fig 4.30).

This calcification is a concern for the longevity of the Gore-Tex sutures because it causes stiffening and rupture. Calcification of ePTFE vascular grafts have also been described and the presence of calcification was significantly related to the duration of the vascular implantation (Fig 4.31) (Metha et al 2011). Calcium deposits within the interstices of grafts can stiffen the graft and lead to fracture and graft failure.

**Fig 4.30:** Mitral valve of sheep 5 (8 months implant) shows a large defect at the medial commissure where mitral regurgitation would have caused a turbulent jet and high shear stress (black circle). There is also a perforation in the central suture line (red circle) which would have caused a turbulent jet through the perforation. Notice how the calcification (red arrows) is concentrated on the side of the mitral regurgitation at the A2 and A3 Gore-Tex chordae while A1 is relatively spared.

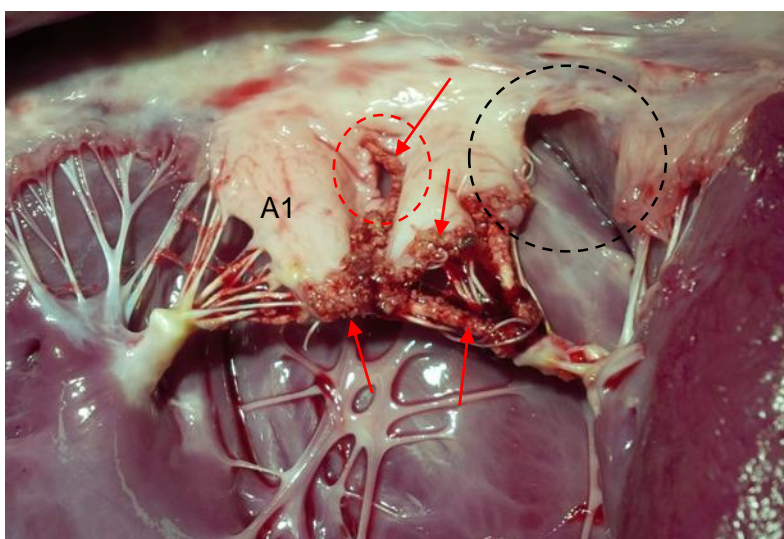
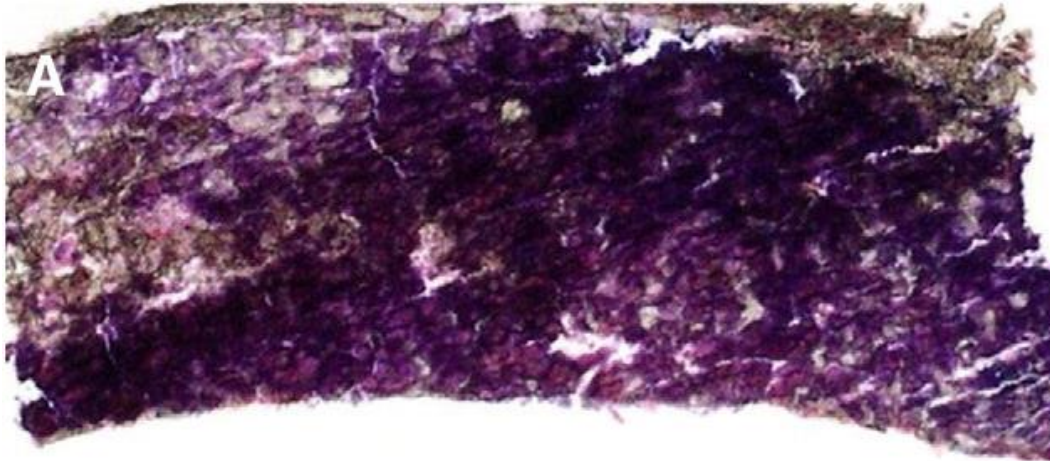


**Fig 4.31:** Calcification in an extended polytetrafluoroethylene (ePTFE) vascular graft (Metha 2011).



Mechanical valves are known to create turbulent flow with increased shear stress across the valves which can cause platelet activation and aggregation and hemolysis of red blood cells (Yoganathan et al 2005). The same increased fluid stresses can also cause damage to endothelial cells with exposure of extracellular matrix proteins which can lead to the adherence, activation and aggregation of platelets. Stented bioprosthetic valves are mildly stenotic compared to native valves because of stent restriction to leaflet opening, construction of the leaflets and stiffness of the fixed tissue (Yoganathan et al 2004). This also creates turbulent flow cross the valve with increased shear stress.

The flow across the vein leaflet was not turbulent on echocardiography and very similar to the native valve with a laminar diastolic flow pattern. Turbulence does occur with mitral regurgitation which was seen on echocardiography at the commissures. This turbulence causes high shear stress which can lead to focal areas of denuded endothelium and can become a source for the development of thrombo-emboli and infective vegetations. We did not notice denuded endothelium in the long term implants, but intimal fibroplasia on the vein leaflet and posterior native leaflets was seen, which may have been from increased shear stress from mitral regurgitation. Focal areas of fibrin was found in 4 of the long term implants (6 months) overlying the endothelium. These areas of fibrin and the infective endocarditis

which was seen in 4 cases may have been from increased shear stress from mitral regurgitation.

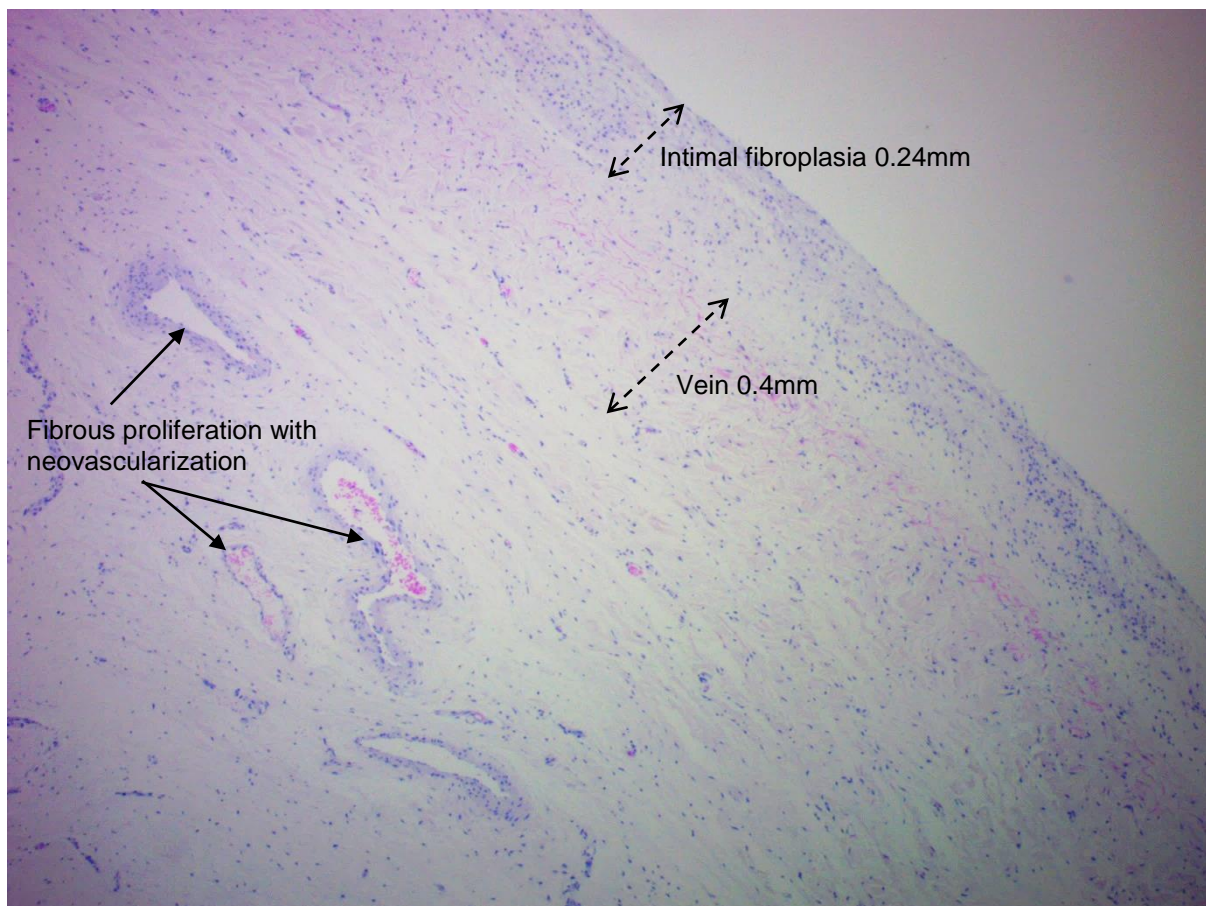
#### **4.7 Durability of the vein leaflet.**

It was encouraging to see how the vein leaflet adapted morphologically and functionally to its new surroundings in the heart as a mitral valve leaflet substitute. Focal areas of endothelial necrosis was noticed in all the early implants as is seen in veins that are used for arterial bypass grafts (Davies and Hagan 1995, Cavallari et al 1997, Kalra and Miller 2000). The later implants showed intimal fibroplasia with normal endothelial covering so it seems that the focal areas of endothelial necrosis heals with time. This was seen in 12 of the 17 implants after 1 month and is evidence that the vein leaflet remains a living viable tissue valve inside the heart that can repair itself and adapt. The intimal fibroplasia that was observed in the vein leaflets is also seen in veins when it is used as arterial bypass grafts (Spray and Roberts 1977). Intimal hyperplasia is also seen in pulmonary autograft leaflets with thickening of the leaflets when it is placed in the aortic and mitral position and it is an effect of adaptive remodelling from increased tensile and shear stress on the leaflets (Buch et al 1971, Schoof et al 2006). The thickening of the leaflets may enhance mechanical strength, but it influences valve function by restricting leaflet extensibility (Schoof et al 2006). The 5 vein implants that had focal areas of necrosis of the vein layers after 1 month either had SBE, a hematoma between the vein layers with pressure on the vein tissue or extreme tension on the leaflet edge from severe annular dilatation.

We chose to use a double layer of vein leaflet for 2 reasons: to ensure endothelium on both sides of the leaflet and to increase the strength of the leaflet. The jugular vein of the sheep is 0.3-0.6 mm thick and has a larger extension ratio than native mitral valve tissue (Wesly et al 1975, May-Newman and Yin 1995, Sacks et al 2006). Using a double layered vein leaflet improved the strength of the leaflet, but it created potential problems. The 2 vein layers were sutured together at the leaflet edges with Gore-Tex CV-8 and the space between the adventitial vein layers creates a potential space. In the early implants it was filled with fibrin and the space was later obliterated by fibrous proliferation and neovascularization. This fibrous proliferation caused significant thickening of the leaflets (2.25mm-6.5mm) and histologically the collagen fibres showed a random orientation in different directions, unlike the organised pattern in native mitral valve tissue. The reactive fibrous proliferation could be a response to

the abnormal forces on the vein leaflet in the heart since distortion of connective tissue is known to stimulate cellular replication and the synthesis of collagen (Buch et al 1971, Schoof et al 2006). These thickened leaflets were still flexible, but not as flexible as the original thin vein leaflets at implantation. The original vein layers were still clearly visible in the long term implants with preserved interstitial cells (myofibroblasts), collagen and elastic fibres (Fig 4.32).

**Fig 4.32:** Histological section of the vein implant in sheep 16 (6 month implant) shows the original vein between the intimal fibroplasia and underlying fibrous proliferation with neovascularization (H and E stain 40x). There are preserved interstitial cells (myofibroblasts), collagen and elastic fibres in the original vein wall.



Although the fibrous proliferation between the vein leaflets caused thickening of the leaflets, it did not cause shortening or shrinkage of the leaflets. The leaflet height was unchanged and although it was not possible to demonstrate growth in the valve, there was no shrinkage or contraction of the leaflet. This is different to the fibrous reaction that was observed with fresh autologous pericardium. When fresh autologous pericardium was used as a heart valve leaflet and was subjected to the hemodynamic forces in the heart, the pericardium contracted and formed scar tissue. This was most likely mediated by pericardial cells that were stimulated by the abnormal forces on the pericardial substrate with very complex bending, compressive stresses and shear stress (Fabiani 1995, Vesely 2003). This experience with autologous pericardium demonstrated that the interstitial cells respond unpredictably when it is subjected to new or abnormal loading conditions (Vesely et al 2003). The scarring problem was solved by treating the autologous pericardium with glutaraldehyde, but this made the pericardium an acellular structure which degenerates with time (Fabiani 1995, Vesely et al 2003, Al Halees et al 2004).

Hematoma formation was seen between the vein layers in 4 implants and this caused vein necrosis in 3 implants because of increased pressure between the vein layers. This is another potential problem of the double layered vein. Blood can enter the potential space between the leaflets, either at the suture line around the edges or through a vein branch opening that is not completely closed. We tried to avoid this complication by suturing the free edges and the vein branches carefully. It may be better to use the vein as a single layer to avoid the complications of the potential space between the layers. The saphenous vein wall is twice as thick as the jugular vein and may be strong enough to be used as a single layer to shape a leaflet (Fig 4.13). This will avoid hematoma formation between the layers and may also prevent the excessive fibrous proliferation between the leaflets that caused the leaflet thickening. If the vein is used as one layer, the endothelium will only be covering the leaflet on the intimal side, leaving the adventitial side uncovered, but with time an endothelial layer should form over the adventitia. Further investigation is needed to see if a saphenous vein can be used as a single layer and if the adventitial layer will remodel and endothelialize. The suture retention of saphenous vein must also be tested and compared to that of the mitral valve leaflet to see if it will be able to hold Gore-Tex sutures for chordae on the leaflet edge (Konig et al 2009).

The central suture line healed well in 17 of the 21 sheep and is evidence that the vein leaflet is viable and has the ability to repair itself. One implant showed a perforation in the proximal central suture line and one implant showed small defects in the central suture line. Two of the specimens showed tearing of the distal central suture line and 7 implants showed tearing of a primary Gore-Tex chord from the leaflet edge of which 3 had infective endocarditis as a cause. It is difficult to attribute the ruptured Gore-Tex chordae from the leaflet edge purely to poor suture retention of the vein tissue, because most of the Gore-Tex chordae healed well to the leaflet edge and did not tear out. Many of the Gore-Tex chordae that pulled loose from the leaflet edge could be the result of extreme tension on the valve leaflet from annular dilatation and decreased coaptation which increased tension on the primary chordae. An annuloplasty ring and secondary chordae may prevent this extreme tension on the leaflet edge as discussed.

The sheep model is a good model to test calcification of a bioprosthetic heart valve, because of the accelerated rate of calcification that is seen in the juvenile sheep model (Schoen et al 1994, Ozaki et al 2004, Flameng et al 2005). Calcification is more common in younger age and more pronounced in areas of increased mechanical stress and strain with the highest calcium concentrations shown in the cusps of mitral valve implants where the mechanical stress is higher than in the aortic or pulmonary position (Flameng et al 2005). The amount of calcification seen in a bioprosthesis implanted in a sheep for 3 months correlates well with the amount of calcification seen in a bioprosthesis implanted in an elderly person for 10 years (Ozaki et al 2004). In this study calcification was seen around the Gore-Tex chordae and sutures from 4 months after implantation.

Calcification was only seen in 4 vein leaflets and this calcification was only seen around Gore-Tex sutures while the rest of the leaflets were free from calcification. This is encouraging, because it means that the vein leaflet is viable and able to manage calcium transport and prevent it from accumulating in the cell membranes and forming hydroxyl apatite (calcium phosphate) crystals. The living vein is also able to prevent the spread of calcification, presumably by secreting inhibitors of apatite crystal growth. Fibroblasts have been shown to inhibit the calcification of bone cells when cultured in the same dish in vitro (Ogiso et al 1991).

Histological evidence for the vein's viability is seen from the normal endothelium and preserved myofibroblasts and connective tissue in the vein leaflets with preservation of the

original vein layers. The myofibroblasts possess characteristics similar to the valvular interstitial cells found in native heart valves (Filip et al. 1986, Della Rocca et al 2000). The absence of calcification in the vein leaflet demonstrates that the vein leaflet is able to regulate calcium transport and mineral deposition for up to 10 months. These results show that autologous venous tissue should last for at least 10 years in a human heart without significant calcification if the accelerated calcification in the sheep model can be extrapolated to humans (Ozaki et al 2004).

The calcification that was seen in this study around the Gore-Tex sutures and the Gore-Tex chordae is a concern, because this may limit the durability of the valve and lead to Gore-Tex rupture. Other biological materials such as autologous pericardium and xenopericardium have failed to perform as chordae tendinae (Bortolotti et al 2012). Fascia lata performed poorly as a valve leaflet substitute with early failure and will not be a good option to use as chordae tendinae (Ionescu and Ross 1969, Silver et al 1975). Tissue engineering of chordae could create chordae that had comparable extensibility, but had 10 times more stiffness and the failure strength was 10 times less than normal chordae (Shi and Vesely 2004). There is currently no ideal substitute for the unique structure and function of native chordae tendinae with its central core of tightly packed collagen, surrounded by elastic fibres and covered with an endocardial cell lining (Fenoglio et al 1972). Gore-Tex chordae is the best substitute we have at present with good long term results and durability in mitral valve repair (Salvato et al 2008, David et al 2013).



## 5. Conclusion:

The purpose of this study was to evaluate whether an autologous vein graft can be used to replace an anterior mitral valve leaflet.

The first question was whether it is technically possible to create a functioning mitral valve leaflet from autologous vein supported by Gore-Tex chordae. This study showed that it was possible to create a functioning valve leaflet with trace to mild mitral regurgitation (MR) in 14 out of 21 sheep. This figure could be improved by ensuring accurate Gore-Tex chordal length of the primary chordae to avoid prolapse or tethering of segments of the vein leaflet. The coaptation length between the vein leaflet and the posterior leaflet can be increased with better valve closure by adding secondary chordal support with Gore-Tex chordae and by adding a ring annuloplasty. This should improve the commissural MR that was found in many of the valves. It is important to create a valve that is competent with a large surface of coaptation to ensure long term function. Mild to moderate MR can progress with time and cause annular and left ventricular dilatation. One of the reasons for increased MR with time, was that the mitral annular-papillary continuity was lost when we cut the secondary chordae and removed the native anterior mitral valve leaflet. A ring annuloplasty and secondary Gore-Tex chordae will support the annulus and restore annular papillary continuity and make the insertion of the valve more reproducible and durable.

A double layer of jugular vein was used to increase the leaflet strength and to ensure an endothelial covering on both sides of the leaflet. The double layer made insertion of the valve more difficult with more suture lines on the edge and it created a potential space between the leaflets where a hematoma could form. This was seen in 4 cases with necrosis of the vein layer overlying the hematoma in 3 cases. The fibrous proliferation with neovascularization that was seen between the 2 vein layers caused significant thickening in the vein leaflet, but the leaflet remained flexible. A human saphenous vein has a wall thickness which is twice as much as the jugular vein wall and may be strong enough to use as a single layer when used as a vein leaflet in humans. This will simplify implantation and avoid the potential space between the 2 vein layers. It is uncertain how the adventitial layer will remodel and endothelialize and whether the fibrous proliferation and thickening will be less when used as a single layer. The suture retention of a saphenous vein will have to be tested and compared to the anterior mitral valve leaflet to see if a single layer saphenous vein could hold the Gore-Tex chordae on the

leaflet edge. It may be necessary to support the edge with an extra strip of vein tissue or vein pledget where the chordae are implanted.

The second question was whether the vein will be able to withstand the stress and strain of deformation when used as a valve leaflet and maintain its flexibility. The vein leaflet has a larger extension ratio than mitral valve tissue and stretches more under pressure. This was seen with the amount of billowing of the leaflet on echocardiography. The amount of billowing was not exclusively from increased vein tissue elasticity, but also because the vein leaflet was not supported by secondary chordae like the native anterior mitral valve leaflet. The vein leaflet developed intimal fibroplasia and fibrous proliferation between the 2 adventitial layers as a response to the increased stress upon the tissue. This caused leaflet thickening, but the vein remained flexible up to 10 months on echocardiography without leaflet shortening or contracture. The suture retention and healing of the Gore-Tex chordae to the leaflet edge was good in most cases and when some of the Gore-Tex chordae pulled out from the leaflet edge (7 cases), there was an underlying cause such as infective endocarditis or excessive tension from annular dilatation and poor coaptation. The progression of mitral regurgitation (MR) that was found in the sheep is a concern, but is most likely from technical reasons such as lack of mitral annular support, lack of secondary chordae and poor coaptation than from primary vein tissue failure. Further studies with mitral annular support and secondary chordae should clarify whether the progressive MR was from technical failure or vein tissue failure.

The third question was whether a vein will remain viable in the intracardiac environment when used as a valve leaflet and be able to adapt and grow. The histological results showed that the vein leaflets had focal areas of endothelial and media necrosis in the early implants, while the older implants showed viable endothelium and the underlying vein layers clearly showed viability with myofibroblasts, collagen and elastin. This, with the healing pattern seen in the suture lines and lack of calcification in the leaflet, is evidence that the vein leaflet remains viable with the ability to repair itself and to morphologically adapt.

Some of the Gore-Tex chordae showed calcification in 7 specimens from as early as 4 months which was a surprising finding, because other studies found no calcification of Gore-Tex chordae in sheep for up to 13 months (Revuelta et al 1989, Bortolotti 2012). One possibility for this could be regurgitant flow causing increased shear stress with platelet activation and aggregation on the Gore-Tex which create foci which can calcify. This calcification can lead to

chord rupture and valve failure and is a concern for valve durability. Gore-Tex chordae is the best substitute for chordae tendinae that is currently available with good long term results of up to 25 years in human mitral valve repairs (Salvato et al 2008, David et al 2013).

The autologous vein supported by Gore-Tex chordae fulfil many of the criteria of the ideal valve prosthesis. It is a living valve that remains viable and functional for up to 10 months in a sheep model and showed the ability to morphologically adapt. There was a normal healing pattern between the vein leaflet and the annulus and no calcification was seen in the vein leaflets apart from the calcification around Gore-Tex sutures in some specimens. Growth potential was not shown, but there was no shrinkage of the leaflet as is seen with autologous pericardium and the leaflet retains flexibility and the ability to deform. Anticoagulation is not necessary in the long term, since it is a biological valve with a viable endothelial layer. Diastolic flow across the valve is laminar and mimics the native mitral valve. Less turbulence means lower shear stress and less damage to endothelium and blood elements.

It was encouraging to see some of the mitral valves functioning well with only mild MR for up to 10 months. There were late valve failures in this study, but many of these failures could be a result of an imperfect technique during replacement and not because of tissue failure from the vein. The ideal valve should be easily implantable and reproducible and the insertion of the vein leaflet does not satisfy these criteria yet. Before one can embark on a clinical study to replace the mitral valve with autologous vein tissue, it will be necessary to refine and standardize the technical aspects to ensure that a competent valve is created each time that will be durable and reproducible. An annuloplasty ring and secondary Gore-Tex chordae will support the vein leaflets by creating a larger surface of coaptation and will result in better long term valve function.

Other possible clinical applications for autologous vein could be for a patch repair of a valve leaflet perforation. It might also be useful for leaflet extension of the posterior or anterior mitral valve leaflet for rheumatic valves or ischaemic mitral regurgitation where autologous pericardium is currently used (Zegdi et al 2007, De Varennes et al 2009). In the aortic valve it could also be used for leaflet extension for congenital or rheumatic aortic valves where pericardium is currently used (Grinda et al 2002, Alsoufi et al 2006). The vein is autologous living tissue and should perform better than autologous pericardium or xenograft pericardium.

Autologous vein may also be useful to create a monocusp valve during a Tetralogy of Fallot repair when a transannular patch is needed. Currently bovine pericardium, Gore-Tex membrane or porcine intestinal submucosa (CorMatrix®) is used for valvuloplasty but it is prone to early degeneration and progressive regurgitation (Bacha 2014, Turrentine et al 2002). Autologous vein should do very well in the pulmonary circulation because of the lower pressure. A drawback of using autologous vein is the extra leg incision if the saphenous vein is harvested and in a child the upper leg vein will need to be used. This will have to be discussed with the patient's family and needs to be done in a clinical trial. Unfortunately in many cases it is not known beforehand whether a patch will be necessary and harvesting of a vein while on bypass is not always practical.

Apart from mitral valve replacement, vein tissue could also be used to replace the aortic or pulmonary valves. These valves have a smaller surface area and enough vein can be harvested to create 3 semilunar leaflets. By using templates to cut out 3 semilunar valve leaflets from the vein, it would be possible to suture these leaflets to the aortic or pulmonary annulus, almost like a stentless valve. The aortic valve closes with diastolic pressure which is less than the systolic pressure that the mitral valve has to face. The feasibility of these techniques will have to be tested in large animal studies.

This study demonstrated that autologous vein has the potential to be used as a valve leaflet substitute, because it remained viable in the intracardiac position for up to 10 months and was able to withstand the stress and deformation of a valve leaflet. Histologically it showed the ability to heal and to morphologically adapt to the new environment.

## 6. References

- Adams, D. H., & Anyanwu, A. C. (2009). Valve Disease: Asymptomatic Mitral Regurgitation: Does Surgery Save Lives? *Nature Reviews Cardiology*, 6(5), 330-332.
- Adams, D. H., Rosenhek, R., & Falk, V. (2010). Degenerative Mitral Valve Regurgitation: Best Practice Revolution. *European Heart Journal*, 31(16), 1958-1966.
- Aicher, D., Kuniyara, T., Abou Issa, O., Brittner, B., Graber, S., & Schafers, H. J. (2011). Valve Configuration Determines Long-Term Results After Repair of the Bicuspid Aortic Valve. *Circulation*, 123(2), 178-185.
- Ali, M., Kumar, S., Bjornstad, K., & Duran, C. (1996). The Sheep as an Animal Model for Heart Valve Research. *Cardiovascular Surgery*, 4(4), 543-549.
- Alsoufi, B., Karamlou, T., Bradley, T., Williams, W. G., Van Arsdell, G. S., Coles, J. G., et al. (2006). Short and Midterm Results of Aortic Valve Cusp Extension in the Treatment of Children with Congenital Aortic Valve Disease. *The Annals of Thoracic Surgery*, 82(4), 1292-1300.
- Angelini, A., Ho, S. Y., Anderson, R. H., Davies, M. J., & Becker, A. E. (1988). A Histological Study of the Atrioventricular Junction in Hearts with Normal and Prolapsed Leaflets of the Mitral Valve. *British Heart Journal*, 59(6), 712-716.
- Anyanwu, A. C., & Adams, D. H. (2007). Etiologic classification of degenerative mitral valve disease: Barlow's disease and fibroelastic deficiency. *Seminars in Thoracic and Cardiovascular Surgery*, 19(2) 90-96.
- Aupart, M. R., Mirza, A., Meurisse, Y. A., Sirinelli, A. L., Neville, P. H., & Marchand, M. A. (2006). Perimount Pericardial Bioprosthesis for Aortic Calcified Stenosis: 18-Year Experience with 1133 Patients. *The Journal of Heart Valve Disease*, 15(6), 768-75; discussion 775-6.
- Avierinos, J. F., Gersh, B. J., Melton, L. J., 3rd, Bailey, K. R., Shub, C., Nishimura, R. A., et al. (2002). Natural History of Asymptomatic Mitral Valve Prolapse in the Community. *Circulation*, 106(11), 1355-1361.

- Bacha, E. (2014). Valve-Sparing Options in Tetralogy of Fallot Surgery. *Operative Techniques in Thoracic and Cardiovascular Surgery*, 18(4), 316-327.
- Barnard, B., le Roux, P., van Wyk, H. (2010). Mitral Valve Replacement at Tygerberg Hospital: A 5 Year Follow-Up. *SA Heart Journal*, 7(1), 30-37.
- Baudet, E. M., Puel, V., McBride, J. T., Grimaud, J., Roques, F., Clerc, F., et al. (1995). Long-Term Results of Valve Replacement with the St. Jude Medical Prosthesis. *The Journal of Thoracic and Cardiovascular Surgery*, 109(5), 858-870.
- Bjoerk, V. O., & Hultquist, G. (1964). Teflon and Pericardial Aortic Valve Prostheses. *The Journal of Thoracic and Cardiovascular Surgery*, 47, 693-701.
- Bokros, J. C. (1989). Carbon in Prosthetic Heart Valves. *The Annals of Thoracic Surgery*, 48(3), S49-S50.
- Bortolotti, U., Milano, A. D., & Frater, R. W. (2012). Mitral Valve Repair with Artificial Chordae: A Review of its History, Technical Details, Long-Term Results, and Pathology. *The Annals of Thoracic Surgery*, 93(2), 684-691.
- Bouten, C., Dankers, P., Driessen-Mol, A., Pedron, S., Brizard, A., & Baaijens, F. (2011). Substrates for Cardiovascular Tissue Engineering. *Advanced Drug Delivery Reviews*, 63(4), 221-241.
- Brais, M. P., & Braunwald, N. S. (1974). Tissue Acceptance of Materials Implanted within the Circulatory System. *Archives of Surgery*, 109(3), 351-358.
- Braunwald, N. S., Cooper, T., & Morrow, A. G. (1960). Complete Replacement of the Mitral Valve. Successful Clinical Application of a Flexible Polyurethane Prosthesis. *The Journal of Thoracic and Cardiovascular Surgery*, 40, 1-11.
- Braunwald, N. S., & Morrow, A. G. (1968). Tissue Ingrowth and the Rigid Heart Valve. Review of Clinical and Experimental Experience during the Past Year. *The Journal of Thoracic and Cardiovascular Surgery*, 56(3), 307-322.
- Brody, W. R., Angeli, W. W., & Kosek, J. C. (1972). Histologic Fate of the Venous Coronary Artery Bypass in Dogs. *The American Journal of Pathology*, 66(1), 111-130.

- Buch, W. S., Kosek, J. C., & Angell, W. W. (1971). The Role of Rejection and Mechanical Trauma on Valve Graft Viability. *The Journal of Thoracic and Cardiovascular Surgery*, 62(5), 696-706.
- Bull, B., & Braunwald, N. S. (1971). Human Histopathologic Response to a Completely Fabric-Covered Prosthetic Heart Valve. *Annals of Surgery*, 174(5), 755-761.
- Burdon, T. A., Miller, D. C., Oyer, P. E., Mitchell, R. S., Stinson, E. B., Starnes, V. A., & Shumway, N. E. (1992). Durability of Porcine Valves at Fifteen Years in a Representative North American Patient Population. *The Journal of Thoracic and Cardiovascular Surgery*, 103(2), 238-51; discussion 251-2.
- Butany, J., Collins, M. J., & David, T. E. (2004). Ruptured Synthetic Expanded Polytetrafluoroethylene Chordae Tendinae. *Cardiovascular Pathology*, 13(3), 182-184.
- Butcher, J. T., Mahler, G. J., & Hockaday, L. A. (2011). Aortic Valve Disease and Treatment: The Need for Naturally Engineered Solutions. *Advanced Drug Delivery Reviews*, 63(4), 242-268.
- Cagli, K. (2010). A Simple Method of Making Artificial Chordal Loops for Mitral Valve Repair. *The Annals of Thoracic Surgery*, 89(2), e12-e14.
- Carapetis, J. R., McDonald, M., & Wilson, N. J. (2005). Acute Rheumatic Fever. *The Lancet*, 366(9480), 155-168.
- Carapetis, J. R., Steer, A. C., Mulholland, E. K., & Weber, M. (2005). The Global Burden of Group A Streptococcal Diseases. *The Lancet Infectious Diseases*, 5(11), 685-694.
- Carpentier, A. (1989). From Valvular Xenograft to Valvular Bioprosthesis: 1965–1970. *The Annals of Thoracic Surgery*, 48(3), S73-S74.
- Carpentier, A. F., Lessana, A., Relland, J. Y., Belli, E., Mihaileanu, S., Berrebi, A. J., et al. (1995). The “physio-Ring”: An Advanced Concept in Mitral Valve Annuloplasty. *The Annals of Thoracic Surgery*, 60(5), 1177-1186.
- Carpentier, A., Adams, D. H., & Filsoufi, F. (2010). Carpentier's reconstructive valve surgery Chapter 5 Surgical anatomy and Physiology. (pp. 27). Missouri: Saunders Elsevier.

- Carpentier, A. (1983). Cardiac Valve Surgery--the "French Correction". *The Journal of Thoracic and Cardiovascular Surgery*, 86(3), 323-337.
- Carpentier, A., Lemaigre, G., Robert, L., Carpentier, S., & Dubost, C. (1969). Biological Factors Affecting Long-Term Results of Valvular Heterografts. *The Journal of Thoracic and Cardiovascular Surgery*, 58(4), 467-483.
- Carpentier, A., Nashef, A., Carpentier, S., Ahmed, A., & Goussef, N. (1984). Techniques for Prevention of Calcification of Valvular Bioprostheses. *Circulation*, 70(3 Pt 2), 1165-8.
- Castillo, J. G., Anyanwu, A. C., Fuster, V., & Adams, D. H. (2012). A Near 100% Repair Rate for Mitral Valve Prolapse is Achievable in a Reference Center: Implications for Future Guidelines. *The Journal of Thoracic and Cardiovascular Surgery*, 144(2), 308-312.
- Cavallari, N., Abebe, W., Mingoli, A., Sapienza, P., Hunter, W. J., Agrawal, D. K., et al. (1997). Short-Term Preservation of Autogenous Vein Grafts: Effectiveness of University of Wisconsin Solution. *Surgery*, 121(1), 64-71.
- Choudhary, S. K., Dhareshwar, J., Govil, A., Airan, B., & Kumar, A. S. (2003). Open Mitral Commissurotomy in the Current Era: Indications, Technique, and Results. *The Annals of Thoracic Surgery*, 75(1), 41-46.
- Christian, A. J., Lin, H., Alferiev, I. S., Connolly, J. M., Ferrari, G., Hazen, S. L., et al. (2014). The Susceptibility of Bioprosthetic Heart Valve Leaflets to Oxidation. *Biomaterials*, 35(7), 2097-2102.
- Cochran, R., & Kunzelman, K. S. (1991). Comparison of Viscoelastic Properties of Suture Versus Porcine Mitral Valve Chordae Tendineae. *Journal of Cardiac Surgery*, 6(4), 508-513.
- Colli, A., D'Amico, R., Mestres, C. A., Pomar, J. L., Cámara, M., Ruyra, X., & Mulet, J. (2010). Is Early Antithrombotic Therapy Necessary After Tissue Mitral Valve Replacement. *J Heart Valve Dis*, 19(4), 405-411.
- Cox, J. L., Chiasson, D. A., & Gotlieb, A. I. (1991). Stranger in a Strange Land: The Pathogenesis of Saphenous Vein Graft Stenosis with Emphasis on Structural and Functional Differences between Veins and Arteries. *Progress in Cardiovascular Diseases*, 34(1), 45-68.



- Dahm, M., Husmann, M., Mayer, E., Prüfer, D., Groh, E., & Oelert, H. (1995). Relevance of Immunologic Reactions for Tissue Failure of Bioprosthetic Heart Valves. *The Annals of Thoracic Surgery*, 60, S348-S352.
- David, T. E. (1989). Replacement of Chordae Tendineae with Expanded Polytetrafluoroethylene Sutures. *Journal of Cardiac Surgery*, 4(4), 286-290.
- David, T. E. (1994). Papillary Muscle-Annular Continuity: Is it Important? *Journal of Cardiac Surgery*, 9(s2), 252-254.
- David, T. E. (2004). Artificial chordae. *Seminars in Thoracic and Cardiovascular Surgery*, 16(2) 161-168.
- David, T. E., & Armstrong, S. (2010). Aortic Cusp Repair with Gore-Tex Sutures during Aortic valve-sparing Operations. *The Journal of Thoracic and Cardiovascular Surgery*, 139(5), 1340-1342.
- David, T.E., Armstrong, S., & Ivanov, J. (2013). Chordal Replacement with Polytetrafluoroethylene Sutures for Mitral Valve Repair: A 25-Year Experience. *The Journal of Thoracic and Cardiovascular Surgery*, 145(6), 1563-1569.
- David, T. E., Ivanov, J., Armstrong, S., Christie, D., & Rakowski, H. (2005). A Comparison of Outcomes of Mitral Valve Repair for Degenerative Disease with Posterior, Anterior, and Bileaflet Prolapse. *The Journal of Thoracic and Cardiovascular Surgery*, 130(5), 1242-1249.
- David, T. E., Ivanov, J., Armstrong, S., & Rakowski, H. (2003). Late Outcomes of Mitral Valve Repair for Floppy Valves: Implications for Asymptomatic Patients. *The Journal of Thoracic and Cardiovascular Surgery*, 125(5), 1143-1152.
- David, T. E., Omran, A., Ivanov, J., Armstrong, S., de Sa, M. P., Sonnenberg, B., & Webb, G. (2000). Dilation of the Pulmonary Autograft After the Ross Procedure. *The Journal of Thoracic and Cardiovascular Surgery*, 119(2), 210-220.
- David, T. E. (2009). Ross Procedure at the Crossroads. *Circulation*, 119(2), 207-209.
- Davies, M. G., & Hagen, P. (1994). Influence of Perioperative Storage Solutions on Long-Term Vein Graft Function and Morphology. *Annals of Vascular Surgery*, 8(2), 150-157.

- Davies, M. G., & Hagen, P. (1995). Pathophysiology of Vein Graft Failure: A Review. *European Journal of Vascular and Endovascular Surgery*, 9(1), 7-18.
- Davila, J. C. (1989). Where is the Ideal Heart Valve Substitute? What has Frustrated its Realization? *The Annals of Thoracic Surgery*, 48(3), S20-S23.
- De Varennes, B., Chaturvedi, R., Sidhu, S., Cote, A. V., Shan, W. L., Goyer, C., et al. (2009). Initial Results of Posterior Leaflet Extension for Severe Type IIIb Ischemic Mitral Regurgitation. *Circulation*, 119(21), 2837-2843.
- De Visscher, G., Blockx, H., Meuris, B., Van Oosterwyck, H., Verbeken, E., Herregods, M., & Flameng, W. (2008). Functional and Biomechanical Evaluation of a Completely Recellularized Stentless Pulmonary Bioprosthesis in Sheep. *The Journal of Thoracic and Cardiovascular Surgery*, 135(2), 395-404.
- Delahaye, J. P., Gare, J. P., Viguier, E., Delahaye, F., De Gevigney, G., & Milon, H. (1991). Natural History of Severe Mitral Regurgitation. *European Heart Journal*, 12 Suppl B, 5-9.
- Della Rocca, F., Sartore, S., Guidolin, D., Bertiplaglia, B., Gerosa, G., Casarotto, D., & Pualetto, P. (2000). Cell Composition of the Human Pulmonary Valve: A Comparative Study with the Aortic valve—the VESALIO\* Project. *The Annals of Thoracic Surgery*, 70(5), 1594-1600.
- Denny, F. W. (1987). T. Duckett Jones and Rheumatic Fever in 1986. T. Duckett Jones Memorial Lecture. *Circulation*, 76(5), 963-970.
- DiBardino, D. J., ElBardissi, A. W., McClure, R. S., Razo-Vasquez, O. A., Kelly, N. E., & Cohn, L. H. (2010). Four Decades of Experience with Mitral Valve Repair: Analysis of Differential Indications, Technical Evolution, and Long-Term Outcome. *The Journal of Thoracic and Cardiovascular Surgery*, 139(1), 76-84.
- Dreyfus, G. D., Bahrami, T., Alayle, N., Mihealainu, S., Dubois, C., & De Lentdecker, P. (2001). Repair of Anterior Leaflet Prolapse by Papillary Muscle Repositioning: A New Surgical Option. *The Annals of Thoracic Surgery*, 71(5), 1464-1470.
- Du Plessis, L. A., & Marchand, P. (1964). The Anatomy of the Mitral Valve and its Associated Structures. *Thorax*, 19(3), 221-227.

- Duan, B., Hockaday, L. A., Kang, K. H., & Butcher, J. T. (2013). 3D Bioprinting of Heterogeneous Aortic Valve Conduits with alginate/gelatin Hydrogels. *Journal of Biomedical Materials Research Part A*, 101(5), 1255-1264.
- Edmunds, L. H., Clark, R. E., Cohn, L. H., Miller, D. C., & Weisel, R. D. (1988). Guidelines for Reporting Morbidity and Mortality After Cardiac Valvular Operations. *The Annals of Thoracic Surgery*, 46(3), 257-259.
- El Khoury, G., & Vohra, H. A. (2012). Polytetrafluoroethylene Leaflet Extensions for Aortic Valve Repair. *European Journal of Cardio-Thoracic Surgery : Official Journal of the European Association for Cardio-Thoracic Surgery*, 41(6), 1258-1259.
- Elkins, R. C., Thompson, D. M., Lane, M. M., Elkins, C. C., & Peyton, M. D. (2008). Ross Operation: 16-Year Experience. *The Journal of Thoracic and Cardiovascular Surgery*, 136(3), 623-630. e5.
- Epstein, F. H., Gibbons, G. H., & Dzau, V. J. (1994). The Emerging Concept of Vascular Remodeling. *New England Journal of Medicine*, 330(20), 1431-1438.
- Fabiani, J., Dreyfus, G. D., Marchand, M., Jourdan, J., Aupard, M., Latrémouille, C., et al (1995). The Autologous Tissue Cardiac Valve: A New Paradigm for Heart Valve Replacement. *The Annals of Thoracic Surgery*, 60, S189-S194.
- Fawzy, M. E. (2009). Long-Term Results Up to 19 Years of Mitral Balloon Valvuloplasty. *Asian Cardiovascular and Thoracic Annals*, 17(6), 627-633.
- Fenoglio, J. J., Pham, T. D., Wit, A. L., Bassett, A. L., & Wagner, B. M. (1972). Canine Mitral Complex: Ultrastructure and Electromechanical Properties. *Circulation Research*, 31(3), 417-430.
- Ferrans, V. J., Spray, T. L., Billingham, M. E., & Roberts, W. C. (1978). Structural Changes in Glutaraldehyde-Treated Porcine Heterografts used as Substitute Cardiac Valves: Transmission and Scanning Electron Microscopic Observations in 12 Patients. *The American Journal of Cardiology*, 41(7), 1159-1184.
- Filip, D., Radu, A., & Simionescu, M. (1986). Interstitial Cells of the Heart Valves Possess Characteristics Similar to Smooth Muscle Cells. *Circulation Research*, 59(3), 310-320.

- Filsoufi, F., & Carpentier, A. (2007). Principles of reconstructive surgery in degenerative mitral valve disease. *Seminars in Thoracic and Cardiovascular Surgery*, 19(2) 103-110.
- Flameng, W., Meuris, B., Yperman, J., De Visscher, G., Herijgers, P., & Verbeken, E. (2006). Factors Influencing Calcification of Cardiac Bioprostheses in Adolescent Sheep. *The Journal of Thoracic and Cardiovascular Surgery*, 132(1), 89-98.
- Flanagan, T. C., & Pandit, A. (2003). Living Artificial Heart Valve Alternatives: A Review. *Eur Cell Mater*, 6(1), 28-45.
- Flynn, B. P., Bhole, A. P., Saeidi, N., Liles, M., Dimarzio, C. A., & Ruberti, J. W. (2010). Mechanical Strain Stabilizes Reconstituted Collagen Fibrils Against Enzymatic Degradation by Mammalian Collagenase Matrix Metalloproteinase 8 (MMP-8). *PLoS One*, 5(8), e12337.
- Fourie, P., Vos, P., & Abiola, S. (2009). The Influence of Supplementary Light on Dorper Lambs Fed Intensively. *South African Journal of Animal Science*, 39(5), 211-214.
- Frater, R. W., Gong, G., Hoffman, D., & Liao, K. (1992). Endothelial Covering of Biological Artificial Heart Valves. *The Annals of Thoracic Surgery*, 53(3), 371-372.
- Freed, L. A., Levy, D., Levine, R. A., Larson, M. G., Evans, J. C., Fuller, D. L., et al. (1999). Prevalence and Clinical Outcome of Mitral-Valve Prolapse. *New England Journal of Medicine*, 341(1), 1-7.
- Frink, R., & Merrick, B. (1974). The Sheep Heart: Coronary and Conduction System Anatomy with Special Reference to the Presence of an Os Cordis. *The Anatomical Record*, 179(2), 189-199.
- Furlong, B., Henderson, A., Lewis, M., & Smith, J. (1987). Endothelium-derived Relaxing Factor Inhibits in Vitro Platelet Aggregation. *British Journal of Pharmacology*, 90(4), 687-692.
- Gao, G., Wu, Y., Grunkemeier, G. L., Furnary, A. P., & Starr, A. (2004). Durability of Pericardial Versus Porcine Aortic Valves. *Journal of the American College of Cardiology*, 44(2), 384-388.
- Giachelli, C. M. (1999). Ectopic Calcification: Gathering Hard Facts about Soft Tissue Mineralization. *The American Journal of Pathology*, 154(3), 671-675.

- Giddens, D. P., Yoganathan, A. P., & Schoen, F. J. (1993). Prosthetic Cardiac Valves. *Cardiovascular Pathology*, 2(3), 167-177.
- Gillinov, A. M., & Cosgrove, D. M. (2004). Chordal transfer for repair of anterior leaflet prolapse. *Seminars in Thoracic and Cardiovascular Surgery*, 16(2) 169-173.
- Gillinov, A. M., Cosgrove, D. M., Blackstone, E. H., Diaz, R., Arnold, J. H., Lytle, B. W., et al. (1998). Durability of Mitral Valve Repair for Degenerative Disease. *The Journal of Thoracic and Cardiovascular Surgery*, 116(5), 734-743.
- Gillinov, A. M., Mihaljevic, T., Blackstone, E. H., George, K., Svensson, L. G., Nowicki, E. R., et al. (2010). Should Patients with Severe Degenerative Mitral Regurgitation Delay Surgery Until Symptoms Develop? *The Annals of Thoracic Surgery*, 90(2), 481-488.
- Gillinov, A. M., Shortt, K. G., & Cosgrove, D. M. (2005). Commissural Closure for Repair of Mitral Commissural Prolapse. *The Annals of Thoracic Surgery*, 80(3), 1135-1136.
- Glasson, J. R., Komeda, M., Daughters, G. T., Niczyporuk, M. A., Bolger, A. F., Ingels, N. B., & Miller, D. C. (1996). Three-Dimensional Regional Dynamics of the Normal Mitral Anulus during Left Ventricular Ejection. *The Journal of Thoracic and Cardiovascular Surgery*, 111(3), 574-585.
- Gogoladze, G., Dellis, S. L., Donnino, R., Ribakove, G., Greenhouse, D. G., Galloway, A., & Grossi, E. (2010). Analysis of the Mitral Coaptation Zone in Normal and Functional Regurgitant Valves. *The Annals of Thoracic Surgery*, 89(4), 1158-1161.
- Golbasi, I., Tasatargil, A., Aksoy, N. H., Sadan, G., Karasu, E., Turkay, C., & Bayezid, O. (2005). A Functional and Histopathological Comparison. *Texas Heart Institute Journal*, 32(3)
- Gough, J. E., Scotchford, C. A., & Downes, S. (2002). Cytotoxicity of Glutaraldehyde Crosslinked collagen/poly (Vinyl Alcohol) Films is by the Mechanism of Apoptosis. *Journal of Biomedical Materials Research*, 61(1), 121-130.
- Green, G. R., Dagum, P., Glasson, J. R., Nistal, J. F., Daughters, G. T., Ingels, N. B., & Miller, D. C. (1999). Restricted Posterior Leaflet Motion After Mitral Ring Annuloplasty. *The Annals of Thoracic Surgery*, 68(6), 2100-2106.

- Grinda, J., Latremouille, C., Berrebi, A. J., Zegdi, R., Chauvaud, S., Carpentier, A. F., et al. (2002). Aortic Cusp Extension Valvuloplasty for Rheumatic Aortic Valve Disease: Midterm Results. *The Annals of Thoracic Surgery*, 74(2), 438-443.
- Gross, L., & Kugel, M. (1931). Topographic Anatomy and Histology of the Valves in the Human Heart. *The American Journal of Pathology*, 7(5), 445.
- Gross, R. I., Cunningham Jr, J. N., Snively, S. L., Catinella, F. P., Nathan, I. M., Adams, P. X., & Spencer, F. C. (1981). Long-Term Results of Open Radical Mitral Commissurotomy: Ten Year Follow-Up Study of 202 Patients. *The American Journal of Cardiology*, 47(4), 821-825.
- Grunkemeier, G. L., Li, H., Naftel, D. C., Starr, A., & Rahimtoola, S. H. (2000). Long-Term Performance of Heart Valve Prostheses. *Current Problems in Cardiology*, 25(2), 78-154.
- Gundry, S. R., Jones, M., Ishihara, T., & Ferrans, V. J. (1980). Optimal Preparation Techniques for Human Saphenous Vein Grafts. *Surgery*, 88(6), 785-794.
- Guyton, R. A., Sundt III, T. M., Albert, N. M., Hochman, F. J. S., Bozkurt, F. B., Kovacs, F. R. J., et al. (2014). 2014 AHA/ACC Guideline for the Management of Patients with Valvular Heart Disease. *Circulation*, 129, 000-000.
- Harken, D. E. (1989). Heart Valves: Ten Commandments and Still Counting. *The Annals of Thoracic Surgery*, 48(3), S18-S19.
- Harrison, D. C., Ibrahim, M. A., Weyman, A. E., Kuller, L. H., Blot, W. J., & Miller, D. E. (2013). The Björk-Shiley Convexo-Concave Heart Valve Experience from the Perspective of the Supervisory Panel. *The American Journal of Cardiology*, 112(12), 1921-1931.
- Hickey, M. S., Blackstone, E. H., Kirklin, J. W., & Dean, L. S. (1991). Outcome Probabilities and Life History After Surgical Mitral Commissurotomy: Implications for Balloon Commissurotomy. *Journal of the American College of Cardiology*, 17(1), 29-42.
- Hinderer, S., Seifert, J., Votteler, M., Shen, N., Rheinlaender, J., Schäffer, T. E., & Schenke-Layland, K. (2014). Engineering of a Bio-Functionalized Hybrid Off-the-Shelf Heart Valve. *Biomaterials*, 35(7), 2130-2139.
- Hinton, R. B., & Yutzey, K. E. (2011). Heart Valve Structure and Function in Development and Disease. *Annual Review of Physiology*, 73, 29-46.

- Ho, S. (2002). Anatomy of the Mitral Valve. *Heart*, 88(suppl 4), iv5-iv10.
- Hopkins, R. (2007). Cardiac surgeon's primer: Tissue-engineered cardiac valves. *Seminars in Thoracic and Cardiovascular Surgery: Pediatric Cardiac Surgery Annual*, 10(1), 125-135.
- Human, P., & Zilla, P. (2001). Characterization of the Immune Response to Valve Bioprostheses and its Role in Primary Tissue Failure. *The Annals of Thoracic Surgery*, 71(5), S385-S388.
- Ibrahim, M., Rao, C., & Athanasiou, T. (2012). Artificial Chordae for Degenerative Mitral Valve Disease: Critical Analysis of Current Techniques. *Interactive Cardiovascular and Thoracic Surgery*, 15(6), 1019-1032.
- Ionescu, M., & Ross, D. (1969). Heart-Valve Replacement with Autologous Fascia Lata. *The Lancet*, 294(7616), 335-338.
- lung, B., & Vahanian, A. (2011). Epidemiology of Valvular Heart Disease in the Adult. *Nature Reviews Cardiology*, 8(3), 162-172.
- Janson, J. T. (2013). Mitral valve repair: The Stellenbosch experience. *Cardio Thoracic Surgery—Quo Vadis: Biennial Conference of the Society of Cardiothoracic Surgeons of South Africa*, Durban.
- Jansson, K., Bengtsson, L., Swedenborg, J., & Haegerstrand, A. (2001). In Vitro Endothelialization of Bioprosthetic Heart Valves Provides a Cell Monolayer with Proliferative Capacities and Resistance to Pulsatile Flow. *The Journal of Thoracic and Cardiovascular Surgery*, 121(1), 108-115.
- Jayakrishnan, A., & Jameela, S. (1996). Glutaraldehyde as a Fixative in Bioprostheses and Drug Delivery Matrices. *Biomaterials*, 17(5), 471-484.
- Jimenez, J. H., Liou, S. W., Padala, M., He, Z., Sacks, M., Gorman, R. C., et al. (2007). A Saddle-Shaped Annulus Reduces Systolic Strain on the Central Region of the Mitral Valve Anterior Leaflet. *The Journal of Thoracic and Cardiovascular Surgery*, 134(6), 1562-1568.
- Jimenez, J. H., Soerensen, D. D., He, Z., Ritchie, J., & Yoganathan, A. P. (2005). Mitral Valve Function and Chordal Force Distribution using a Flexible Annulus Model: An in Vitro Study. *Annals of Biomedical Engineering*, 33(5), 557-566.

- Johnson, C. M., Hanson, M. N., & Helgeson, S. C. (1987). Porcine Cardiac Valvular Subendothelial Cells in Culture: Cell Isolation and Growth Characteristics. *Journal of Molecular and Cellular Cardiology*, 19(12), 1185-1193.
- Jones, M., Conkle, D. M., Ferrans, V. J., Roberts, W. C., Levine, F. H., Melvin, D. B., & Stinson, E. B. (1973). Lesions Observed in Arterial Autogenous Vein Grafts Light and Electron Microscopic Evaluation. *Circulation*, 48(1S3), III-198-III-210.
- Joudinaud, T. M., Kegel, C. L., Flecher, E. M., Weber, P. A., Lansac, E., Hvass, U., & Duran, C. M. (2007). The Papillary Muscles as Shock Absorbers of the Mitral Valve Complex. An Experimental Study. *European Journal of Cardio-Thoracic Surgery* 32(1), 96-101.
- Kabbani, S., Jamil, H., Nabhani, F., Hamoud, A., Katan, K., Sabbagh, N., et al. (2007). Analysis of 92 Mitral Pulmonary Autograft Replacement (Ross II) Operations. *The Journal of Thoracic and Cardiovascular Surgery*, 134(4), 902-908.
- Kalra, M., & Miller, V. M. (2000). Early Remodeling of Saphenous Vein Grafts: Proliferation, Migration and Apoptosis of Adventitial and Medial Cells Occur Simultaneously with Changes in Graft Diameter and Blood Flow. *Journal of Vascular Research*, 37(6), 576-584.
- Kilner, P. J., Yang, G., Wilkes, A. J., Mohiaddin, R. H., Firmin, D. N., & Yacoub, M. H. (2000). Asymmetric Redirection of Flow through the Heart. *Nature*, 404(6779), 759-761.
- Kim, K. M., Herrera, G. A., & Battarbee, H. D. (1999). Role of Glutaraldehyde in Calcification of Porcine Aortic Valve Fibroblasts. *The American Journal of Pathology*, 154(3), 843-852.
- Kim, W. Y., Bisgaard, T., Nielsen, S. L., Poulsen, J. K., Pedersen, E. M., Hasenkam, J. M., et al. . (1994). Two-Dimensional Mitral Flow Velocity Profiles in Pig Models using Epicardial Doppler Echocardiography. *Journal of the American College of Cardiology*, 24(2), 532-545.
- Kim, J. B., Kim, H. J., Moon, D. H., Jung, S. H., Choo, S. J., Chung, C. H., et al. (2010). Long-Term Outcomes After Surgery for Rheumatic Mitral Valve Disease: Valve Repair Versus Mechanical Valve Replacement. *European Journal of Cardio-Thoracic Surgery*, 37(5), 1039-1046.



- Komoda, T., Hetzer, R., Oellinger, J., Siniawski, H., Hofmeister, J., HÜBLER, M., . . . Maeta, H. (1997). The Relationship between the Mitral Annulus and Left Ventricular Outflow Tract. *ASAIO Journal*, 43(6), 932-936.
- Konig, G., McAllister, T. N., Dusserre, N., Garrido, S. A., Iyican, C., Marini, A., . . . Zagalski, K. (2009). Mechanical Properties of Completely Autologous Human Tissue Engineered Blood Vessels Compared to Human Saphenous Vein and Mammary Artery. *Biomaterials*, 30(8), 1542-1550.
- Kouchoukos, N. T., Masetti, P., Nickerson, N. J., Castner, C. F., Shannon, W. D., & Dávila-Román, V. G. (2004). The Ross Procedure: Long-Term Clinical and Echocardiographic Follow-Up. *The Annals of Thoracic Surgery*, 78(3), 773-781.
- Kouzi-Koliakos, K., Kanellaki-Kyparissi, M., Marinov, G., Knyazhev, V., Tsalie, E., Batzios, C., & Kovachev, D. (2006). Prebypass Histological and Ultrastructural Evaluation of the Long Saphenous Vein as a Predictor of Early Graft Failure. *Cardiovascular Pathology*, 15(6), 336-346.
- Kumar, A. S., Choudhary, S. K., Mathur, A., Saxena, A., Roy, R., & Chopra, P. (2000). Homograft Mitral Valve Replacement: Five Years' Results. *The Journal of Thoracic and Cardiovascular Surgery*, 120(3), 450-458.
- Kumar, A. S., Rao, P. N., & Saxena, A. (1995). Results of Mitral Valve Reconstruction in Children with Rheumatic Heart Disease. *The Annals of Thoracic Surgery*, 60(4), 1044-1047.
- Kunzelman, K. S., Cochran, R. P., Murphree, S. S., Ring, W. S., Verrier, E. D., & Eberhart, R. C. (1993). Differential Collagen Distribution in the Mitral Valve and its Influence on Biomechanical Behaviour. *The Journal of Heart Valve Disease*, 2(2), 236-244.
- Kunzelman, K., Reimink, M., & Cochran, R. (1997). Annular Dilatation Increases Stress in the Mitral Valve and Delays Coaptation: A Finite Element Computer Model. *Vascular*, 5(4), 427-434.
- Lam, J. H., Ranganathan, N., Wigle, E. D., & Silver, M. D. (1970). Morphology of the Human Mitral Valve. I. Chordae Tendineae: A New Classification. *Circulation*, 41(3), 449-458.

- Langer, F., Kuniyama, T., Hell, K., Schramm, R., Schmidt, K. I., Aicher, D., et al. (2009). RING+STRING: Successful Repair Technique for Ischemic Mitral Regurgitation with Severe Leaflet Tethering. *Circulation*, *120*(11 Suppl), S85-91.
- Lansac, E., Lim, K. H., Shomura, Y., Goetz, W. A., Lim, H. S., Rice, N. T., et al. (2002). Dynamic Balance of the Aortomitral Junction. *The Journal of Thoracic and Cardiovascular Surgery*, *123*(5), 911-918.
- Lawrence, J. G., Carapetis, J. R., Griffiths, K., Edwards, K., & Condon, J. R. (2013). Acute Rheumatic Fever and Rheumatic Heart Disease: Incidence and Progression in the Northern Territory of Australia 1997-2010. *Circulation*, *128*(5), 492-501.
- Lawrie, G. M., Earle, E. A., & Earle, N. (2011). Intermediate-Term Results of a Nonresectional Dynamic Repair Technique in 662 Patients with Mitral Valve Prolapse and Mitral Regurgitation. *The Journal of Thoracic and Cardiovascular Surgery*, *141*(2), 368-376.
- Lehner, G., Fischlein, T., Baretton, G., Murphy, J. G., & Reichart, B. (1997). Endothelialized Biological Heart Valve Prostheses in the Non-Human Primate Model. *European Journal of Cardio-Thoracic Surgery*, *11*(3), 498-504.
- Liao, J., Joyce, E. M., & Sacks, M. S. (2008). Effects of Decellularization on the Mechanical and Structural Properties of the Porcine Aortic Valve Leaflet. *Biomaterials*, *29*(8), 1065-1074.
- Liao, J., & Vesely, I. (2004). Relationship between Collagen Fibrils, Glycosaminoglycans, and Stress Relaxation in Mitral Valve Chordae Tendineae. *Annals of Biomedical Engineering*, *32*(7), 977-983.
- Liao, J., Yang, L., Grashow, J., & Sacks, M. S. (2007). The Relation between Collagen Fibril Kinematics and Mechanical Properties in the Mitral Valve Anterior Leaflet. *Journal of Biomechanical Engineering*, *129*(1), 78-87.
- Lis, Y., Burleigh, M., Parker, D., Child, A., Hogg, J., & Davies, M. (1987). Biochemical Characterization of Individual Normal, Floppy and Rheumatic Human Mitral Valves. *Biochem.J*, *244*, 597-603.
- Liu, A. C., Joag, V. R., & Gotlieb, A. I. (2007). The Emerging Role of Valve Interstitial Cell Phenotypes in Regulating Heart Valve Pathobiology. *The American Journal of Pathology*, *171*(5), 1407-1418.

- Liu, X., Han, L., Song, Z., Tan, M., Gong, D., & Xu, Z. (2013). Aortic Valve Replacement with Autologous Pericardium: Long-Term Follow-Up of 15 Patients and in Vivo Histopathological Changes of Autologous Pericardium. *Interactive Cardiovascular and Thoracic Surgery*, 16(2), 123-128.
- LoGerfo, F. W., Quist, W. C., Cantelmo, N. L., & Haudenschild, C. C. (1983). Integrity of Vein Grafts as a Function of Initial Intimal and Medial Preservation. *Circulation*, 68(3 Pt 2), II117-24.
- Longnecker, C. R., & Lim, M. J. (2011). Prosthetic Heart Valves. *Cardiology Clinics*, 29(2), 229-236.
- Love, J. W. (1998). Autologous Pericardial Reconstruction of Semilunar Valves. *The Journal of Heart Valve Disease*, 7(1), 40-47.
- Lower, R. R., Stofer, R. C., & Shumway, N. E. (1960). Autotransplantation of the Pulmonic Valve into the Aorta. *The Journal of Thoracic and Cardiovascular Surgery*, 39, 680-687.
- Magne, J., Mathieu, P., Dumesnil, J. G., Tanne, D., Dagenais, F., Doyle, D., & Pibarot, P. (2007). Impact of Prosthesis-Patient Mismatch on Survival After Mitral Valve Replacement. *Circulation*, 115(11), 1417-1425.
- Manji, R. A., Zhu, L. F., Nijjar, N. K., Rayner, D. C., Korbitt, G. S., Churchill, T. A., et al. (2006). Glutaraldehyde-Fixed Bioprosthetic Heart Valve Conduits Calcify and Fail from Xenograft Rejection. *Circulation*, 114(4), 318-327.
- Marijon, E., Ou, P., Celermajer, D. S., Ferreira, B., Mocumbi, A. O., Jani, D., et al. (2007). Prevalence of Rheumatic Heart Disease Detected by Echocardiographic Screening. *New England Journal of Medicine*, 357(5), 470-476.
- Markl, M., Kilner, P. J., & Ebbers, T. (2011). Comprehensive 4D Velocity Mapping of the Heart and Great Vessels by Cardiovascular Magnetic Resonance. *J Cardiovasc Magn Reson*, 13(7), 10.1186.
- Marron, K., Yacoub, M. H., Polak, J. M., Sheppard, M. N., Fagan, D., Whitehead, B. F., et al. (1996). Innervation of Human Atrioventricular and Arterial Valves. *Circulation*, 94(3), 368-375.

- Martinez, R., Fierro, C. A., Shireman, P. K., & Han, H. (2010). Mechanical Buckling of Veins Under Internal Pressure. *Annals of Biomedical Engineering*, 38(4), 1345-1353.
- Matsuki, O., Robles, A., Gibbs, S., Bodnar, E., & Ross, D. N. (1988). Long-Term Performance of 555 Aortic Homografts in the Aortic Position. *The Annals of Thoracic Surgery*, 46(2), 187-191.
- May-Newman, K., & Yin, F. (1998). A Constitutive Law for Mitral Valve Tissue. *Journal of Biomechanical Engineering*, 120(1), 38-47.
- McCarthy, K. P., Ring, L., & Rana, B. S. (2010). Anatomy of the Mitral Valve: Understanding the Mitral Valve Complex in Mitral Regurgitation. *European Journal of Echocardiography*, 11(10), i3-i9.
- Mehta, R. I., Mukherjee, A. K., Patterson, T. D., & Fishbein, M. C. (2011). Pathology of Explanted Polytetrafluoroethylene Vascular Grafts. *Cardiovascular Pathology*, 20(4), 213-221.
- Misfeld, M., & Sievers, H. (2007). Heart Valve Macro-and Microstructure. *Philosophical Transactions of the Royal Society B: Biological Sciences*, 362(1484), 1421-1436.
- Mitchell, R. N., Jonas, R. A., & Schoen, F. J. (1995). Structure-Function Correlations in Cryopreserved Allograft Cardiac Valves. *The Annals of Thoracic Surgery*, 60, S108-S113.
- Mulholland, D. L., & Gotlieb, A. I. (1997). Cardiac Valve Interstitial Cells: Regulator of Valve Structure and Function. *Cardiovascular Pathology*, 6(3), 167-174.
- Muresian, H. (2009). The Clinical Anatomy of the Mitral Valve. *Clinical Anatomy*, 22(1), 85-98.
- National Institutes of Health. (1985). *Guide for the care and use of laboratory animals*. National Academies.
- Netter, F. H. (2010). *Atlas of human anatomy* (5th edition) Elsevier Health Sciences.
- Nielsen, S. L., Lomholt, M., Johansen, P., Hansen, S. B., Andersen, N. T., & Hasenkam, J. M. (2011). Mitral Ring Annuloplasty Relieves Tension of the Secondary but Not Primary Chordae Tendineae in the Anterior Mitral Leaflet. *The Journal of Thoracic and Cardiovascular Surgery*, 141(3), 732-737.

- Nielsen, S. L., Timek, T. A., Green, G. R., Dagum, P., Daughters, G. T., Hasenkam, J. M., et al. (2003). Influence of Anterior Mitral Leaflet Second-Order Chordae Tendineae on Left Ventricular Systolic Function. *Circulation*, *108*(4), 486-491.
- Nkomo, V. T., Gardin, J. M., Skelton, T. N., Gottdiener, J. S., Scott, C. G., & Enriquez-Sarano, M. (2006). Burden of Valvular Heart Diseases: A Population-Based Study. *The Lancet*, *368*(9540), 1005-1011.
- Nkomo, V. T. (2007). Epidemiology and Prevention of Valvular Heart Diseases and Infective Endocarditis in Africa. *Heart (British Cardiac Society)*, *93*(12), 1510-1519.
- O'Brien, J. E., Shi, Y., Fard, A., Bauer, T., Zalewski, A., & Mannion, J. D. (1997). Wound Healing Around and within Saphenous Vein Bypass Grafts. *The Journal of Thoracic and Cardiovascular Surgery*, *114*(1), 38-45.
- Ogiso, B., Hughes, F. J., Melcher, A. H., & McCulloch, C. A. (1991). Fibroblasts Inhibit Mineralised Bone Nodule Formation by Rat Bone Marrow Stromal Cells in Vitro. *Journal of Cellular Physiology*, *146*(3), 442-450.
- Oh, J. K., Appleton, C. P., Hatle, L. K., Nishimura, R. A., Seward, J. B., & Tajik, A. J. (1997). The Noninvasive Assessment of Left Ventricular Diastolic Function with Two-Dimensional and Doppler Echocardiography. *Journal of the American Society of Echocardiography*, *10*(3), 246-270.
- Okita, Y., Miki, S., Ueda, Y., Tahata, T., & Sakai, T. (1995). Left Ventricular Function After Mitral Valve Replacement with Or without Chordal Preservation. *The Journal of Heart Valve Disease*, *4 Suppl 2*, S181-92.
- Olesen, K. H. (1962). The Natural History of 271 Patients with Mitral Stenosis Under Medical Treatment. *British Heart Journal*, *24*, 349-357.
- Ormiston, J. A., Shah, P. M., Tei, C., & Wong, M. (1981). Size and Motion of the Mitral Valve Annulus in Man. I. A Two-Dimensional Echocardiographic Method and Findings in Normal Subjects. *Circulation*, *64*(1), 113-120.
- Owens, C. D. (2010). Adaptive Changes in Autogenous Vein Grafts for Arterial Reconstruction: Clinical Implications. *Journal of Vascular Surgery*, *51*(3), 736-746.

- Ozaki, S., Herijgers, P., & Flameng, W. (2004). A New Model to Test the Calcification Characteristics of Bioprosthetic Heart Valves. *Annals of Thoracic and Cardiovascular Surgery*, 10(1), 23-28.
- Padala, M., Gyoneva, L., & Yoganathan, A. P. (2012). Effect of Anterior Strut Chordal Transection on the Force Distribution on the Marginal Chordae of the Mitral Valve. *The Journal of Thoracic and Cardiovascular Surgery*, 144(3), 624-633.
- Perier, P., Hohenberger, W., Lakew, F., Batz, G., Urbanski, P., Zacher, M., et al. (2008). Toward a New Paradigm for the Reconstruction of Posterior Leaflet Prolapse: Midterm Results of the “respect rather than Resect” Approach. *The Annals of Thoracic Surgery*, 86(3), 718-725.
- Price, J., De Kerchove, L., Glineur, D., Vanoverschelde, J., Noirhomme, P., & El Khoury, G. (2013). Risk of Valve-Related Events After Aortic Valve Repair. *The Annals of Thoracic Surgery*, 95(2), 606-613.
- Rabbah, J. M., Saikrishnan, N., Siefert, A. W., Santhanakrishnan, A., & Yoganathan, A. P. (2013). Mechanics of Healthy and Functionally Diseased Mitral Valves: A Critical Review. *Journal of Biomechanical Engineering*, 135(2), 021007.
- Radomski, M., Palmer, R., & Moncada, S. (1987). Endogenous Nitric Oxide Inhibits Human Platelet Adhesion to Vascular Endothelium. *The Lancet*, 330(8567), 1057-1058.
- Rapaport, E. (1975). Natural History of Aortic and Mitral Valve Disease. *The American Journal of Cardiology*, 35(2), 221-227.
- Reul, H., & Talukder, N. (1981). Fluid Mechanics of the Natural Mitral Valve. *Journal of Biomechanics*, 14(5), 361-372.
- Revuelta, J. M., Garcia-Rinaldi, R., Gaité, L., Val, F., & Garijo, F. (1989). Generation of Chordae Tendineae with Polytetrafluoroethylene Stents. Results of Mitral Valve Chordal Replacement in Sheep. *The Journal of Thoracic and Cardiovascular Surgery*, 97(1), 98-103.
- Robertson, K. A., Volmink, J. A., & Mayosi, B. M. (2006). Towards a Uniform Plan for the Control of Rheumatic Fever and Rheumatic Heart Disease in Africa-the Awareness Surveillance Advocacy Prevention (ASAP) Programme. *South African Medical Journal*, 96(3), 241.

- Rosenfeldt, F. L., He, G., Buxton, B. F., & Angus, J. A. (1999). Pharmacology of Coronary Artery Bypass Grafts. *The Annals of Thoracic Surgery*, 67(3), 878-888.
- Ross, D. (1967). Replacement of Aortic and Mitral Valves with a Pulmonary Autograft. *The Lancet*, 290(7523), 956-958.
- Ross, D. N., & Kabbani, S. (1997). Mitral Valve Replacement with a Pulmonary Autograft: The Mitral Top Hat. *The Journal of Heart Valve Disease*, 6(5), 542-545.
- Ruel, M., Masters, R. G., Rubens, F. D., Bédard, P. J., Pipe, A. L., Goldstein, W. G., et al. (2004). Late Incidence and Determinants of Stroke After Aortic and Mitral Valve Replacement. *The Annals of Thoracic Surgery*, 78(1), 77-83.
- Sacks, M. S., David Merryman, W., & Schmidt, D. E. (2009). On the Biomechanics of Heart Valve Function. *Journal of Biomechanics*, 42(12), 1804-1824.
- Sacks, M. S., Enomoto, Y., Graybill, J. R., Merryman, W. D., Zeeshan, A., Yoganathan, A. P., et al. (2006). In-Vivo Dynamic Deformation of the Mitral Valve Anterior Leaflet. *The Annals of Thoracic Surgery*, 82(4), 1369-1377.
- Sacks, M. S., Schoen, F. J., & Mayer Jr, J. E. (2009). Bioengineering Challenges for Heart Valve Tissue Engineering. *Annual Review of Biomedical Engineering*, 11, 289-313.
- Sacks, M. S., & Yoganathan, A. P. (2007). Heart Valve Function: A Biomechanical Perspective. *Philosophical Transactions of the Royal Society of London. Series B, Biological Sciences*, 362(1484), 1369-1391.
- Salgo, I. S., Gorman, J. H., Gorman, R. C., Jackson, B. M., Bowen, F. W., Plappert, T., et al. (2002). Effect of Annular Shape on Leaflet Curvature in Reducing Mitral Leaflet Stress. *Circulation*, 106(6), 711-717.
- Salvador, L., Mirone, S., Bianchini, R., Regesta, T., Patelli, F., Minniti, G., et al. (2008). A 20-Year Experience with Mitral Valve Repair with Artificial Chordae in 608 Patients. *The Journal of Thoracic and Cardiovascular Surgery*, 135(6), 1280-1287. e1.
- Sanfilippo, A. J., Harrigan, P., Popovic, A. D., Weyman, A. E., & Levine, R. A. (1992). Papillary Muscle Traction in Mitral Valve Prolapse: Quantitation by Two-Dimensional Echocardiography. *Journal of the American College of Cardiology*, 19(3), 564-571.

- Schoen, F. J., & Levy, R. J. (2005). Calcification of Tissue Heart Valve Substitutes: Progress Toward Understanding and Prevention. *The Annals of Thoracic Surgery*, 79(3), 1072-1080.
- Schoen, F. J., Hirsch, D., Bianco, R. W., & Levy, R. J. (1994). Onset and Progression of Calcification in Porcine Aortic Bioprosthetic Valves Implanted as Orthotopic Mitral Valve Replacements in Juvenile Sheep. *The Journal of Thoracic and Cardiovascular Surgery*, 108(5), 880-887.
- Schoof, P. H., Takkenberg, J. J., van Suylen, R., Zondervan, P. E., Hazekamp, M. G., Dion, R. A., & Bogers, A. J. (2006). Degeneration of the Pulmonary Autograft: An Explant Study. *The Journal of Thoracic and Cardiovascular Surgery*, 132(6), 1426-1432.
- Schwann, T. A., Engoren, M., Bonnell, M., Clancy, C., Khouri, S., Kabour, A., et al. (2013). Mitral Valve Repair and Bioprosthetic Replacement without Postoperative Anticoagulation does Not Increase the Risk of Stroke Or Mortality. *European Journal of Cardio-Thoracic Surgery*, 44(1), 24-31.
- Senning, A. (1967). Fascia Lata Replacement of Aortic Valves. *The Journal of Thoracic and Cardiovascular Surgery*, 54(4), 465-470.
- Shi, Y., & Vesely, I. (2004). Characterization of Statically Loaded tissue-engineered Mitral Valve Chordae Tendineae. *Journal of Biomedical Materials Research Part A*, 69(1), 26-39.
- Siddiqui, R. F., Abraham, J. R., & Butany, J. (2009). Bioprosthetic Heart Valves: Modes of Failure. *Histopathology*, 55(2), 135-144.
- Silbiger, J. J., & Bazaz, R. (2009). Contemporary Insights into the Functional Anatomy of the Mitral Valve. *American Heart Journal*, 158(6), 887-895.
- Silver, M., Hudson, R. E., & Trimble, A. S. (1975). Morphologic Observations on Heart Valve Prostheses made of Fascia Lata. *The Journal of Thoracic and Cardiovascular Surgery*, 70(2), 360-366.
- Siney, L., & Lewis, M. J. (1993). Nitric Oxide Release from Porcine Mitral Valves. *Cardiovascular Research*, 27(9), 1657-1661.



- Skoularigis, J., Essop, M. R., Skudicky, D., Middlemost, S. J., & Sareli, P. (1993). Frequency and Severity of Intravascular Hemolysis After Left-Sided Cardiac Valve Replacement with Medtronic Hall and St. Jude Medical Prostheses, and Influence of Prosthetic Type, Position, Size and Number. *The American Journal of Cardiology*, 71(7), 587-591.
- Smedira, N. G., Selman, R., Cosgrove, D. M., McCarthy, P. M., Lytle, B. W., Taylor, P. C., et al. (1996). Repair of Anterior Leaflet Prolapse: Chordal Transfer is Superior to Chordal Shortening. *The Journal of Thoracic and Cardiovascular Surgery*, 112(2), 287-292.
- Smith, J. C. (1967). The Pathology of Human Aortic Valve Homografts. *Thorax*, 22(2), 114-138.
- Soler-Soler, J., & Galve, E. (2000). Worldwide Perspective of Valve Disease. *Heart (British Cardiac Society)*, 83(6), 721-725.
- Spina, M., Ortolani, F., Messlemani, A. E., Gandaglia, A., Bujan, J., Garcia-Honduvilla, N., (2003). Isolation of Intact Aortic Valve Scaffolds for heart-valve Bioprotheses: Extracellular Matrix Structure, Prevention from Calcification, and Cell Repopulation Features. *Journal of Biomedical Materials Research Part A*, 67(4), 1338-1350.
- Spray, T. L., & Roberts, W. C. (1977). Changes in Saphenous Veins used as Aortocoronary Bypass Grafts. *American Heart Journal*, 94(4), 500-516.
- Stoker, W., Gök, M., Sipkema, P., Niessen, H. W., Baidoshvili, A., Westerhof, N., Eijssman, L. (2003). Pressure-Diameter Relationship in the Human Greater Saphenous Vein. *The Annals of Thoracic Surgery*, 76(5), 1533-1538.
- Straub, U. J., Huwer, H., Kalweit, G., Volkmer, I., & Gams, E. (1997). Improved Regional Left Ventricular Performance in Mitral Valve Replacement with Orthotopic Refixation of the Anterior Mitral Leaflet. *The Journal of Heart Valve Disease*, 6(4), 395-403.
- Tamura, K., Fukuda, Y., Ishizaki, M., Masuda, Y., Yamanaka, N., & Ferrans, V. J. (1995). Abnormalities in Elastic Fibers and Other Connective-Tissue Components of Floppy Mitral Valve. *American Heart Journal*, 129(6), 1149-1158.
- Tamura, K., Jones, M., Yamada, I., & Ferrans, V. J. (1995). A Comparison of Failure Modes of Glutaraldehyde-Treated Versus Antibiotic-Preserved Mitral Valve Allografts Implanted in Sheep. *The Journal of Thoracic and Cardiovascular Surgery*, 110(1), 224-238.

- Taylor, P. M., Batten, P., Brand, N. J., Thomas, P. S., & Yacoub, M. H. (2003). The Cardiac Valve Interstitial Cell. *The International Journal of Biochemistry & Cell Biology*, 35(2), 113-118.
- Teshima, H., Hayashida, N., Yano, H., Nishimi, M., Tayama, E., Fukunaga, S., Aoyagi, S. (2003). Obstruction of St Jude Medical Valves in the Aortic Position: Histology and Immunohistochemistry of Pannus. *The Journal of Thoracic and Cardiovascular Surgery*, 126(2), 401-407.
- Timek, T. A., & Miller, D. C. (2001). Experimental and Clinical Assessment of Mitral Annular Area and Dynamics: What are we Actually Measuring? *The Annals of Thoracic Surgery*, 72(3), 966-974.
- Timek, T. A., Green, G. R., Tibayan, F. A., Lai, D. T., Rodriguez, F., Liang, D., et al. (2003). Aorto-Mitral Annular Dynamics. *The Annals of Thoracic Surgery*, 76(6), 1944-1950.
- Topilsky, Y., Suri, R., Schaff, H. V., & Enriquez-Sarano, M. (2010). When to intervene for asymptomatic mitral valve regurgitation. *Seminars in Thoracic and Cardiovascular Surgery*, 22(3) 216-224.
- Turrentine, M. W., McCarthy, R. P., Vijay, P., McConnell, K. W., & Brown, J. W. (2002). PTFE Monocusp Valve Reconstruction of the Right Ventricular Outflow Tract. *The Annals of Thoracic Surgery*, 73(3), 871-880.
- Underwood, M., More, R., Weeresena, N., Firmin, R., & De Bono, D. (1993). The Effect of Surgical Preparation and in-Vitro Distension on the Intrinsic Fibrinolytic Activity of Human Saphenous Vein. *European Journal of Vascular Surgery*, 7(5), 518-522.
- Une, D., Ruel, M., & David, T. E. (2014). Twenty-Year Durability of the Aortic Hancock II Bioprosthesis in Young Patients: Is it Durable enough? *European Journal of Cardio-Thoracic Surgery*, 46(5), 825-830.
- Vahanian, A., & Iung, B. (2012). The New ESC/EACTS Guidelines on the Management of Valvular Heart Disease. *Archives of Cardiovascular Diseases*, 105(10), 465-467.
- Valente, M., Bortolotti, U., & Thiene, G. (1985). Ultrastructural Substrates of Dystrophic Calcification in Porcine Bioprosthetic Valve Failure. *The American Journal of Pathology*, 119(1), 12-21.

- Vesely, I. (2003). The Evolution of Bioprosthetic Heart Valve Design and its Impact on Durability. *Cardiovascular Pathology*, 12(5), 277-286.
- Vesely, I. (2005). Heart Valve Tissue Engineering. *Circulation Research*, 97(8), 743-755.
- Vongpatanasin, W., Hillis, L. D., & Lange, R. A. (1996). Prosthetic Heart Valves. *New England Journal of Medicine*, 335(6), 407-416.
- Wesly, R. L., Vaishnav, R. N., Fuchs, J. C., Patel, D. J., & Greenfield, J. C., Jr. (1975). Static Linear and Nonlinear Elastic Properties of Normal and Arterialized Venous Tissue in Dog and Man. *Circulation Research*, 37(4), 509-520.
- White, J. K., Agnihotri, A. K., Titus, J. S., & Torchiana, D. F. (2005). A Stentless Trileaflet Valve from a Sheet of Decellularized Porcine Small Intestinal Submucosa. *The Annals of Thoracic Surgery*, 80(2), 704-707.
- Wilcox, B. R., Cook, A. C., & Anderson, R. H. (2005). *Surgical anatomy of the heart* Cambridge University press.
- Wilkins, G. T., Weyman, A. E., Abascal, V. M., Block, P. C., & Palacios, I. F. (1988). Percutaneous Balloon Dilatation of the Mitral Valve: An Analysis of Echocardiographic Variables Related to Outcome and the Mechanism of Dilatation. *British Heart Journal*, 60(4), 299-308.
- Williams, D. F. (2008). On the Mechanisms of Biocompatibility. *Biomaterials*, 29(20), 2941-2953.
- World Heart Federation (2014, March 24). *Rheumatic heart disease-Demonstration projects in Africa*. Retrieved from the World Heart Federation website: <http://www.world-heart-federation.org/what-we-do/applied-research/rheumatic-heart-disease-demonstration-projects/africa/>
- Yacoub, M. H., & Cohn, L. H. (2004). Novel Approaches to Cardiac Valve Repair from Structure to Function: Part II. *Circulation*, 109(9), 1064-1072.
- Yacoub, M. H., Klieverik, L. M., Melina, G., Edwards, S. E., Sarathchandra, P., Bogers, A. J., et al. (2006). An Evaluation of the Ross Operation in Adults. *The Journal of Heart Valve Disease*, 15(4), 531-539.

- Yamauchi, T., Taniguchi, K., Kuki, S., Masai, T., Noro, M., Nishino, M., & Fujita, S. (2005). Evaluation of the Mitral Valve Leaflet Morphology after Mitral Valve Reconstruction with a Concept "Coaptation Length Index". *Journal of Cardiac Surgery*, 20(5), 432-435.
- Yamaura, Y., Yoshikawa, J., Yoshida, K., Hozumi, T., Akasaka, T., & Okada, Y. (1995). Three-Dimensional Analysis of Configuration and Dynamics in Patients with an Annuloplasty Ring by Multiplane Transesophageal Echocardiography: Comparison between Flexible and Rigid Annuloplasty Rings. *The Journal of Heart Valve Disease*, 4(6), 618-622.
- Yavuz, T., Nisli, K., Oner, N., Dindar, A., Aydogan, U., Omeroglu, R. E., & Ertugrul, T. (2008). Long Term Follow-Up Results of 139 Turkish Children and Adolescents with Rheumatic Heart Disease. *European Journal of Pediatrics*, 167(11), 1321-1326.
- Yoganathan, A. P., Chandran, K., & Sotiropoulos, F. (2005). Flow in Prosthetic Heart Valves: State-of-the-Art and Future Directions. *Annals of Biomedical Engineering*, 33(12), 1689-1694.
- Yoganathan, A. P., He, Z., & Casey Jones, S. (2004). Fluid Mechanics of Heart Valves. *Annu.Rev.Biomed.Eng.*, 6, 331-362.
- Zaidi, A. H., Nathan, M., Emani, S., Baird, C., Pedro, J., Gauvreau, K., et al. (2014). Preliminary Experience with Porcine Intestinal Submucosa (CorMatrix) for Valve Reconstruction in Congenital Heart Disease: Histologic Evaluation of Explanted Valves. *The Journal of Thoracic and Cardiovascular Surgery*, 148(5), 2216-2225. e1.
- Zegdi, R., Khabbaz, Z., Chauvaud, S., Latremouille, C., Fabiani, J., & Deloche, A. (2007). Posterior Leaflet Extension with an Autologous Pericardial Patch in Rheumatic Mitral Insufficiency. *The Annals of Thoracic Surgery*, 84(3), 1043-1044.
- Zou, R., Sun, M., Lu, Z., & Guo, Q. (2012). Influence of Ischemia before Vein Grafting on Early Hyperplasia of the Graft and the Dynamic Changes of the Intima after Grafting. *Journal of Cardiothoracic Surgery*, 7, 90-8090-7-90.
- Zussa, C., Frater, R. W., Polesel, E., Galloni, M., & Valfré, C. (1990). Artificial Mitral Valve Chordae: Experimental and Clinical Experience. *The Annals of Thoracic Surgery*, 50(3), 367-373.